UNESCO

United Nations
Educational, Scientific and
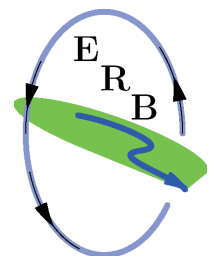Cultural Organization

International
Hydrological
Programme

Hydrological extremes
in small basins

**12th Biennial International Conference of the Euromediterranean Network
of Experimental and Representative Basins (ERB)
Kraków, Poland, 18–20 September 2008**

*Convened by: ERB, UNESCO/IHP (NE FRIEND Project 5)
Jagiellonian University,
Institute of Geography and Spatial Management*

ERB

PROCEEDINGS

Edited by W. Chełmicki and J. Siwek

HYDROLOGICAL EXTREMES IN SMALL BASINS

International conference, Kraków, 18–20 September, 2008

Convened by:
Euromediterranean Network of Experimental and Representative Basins (ERB)
UNESCO IHP Northern European FRIEND Project 5

Organised by:
Jagiellonian University, Institute of Geography and Spatial Management, Kraków (Poland)

International Scientific Committee
– Piet Warmerdam, ERB international coordinator, Wageningen, The Netherlands
– Mitja Brilly, Ljubljana, Slovenia
– Wojciech Chełmicki, Kraków, Poland
– Niko Verhoest, Ghent, Belgium
– Francesc Gallart, Barcelona, Spain
– Jūratè Kriaučiūnienè, Kaunas, Lithuania
– Sergei Zhuravin, St.Petersburg, Russia
– Hubert Holzmann, Vienna, Austria
– João de Lima, Coimbra, Portugal
– Ian Littlewood, PUB-IAHS representative, Wallingford, GB
– Franca Maraga, Torino, Italy
– Pavol Miklánek, Bratislava, Slovakia
– Pompiliu Mita, Bucharest, Romania
– Laurent Pfister, Belvaux, NE Friend 5 coordinator, Luxembourg
– Manfred Spreafico, Bern, Switzerland
– Miroslav Tesař, Stachy, Czech Republic
– Stefan Uhlenbrook, Delft, The Netherlands
– Daniel Viville, Strasbourg, France

Local Organising Committee
– Maria Baścik, Jagiellonian University
– Wojciech Chełmicki, Jagiellonian University
– Michał Kasina, Jagiellonian University
– Artur Magnuszewski, University of Warsaw
– Joanna Pociask-Karteczka, Jagiellonian University
– Bartomiej Rzonca, Jagiellonian University
– Janusz Siwek, Jagiellonian University
– Roman Soja, Polish Academy of Sciences
– Mirosław Żelazny, Jagiellonian University

Previous ERB conferences and proceedings

October 1986 : Aix en Provence (France)

October 1988 : Perugia (Italy)
Erosion and sediment transport.
European Network of Representative and Experimental Basins, 2nd General Meeting,
Perugia. Associazione Italiana di Idronomia, Publ. No. 9, Padova, 1989, 203 pp.

September 1990 : Wageningen (The Netherlands)
Hydrological research basins and the environment.
TNO Comm. on Hydrol. Res., Proc. and Informat. No. 44, The Hague, 347 pp.

September 1992 : Oxford (United Kingdom)
Methods of hydrological basin comparison.
Institute of Hydrology Rep. No. 120, Wallingford, 198 pp.

September 1994 : Barcelona (Spain)
Assessment of hydrological temporal variability and changes.
Acta Geol. Hisp., (Special Issue), vol. 28, no. 2-3, Barcelona, 1995, 138 pp.

September 1996 : Strasbourg (France)
Ecohydrological processes in small basins.
Technical Documents in Hydrology 14, IHP UNESCO, Paris, 1997, 199 pp.

September 1998 : Liblice (Czech Republic)
Catchment hydrological and biochemical processes in a changing environment.
Technical Documents in Hydrology 37, IHP UNESCO, Paris, 2000, 296 pp.

September 2000 : Ghent (Belgium)
Monitoring and modelling catchment water quantity and quality.
Technical Documents in Hydrology 66, IHP UNESCO, Paris, 2003, 112 pp.

September 2002 : Demänovská dolina (Slovakia)
Interdisciplinary approaches in small catchment hydrology: monitoring and research.
Technical Documents in Hydrology 67, IHP UNESCO, Paris, 2003, 256 pp.

October 2004 : Torino (Italy)
Progress in surface and subsurface water studies at plot and small basin scale.
Technical Documents in Hydrology 77, IHP UNESCO, Paris, 2005, 194 pp.

September 2006 : Luxembourg (Luxembourg)
Uncertainties in the 'monitoring-conceptualisation-modelling' sequence of catchment research.
Technical Documents in Hydrology 81, IHP UNESCO, Paris, 2007, 192 pp.

PREFACE

Changes in the natural environment taking place today are to a significant extent the result of human pressure. These changes are having an effect on water circulation and the flow of matter in river catchments. This is particularly clear in terms of the intensity and the frequency of extreme events such as floods and low flow events. Given the economic and social consequences of extreme events, the study of such events has become an important issue in science. The goal of this type of research is to gain insight into the mechanisms that drive extreme events. Small research catchments are especially useful in this type of research. Such catchments help researchers understand the genesis of extreme events at different stages of water circulation. Research results can then be used to create advanced models designed to predict water phenomena as well as to produce extreme event scenarios for a changing natural environment.

On September 18–20, 2008, The Twelfth Biennial Conference of the Euromediterranean Network of Representative and Experimental Basins (ERB) was held in Kraków. The conference addressed the issue of hydrological extremes in small basins and was organized by the Institute of Geography and Spatial Management of the Jagiellonian University under the umbrella of the IAHS (International Association of Hydrological Sciences),"PUB" initiative (Prediction in Ungauged Basins) and the UNESCO-IHP Northern European FRIEND Project. The 109 researchers who took part in the conference presented 41 papers and 50 posters.

The conference focused on the following themes:
- Prediction of the hydrological response based on different quality measurement data;
- Hydrological model calibration for extreme conditions;
- Hydro-chemical and geomorphological response to hydrological extremes;
- Surface water–groundwater interactions under extreme conditions;
- Extreme value statistics;
- Extreme streamflow prediction in ungauged basins;
- New ideas, monitoring, and model developments; experiences in small basin research.

The conference also included a field session where the participants could become familiar with the research being conducted in research catchments by the Field Research Station of the Institute of Geography and Spatial Management of the Jagiellonian University located in the Wieliczka Foothills.

All abstracts submitted by authors of papers and posters were published in the Book of Abstracts. This volume contains 24 articles submitted by authors after the conference. It also contains the text of the keynote presentation by Ian G. Littlewood.

Full-text versions of all keynote lectures given by Ian G. Littlewood, Zbigniew W. Kundzewicz, and Maciej Zalewski have been published in the journal Folia Geographica, Geographica-Physica Series (2008, vol. 39) and are available on the journal's website http://www.geo.uj.edu.pl/foliageographica/index2.php .

Papers based on the posters presented at the conference will be published in 2009 and 2010 in the journal Folia Geographica (vols. 40 and 41).

The conference organisers and the editors of this volume would like to thank all participants for their active role in the conference. Special thanks are also being extended to authors for their contributions and to reviewers for their critical comments which had helped make the published works better.

Thanks are also being directed to Piet Warmerdam – the international coordinator of ERB in 2002–2008 – for his work, his organizational help, and the creation of a cordial and productive discussion atmosphere. We would like to wish his successor, Ladislav Holko of Slovakia, a successful term in managing the ERB for the next few years. Finally, thanks are being extended to the UNESCO-IHP which had financially supported more than a dozen conference participants and also had provided financial support – along with the Institute of Geography and Spatial Management of the Jagiellonian University – for the publication of this volume.

The Editors

TABLE OF CONTENTS

Session 7: New ideas, monitoring, and model developments; experiences in small basin research

MODELLING THE HYDROLOGICAL EXTREME EVENT OF SUMMER 2007 IN THE SEVERN UPLANDS FROM GAUGE AND RADAR RAINFALL SOURCES

E.M. Biggs [1], P.M. Atkinson[1] and D.C. De Roure[2]

[1] *School of Geography, University of Southampton, Southampton, SO17 1BJ, UK*

[2] *School of Electronics and Computer Science, University of Southampton, Southampton, SO17 1BJ, UK*
Corresponding author: Eloise Biggs, e-mail: Eloise.Biggs@soton.ac.uk

ABSTRACT

This paper provides a comparison of gauge interpolated and radar derived precipitation data sources for an upland catchment in the UK for a time period when extreme hydrological conditions were prevalent. Subsequently, a performance measure was used to evaluate the accuracy of hydrological simulation of extreme conditions using the two independent precipitation data sources within a HEC-HMS modelling framework. Discrepancies between gauge and radar time-series precipitation records were found to coincide with elevation, spatial distribution of precipitation and distance from the radar source. The Nash-Sutcliffe performance measure indicated that despite the higher temporal and spatial resolution of the radar data, interpolated gauging station records produced comparative accuracy when replicating the extreme hydrological event of Summer 2007.

Key words: extremes, radar rainfall, HEC-HMS, rainfall-runoff modelling

INTRODUCTION

Global changes in climate are likely to induce an increase in the frequency and magnitude of hydrological extremes (Cunderlik and Simonovic, 2005). There is evidence to suggest that both precipitation and flow extremes have increased in the UK over the last 30–40 years (DEFRA, 2001; Osborn *et al*., 2000; Fowler and Kilsby, 2003). Flooding is the most damaging and costly natural hazard in the UK, costing the nation billions of pounds every year (Brown and Damery, 2002) and extreme floods such as those experienced in 1998, 2000 and 2007 are likely to occur more frequently due to changes in precipitation. Accurate monitoring and modelling of these extreme events is essential if future extremes under a changing climate are to be characterised accurately. The quality of hydrological forecasts will, in general, depend on the quality of the simulation model, the accuracy of the precipitation and boundary forecasts, and the efficiency of the data assimilation procedure. Recent efforts in fluvial forecasting have focused on quantifying rainfall amounts from radar images. As the spatial and temporal resolution of distributed gridded data has increased it has become more desirable to incorporate gauge-corrected radar imagery into hydrological modelling to increase accuracy. This paper investigates the effectiveness of tipping-bucket rain gauges and Nimrod radar rainfall imagery to simulate a recent extreme flood event in the UK and to determine where the differences in accuracy lie given the different data resources used for model simulation.

STUDY SITE AND DATA

The Severn Uplands

The Severn Uplands is located at the headwaters of the River Severn, UK, and encompasses a drainage area of approximately 2000 km² (Fig. 1). The strong maritime influence in the Severn Uplands leads to high rainfall quantities and frequencies. To the west, the catchment is bordered by the Cambrian Mountains and prevailing
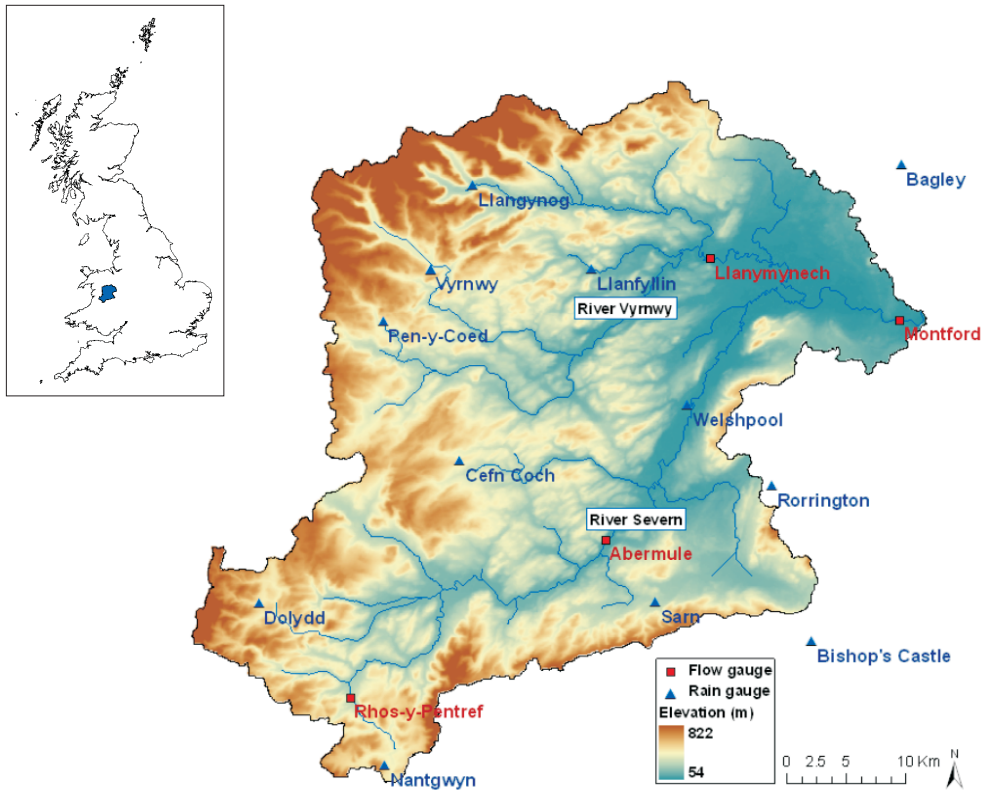
Fig. 1:   The Severn Uplands catchment.

weather systems from the south-west bring precipitation as air streams are forced to uplift by the mountains. Rainfall is high in the west, totalling more than 2500 mm·annum^{-1}, and runoff regimes are flashy. Towards the east of the basin rainfall reduces to around 660 mm·annum^{-1} and drastic reductions in elevation give way to a wider fluvial system which meanders through low-lying floodplains. Elevation ranges from heights of approximately 820 m AOD in the west to lows of 50 m AOD in the east. The Vyrnwy, a major tributary, adjoins the River Severn just upstream of the catchment outlet at the Severn-Vyrnwy confluence zone where flood inundation occurs frequently. The Severn Uplands is a predominantly rural catchment with widespread grassland constituting approximately two-thirds of the land cover and woodland comprising the majority of the remaining third. The catchment largely constitutes impermeable geology, which leads to the generation of rapid runoff processes, particularly in the upper reaches where slopes are steep.

Summer 2007

During the summer of 2007 many parts of the UK were inundated following a series of unseasonably low depression systems throughout June and July. The heavy rainfall was the result of a series of statistically unusual weather patterns that have been attributed to two major causes; the position of the Polar Front Jet Stream and high North Atlantic sea surface temperatures (Marsh and Hannaford, 2007). In June, heavy thunderstorms led to wide extents of ground saturation, then in July slow moving depressions resulted in the largest flood inundation peaks. Rainfall intensity was high and June was one of the wettest months on record in the UK.

Two main sources of precipitation data are available in the UK; (i) gauged data recorded by the Environment Agency and (ii) Nimrod radar imagery sourced from the Met Office and supplied through the British Atmospheric Data Centre (BADC). Gauge records were obtained at 15-minute intervals for 12 gauges across the catchment (Figure 1) and radar images were acquired at 5-minute temporal resolution with 1 km^2 spatial resolution. Flow gauge data (Environment Agency) for model calibration were retrieved at 15-minute intervals for four locations (Figure 1). Radar data were aggregated to 15-minute intervals to temporally coincide with

2

the gauge time-series. All precipitation and flow records were retrieved for the time period 1st June to 31st July 2007, which is referred to in this paper as 'Summer 2007'.

METHODS

HEC-HMS, a one-dimensional rainfall-runoff model, was used to replicate hydrological processes in the Severn Uplands. Rainfall inputs were used to drive the hydrological model where subbasin (Clark unit hydrograph (gauge) and ModClark (radar) transform; recession baseflow; initial and constant loss) and river routing (Muskingum-Cunge) parameters acted to translate rainfall into runoff. Model calibration was undertaken using the HEC-HMS optimisation procedure with a combination of two objective functions and two minimising algorithms to determine optimal accuracy. The models (gauge- and radar-driven) were calibrated independently and optimum parameter sets were derived which generated the most accurate hydrograph simulations. Gauge rainfall was modelled within HEC-HMS using time and depth weights. Rainfall inputs were compared using error and correlation calculations and model outputs were assessed using a performance measure as described below.

Rainfall comparison

Root-mean square error (RMSE) was used as a measure of the quantitative agreement between the gauge and radar time-series. Lewis and Harrison (2007) state that RMSE is highly correlated with the magnitude of land surface rain-rate such that poorly performing radars in light rain could appear more accurate in predicting reference data than relatively accurately performing radar in heavy rainfall. Therefore, in addition to RMSE, the root-mean square factor (RMSF) was used as it overcomes this problem. RMSF is interpreted as giving scale to the multiplicative error (Golding, 1998) and is calculated as

$$RMSF = \exp \left\{ \frac{1}{n} \sum_{i=1}^{n} \left[h\left(\frac{R_i}{G_i}\right) \right]^2 \right\}^{\frac{1}{2}}$$
Eq.1

where R_i is radar precipitation and G_i is rain gauge precipitation at observation i and n is number of observations. Radar time-series were calculated by extracting cell values located at each of the gauging station locations and amalgamated to coincide with the temporal resolution of the gauge time-series. To avoid division by zero, only values ≥ 0.05 mm (a quarter of the standard 0.2 mm threshold for hourly readings) present in both 15-minute time-series were analysed. In addition to RMSE and RMSF, the Pearson product-moment correlation coefficient r was used to determine correlation and systematic bias was estimated as the difference between time-series totals.

Performance measure

The Nash-Sutcliffe efficiency index E_f (Nash and Sutcliffe, 1971) is a performance measure which compares optimal model simulations, rendered from strategic sampling of the parameter space, to that of the observational data, as follows

$$E_f = 1 - \frac{\sum_{i=1}^{n} (\hat{Y}_i - Y_i)^2}{\sum_{i=1}^{n} (Y_i - \bar{Y})^2}$$
Eq. 2

where: $\hat{Y}_i$ is the predicted value and Y_i is the measured value of the dependent variable Y for observation i, $\bar{Y}$ is the mean of the measured values and n is the sample size. E_f will return a value of 1 for a perfect fit.

A value close to 0 is equivalent to saying that the hydrological model is equal to a one-parameter "no-knowledge" model. Negative values indicate that the model is performing below that of a "no-knowledge" model (Beven, 2001).

RESULTS

Time-series precipitation residuals at 15-minute intervals for Summer 2007 indicate an average RMSE of 0.18 mm across the Severn Uplands catchment (Table 1). No obvious spatial pattern in RMSE is apparent. However, RMSF values are generally smaller towards the east of the catchment and larger in the west (Table 1). Harrison *et al.* (2000) found that sampling difference alone can account for a RMSF difference of between 1.26 and 2.51 for hourly radar data at a 5 km² spatial resolution. Quality controlled and corrected Nimrod radar data have a typical RMSF value of around 2 when compared to surface gauges (Harrison *et al.*, 2000). With respect to these findings, RMSF values for the Severn Uplands indicate less error between precipitation residuals at analysed sites than expected, with a maximum observed RMSF value of 1.29. Correlations between the two time-series are large, particularly at sites in the south-east of the catchment where large positive correlations indicate a near-perfect fit (Table 1). Bias between Summer 2007 precipitation totals (radar minus gauge) indicates systematic errors of approximately ± 50 mm (Table 1). Radar time-series data over-predict ground observations at half of the gauging station locations. In terms of absolute error the most accurate radar predictions (in relation to reference data for the Summer 2007 hydrological event) are situated in the north-west of the catchment.

Table 1: Comparison of gauge and radar time-series at gauge station locations.

Station	RMSE [mm]	RMSF	r	Bias [mm]
Bagley	0.15	1.22	0.85	15.22
Bishop's Castle	0.13	1.22	0.85	30.71
Cefn Coch	0.20	1.26	0.63	41.97
Dolydd	0.18	1.29	0.81	-40.76
Llanfyllin	0.19	1.22	0.74	-56.37
Llangynog	0.18	1.25	0.79	4.22
Nantgwyn	0.19	1.26	0.75	17.46
Pen-y-Coed	0.21	1.29	0.71	0.77
Rorrington	0.17	1.19	0.90	-53.87
Sarn	0.16	1.21	0.86	-51.10
Vyrnwy	0.15	1.26	0.80	-1.29
Welshpool	0.22	1.23	0.80	-59.86

Model simulations were run initially to test the July 2007 predictions only. E_f indices of these preliminary results indicate little difference between simulated and observed flows derived from gauge and radar data inputs (Table 2). E_f values signify greater prediction accuracy in the upper reaches of the catchment, with accuracy decreasing with distance downstream. The gauge network generates a larger E_f value at Rhos-y-Pentref than that produced from the radar, but all three other sites are predicted more accurately using radar data. In contrast, when the entire Summer 2007 period is modelled the gauging network predicts more accurately in all cases (Table 2). The differences between July and Summer 2007 predictions are visualised in Figure 2 for Rhos-y-Pentref where the latter part of the gauge and radar time-series clearly fit the observed data more accurately.

Table 2: Nash-Sutcliffe performance measure E_f for calibrated gauge- and radar-driven model simulations in comparison to observed flows.

	July		Summer 2007	
	Radar	Gauge	Radar	Gauge
Rhos-y-rentref	0.813	0.835	0.522	0.653
Abermule	0.672	0.597	0.315	0.540
Llanymynech	0.607	0.448	0.405	0.802
Montford	0.406	0.397	0.197	0.578

INTERPRETATION AND DISCUSSION

Differences between the precipitation time-series are likely to have arisen from the ability of the radar to represent rainfall accurately. Several sources of uncertainty are present when processing radar data and two main factors seem to influence accuracy in the Severn Uplands. Firstly, the occultation and echoes of the radar

4
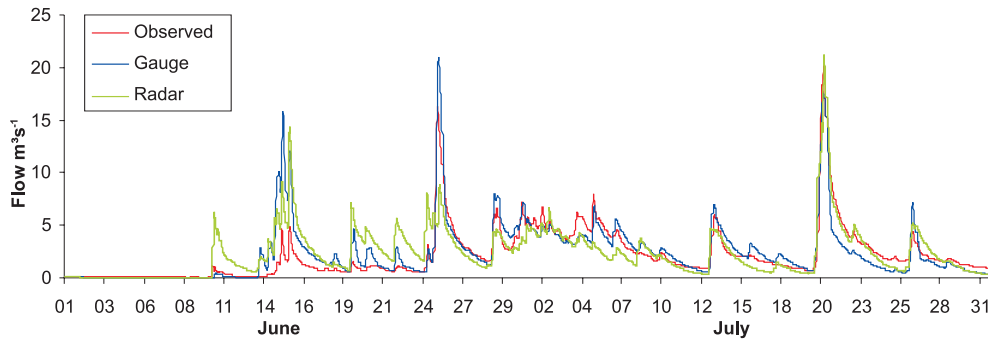
Fig. 2: Calibrated gauge- and radar-driven model simulations and observational data at Rhos-y-Pentref.

beam due to topographic changes and issues arising from orographic enhancement may have resulted in larger inaccuracies in the higher elevations to the north and west of the Severn Uplands. Secondly, the greater the distance from the radar source the greater the error, which could be due to the overshooting of precipitation by the radar beam at long ranges (Tilford *et al*., 2003). In addition to these radar-sourced inaccuracies, the actual total amount of precipitation may have an effect on gauge-radar residuals.

These three factors are illustrated in Figure 3 where RMSF has been plotted against Summer 2007 rainfall totals, the distance of the site from the radar source and the elevation of the site. Significant positive correlations ($p < 0.05$) are identified between RMSF and all variables with values of 0.64 (radar), 0.91 (gauge), 0.73 (distance) and 0.68 (elevation). Larger error values at sites in the west of the Severn Uplands are likely to have
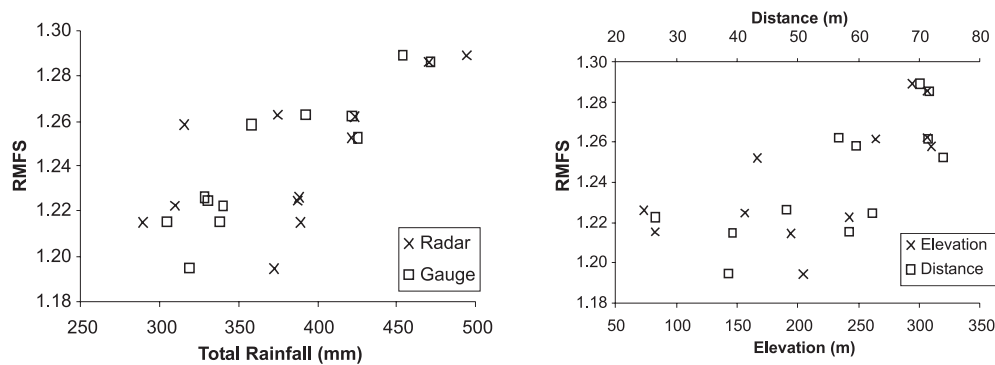
Fig. 3: Variations in RMSF in accordance with changes in total Summer 2007 rainfall (left) and elevation and distance from nearest radar source for time-series recorded locations (right).

resulted from higher rainfall due to orographic enhancement (elevation) which in turn results in increased radar distortion. These locations also happen to be furthest away from the nearest radar source which is situated to the south-east of the catchment. By multiplying the radar variables together, then scaling the values from 0 to 1, the spatial distribution of error likelihood was defined (Fig. 4). The scaled values show a significant positive correlation with RMSF at a value of 0.92 ($p < 0.001$).

The increased predictive power at upstream locations is likely to have occurred due to more clearly defined rainfall-runoff processes, as the steep topography and impermeable geology aid rapid transition of rainfall into runoff which directly inputs into river channels. Contrastingly, further downstream clear-cut rainfall-runoff processes diminish as the topography flattens out and basin properties such as floodplain storage and groundwater aquifers become increasingly influential. In terms of model output differences arising from precipitation data inputs, the E_f values suggest that HEC-HMS is capable of using both gauge and radar sources
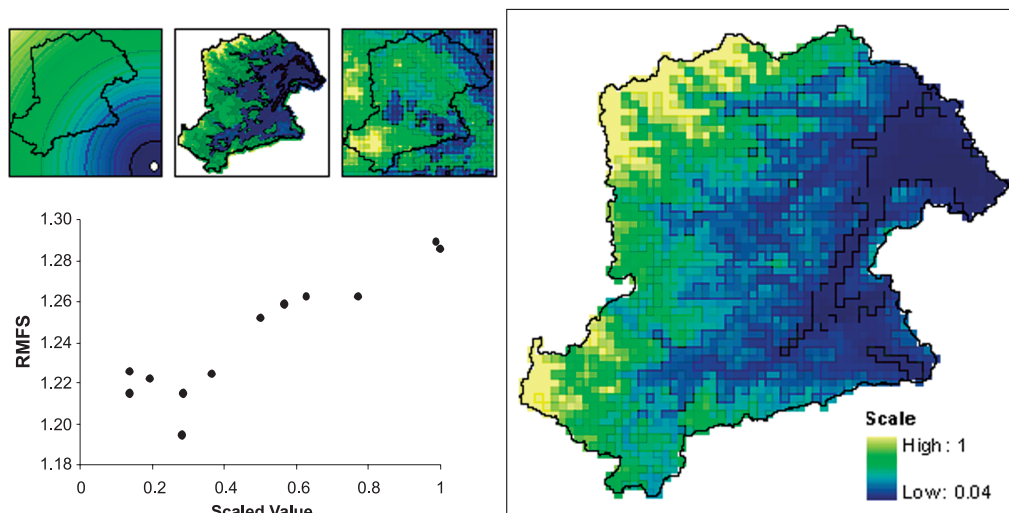
Fig. 4: Distance from radar source (top left), elevation (top middle) and rainfall total (top right) were multiplied and scaled then mapped (right) and plotted against RMSF.

to replicate Summer 2007 extreme flows with suitable accuracy, particularly at the more upstream locations. The lack of difference between the time-series E_f values may be due to the effectiveness of the modelling and calibration procedures within HEC-HMS. It may be beneficial in future research to correct the bias within the radar data by using the variables discussed above.

CONCLUSIONS

It has to be reiterated that neither rain gauge nor weather radar data can be taken as 'truth' (Tilford *et al.*, 2003). Despite differences in the gauge and radar time-series records, both point-interpolated and grid-distributed precipitation produced comparable results when using HEC-HMS to model the extreme hydrological event of Summer 2007 in the Severn Uplands. Greater accuracy was achieved in the upper reaches of the catchment and simulation accuracy increased in the latter part of the time period simulated. Overall, although some error remains, the Summer 2007 extreme hydrological event, one of the wettest events on record in the UK, was modelled adequately using both gauge and radar precipitation inputs. This provides encouragement for using the HEC-HMS software to model other extreme events which have occurred in the Severn Uplands; firstly, to validate the parameter sets for alternative extreme hydrological conditions, and secondly, to further research on how future precipitation extremes will influence fluvial extremes given current climate change predictions.

REFERENCES

Brown J.D. and Damery S.D. (2002). Managing flood risk in the UK: towards an integration of social and technical perspectives. *Transactions of the Inst. of Br. Geogr*., **27**: 412–426.

Cunderlik J.M. and Simonovic S.P. (2005). Hydrological extremes in a south-western Ontario river basin under future climate conditions. *Hydrol. Sci. J.*, **50**(4): 361–654.

DEFRA (2001). *National Appraisal of Assets at Risk from Flooding and Coastal Erosion, including the potential impact of climate change: Final Report*. Halcrow, Swindon: 61pp.

Fowler H.J. and Kilsby C.G. (2003). A regional frequency analysis of United Kingdom extreme rainfall from 1964 to 2000. *Int. J. Climatol.*, **23**(11): 1313–1334.

Golding B.W. (1998). Nimrod: system for generating automated very short forecasts. *Meteorol. Appl.*, **5**: 1–16.

Harrison D.L., Driscoll S.J. and Kitchen M. (2000). Improving precipitation estimated from weather radar using quality control and correction techniques. *Meteorol. Appl.*, **6**: 135–144.

Lewis H.W. and Harrison D.L. (2007). Assessment of radar data quality in upland catchments. *Meteorol. Appl.*, **14**: 441–454.

Marsh T.J. and Hannaford J. (2007). *The summer 2007 floods in England and Wales – a hydrological appraisal*. Centre for Ecology and Hydrology, Wallingford, UK: 32pp.

Nash J.E. and Sutcliffe J.V. (1971). River flow forecasting through conceptual models. Part 1: A discussion of principles. *J. Hydrol.*, **10**(3): 282–290.

Osborn T.J., Hulme M., Jones P.S. and Basnett T.A. (2000). Observed trends in the daily intensity of United Kingdom precipitation. *Int. J. Climatol.*, **20**: 347–364.

Tilford K.A., Sene K., Chatterton J.B., and Whitlow C. (2003). *Flood Forecasting – Real Time Modelling*. Defra/Environment Agency R&D Technical Report W5C-013/5/TR.

IDENTIFICATION OF SMALL BASINS PRONE TO FLASH FLOODING AS A METHOD SUPPORTING LOCAL FLOOD FORECASTING – BASED ON THE EXAMPLE OF THE SOUTHERN PART OF THE NIDA RIVER BASIN (POLAND)

T. Bryndal

Institute of Geography, Pedagogical University, Podchorążych 2, 30-082 Kraków, Poland
e-mail:tbryndal@ap.krakow.pl

ABSTRACT

Flash floods induced by heavy rainstorms can cause significant property damage as well as loss of human life (local floods). Today, the ability to predict such events is primarily based on local weather forecasts. However, given the haphazard temporal and spatial distribution of convective rainstorms, the forecasting of local floods must take into account additional factors. In this research study, models of basins prone to flash flooding were created. The models were characterized by ten physiographic parameters. Next, natural basins resembling the models were delineated in the southern part of the Nida Basin. Available information about flash floods in this region confirmed that the delineated basins had been affected by flash floods in the past. Hence, the identification of basins susceptible to flash floods may improve flood forecasting ability.

Key words: flash flood, forecast, small basin, Nida Basin

INTRODUCTION

Flash floods in small river basins are the result of intense short-duration convective rainstorms. Given their local reach, they are considered local floods. Both overland flow and flood waves can be reasons for considerable soil erosion, property damage, and loss of human life (Bielders *et al.*, 2003; Gutiérres *et al.*, 1998; Verstraeten and Poesen, 1999).

Fieldwork (Bryndal, 2008) has shown that flash floods have a specific course of action. In most cases, only a certain part of a basin suffers flooding. It is well known that flood wave parameters depend on rainfall characteristics and a basin's features such as area, relief, geomorphology, land use, and geology (Gregory and Walling, 1973; Ramachado Rao, 2003). The part of the basin which is affected by flooding can be described using certain physiographic parameters. Eighty three basins located in the southern part of Poland (the Carpathian Mts. and the Polish part of the Uplands) were described using the parameters. They were selected on the basis of the hydrological literature relevant to the mechanisms of outflow formation during intense short-duration precipitation events. In this manner, 14 parameters were calculated describing a basin's dimensions (area, maximum length, average width), shape (shape index), relief conditions (average slope gradient, average slope length, relief, average valley bottom gradient), valley and road network (valley density, bifurcation ratio, road density), structure of land use (forest area, settlement area, arable area), and soil conditions. Detailed analysis of the parameters used (Bryndal, 2006) has indicated that the basins were similar in spite of the fact that they were situated in different regions – highlands, foothills, mid-mountain terrain, and basins. Moreover, research has revealed characteristic features of the basins. The basins analyzed were small in area. Three quarters of them were smaller than 12 km². Only a few basins were larger than 20 km². The largest basin was under 40 km². During a rainstorm, such a basin is completely covered by heavy precipitation which leads to a rapid response on the part of the basin. Most of the investigated basins had steep slopes – steeper than 6º. Steep slopes accelerate overland flow velocity reducing time to peak and increasing peak discharge. The majority of the basins possessed a main valley bottom gradient larger than 11%. This feature accelerates flood wave

propagation. The basins in question had dense and well developed road and valley networks. Three quarters of the basins possessed a valley and road network density higher than 2.7 km·km^{-2} and 3.4 km·km^{-2}, respectively. These elements play a crucial role in delivering rainstorm water from slopes to valley bottoms. The basins investigated have been substantially deforested. On average, forest occupied only one fifth of the basin's area, usually as riparian forest. Arable lands which predispose overland flow generation were dominant in the basins investigated. The majority of the basins possessed arable land content above 60%. Most of the basins possessed soil cover developed on bedrock rich in clay minerals. Such soil structure affects overland flow generation. Given that the investigated basins were ungauged and hydrological data was unavailable, the process of transformation from rainfall to outflow was investigated using the Geomorphological Instantaneous Unit Hydrograph Model (Rodriguez-Iturbe and Valdes, 1979). The results have revealed comparable basin response which was also confirmed by specific runoff values (Bryndal, 2006; 2007). Moreover, the basins analysed possessed high outflow coefficients values. The Soil Conservation Service Method (Ramachado Rao, 2003) indicated that this parameter ranged from 0.4 to 0.7. The outflow coefficient, calculated using a method based on soil structure and basin topography (Czarnecka, 1976), was slightly higher and ranged from 0.4 to 0.9.

Results of the research have revealed that some basins are more prone to flash flooding than others. If a certain type of basin is affected by heavy rainstorms, then there is a high probability that flash floods will occur. Therefore, the identification of such basins may support local flood forecasting efforts. The goal of this study is to identify basins prone to flash flooding in the southern part of the Nida Basin.

MATERIALS AND METHODS

Identification of basins was performed on the basis of models which had been created as the result of a classification process. Eighty three basins which had been described by 14 physiographic parameters (Bryndal, 2006) were divided into smaller groups. These groups can be described as models of basins prone to flash flooding. Cluster analysis was performed as a classification method. At the beginning, correlation analysis was performed and the features that had a coefficient of correlation larger than |0.5| were eliminated. In this way, 10 physiographic parameters were selected (Table 1). Input data was standardized in order to minimize the influence of data on the distance measure. Euclidean distance was used as a measure of similarity and agglomeration was performed using Ward's Method (Marques de Sà, 2007). Division of the hierarchical tree was performed according to the method proposed by Z. Hellig (1968), using the critical value (W_k). The value was computed on the basis of a distance matrix according to following equation:

$$W_k = \mu + 2\sigma \qquad\qquad \text{Eq. 1}$$

where: W_k – critical value, μ, σ – mean value and standard deviation of the series of the smallest values in the distance matrix rows.

This value divides the hierarchical tree into the most homogeneous clusters (Hellig, 1968). Reductions in the number of clusters using multiples of the critical value allowed for the determination of the models. They were characterized using descriptive characteristics such as mean value, coefficient of variability, and minimum and maximum values. Such characteristics enabled an assessment of the diversity of physiographic parameters of the models and the identification of natural basins similar to those portrayed by the models.

Geographic Information System tools were utilized to create a geo-database for the southern part of the Nida Basin. The following vector data was used: 1:50 000. The geo-database was analyzed in order to identify basins similar to those in particular models. Minimum and maximum values of physiographic parameters were used during the identification process. In this way, natural basins comparable to those in the models generated were delineated. Finally, the delineated basins were researched for previous reported flash flood activity.

RESULTS

Models of Basins

Figure 1 presents the results of the agglomeration process. The low level of the linkage distance value during the agglomeration process deserved special emphasis. It may be interpreted to mean that the basins analyzed were alike. The critical value was equal to 3.25 and divided the hierarchical tree into 31 clusters. According to Z. Hellig (1968), these clusters are the most homogeneous. However, some clusters consisted of a small number of basins. More than 10% of the clusters consisted of only a single basin. Therefore, in order to create models of the basins, the number of clusters had to be reduced. It should be noted that the critical value, which divided the population into 31 clusters, constituted only 9% of the maximum linkage value. If the critical value had been doubled, then the number of clusters would have been reduced from 31 to 12. If the critical value had been tripled, the number of clusters would have been reduced from 31 to 7, which would constitute about 78% of all the basins (Fig. 1), whereas a tripled critical value would constitute only 27% of the maximum linkage value. Clusters, which comprise of one or two basins, were reduced completely. Three clusters consisted of 17 to 19 basins each which constituted 65% of the basins studied. Three remaining clusters contained three, four, and eight basins. Table 1 presents the descriptive parameters of the models.
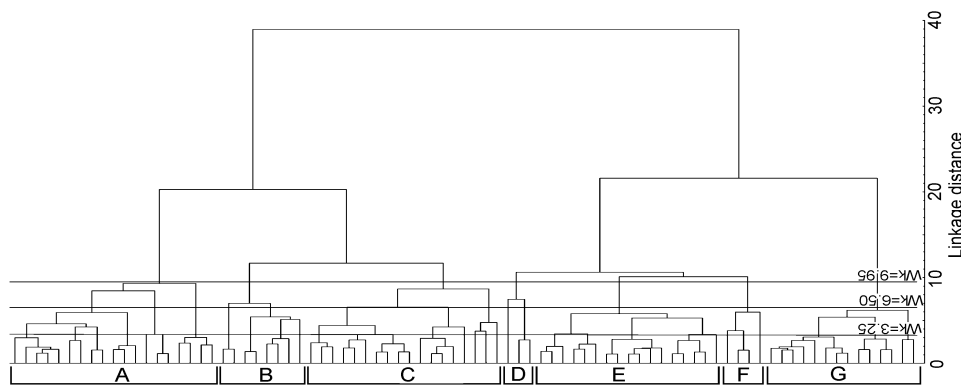
Fig. 1:   Division of the hierarchical tree into clusters. A-G – the models.

The models are varied in terms of dimensions, relief, and land use structure. Models A, B, C, and D are based on medium size basins (5.6–9.0 km^2). Moreover, Model A possesses very steep slopes (11°) and a high percentage of forest area (67%). The others, except Model G, possess steep slopes (6–8˚). Arable lands dominate slightly in Model B (56%), whereas they cover almost three quarters of the land in Model C. Model C contains the largest basins (16km^2) where arable lands occupy almost three quarters of basin area. Model G possesses a gentle slope gradient (3°) and it is almost completely deforested (1%).

The models are different in terms of the number of basins. Two models, D and F, are based on a small number of basins – 3 and 4, respectively. This indicates that these models vary from the others significantly. Models D and F cover a very small area (less than 4 km^2). These models are significantly different in terms of their shape. Model D is based on circular basins (shape ratio: 0.8) whereas Model F is based on the most elongated basins (shape ratio 0.5). Model D possesses the highest urban area content (19%) as well as road network density (10.8 km·km^{-2}) whereas Model F possesses the highest valley network density (6.1 km·km^{-2}) and the lowest bifurcation ratio (4.6).

Identification of Basins

The research was performed in the southern part of the Nida Basin. The region consists of three sub-regions (Fig. 2). It is rolling terrain where elevations range from 200 to 400 m. above sea level. The bedrock consists

Table 1: Models of basins prone to flash floods – descriptive characteristics.

	A [km^2]	Ck	ø [°]	VD [km·km^{-2}]	Rb	FA [%]	BA [%]	AA [%]	RD [km·km^{-2}]	ö
					Model A					
x	7.7	0.7	11	3.2	3.5	64.0	3.0	33.0	5.5	0.7
V x	69.2	18.5	26.2	16.6	20.6	32.0	67.2	58.9	34.1	14.0
min	1.0	0.4	6.0	2.3	2.2	29.0	0.4	4.7	1.5	0.5
max	19.0	1.0	17.0	4.4	5.1	93.3	9.8	65.2	9.3	0.8
					Model B					
x	6.5	0.6	8.0	3.3	5.3	39.0	5.0	56.0	4.9	0.8
V x	38.2	46.1	25.2	14.9	13.9	66.5	60.1	41.7	35.1	3.0
min	3.6	0.3	6.0	2.7	4.2	0.0	0.9	22.4	3.0	0.8
max	9.3	0.9	12.0	4.0	6.2	76.7	8.4	92.3	7.9	0.9
					Model C					
x	15.9	0.7	7.0	3.0	4.0	26.0	5.0	70.0	4.8	0.7
V x	55.0	15.8	27.2	27.7	14.3	59.4	53.4	20.7	43.6	10.6
min	4.1	0.5	3.0	2.1	3.3	0.0	0.6	45.9	1.4	0.5
max	38.7	1.0	11.0	5.8	4.9	50.0	9.4	96.2	8.7	0.9
					Model D					
x	3.1	0.8	6.0	3.8	3.6	7.0	19.0	74.0	10.8	0.6
V x	55.5	15.9	36.7	35.6	2.8	132.9	55.5	26.0	40.2	23.6
min	1.4	0.7	4.0	2.3	3.5	1.5	10.5	52.2	5.9	0.6
max	4.8	0.9	8.0	5.0	3.7	17.0	30.8	88.0	14.3	0.8
					Model E					
x	9.0	0.7	7.0	3.7	4.1	17.0	7.0	76.0	7.2	0.5
V x	53.2	13.7	19.9	15.3	10.6	55.6	51.7	13.9	16.0	12.2
min	2.7	0.5	3.0	2.7	3.4	0.5	2.7	56.6	5.6	0.4
max	18.7	0.8	9.0	4.4	4.8	37.0	16.2	92.2	10.3	0.7
					Model F					
x	4.0	0.5	7.0	6.1	4.6	33.0	5.0	62.0	6.0	0.5
V x	31.7	29.8	42.7	17.0	15.5	104.5	65.5	53.3	8.9	9.5
min	2.9	0.3	3.0	5.2	3.6	6.9	1.7	16.5	5.5	0.5
max	5.5	0.7	10.0	7.3	5.3	81.8	8.9	90.1	6.5	0.7
					Model G					
x	5.6	0.7	3.0	2.7	4.1	1.0	7.0	92.0	3.3	0.5
V x	56.5	21.2	43.0	24.8	26.3	148.1	40.7	3.6	19.4	11.7
min	2.5	0.6	1.0	1.5	2.6	0.0	3.3	87.3	2.2	0.4
max	11.3	0.9	6.0	3.5	6.0	5.0	11.0	96.7	4.1	0.6

A – area of basin, Ck – shape ratio, ψ – average slope gradient, VD – valley network density, Rb – bifurcation ratio, FA – forest areas, BA – built-up areas, AA – arable land, RD – road network density. φ – outflow ratio computed on the basis of a 1:300 000 soil map according to the method proposed by H. Czarnecka (1976), x – mean value of parameter, Vx – coefficient of variability, Source: Own data.

of Cretaceous Period marlstone, limestone, gaize, as well as Miocene Period clays and sands. Various types of Quaternary Period deposits cover more than three quarters of the region. Loess deposits, 1 to 10 m thick, cover about 60% of the region (Cabaj and Nowak, 1986). Average annual precipitation ranges form 550–650 mm whereas average annual temperature exceeds 7ºC (Paszyński and Klunge, 1986). The soil cover consists primarily of cambisoils and chernozems. The southern part of the Nida Basin is an agricultural region.

Figure 3 presents the spatial distribution of these basins. Natural basins, similar to those in Models A and B, have not been identified. Natural basins similar to those in Model C have been identified and they are the most numerous (36 basins). This model is based on the largest basins ($x_A \approx 16$ km^2), basins with steep slope gradients ($x_\psi \approx 7°$), the most forested basins ($x_{FA} = 26\%$), and basins with dense and well developed valley and road networks ($x_{VD} \approx 3$ km·km^{-1}; $x_{Rb} \approx 4$; $x_{RD} \approx 4.8$ km·km^{-1}).
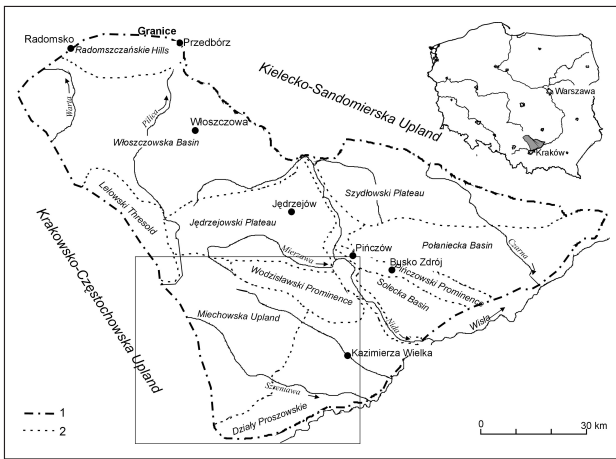
Fig. 2: The research area. 1 – Boundary of the Nida Basin region, 2 – Sub-region boundaries based on J. Flis (1956) (modified).
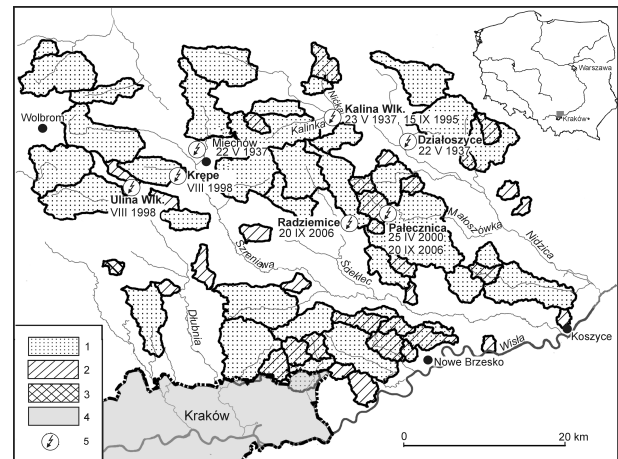
Fig. 3: Spatial distribution of small basins prone to flash floods.

1–3 – Basins resembling Models C, E, and G, 4 – Kraków city boundary, 5 – Places where downpours have caused flash floods in small basins in the past.

Model E is based on 13 basins. These basins are smaller in area ($x_A \approx 9$ km^2) with slope gradients similar to those in Model C. These basins have denser (vs. Model C) road and valley networks ($x_{VD} \approx 3.7$ km·km^{-2}; $x_{Rb} \approx 4.1$; $x_{RD} \approx 7.2$ km·km^{-2}) and they are more deforested ($x_{FA} = 17\%$). Only one basin has been identified as similar to Model G. This model is based on basins which are smallest in area ($x_A = 5.6$ km^2) with a gentle slope ($x_\psi = 3°$) and the smallest density of valley and road networks ($x_{VD} \approx 2.7$ km·km^{-2}; $x_{Rb} = 4.1$; $x_{RD} \approx 3.3$ km·km^{-2}). They are almost completely deforested ($x_{FA} = 1\%$). Eighteen basins have been identified as resembling Model E, inside of the largest basins, which were included in Model C.

Flash flood information available in the literature confirmed that the delineated natural basins had been affected by flash floods in the past (Fig. 3).

DISCUSSION

One of the methods that may limit the negative effects of local floods is successful forecasting. Currently, the prediction of flash floods is based on local weather forecasts. However, even short-term forecasting offers only superficial information that a given region may be affected by heavy rainstorms. Meteorological models which rely on real-time radar data may improve rainstorm forecasts. For instance, the results of research carried out in Switzerland indicate that it is possible to predict convective cell movement and velocity up to three hours in advance using real-time radar data. (Macklemburg *et al.*, 2000). This type of model allows for the identification of a particular zone where the probability of a rainstorm is the highest. Nevertheless, given the haphazard temporal and spatial distribution of convective precipitation, it is difficult to accurately predict the time and location where it may occur. Therefore, the prediction of local floods, apart from the local weather forecast, should take into account additional factors. Information about the spatial distribution of basins vulnerable to flash floods may be treated as such an additional factor. The agreement between the nature of scientifically delineated basins and historical flash flood information about particular basins suggests that the identification of basins resembling those in theoretical models may be a valuable tool in the process of forecasting flash floods in a region.

CONCLUSIONS

The forecasting of flash floods in small river basins is one of the most difficult aspects of operational hydrology. This is due to the fact that convective rainstorms are almost unpredictable. Formal identification of basins prone to flash floods may improve local flood prediction abilities. Information about the spatial distribution of such basins in conjunction with weather forecasts (mainly radar data) may support short-term flood forecasting as it would allow the identification of basins where flood risk is the highest. Such information may be very valuable to decision makers and rescue workers. Moreover, a knowledge of the distribution of flood-prone basins may be useful for purposes of regional spatial management. This may result in organized efforts to minimize flood damage in flood-prone river basins.

REFERENCES

Bielders C.L. and Ramelot C. (2003). Farmer perception of runoff and erosion and extent of flooding in the silt-loam belt of the Belgian Walloon Region. *Environ. Sci. Policy*, **6**: 85–93.

Bryndal T. (2006). *Natural and anthropogenic causes of small-scale flooding in Poland*. Ph.D. Dissertation, Institute of Geography, Pedagogical University in Kraków: 120 pp.

Bryndal T. (2007). Transformacja opadu w odpływ w karpackich zlewniach przy wykorzystaniu GUH. (Transformation of rainfall into runoff in Carpathian drainage basins using GUH). In: Michalczyk Z. (ed.) *Badania hydrograficzne w poznaniu środowiska (Hydrographic research in environmental science),* **8**, Obieg wody w środowisku naturalnym i przekształconym (Water circulation in natural and transformed environments). UMCS, Lublin: 117–126.

Cabaj W. and Nowak W. (1986). Rzeźba Niecki Nidziańskiej (Relief of the Nida Basin). *Studia Ośrodka Dokumentacji Fizjograficznej*, **14**: 119–208.

Czarnecka H. (1976). Próba obliczenia współczynnika odpływu „fi" przepływów maksymalnych, w małych niekontrolowanych zlewniach, na podstawie pokrywy glebowej (An attempt to calculate the outflow coefficient φ of maximum discharge in small uncontrolled basins based on soil cover). *Gospodarka Wodna*, **8–9**: 225–237.

Flis J. (1956). Szkic fizyczno-geograficzny Niecki Nidziańskiej (A physical and geographic sketch of the Nida Basin). *Czasopismo Geograficzne*, **27**(2): 123–158.

Gregory K.J. and Walling D.E. (1973). *Drainage basin form and processes*. Edward Arnold, London: 456 pp.

Hellig Z. (1968). Zastosowanie metody taksonomicznej do typologicznego podziału krajów ze względu na poziom ich rozwoju oraz zasoby i strukturę wykwalifikowanych kadr (Application of the taxonomic method to a typological classification of countries based on their development level, resources, and structure of work professionals). *Przegląd Statystyczny*, **4**: 65 pp.

Maclemburg S., Bell V.A, Moore R.J. and Joss J. (2000). Interfacing and enhanced radar echo tracking algorithm with a rainfall-runoff model for real-time flood forecasting, *Phys. Chem. Earth Pt B*, **25**(10-12): 1325–1333.

Marques de Sà J.P. (2007). *Applied statistics using SPSS, Statistica, Matlab and R*, Springer-Verlag Berlin Heidelberg: 505 pp.

Paszyński J., Kluge M. (1986). Klimat Niecki Nidziańskiej (Climate of the Nida Basin). *Studia Ośrodka Dokumentacji Fizjograficznej*, **14**: 211–238.

Ramachado Rao A. (2003). Surface water hydrology. In: Chen W.F and Richard Liew J.Y., (ed.), *The Civil Engineering Handbook*, Second Edition, CRC Press, New York: 1116–1144.

Rodriguez-Iturbe I. and Valdes J.B. (1979). The geomorphologic structure of hydrologic response. *Water Resour. Res.*, **15**: 1409–1420.

Verstraeten G. and Poesen J. (1999). The nature of small scale flooding, muddy floods and retention pond sedimentation in central Belgium. *Geomorphology*, **29**: 275–292.

FLASH FLOOD SIMULATION IN SMALL BASINS USING A TWO-DIMENSIONAL HYDRAULIC MODEL

S. Matreata, M. Birsan and R. Amaftiesei

National Institute of Hydrology and Water Management Sos. Bucuresti - Ploiesti, no.97, Bucharest, Romania

Corresponding authors: simona.matreata@hidro.ro, marius.birsan@hidro.ro

ABSTRACT

Given the growing number of high intensity precipitation events in recent years in many countries and the perspective of a further increase in the frequency of such extreme events resulting from climate change, the need for analysis and simulation of hydrological processes associated with flash floods has become a growing priority for the scientific community.

This paper describes the simulation of extreme floods in a small basin (Moneasa River Basin, area of 76.2 km^2) using a two-dimensional hydraulic model (the POTOP model) which takes into account various precipitation and roughness coefficient scenarios that correspond to levels of forestation/deforestation. This model also serves as a tool for the analysis of the efficiency of different flood control measures and actions (e.g. building internal dams). The POTOP model is a hydraulic model of flood formation and propagation, modelling non-permanent two-dimensional water movement with free surfaces via numerical integration of the Saint Vénant equation system. The model approximates the evolution of different hydraulic elements in time and space (flooded areas, water levels, depths, speeds, discharges, flood volumes, rise durations, and propagation times).

Key words: flash flood, simulation, POTOP model

INTRODUCTION

A growing number of high intensity precipitation events in recent years has induced the incidence of flash floods in small and very small basins in Romania. Such floods have generated extensive damage ranging from the loss of human life to substantial property destruction.

Flash floods have occurred in almost every region of the country, often with catastrophic consequences. The main cause of flash floods is rainfall with a torrential character, featuring very high intensity of precipitation. Precipitation which exceeds 25 millimetres per hour can induce flash floods in basins with surface areas smaller than 200 km^2.

Another factor that accommodates the occurrence of flash floods is the nature of the terrain itself with a low degree of permeability which is especially common in urban areas.The severity of flash floods increases in cases where slopes are seriously deforested, agricultural areas are ploughed along slopes, and in situations where basins with normally rough terrain had been transformed by large scale urbanization.

BASINS AND DATA

The Moneasa River Basin, up to the town of Ranusa, is located in the Codru Moma mountain region and stretches towards the south. Although this mountain range is quite low, the maximum altitude being only 1098 m (Mount Izoi), basin slopes are very steep: 40-50% (Fig. 1).
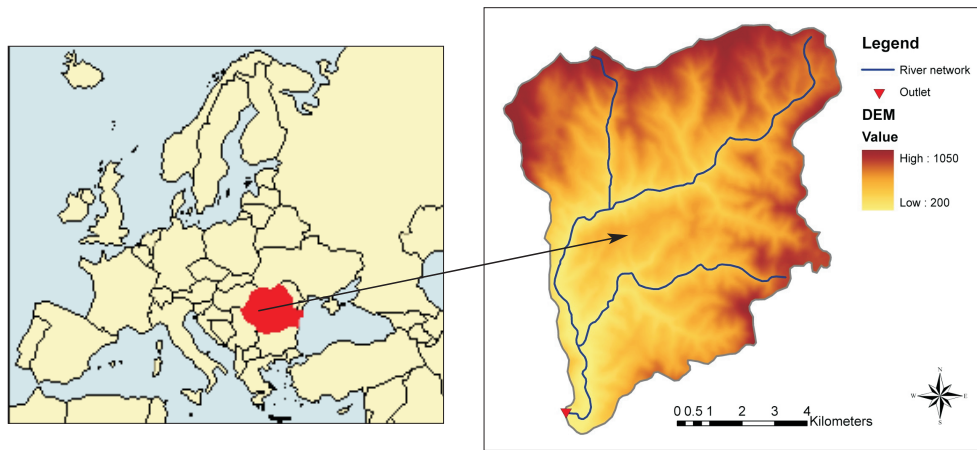
Fig. 1:   The Moneasa Basin.

The Moneasa Basin is characterized by a large forestation coefficient with the majority of its sub-basins being covered by deciduous forests – beech trees prevail in the North (70–80%) while durmast trees prevail in the South (50–60%).

Two types of soil prevail in the basin area (weighted average): poorly podsoled brown forest soil and brown yellow forest soil.

From a geological point of view, the basin area is characterized by Neocene, Mesozoic, and Permian rocks. There are also rocks that are considered permeable because of existing splits (lime, limestone) and rocks that are considered impermeable (andesite, rhyolite, clay shale).

The basin's large opening towards the southwest allows for the penetration of air masses rich in water content. As a consequence, the quantity of water available from atmospheric precipitation is very large (mean multi-year precipitation = 950 millimetres). The lowest mean multi-year temperature in January ranges from -2 to -30 ^{0}C while the highest mean multi-year temperature is 16–18 ^{0}C in the month of June.

There are 7 functioning hydrometric stations in the Moneasa Basin which monitor 6 sub-basins with areas ranging from 5.50 to 49 km^2 as well as the basin outlet with a total area of 76.2 km^2. The main characteristics of the Moneasa Basin are available in Table 1.

Table 1: Fundamental basin data: area (F), mean altitude (H), river length (L), mean basin slope (Ib), mean annual discharge (Q_{med}), maximum recorded discharge, (Q_{max}), and minimum discharge with an 80% ($Q_{min\,80\%}$) probability of exceedance.

River	Hydrometric station	F [km^2]	H [m]	L [m]	Ib [%]	Q_{med} [m$^3 \cdot$s^{-1}]	Q_{max} [m$^3 \cdot$s^{-1}]	$Q_{min\,80\%}$ [m$^3 \cdot$s^{-1}]
Moneasa	Boroaia	14.3	661	4.5	35.6	0.250	13.6	0.017
Valea Rujii	Ruja	6.60	660	4.0	40.6	0.128	6.24	0.012
Valea Lunga	Pastravarie	5.50	578	4.0	43.9	0.079	6.05	0.013
Meghes	Sonda	10.0	547	3.5	37.2	0.085	10.9	0.010
Moneasa	Moneasa	49.4	608	9.4	40.8	0.946	50.2	0.172
Fanuri	Ranusa	19.5	475	6.0	34.7	0.262	20.8	0.0364
Moneasa	Ranusa	76.2	586	14.2	38.1	1.27	73.0	0.236

POTOP MODEL

A hydraulic model of flood formation and propagation in two-dimensional space (with or without initial runoff) called POTOP was used to simulate flash floods within the Moneasa Basin. (Amaftiesei, R., 2006, 2007). The model approximates the evolution of different hydraulic elements in time and space (flooded areas, water levels, depths, speeds, discharges, flood volumes, rise durations, and propagation times) based on different rain-producing configuration scenarios and selected limitations.

For the GRID-type ASCII obtained with GIS terrain support (in this case the SRTM DTM with 90 m resolution have been used, after the interpolation at 30 m), the model uses a level-discharge curve (a rating curve) in sections contracted naturally or by works (limit conditions) using rain-producing scenarios based on regional historical records.

The program models non-permanent two-dimensional water movement with free surfaces via numerical integration of the Saint Vénant equation system formed by the continuity equation and the simplified movement equations – keeping only the friction term – placed on the map in the OX and OY directions. The numerical integration is performed using an implicit scheme – by linearization and the application of the double deflection method onto the map, alternating between network lines and columns.

Representative results produced by the model consist of maps which contain the network scheme and the terrain topography. Furthermore, the following values are produced for every time interval of a flood: free water surface levels, instantaneous or maximum recorded depths, water speeds, precipitation variability graphics, depth hydrographs, free water surface levels within any network knot, discharge hydrographs for any section of interest or within a single knot associated with a rating curve or a discharge hydrograph.

RESULTS AND DISCUSSION

The first simulation was performed as a general validation check for the model using model roughness parameters corresponding to present runoff formation conditions within the basin with a mean roughness coefficient of 0.1 (well-forested basin) and 1-hour rainfall (100-year return period) set at around 120 mm.

The runoff coefficient (α) was estimated using existing relationships for the runoff coefficient (Mita P. 1986, 2003) as a function of the rainfall amount (hc) and the 10-day antecedent precipitation index (API_{10}) for the Moneasa Basin (Fig. 2). The simulation used a runoff coefficient of 0.55, corresponding to an API of 60 mm.

For the purpose of model validation, simulation results were compared to maximum discharges with 100-year return periods computed using common statistical methods of maximum discharge estimation in small basins. This analysis was performed for the basin outlet – at the town of Ranusa on the Moneasa River – and for another three areas within the basin (Boroaia and Moneasa on the Moneasa River and Ranusa on the Fanuri River).
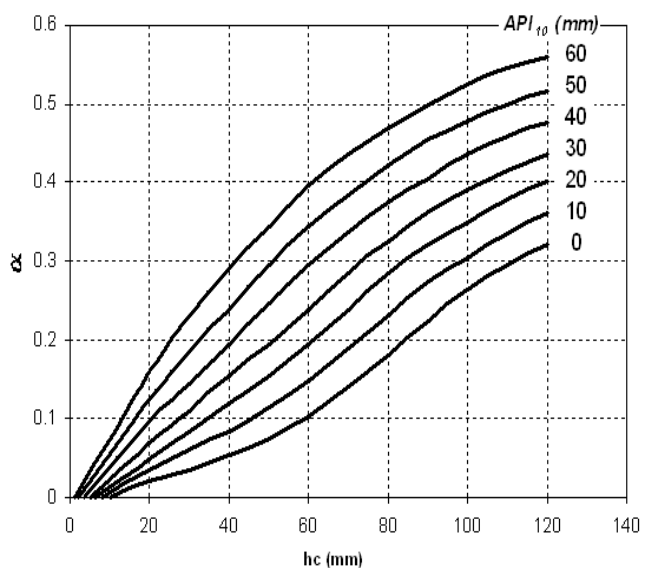
Fig. 2:   The runoff coefficient relationship $\alpha = f(hc, API_{10})$ for the Moneasa Basin

As seen in Table 2, the simulated maximum discharge values produced by the POTOP model are very close to those within the corresponding 100-year return period computed using statistical methods for all four river sections.

Table 2: Maximum discharges with 100-year return periods computed using standard statistical methods and POTOP simulations for the main four hydrometric stations within the Moneasa Basin.

River	Hydrometric station	F [km^2]	H [m]	$Q_{max\ 1\%}$ statistical method [m^3·s^{-1}]	$Q_{max\ 1\%}$ model simulation [m^3·s^{-1}]
Moneasa	Boroaia	14.3	661	60.0	68.0
Moneasa	Moneasa	49.4	608	120.0	115.0
Fanuri	Ranusa	19.5	475	76.0	72.0
Moneasa	Ranusa	76.2	586	145.0	155.0

The second series of simulations was performed using the same amount of rainfall (100 mm) but using different values of the mean roughness coefficient (0.07 and 0.05) and applying different degrees of deforestation compared to the present situation (0.1) in order to estimate the influence of land use and land cover changes on peak discharges at the outlet of the Moneasa Basin.
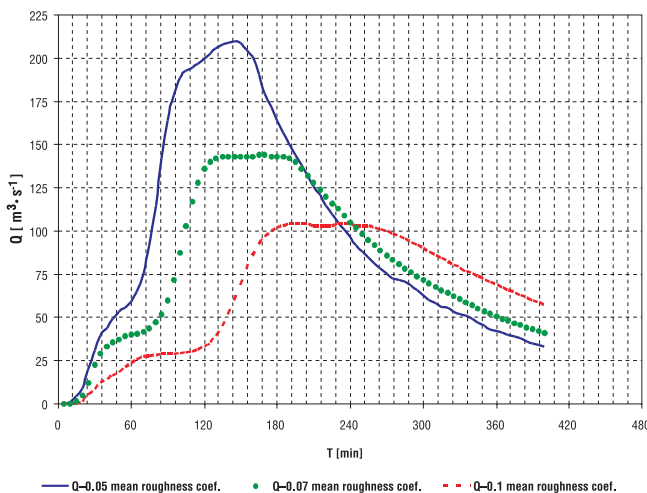
Fig. 3:   Simulated hydrographs for different mean roughness coefficients

The simulation results indicate that there is a significant increase in maximum discharge. A value of 104 m^3·s^{-1} is obtained for a mean roughness coefficient of 0.1 (Q – 0.1) under present conditions. A value of 145.7 m^3·s^{-1} is obtained for a mean roughness coefficient of 0.07 (Q – 0.07). Finally, a value of 209 m^3·s^{-1} is obtained for a mean roughness coefficient of 0.05 (Q – 0.05) – see Fig. 3.

The simulation results also show the influence of deforestation on the duration of the rising limb and on total flood duration. This indicates a significant decrease in the values of such flood characteristics with an increase in the degree of deforestation.

The last series of simulations were performed for the purpose of analysing the influence of the building of internal dams on peak discharge values. As seen in Figure 4, the model simulates a significant effect of peak flood discharge attenuation, in this case, 28% attenuation based on a 0.05 mean roughness coefficient (a), as well as 22% attenuation based on a 0.07 mean roughness coefficient (b), as a result of the influence of the building of one internal dam within the basin.
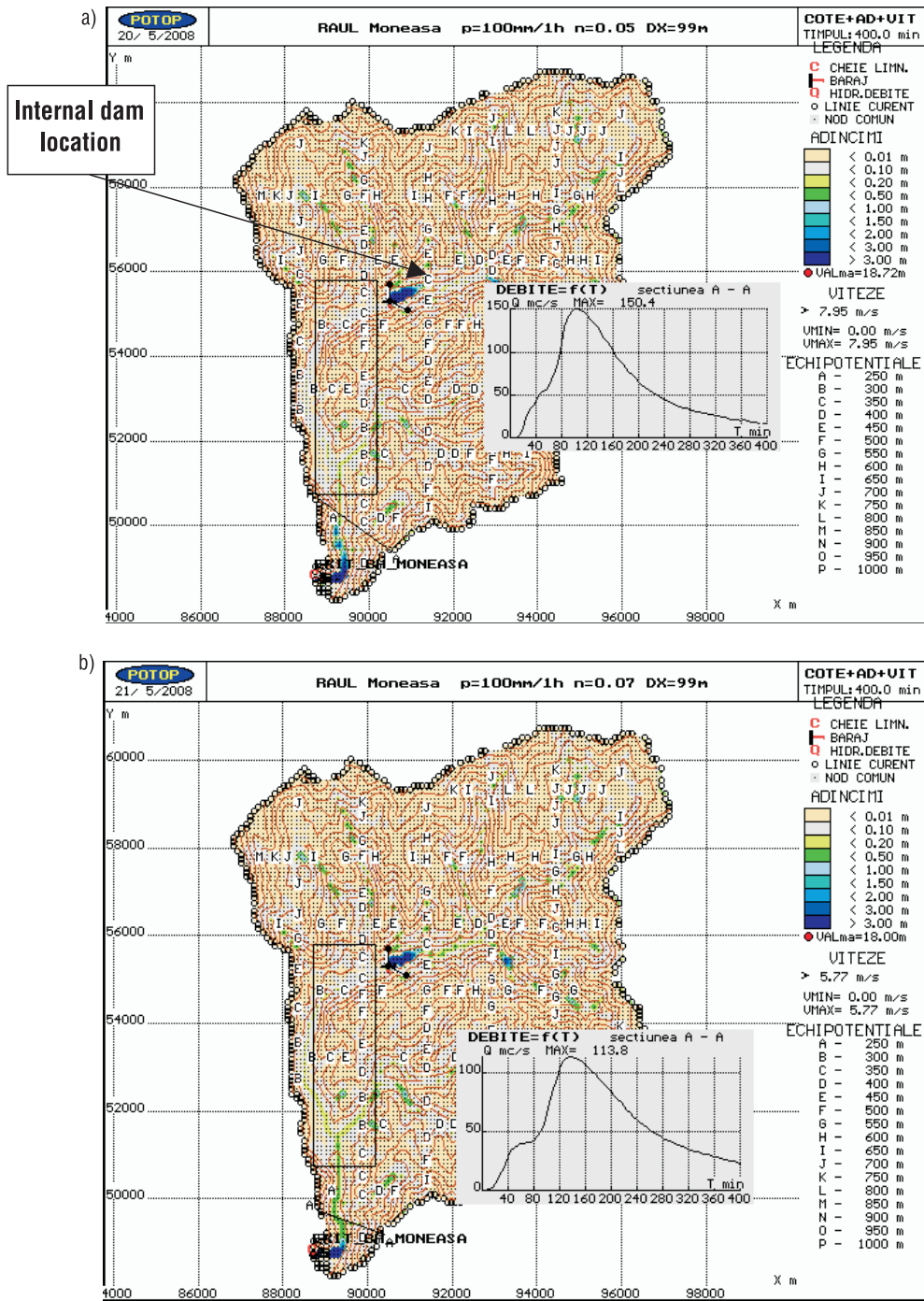
Fig. 4: Simulation results for a 100 mm and 1-hour rainfall scenario with 0.05 (a) and 0.07 (b) as the values of the mean roughness coefficient, illustrating the influence of the building of internal dams for the purpose of flood attenuation.

CONCLUSIONS

Considering the fact that the model configuration was produced based on a limited amount of topographic data, all the simulation results should be regarded as general and preliminary.

Despite the preliminary nature of the results, they do show the potential of using a two-dimension hydraulic modelling approach for the simulation of flash flood formation in small basins. This approach is especially useful for the purpose of assessing the influence of land use and land cover changes on flood characteristics (peak discharge, time to peak, and total time) at any location within a river network or within a basin.

This model can be used for the purpose of the identification of the most vulnerable and critical areas within a basin. The various simulation results produced by this model (flooded areas, water levels, depths, speeds, discharges, flood volumes, time increases, and propagation times) can be used to assess the efficiency of different flood control measures and actions.

Future research will consist of using more detailed GIS data for the model configuration. Different spatial rainfall distribution scenarios within the basin will be generated in order to analyze the effects of rainfall distribution on peak discharge and to further investigate methods designed to assess flood risk in the most vulnerable of areas.

REFERENCES

Amaftiesei R., Chelcea S. and Dinu R. (2006). *Arbore Hazard Map – POTOP Model Application*, "Hydrological Hazards" International Conference, Bucuresti, Romania, 6–8 November 2006.

Amaftiesei R. (2007). *Potop Model User Manual*, Bucuresti.

Mita P. and Matreata S. (2003). *Runoff coefficient relationships for different physiographic factors*, National Institute of Geography, Annual Meeting, Bucuresti.

Mita P. and Muscanu M. (1986). Runoff coefficient relationships in small basins. *Hydrological Studies*, I.M.H., LIII, Bucuresti.

TOWARDS OBJECTIVE DESIGN OF DRY DAMS AT WATERSHED SCALE: HOW TO TAKE INTO ACCOUNT THE SPATIAL STRUCTURE OF THE RAINFALL AND ITS VARIABILITY

C. Poulard, E. Leblois, D. Narbais and S. Chennu

Cemagref, UR HHLY, 3 bis quai Chauveau - CP 220, F-69336 Lyon, France
Corresponding author: Christine Poulard, christine.poulard@cemagref.fr

ABSTRACT

This exploratory study is a contribution to the development of an objective method to design flood mitigation structures distributed over the catchment. Its main issue is to analyse the influence of the input (rainfall scenarios), on the choice of a technical solution (here, the best location for 1 or 3 dry dams). To take into account the spatial variability of the rainfall, we used a simulator of stochastic distributed rainfall fields. A very simple rainfall-runoff model was then implemented on a test case, a 150 km² catchment near Lyon. It was divided into only 63 computation units, following subcatchments delineation. A dry dam can be placed at the outlet of any unit. Such a simple model has short computation times, allowing to run numerous tests and optimization procedures. This study illustrates frequent flaws in operational studies, such as the subjectivity of the definition of an indicator, the ignorance of the exact pattern of the rainfall and of rainfall variability. The main results are summed up in this paper through six didactic remarks. Important issues arising from this study are (i) how to include extreme events in the set of input scenarios, and (ii) how to define efficiency indicators - relying on hydrological variables alone is clearly insufficient. The efficiency indicator should be based on economic terms ; our suggestion is to use a cost-benefit approach. Indeed, it implies annualizing the cost of damages, and so the estimated damages for each flood event are weighted by the range of frequency it represents, and thus the problem of the weight of extreme events is at least partly solved.

Keywords: dry dams, flood mitigation, flood regime, stochastic distributed rainfall fields

INTRODUCTION

Structural measures for flood mitigation must be designed at the right spatial scale, to avoid transferring the problems from one area to another. In this light, upstream retention by dry dams has many advantages compared to river training or levees; moreover, they do not hinder the river natural dynamics. Besides, mitigation structures should be designed in a coordinated manner, to assess the overall effect. The aim of this study is to test a methodology to design dams distributed over the catchment. The effect must be quantified through a comparison of the consequences with and without mitigation structures over the whole flood regime. The main difficulty is to define the input at catchment scale. We chose a rainfall-runoff approach, using stochastic distributed rainfall fields fed into a simple rainfall-runoff model developed for the study, called MHYSTER. As computation time is very short, numerous sensitivity analyses can be easily carried out to study and improve assessment methodologies. The tests highlighted significant differences in calculated hydrographs when using distributed fields or homogenous fields obtained by spatial averaging. The second question addressed is how to define a set of distributed rainfall events representative of the flood regime, knowing that the return period of flood generated by a distributed rainfall event varies in space. We also discussed the definition of a quantified efficiency indicator, necessary to compare several sets of dams.

MODELS: FROM RAINFALL FIELDS TO HYDROGRAPHS

With retention structures dispersed throughout the catchment, input scenarios have to be built at catchment scale. One approach is to define hydrographs at each upstream node and lateral inputs. We chose the other

approach, *i.e.* to feed rainfall fields, obtained from a spatially distributed rainfall field generator, into a distributed hydrologic model. Our rainfall generator is based on the turning bands method, according to the perspective presented in Ramos *et al.* (2006). Our test case is a 150 km² catchment near Lyons. First, the temporal and spatial characteristics of the rainfall regime over the catchment were estimated using data from 5 raingauges (Chennu *et al.,* 2008). The model then generated 9000 72h-events of 3h time-step on a grid of 500mx500m (Fig. 1), assumed to represent 9 major events per year over 1000 years. The observed data used to calibrate the generator integrate various rainfall forms, but none of the observed events has an estimated return period over 100-year. The relevance of the simulated extreme events thus obtained is disputable, since climatic conditions leading to extreme events can be very different from the observed ones. This point is open for further studies.

a) Map of the rainfall on the catchment for event #1 (500m x 500m grid) and main river network

b) Map of resulting peak flood Qmax (without dams) compared to the local flood quantiles on each element
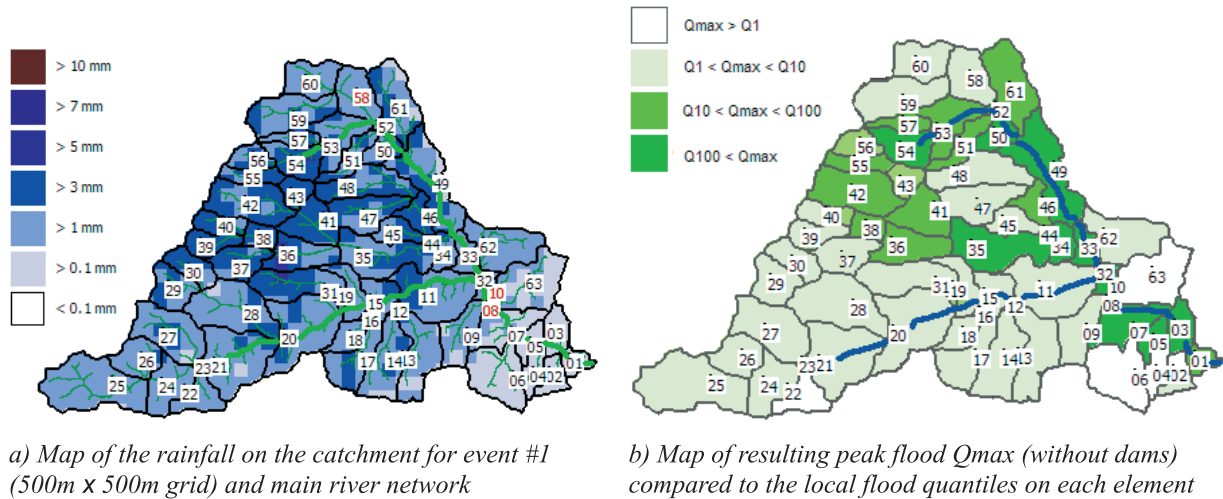
Fig.1:   Representations of input and output of the MHYSTER model for distributed rainfall event no. 1.

A physically-based chain of models was already implemented on this catchment and calibrated against observed events (Chennu *et al,.* 2008). It is composed of MARINE, an event-based distributed rainfall-runoff model simulating infiltration with the Green-Ampt model (Estupina–Borrell, 2004) and MAGE, a 1-D hydraulic model based on St-Venant equations (Giraud, 1997). We wanted a simpler, easy-to-use distributed model on the same test-case to allow quicker exploratory computations and carry out numerous sensitivity analyses. We therefore developed MHYSTER to meet the minimum requirements to reproduce hydrographs all over the watershed. The computation units are 63 subcatchments elements (Fig. 1 and Fig. 2). Hydrographs are computed by adding upstream contributions to local rainfall; Fig. 3 presents the algorithm. The main module in MHYSTER, Module 1 (Fig. 3), computes hydrographs at each element's outlet (Fig. 4). Outflow from

Local production is computed for each element for the current time-step: rainfall volume over the area of the element, multiplied by a runoff coefficient.
For upstream elements, outflow is equal to this volume divided by the time step (if there is no dry dam at this element)

Outflow from an element is added to the water balance of the element downstream within the same time-step.
Outflow from one element may be modified by the presence of a dry dam at the outlet of this element.

Fig. 2:   Principle of discharge computation along the drainage system (subcatchment down to element no. 20).

a) User's main choices   b) Algorithm – modules 1 and 2
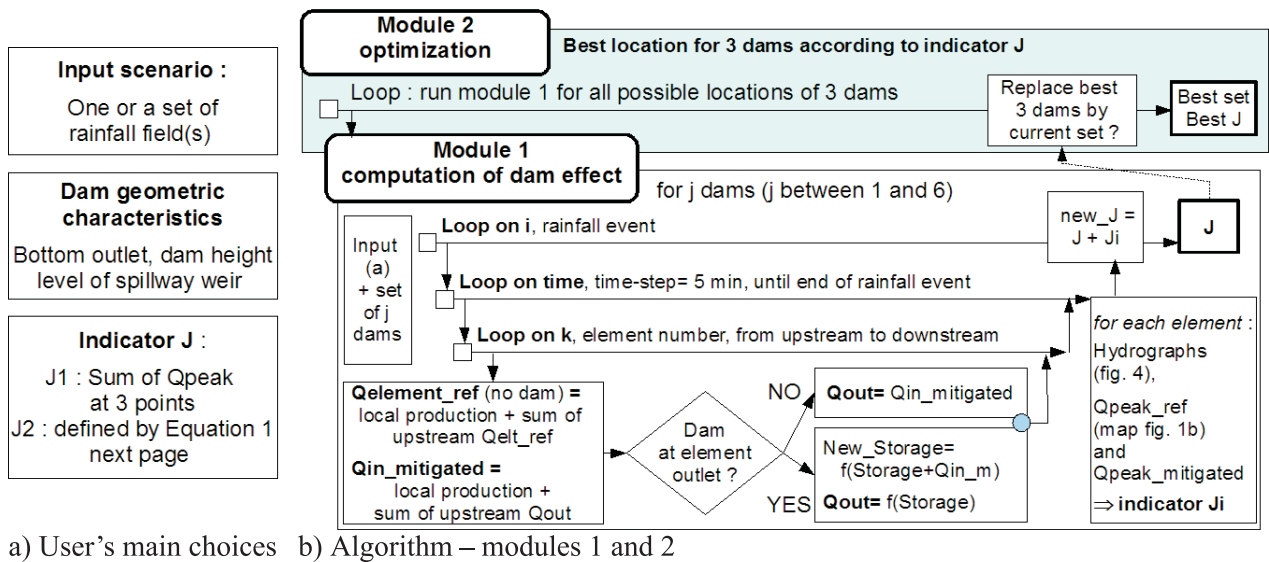
Fig. 3:   Structure of MHYSTER.

a) distributed event #1   averaged in space (#1h)   c) distributed event   averaged in space (#1h)
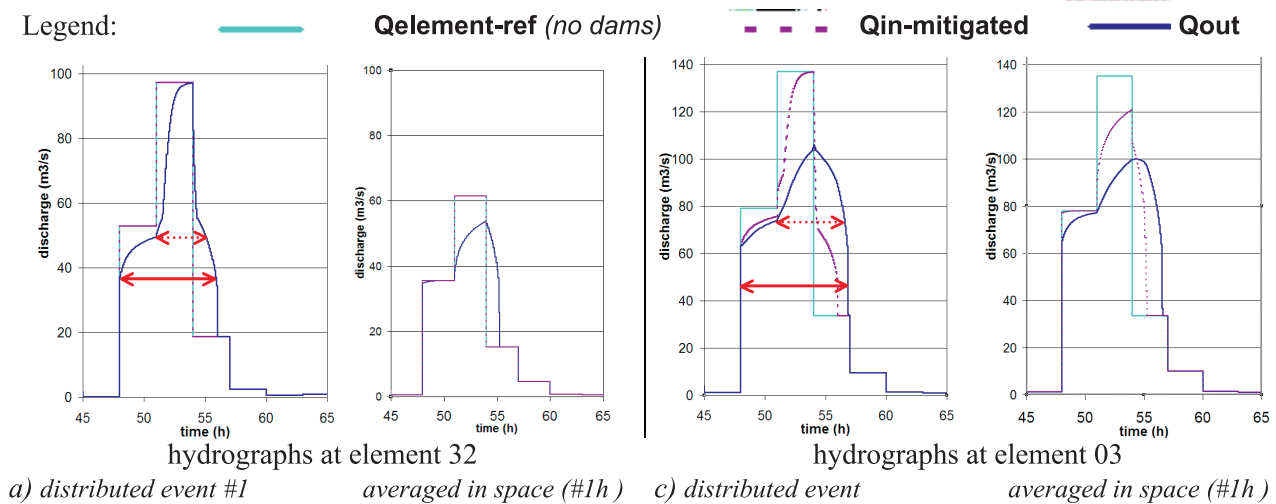
Fig. 4:   Peak of hydrographs computed by Module 1 for rainfall event no. 1, with dams at outlets of elements 32, 11 and 03. *Arrow: duration of mitigation by the element's dam; dotted arrow: overflow.*

one element is immediately transferred to the element downstream within the same time-step. Because there is no routing delay, the reference hydrographs without any dam-denoted **Qelement_ref** in Fig. 4 – follow the rainfall 3h-pattern. Although possible dam locations are generally limited in real catchments, we allowed dams to be placed at the outlet of any of the 63 elements, in order to investigate thoroughly the effect of spatial rainfall distribution in this study. Hydrograph **Qin_mitigated** is computed using inflow already mitigated by upstream dams. If there is a dam at the outlet of the element, the outflow from element, denoted **Qout**, is further mitigated by this dam. Water stage behind the dam is obtained from the volume budget, assuming a simplified topography ; outflow is then deduced from the water stage, using the same standard formula as in MAGE. Cumulative rainfall maps and peak floods maps are also produced (Fig. 1). Module 1 also calculates a mitigation efficiency indicator J, that can be used in an optimization procedure, Module 2, to find the best set of three dams for a given set of rainfall scenarios.

The simplicity of the rainfall-runoff model also serves didactic purposes. In operational studies, many efforts are generally made to fine-tune hydraulic models, while far less attention is given to the input. Very often, only one or two input scenarios are defined and tested ; flood reduction is optimised for these one or two events. The objective should be rather to obtain the best behaviour on average, with respect to flood probability. So, we explicitly shift the focus towards the definition of input scenarios. Wrong assumptions and choices in the model input lead to flawed conclusion – even if the hydraulic model is excellent.

RATIONALE TO TEST A SET OF DAMS AND QUANTIFY THEIR EFFICIENCY

Fig. 3a presents the three main choices the user has to make. The most important one is probably **to define the efficiency indicator**(s), denoted J, used to quantify the effect in order to compare solutions (Module 1), and necessary in optimization procedures (Module 2). In a real study, J should take into account the reduction of damages given by the dams, and also the costs of the dams. MHYSTER uses only one hydrological variable, the discharge ; it can estimate neither flood spatial extent nor water depths. So, a simplified benefit function J was proposed for this study. We assumed that reduction of damages in an element k is proportional to ΔQ_k, peak discharge decrease above an overflow threshold, and to element reach length l_k. All the weight coefficient w_i were left equal to 1 in this study. A cost coefficient c_k accounts for the land uses. The benefit function J is the average of the benefits of the N rainfall event:

$$J = \frac{1}{N} \sum_{i=1}^{N} \mathrm{W}i \sum_{k=1}^{63} f(\Delta Q_k; l_k) c_k$$

Eq. 1

This definition suffices for this exploratory stage, but not for operational use. Moreover, damages are not necessarily proportional to flooded areas; submersion durations are also important. Futures versions should include damage evaluation tables, and account for building and maintenance costs. Besides, using the bowl area for water storage has a significant cost, whether through land purchase or indemnifying procedures.

Then**, dam outlets and height** must be defined. To limit the number of parameters, we define dam characteristics with respect to the local estimated 10- and 100-year return period floods at the element outlets, with the same ratio for all dams. The 10- and 100-year quantiles were derived from flood peak quantiles calculated at one gauging station, assuming a proportionality with the catchment area to a power 0.8 (Myers formula).

Finally, the user must choose the input ; he can work with **one or a set of rainfall event**(s). The methodology is to be implemented afterwards with accurate models, with long processing time, which will not be able to handle all 9000 produced by the stochastic generator. So, we tested procedures to extract automatically events sub-sets, in two stages (Chopart *et al.*, 2007):
   • selecting the maximum rainfall events at 9 locations and for 6 durations (from 3 to 72h) ;
   • reducing the sample size while keeping a fair intra-sample variability (almost uniform marginal distribution on all variables). The sub-set size was fixed at 30.

Two different sampling methods were applied twice: first on the set of 9000 events, representing 1000 years of data, and then on a subset representing 100 years of data. So, 4 sub-sets of 30 events were formed.

RESULTS AND DISCUSSION

The indicator defined by Eq. 1 was used to compare solutions and to carry out optimization procedures. This study allowed to test the sensitivity of the results to explicit or implicit choices made during the procedure. Some of the results only confirm what was logically expected, but are anyway presented and commented for didactic purposes, to point out flaws existing in too many operational studies (authors' experience).

a) Influence of the definition of the indicator

The influence of different damage coefficients was tested (Table 1), as well as other definitions for benefit function J (not shown here). Results are summarised in **Remark 1**: "Definition of the indicator strongly impacts the results of comparisons between dam locations."

Table 1: Results of the optimisation procedure for 6 input scenarios:
best set of 3 dams and indicator value (Eq1)
(indications 'Upstream' and 'South' refer to location of the area of maximum rainfall in the scenario).

Input scenario =		All damage coefficient $c_k = 1$		Different damage coefficient c_k	
		Best set of 3 dams	Indicator value	Best set of 3 dams	Indicator value
one single event	no. 1 (*see* Fig. 1)	**8 ; 10** ; 58	0.88	**10** ; 32 ; 33	87.42
	no. 2 (Upstream)	**8 ; 10** ; 33	0.40	**8 ; 10** ; 33	39.34
	no. 3 (South)	11 ; 14 ; 29	0.11	11 ; 15 ; 31	7.33
	no. 3h (no. 3 averaged in space)	7 ; **8 ; 10**	0.05	7 ; **8 ; 10**	5.29
set of 30 events	Set "Class 100"	32 ; 33 ; 34	0.10	32 ; 33 ; 58	9.38
	Set "Class 1000"	7 ; **8 ; 10**	0.24	7 ; **8 ; 10**	24.35

Numerical values of the indicator should be interpreted carefully. Smaller values mean smaller mitigation and/or a smaller flood. So, comparisons are relevant only for a given set of events or for a given set of dams. Moreover, the global indicator may hide local peculiarities: the peak flood may locally increase if contributions are made concomitant. Mapping elementary indicators could be useful to identify these effects.

b) Influence of the pattern and choice of the (set of) rainfall scenario(s)

Major differences appear between the hydrographs obtained for a rainfall scenario and the same averaged in space for each time-step (Fig. 4). The hydrographs obtained from distributed and averaged events are even more different with the "MARINE+MAGE" chain, where infiltration is taken into account (Chennu *et al.*, 2008). Consequently, the difference in hydrographs has a strong impact on dam efficiency (example of event no. 1, Fig. 4). Differences are more acute in the upstream part and decrease in the downstream part. An example of optimization is shown for event no. 3: resulting dam locations are in the south part of the catchment, where the rainfall intensity is maximum (Table 1). Optimum indicator value is 0.11. For the same event averaged in space, event no. 3h, spatial contrast is obliterated and optimization favours dams in the downstream part, with an indicator of only 0.05. So, **Remark 2** is issued as follows: "Ignorance of the exact spatial pattern of the rainfall leads to errors in the hydrographs and in mitigation assessment".

Table 1 illustrates that each choice of set or sub-set of events leads to a different optimum solution, although some locations are selected more often that others in these cases (elements 8 and 10, in the lower part of the catchment). Optimization generally selects dams in the area of the most intense precipitations. Table 2 displays some cross-comparisons of rainfall scenarios and set of dams. The optimum solution obtained for each scenario selected in Table 1 was tested for the other events or sets of events, and showed contrasted efficiency. Hence **Remark 3**: "The optimum choice of dams for a rainfall scenario might give very poor results for other events". The results with sets of rainfall events lead to remarks 4 and 5.

Remark 4: "Solutions obtained for a set of events yield smaller values of the indicator. This value is an average, since the dams have a significant effect on some events and a much reduced one on other events".

Table2: Cross-comparison of indicator values with respect to input and set of dams (all c_k=1) – in bold: optimum set of dams for this (set of) event(s) according to current indicator.

Set of 3 dams Rainfall (set of) event(s)	**8; 10**; 58	**8; 10**; 33	11; 14; 29	7; **8; 10**	32; 33; 34
#1 (Fig. 1)	**0.88**	0.85	0.003	0.858	0.150
#2 (Upstream)	0.28	**0.40**	0.06	0.32	0.32
#3 (South)	0.002	0.002	**0.11**	0.01	0.000
#3h (#3 averaged in space)	0.027	0.027	0.000	**0.05**	0.000
Set "Class 100"	0.04	0.06	0.015	0.04	**0.10**
Set "Class 1000"	0.19	0.24	0.04	**0.24**	0.12

c) Weight and representativity of extreme events

Remark 5: "The sub-set used to find the best solutions must be representative of the rainfall hazard regime". Tests showed that this important requirement is not met in our tests, because of the reduced number of events in the set. Table 2 illustrates the variability of the indicator value depending on the set of events considered. Our present approach, with one or two extreme events in a set of 30 events and with all the weight coefficients equal to 1, is not satisfactory. Extreme events, such as existing in set "Class1000", are too specific: events can be very strong on part of the catchment and rather moderate elsewhere. These individual peculiarities strongly impact the result. And yet, extreme events must be taken into account because they might account significantly in the damages.

This study highlights the danger to carry out an optimisation procedure based on flawed hypotheses and raises two key issues: how to define an objective and relevant benefit function J, and how to build a representative set of rainfall events.

CONCLUSION AND PERSPECTIVES

Dry dams are effective structures (*e.g.* Poulard *et al*., 2005), but designing a set of several dams to maximize their combined efficiency is a difficult task because it implies building rainfall scenarios at catchment scale. This study shows how a stochastic rainfall simulator can be efficiently used, and emphasizes the importance of taking into account the variability and spatial properties of rainfall. In its present state, MHYSTER is a very simple model, and yet it can carry out informative sensitivity analyses and investigate some recurrent flaws observed in operational studies. Our results clearly illustrates the main flaws, and MHYSTER could be used as a didactic tool: students could test the consequences of their choices or constraints on the final result.

This study also raised interesting questions, and in particular how to take into account extreme events. A promising solution is to define the cost function J according to a complete cost-benefit approach. This implies to estimate damages annualized values, once without and once with the dams. In this approach, extreme events are weighted by the range of frequency they represent. This partly solves the problem of assigning reasonable weights to extreme events. However, a given rainfall event has no intrinsic frequency at catchment scale; the estimated frequency of the resulting flood varies over the catchment (Fig. 1b). We therefore propose to estimate the annualized damages separately on each element. The overall benefits for a set of dams would be the sum of the annualized benefits of each element. Of course, the cost of dams construction and of maintenance should also be included into the cost function *J*, after being also annualized.

Remark 6: "*For an objective efficiency assessment, the indicator must account for both cost and benefits integrated over the regime, using a cost-benefit analysis*". This implies that the set of events include enough diversity to estimate a comprehensive benefit/frequency rate on each element (*see* Remark 5).

This study leads the way towards the development of an objective assessment method, to be used afterwards with state-of-the-art models, such as the MARINE+MAGE chain of models. One very strong assumption is the ability of the rainfall fields simulator to yield sets of events representative of the rainfall hazard regime, including extreme events. Further research is needed to improve extreme events simulation, which is a necessary condition to consolidate this approach.

REFERENCES

Chennu S., Grésillon J.-M., Faure J.-B., Leblois E., Poulard C. and Dartus D. (2008). Flood mitigation strategies at watershed scale through dispersed structural measures, 4th International Symposium on Flood Defence: *Managing Flood Risk, Reliability and Vulnerability*; Toronto, Canada, May 6–8, 2008.

Chopart S., Leblois E. and El Kadi K. (2007). *Selecting representative rain events considering a given structured basin,* EGU General Assembly, Vienna, Austria (poster).

Estupina–Borrell, V. (2004). *Towards a hydrological model suitable for operational flash flood forecasting – Application to Southern France small catchments* (in French), INPT Ph-D Thesis, Toulouse.

Giraud F., Faure J.-B., Zimmer D., Lefeuvre J.-C., Skaggs R. W. (1997). Hydrological modelling of a complex wetland (in French), *J. Irrig.*, **123**(5): 1531–1540.

Poulard C., Szczesny J., Witkowska H. and Radzicki K. (2005). Dynamic Slowdown: A flood mitigation strategy complying with the Integrated Management concept - Implementation in a small mountainous catchment, *Int. J. River Basin Manage.*, **3**(2): 75–85.

Ramos M.-H., Leblois E., Creutin J.-D. (2006). From point to areal rainfall: linking the different approaches for the frequency characterisation of rainfalls in urban areas. *Water Sci. Technol.*, **54**(6–7): 33–40.

HYDROLOGICAL RESPONSE OF A SMALL CATCHMENT EXAMINED BY ISOTOPIC AND MODELLING TOOLS

M. Šanda[1], A. Kulasová[2] and M. Císlerová[1]

[1] *Czech Technical University, Faculty of Civil Engineering, Prague*

[2] *Institute of Hydrodynamics, Czech Academy of Sciences, Public Research Institution, Prague*

Corresponding author: Martin Sanda, email: martin.sanda@fsv.cvut.cz

ABSTRACT

Stream-aquifer interactions, hydrological responses, and groundwater fluxes were examined in the small mountainous headwater catchment of Uhlířská in the Jizera Mountains (Czech Republic). The bedrock is composed of Paleozoic crystalline rocks overlaid by highly permeable shallow cambisols as well as of thick saturated glacial deposits in the valley, overlaid by histosols. These properties allow for rapid interaction between the vadose zone and the granitic bedrock via preferential subsurface flowpaths. As a result of instant water pressure transformation throughout these structures, outflow caused by storms is regularly of a quick response and high magnitude, although surface runoff occurs very rarely. Standard climatic and surface runoff monitoring is supplemented by measurements of soil moisture, soil pore water suction, subsurface hillslope stormflow in the vadose zone, and water table fluctuation in the saturated subsurface, and accompanied by water sampling for analysis of isotopes ^{18}O, ^{2}H and ^{3}H. Seasonal fluctuations of ^{18}O in precipitation and stream outflows are approximated by sine waves and by a lumped parameter residence time distribution approach in order to evaluate the mean residence time of water in the catchment.

A numerical groundwater model combines hydrological and geological information to specify the travel time of water in the deep subsurface. The mean water residence times obtained for this catchment ranged from five months to about a decade. It was concluded that a significant transformation effect takes place in the subsurface zone, supporting the initially hypothesized key role of rapid groundwater recharge through permeable soils and storage within the glacial valley sediments.

Keywords: catchment response, isotopes, geochemical tracers, monitoring, modelling

STUDY AREA AND EXPERIMENTAL SETUP

The Uhlířská catchment is situated in a humid temperate mountainous region of the Jizera Mountains (northern Czech Republic) in the headwater area of the Nisa and Labe rivers. It has a surface area of 1.78 km^2 and covers an altitude range between 777 and 895 m a.s.l. The bedrock is composed of Paleozoic crystalline rocks overlaid by highly permeable shallow cambisols as well as of thick saturated glacial deposits in the valley, overlaid by histosols. These properties allow for rapid interaction between the vadose zone and the granitic bedrock via preferential subsurface flowpaths. As a result of instant water pressure transformation throughout these structures, outflow caused by storms is regularly of a quick response and high magnitude, although surface runoff occurs very rarely. Analysis for the ^{18}O isotope was performed for the following water types and at the following sites in the catchment (Šanda *et. al*, 2007b): precipitation, snowmelt, snowcover, subsurface stormflow, groundwater, soil water from soil suction cups, and stream outflow at two gauging stations (Fig. 1). Water
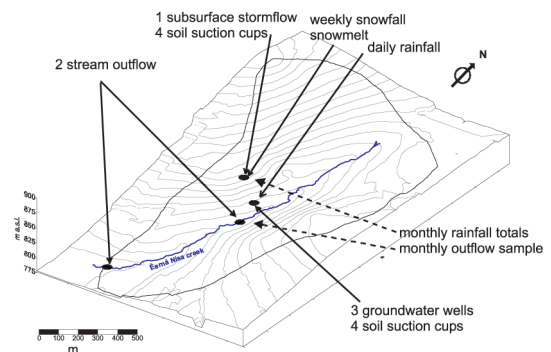

Fig. 1: Water sampling locations in the studied catchment of Uhlířská, Černá Nisa Creek.

29

samples for [18]O analysis were obtained daily in the form of rainfall, weekly in the form of snowfall, weekly in the form of snowcover, every 6 hours (episode-based) in the form of soil subsurface stormflow, daily (event-based) in the form of snowmelt, daily or episodically every 6 hours in the form of streamflow at two gauging profiles, monthly in the form of soil pore water (4 locations, 2 horizons), and monthly in the form of shallow groundwater (4 locations). The [18]O concentration analysis of these samples was performed at the Czech Geological Survey in Prague using a Finnigan Mat 250 mass spectrometer. Some of the samples were authenticated using a Liquid Isotope Analyzer – LGR laser spectrometer at the Slovak Geological Survey of Dionyz Stur, Bratislava. Finally, precipitation and stream outflow are monitored on a monthly basis within the framework of the GNIP and the GNIR programmes run by IAEA (IAEA, 2006; Vitvar *et al.*, 2007). These samples are analysed for [18]O at the IAEA Isotope Hydrology Laboratory in Vienna using a Finnigan MAT DeltaPlus mass spectrometer. All [18]O values are expressed as $\delta^{18}O$ in per-mil of the Vienna Standard Mean Ocean Water, with precision of ±0.1 per mil V-SMOW (±0.2 per mil V-SMOW for laser spectrometer). Monthly [18]O data for precipitation, streamflow, and groundwater are have been selected for this paper.

The amplitudes of annual $\delta^{18}O$ fluctuations in monthly composite precipitation, instantaneous and composite streamwater, and instantaneous monthly groundwater samples are presented on Fig. 2. Shallow groundwater in the catchment exhibits low levels of fluctuation. This is due to the mixing of water volumes with varying [18]O content during the seasons.
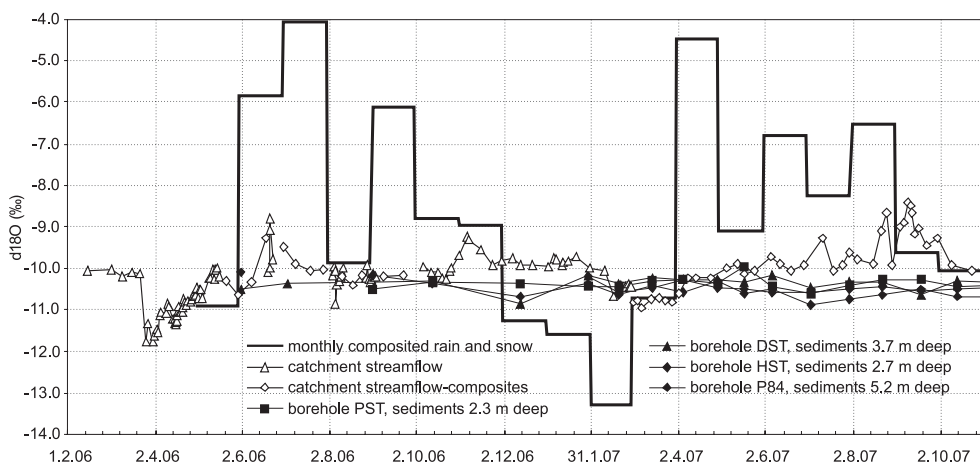
Fig. 2:   Variability in $\delta^{18}O$ content in precipitation, snowfall, streamflow, and groundwater from February 2006 to October 2007 in the Uhlířská catchment.

MEAN RESIDENCE TIME CALCULATION

The mean residence time of water (MRT) in the catchment is calculated via a comparison of $\delta^{18}O$ values in precipitation and streamwater, assuming a steady-state mixing of precipitation with water in the subsurface system, and the conservative tracer behaviour of $\delta^{18}O$. Based on these assumptions – the attenuation of precipitation to streamflow or groundwater $\delta^{18}O$ values – the mean residence time of water can be estimated via an analysis of $\delta^{18}O$ fluctuations using hypothetical residence time distributions. Mathematically simpler methods compare idealized sine wave approximations of both precipitation and streamflow/groundwater $\delta^{18}O$ fluctuations, whereas more complex approaches simulate the transfer of any variable form of $\delta^{18}O$ - fluctuations in precipitation into any $\delta^{18}O$ record in streamflow/groundwater (McGuire and McDonnell, 2006).

Sine wave approximation of $\delta^{18}O$ fluctuations

Based on the correlation of measured monthly temperature averages and monthly records of $\delta^{18}O$ in precipitation for the V/06-X/07 time period (Fig. 3 – left), a set of monthly $\delta^{18}O$ precipitation values
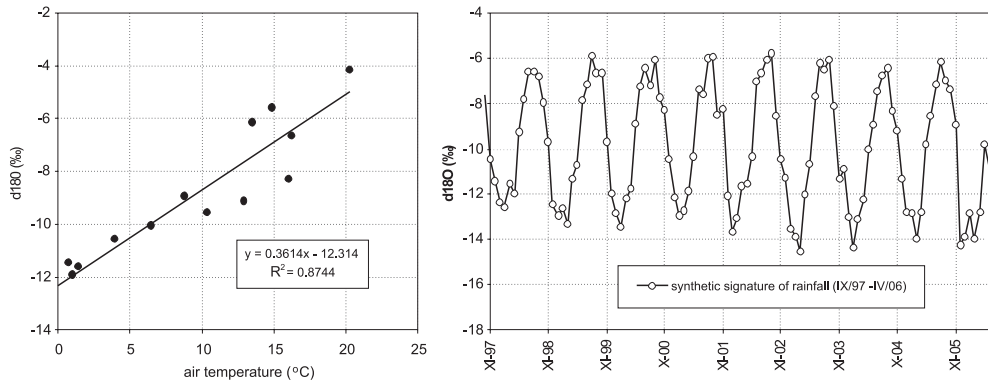
Fig. 3:   Correlation of δ¹⁸O in monthly precipitation totals with monthly mean air temperature (left) and computed record values of δ¹⁸O in monthly composite precipitation (right).

was calculated according to the linear relationship between mean monthly air temperature and δ¹⁸O in the monthly precipitation composite (Fig. 3 – right). The aim of this calculation was to provide long term data for the modelling approaches described below.

Seasonal fluctuations in both computed and measured δ¹⁸O precipitation data and measured δ¹⁸O stream outflow values were fitted to a sine function (Fig. 4), as described by the equation below (Reddy *et al.*, 2006):
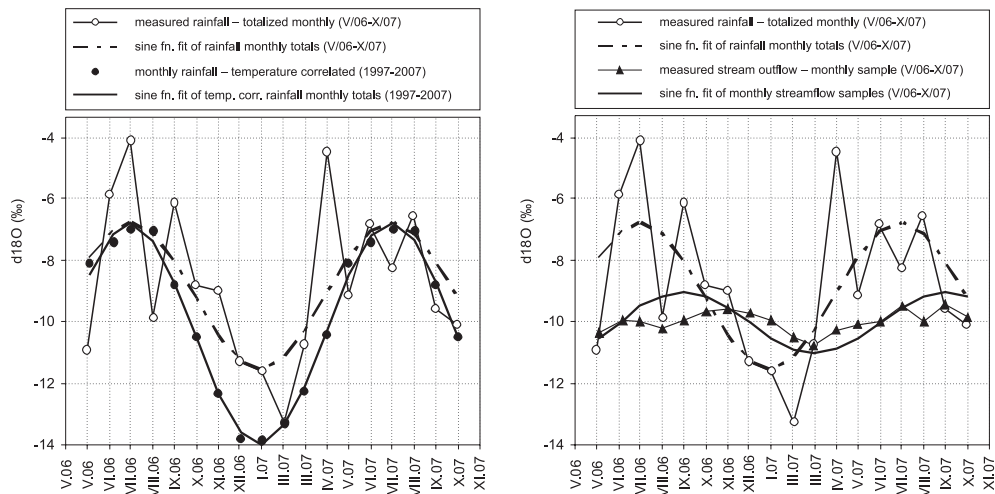
Fig. 4:   Variability in δ¹⁸O levels in monthly precipitation totals (left), computed precipitation and measured streamflow (right).

$$\delta^{18}O = mean(\delta^{18}O) + A\,sin[(2\pi \cdot t\,/\,b) + c] \qquad \text{Eq. 1}$$

where mean(δ¹⁸O) (‰) is the annual mean of δ¹⁸O, A (‰) is the seasonal amplitude of δ¹⁸O, b is the period of the seasonal cycle (e.g. 12 months), t (months) is time, and c (radians) is the phase lag. The parameters mean (δ¹⁸O), A, and c are calculated by fitting Eq. (1) to experimental data via regression. The fit of measured δ¹⁸O precipitation data indicates a higher mean and a smaller amplitude compared to long term computed data due to the warmer winter season of 2006/2007. A comparison of the fitted sine functions of precipitation and stream outflow shows attenuation of the δ¹⁸O signal in streamflow. The decreased level of δ¹⁸O variability in outflow indicates the presence of a strong transformation effect performed by subsurface mixing in the catchment.

31

The MRT was obtained by damping sine wave amplitudes:

$$MRT = \left(\frac{1}{b'}\right)\left[\left(\frac{A}{A_p}\right)^{-2} - 1\right]^{0.5}$$

Eq. 2

where A_p is the seasonal amplitude of $\delta^{18}O$ for precipitation, A is the amplitude of $\delta^{18}O$ for the examined component (i.e. streamflow or groundwater), and b' (rad·time^{-1}) is a conversion factor (Maloszewski and Zuber, 1982).

The mean value of the sine wave fit of $\delta^{18}O$ in streamflow is –10.0‰, the mean computed precipitation $\delta^{18}O$ content is -10.4‰, while the mean value of the sine wave fit of $\delta^{18}O$ in measured precipitation for the examined V/06-X/07 time period is -9.2‰. The values of $\delta^{18}O$ for shallow groundwater range from -10.4 to -10.6‰ (Fig. 2). Experimentally fitted $\delta^{18}O$ data for precipitation and computed precipitation exhibit $\delta^{18}O$ amplitudes of 4.78‰ and 7.23‰, respectively. The sine wave amplitude of $\delta^{18}O$ in outflow is 2.00‰. Therefore, the mean residence time of water in the catchment ranges from approximately 9 to 14 months for $\delta^{18}O$ for either measured or computed precipitation. This comparison illustrates the long term mixing effect present in the subsurface system in the transformation of precipitation into runoff.

General "lumped-parameter" approximation of $\delta^{18}O$ – fluctuations

This approach relates the variable isotope content of precipitation (C_{in}) and that of streams/aquifers (C) with a convolution integral (Maloszewski and Zuber, 1996):

$$C(t) = \int_0^\infty C_{in}(t - t')g(t')\exp(-\lambda t')dt'$$

Eq. 3

where t′ is time of entry, t-t′ is the residence time of streamwater/groundwater, and g(t′) describes the assumed distribution of residence times. In this study, a dispersion distribution of residence times (Eq. 4) was used (Maloszewski and Zuber, 1996):

$$g(t') = \left(4\pi P_D \frac{t'}{t_t}\right)^{-\frac{1}{2}}(t'^{-1})\exp\left[\frac{-\left(1 - \frac{t'}{t_t}\right)^2}{\frac{4P_D t'}{t_t}}\right]$$

Eq. 4

where P_D is the apparent dispersion parameter.

The distribution of the dispersion was applied based on the assumption that the catchment consists of two reservoirs of water where total discharge receives a constant $\delta^{18}O$ "signal" from groundwater and a variable "signal" from the shallow subsurface water supply. The constant $\delta^{18}O$ groundwater signature, as averaged according to Fig. 2, was used ($\delta^{18}O$ = -10.5‰) as an approximate value for the groundwater concentration of $\delta^{18}O$. Fitting the dispersion function model to the experimental data shows that approximately 53% of long term discharge is composed of groundwater of considerable age: i.e. older than can be detected by stable isotopes on the order of 6-7 years. The remaining 47% of discharge is composed of water passing through the catchment relatively quickly. The latter component fits experimental streamflow data best with the mean residence time equal to 4.75 months (Fig. 5).
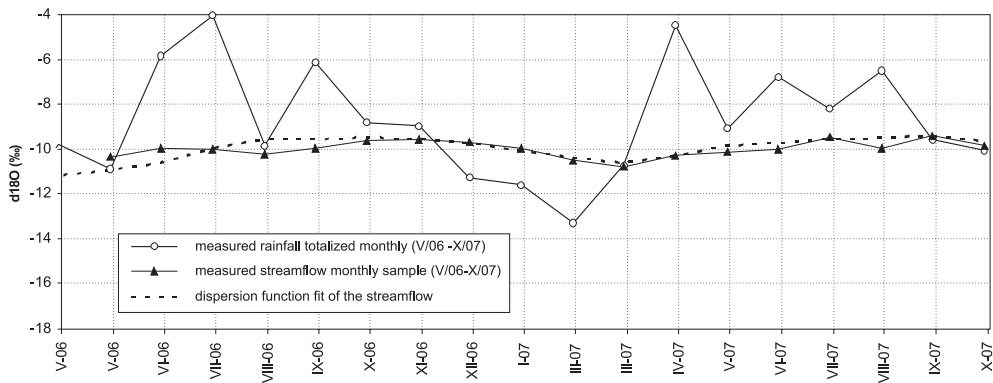
Fig. 5:   Application of dispersion based on a model by Maloszewski and Zuber (1982).

MODELLING GROUNDWATER FLOW

A steady-state one-layer groundwater model was designed to assess the spatial variability of groundwater MRT across various aquifer depths. The MODFLOW2000 code, a part the Groundwater Vistas 4 package, was used. Aquifer thickness was evaluated by means of electrical resistivity tomography (Šanda *et al*., 2007b), approximating the increasing depth of sediment (10–40 meters) along the valley axis towards the catchment outlet. Water table observations in shallow wells were performed during the last decade in the catchment. Detailed mapping using GPS produced distributed water drainage network data. Boundary conditions were set to "no-flow boundary" at the catchment divide and "river discharge" (a Cauchy-type boundary condition) in the streams. Based on an analysis of the outflow hydrograph (2000–2005) generated, multiple approaches were taken with respect to Kille's standard baseflow separation analysis (1970) and the Kliner-Kněžek Method (Kněžek, 1988). A combination of these two methods yielded a baseflow to precipitation of 36% and to streamflow of 46%. In other words, streamflow constitutes approximately 80% of the precipitation. The calibration of the model, i.e. the spatial distribution of the water table, was achieved by modifying saturated hydraulic conductivity values throughout the model cell network (Fig. 6).
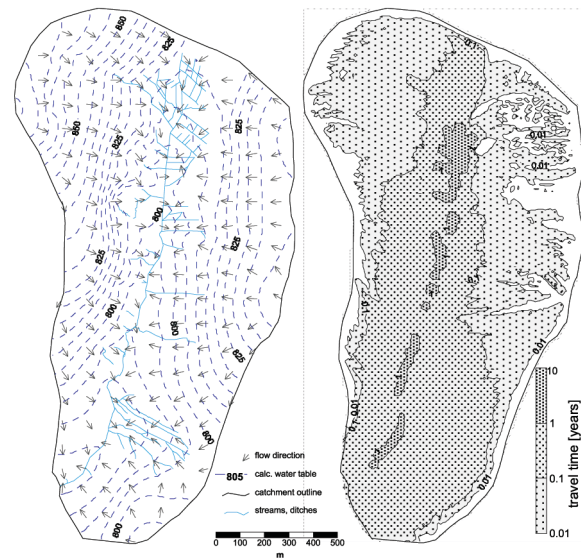
Fig. 6:   Water table and flow directions modeled using Modflow2000.

The application of the modelling results was performed via the tracing of virtual water particles under steady state conditions and under the assumption of evenly distributed porosity = 0.1[-] for weathered upslope structures and glacial sediments in the valley. A virtual particle was inserted into each of the active model cells (10x10 m) and the spatial distribution of mean groundwater travel times was obtained for each cell. Using a flow and particle tracking approach, a preliminary spectrum of groundwater travel times was obtained. It must be noted, however, that the estimation of travel time is strongly affected by the assumed porosity scenario. Measured porosity within the shallow subsurface ranges from 0.4 to 0.6 whereas fractured granite porosity may range from 0.01 to 0.1 (Maloszewski *et al*., 1999). Water travel time within hill slopes formed by 0–10 m deep weathered granite structures ranges from 0.01 to 1.0 years while the residence time of water in the 10–40 m deep sedimentary aquifer is over one year, as mentioned above. The model indicates an MRT of up to one decade for deep groundwater in the deepest and/or the flattest parts of the aquifer. These results support the two component MRT concept obtained from $\delta^{18}O$ analysis. More detailed quantitative results, however, need to be verified through the use of other water dating tools which are more suitable for the assessment of residence times in the range of multiple decades – such dating tools include ^3H and ^3He methods.

CONCLUSIONS

This paper combines an analysis of $\delta^{18}O$ in precipitation, streamflow, and groundwater with an analysis based on a groundwater flow model. The combined use of both approaches revealed a deeper insight into the processes of runoff generation and rainfall-runoff transformation within a catchment's subsurface system. The hypothesis of a relatively low portion of rapid near-surface runoff combined with rather rapid recharging and mixing within the lower soil horizons and the upper less-consolidated bedrock was confirmed. This type of rapid subsurface mixing is assumed to be the principal runoff generation process in the catchment. A runoff component with a uniform isotopic composition and a modelled residence on the order of one decade suggests the existence of a periodically stagnant subsurface water pool within deeper sediment horizons – below peatlands – supplying streamflow under pronounced dry conditions. The approaches used in this study demonstrate the need for mutual application. This is particularly important when interpreting the origin and pathways of slower runoff components. The results obtained are important for purposes of water and landscape management in the temperate humid regions of Central Europe. This is especially true in view of anticipated climate changes as well as changes in water regimes and the role that mountainous headwaters play in supplying water to adjacent lowlands.

REFERENCES

IAEA (2006). *Isotope Hydrology Information System*. ISOHIS Database. Available at: http://isohis.iaea.org

Kille K. (1970). Das Verfahren MoMNQ – ein Beitrag zur Berechnung der mittleren langjährigen Grundwasserneubildung mit Hilfe der monatlichen Niedrigwasserabflüsse. *Z. dt. geol., Ges., Sonderh. Hydrogeol. Hydrogeochem.*: 89-95.

Kněžek, M. (1988). Groundwater flow (In Czech). *Práce a studie. Water Res. Inst.,* **171**, Prague: 64 pp.

Maloszewski P and Zuber A. (1982). Determining the turnover time of groundwater systems with the aid of environmental tracers. 1. Models and their applicability. *J.Hydrol.,* **57**: 207–231.

Maloszewski P. and Zuber A. (1996). Lumped parameter models for the interpretation of environmental tracer data. In: *Manual on mathematical models in isotope hydrology*; TECDOC-910, IAEA, Vienna.

Maloszewski P., Herrmann A. and Zuber A. (1999). Interpretation of tracer tests performed in fractured rock of the Lange Bramke Basin, Germany. *Hydrogeol. J.,* **7**(2): 209-218.

McGuire K.J., McDonnell J.J. (2006). A review and evaluation of catchment transit time modeling. *J. Hydrol.,* **330**(3-4): 543-563.

Reddy, M.M., Schuster, P.F., Kendall, C. and Reddy, M.B. (2006). Characterization of surface and ground water $\delta^{18}O$ seasonal variation and its use for estimating groundwater residence times. *Hydrol. Process.,* **20**: 1753–1772.

Šanda M., Novák L. and Císlerová M. (2007a). Tracing of water flowpaths in a mountainous watershed. In: Pfister L. and Hoffmann P. (ed.). Uncertainties in the 'monitoring-conceptualisation-modelling' sequence of catchment research. Proceedings of the 11th Conference of the Euromediterranean Network of Experimental and Representative Basins (ERB), Luxembourg, 20–22 September 2006, IHP-VI, *Technical Documents in Hydrology*, **81**, UNESCO, Paris.

Šanda, M., Sobotková, M. and Císlerová, M. (2007b). Water Flowpaths in the Mountainous Watershed Traced by 18-oxygen Isotope. In: *Advances in Isotope Hydrology and its Role in Sustainable Water Resources Management* (IHS-2007). Vienna, IAEA: 419–425.

Vitvar T., Aggarwal P. K. and Herczeg A. L. (2007). Global Network is Launched to Monitor Isotopes in Rivers. *Eos Trans. AGU*, **88**(33), 325 pp.

EXTREME GLACIER RETREAT IN SUMMER 2003
– EXAMPLE OF THE AUSTRIAN TEST BASIN *GOLDBERGKEES*

H. Holzmann[1], G. Koboltschnig[2] and W. Schöner[3]

[1] *University of Natural Resources and Applied Life Sciences (BOKU), Vienna, Austria.*

[2] *Provincial Government of Carinthia, Klagenfurt, Austria.*

[3] *Central Institute for Meteorology and Geodynamics (ZAMG), Vienna, Austria.*

Corresponding author: Hubert Holzmann, e-mail: hubert.holzmann@boku.ac.at

ABSTRACT

In the year 2003, Central Europe suffered a very warm and dry summer period. The impact of the high temperatures and low precipitation led to plant stress, crop losses, shortages of drinking water, and low discharge in rivers. One further consequence was a strong melt and depletion of high alpine glaciers. As a positive effect, this meltwater contribution significantly increased the discharge of alpine rivers but on the other hand, it led to a dramatic reduction in glacier volume. This paper describes the hydrologic response and the field monitoring activities conducted in the high alpine test basin of Goldbergkees where hydro-meteorological data, including data on snow and ice melt processes, were obtained during the 2002–2006 time period. It also describes the application of hydrologic water balance models and their conceptualisations and design.

Key words: snow melt, glacier melt, glacier monitoring, melt modelling

INTRODUCTION

Water balance observations in high alpine basins constitute a major challenge due to the exposed conditions of this environment. Precipitation observations at high altitudes are plagued by significant errors resulting from frequent wind and storm events and by a high rate of precipitation falling as snow. Snow distribution is subject to redistribution by wind and avalanches. Runoff response is not directly related to precipitation as there is a temporal shift between snow accumulation and snowmelt. In addition, icemelt contributions from glacier areas significantly affect summer runoff. Within the framework of the research project SNOWTRANS – *Regionalisation of snow- and ice melt processes in the Hohe Tauern mountains in Austria (*Holzmann *et al*., 2008*),* the authors monitored the small partially glaciered basin of Goldbergkees glacier from 2002 to 2006. One of the objectives of the project was to build a good database for the description of the entire hydro-glaciological process in the basin which would enable the application and testing of different types of water balance and snow and ice melt models. Fortunately, different meteorological conditions were present during the observation period including also the extremely warm conditions of the year 2003 which allowed the opportunity to observe and model extreme melting conditions.

BASIN DESCRIPTION

The Goldbergkees basin at Rauriser (Hoher) Sonnblick mountain served as the reference basin for the various applied modelling approaches and field measurement techniques used as this region benefits from a database available from the meteorological observatory and hydro-glaciological network. Mount Hoher Sonnblick, as a major peak of the Hohe Tauern region in the Austrian Alps, is well known because of the meteorological observatory on its top at 3106 m a.s.l. The observatory offers a wide spectrum of meteorological and climatologic measurements dating back to the year 1886. Furthermore, the Sonnblick region stands out because of a detailed glacier monitoring programme running about 25 years now which includes the Goldbergkees glacier (close to

the observatory). The watershed of the Goldbergkees basin is more than 50% glacier (1.5 km² in the year 1998) and its elevation ranges from 2350 and 3106 m a.s.l. Fig. 1 shows the boundaries of the small catchment and the range of its glacier as well as its retreat from 1979 to 2003.
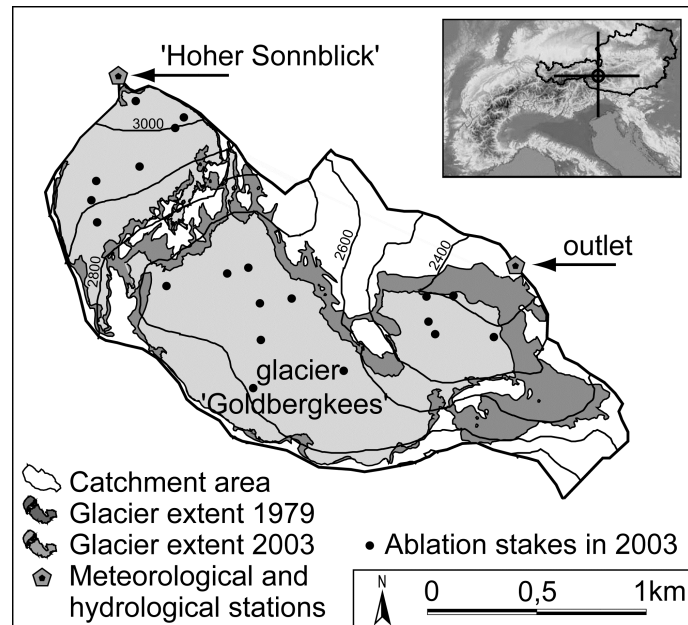
Fig. 1:   Glaciered areas of the Goldbergkees glacier: 1979 (dark grey) and 2003 (bright grey). Black dots show snow stakes from the ablation period in 2003 (From Koboltschnig, 2007).

CLIMATIC CHARACTERISTICS OF THE YEAR 2003

The year 2003 exhibited little rainfall and high temperatures in spring and summer all over Europe. Compared with the mean values from 1990 to 2000, the temperature increase in the test basin during the summer months from May to August was significant and reached its maximum of 4 °C in June (see Fig. 2). Two factors of the alpine environment affected melting processes: (1) Winter accumulation of snow was small and (2) snowmelt had already started in May which was approximately four to six weeks earlier than usual. This caused early snow cover depletion and a quite long period of uncovered bare glacier ice.
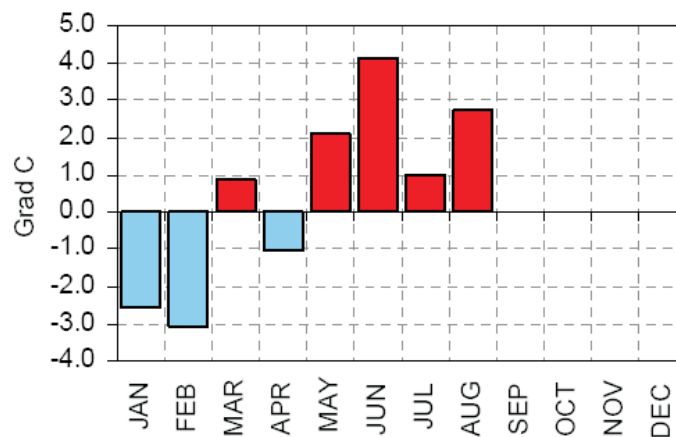
Fig. 2:   Differences in air temperature in the year 2003 compared with the 1990–2000 period. (From Schöner *et al.*, 2004).

In addition to the high rate of energy input during summer 2003 (direct and indirect radiation; see Michlmayr *et al.*, 2008), accumulated deposition of debris from the atmosphere decreased the rate of energy reflectance (albedo) which caused an increase in ice melt.

MONITORING OF SNOW AND ICEMELT

Activities related to those of the meteorological observatory were carried out by staff members. These included permanent observations of snow depth and ice depletion. Snow depth was monitored by ultrasonic snow sensors and snow ablation stakes. The latter had a weekly observation interval. Glacier depletion was observed by ice stakes which were drilled into the ice as well as by field surveys of the glacier terminus and boundary zones. Snow density measurements were carried out as part of students' practical field training in May of each year to detect maximum accumulation which was required for the regular glacier mass balance calculation. In May, some snow profiles possessed a snow depth of more than five meters.

Fig. 3 compares snow accumulation and snowmelt at permanent snow stakes. Table 1 lists the names of the permanent snow stakes and their elevations. In the early winter of 2002, a large increase in snow depth could be observed for the higher elevations. The total maximum was about 400 cm near the peak location. Melting started in May already and in July, most of the snow cover was depleted. In 2004, the snow depth maximum occurred in June and snowmelt lasted until September where some snow was still left at higher altitudes.
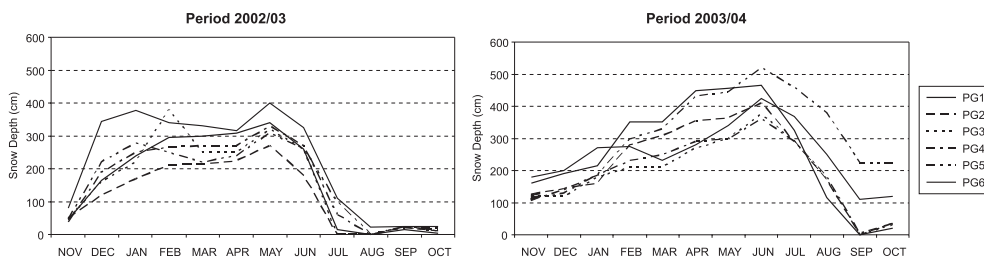
Fig. 3:   Comparison of snow depth distribution in the hydrological years 02/03 (left) and 03/04 (right) (From Rauch, 2007).

Table 1: Snow stakes and elevations.

Code	Name	Elevation (m a.s.l.)
G 1	Unterer Goldbergkeesboden	2450 m
PG 2	Oberer Goldbergkeesboden	2650 m
PG 3	Goldbergkees – Oberer Steilhang	2850 m
PG 4	Goldbergkees – Brettscharte unten	2950 m
PG 5	Goldbergkees – Brettscharte oben	2950 m
PG 6	Fleissscharte	3050 m

A runoff gauge based on a bubbling pressure system, installed in 2002, allows remote data access to the water level at the basin outlet near the glacier's terminus. Temporal runoff measurements using flow velocimeters were carried out to ascertain the rating curve relationship. Fig. 4 shows the discharge time series of the melt period from September 2002 to October 2006 based on hourly time resolution. It can easily be observed that in 2003, the daily intensities of runoff as well as discharge maxima were higher than for other years. As runoff from snow is affected by the retention capacity of the snow column, the runoff pattern is smoother than that with bare ice cover.
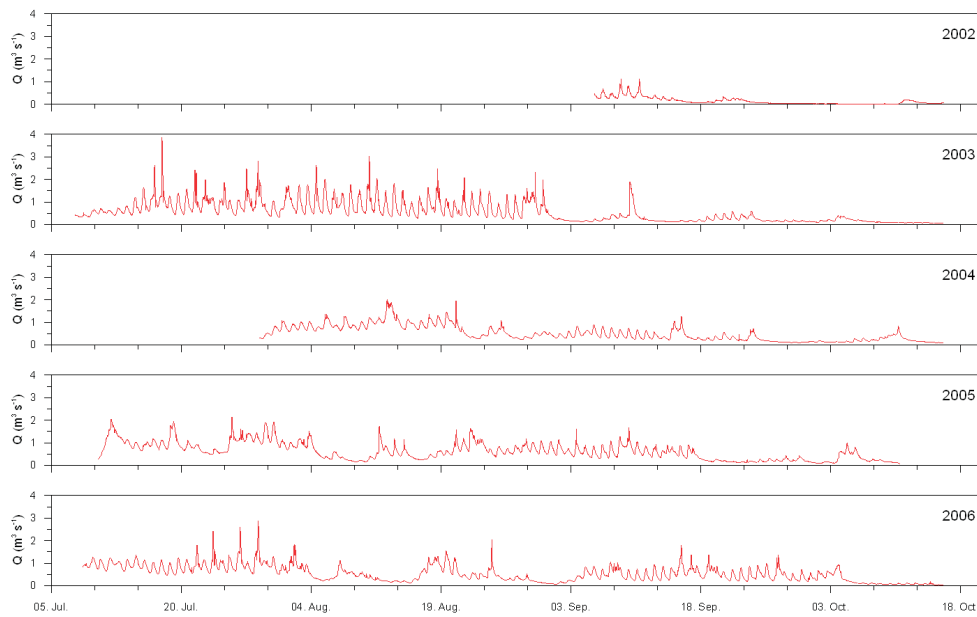
Fig. 4: Discharge observations: 2002–2006 (From Koboltschnig, 2007).
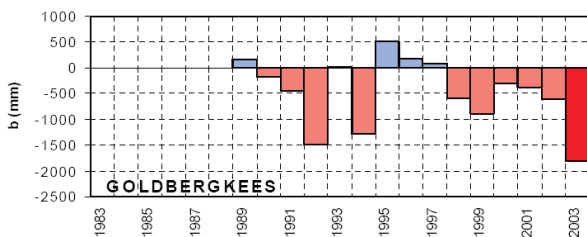
Fig. 5: Annual glacier mass balance for the Goldbergkees glacier. (From Schöner *et al.*, 2004).

All these observation data enable the description of the time and space-dependent melt and runoff formation processes which form the basis for the application and testing of different snow and ice melt routines**.** A further task for the glaciologists was to estimate the net mass balance of the glacier, considering areas of accumulation and depletion. Fig. 5 shows the glacier mass balance for the past twenty years. It can clearly be seen that 2003 had an extremely negative mass balance of 1.8 meters. Only the years 1992 and 1994 showed comparable deficits. Some ice stake readings in 2003 indicated vertical depletion of up to 5 meters in the lower zones of the glacier.

MELT MODELLING

Different types of index-based snow- and icemelt models were applied (Koboltschnig *et al.*, 2008). Furthermore, a physically based energy balance model type was tested (Michlmayr *et al.*, 2008). It could be shown that for mean daily time intervals, temperature index models (day-degree type models) worked sufficiently. For hourly time resolution, combined temperature-radiation index models exhibited better performance with respect to the strong diurnal variability of melt (see Holzmann *et al.*, 2008).

$$M_{i,k,j} = \alpha \cdot TI_k \cdot Temp_{i,j} + \beta \cdot RI \cdot Rad_i \qquad\qquad \text{Eq. 1}$$

where:
M – Snowmelt Rate (mm), TI – Temperature Index RI – Radiation Index, *Temp* – Air Temperature, Rad – Global Radiation, k – seasonal Index, i – temporal Index, j – elevation index, $\alpha + \beta = 1$ – weighting factors

As an example, the combined temperature-radiation index model is briefly introduced herein (see equation 1). Air temperature shows a significant dependence on altitude. Therefore, the basin area has been subdivided into

elevation bands of 100 meters, considering a moist adiabatic lapse rate of 0.65 °C per 100 meters. The above equation was applied for each time interval for all the zones studied.

The calculated melt rates for each zone constitute the inputs for a runoff transformation scheme which is based on the concept portrayed in Figure 6. The variability of the particular subprocesses in melt runoff is substituted by the storage concept on the right. The lowest storage represents subsurface runoff and only need be considered in case of subglacial flow within porous media such as moraines or sediment layers. It should be noted that for this calculation, two separate melt routines for snow and ice were applied. Both use the same concept but have a different parameterization – in particular in the case of the melt indices.
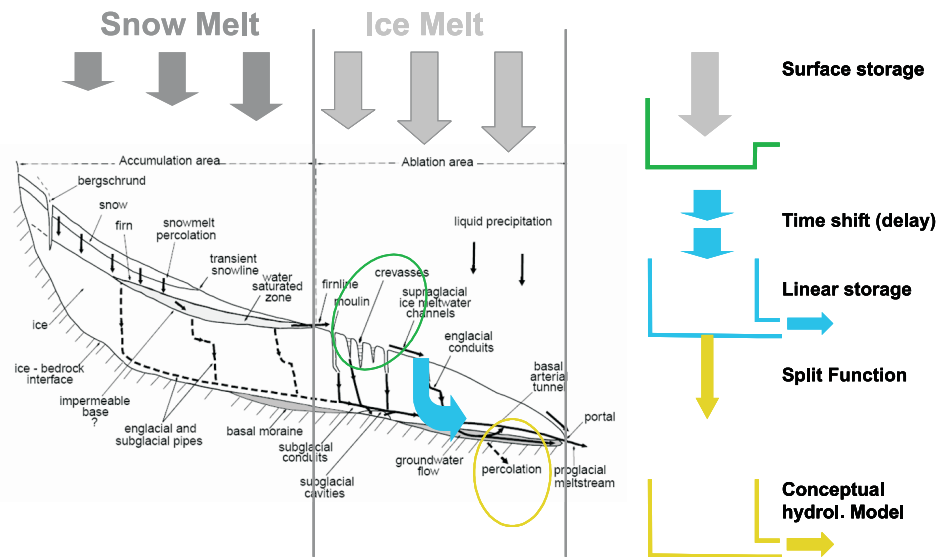
Fig. 6:　　　　　　Conceptualisation of glacier melt runoff.

The hydrologic runoff model enables the estimation of the particular runoff components, their temporal incidence, as well as variability. In Figure 7, it can be seen that significant runoff only takes place from May to September. May and June were dominated by snowmelt while during July and August, ice melt constituted the largest contribution to runoff. In August, almost 90% of runoff was originated from ice melt.
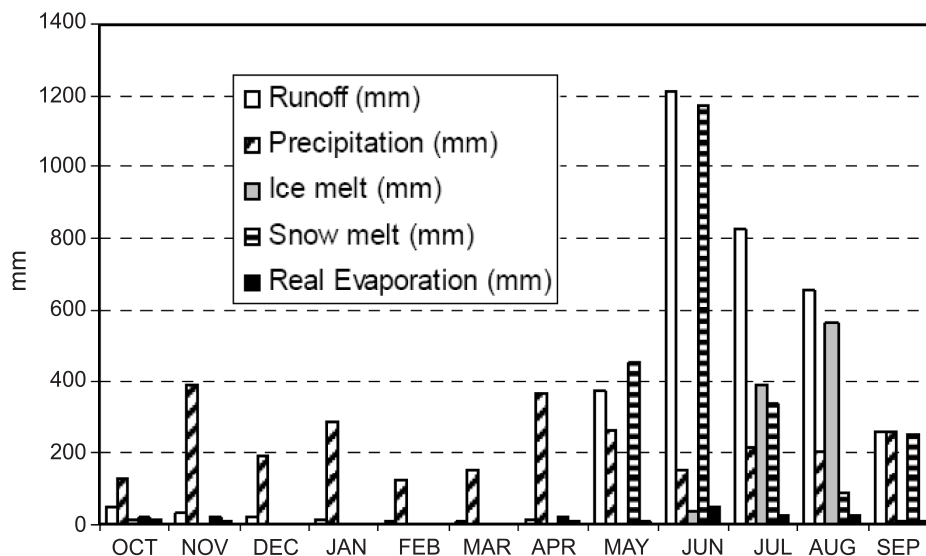
Fig. 7:　　　　　　Runoff components for the Goldbergkees basin for the year 2003 (from Koboltschnig, 2007).

SUMMARY AND CONCLUSIONS

The year 2003 was an extreme year in terms of climatic conditions (high temperatures, low precipitation). In the Goldbergkees basin, an average glacier mass balance loss of 1.8 m could be observed with the mean annual mass balance loss between 1983 and 2005 being only 0.55 m. Due to greenhouse gas emissions, climate models forecast similar conditions for the end of the century. In 2003, glacier melt runoff substituted for the lack of precipitation in high alpine basins but in future, climate trends predict a total depletion of glaciers below 3000 m.a.s.l. during the remainder of the current century. This will lead to low summer flow, temperature increases of river water, and will lead to corresponding consequences for ecology, hydro-energy production, and landscape-based attractions (tourism). In the described project, it was shown that hydrologic models reliably enable the computation of runoff components and are useful for the purpose of forecasting environmental changes.

As a basis for such applications, meteorological and hydrological observation data are required. Due to the difficult environmental conditions in high alpine areas, experimental test basins are of utmost importance. Future research should also focus on the transformation and extrapolation of these results to ungauged basins.

REFERENCES

Holzmann H., Schöner W., Koboltschnig G., Kroisleitner Ch., Hynek B., Mott R., Michlmayer G., Schneider W., Kaiser G., Vollmann M. and Rauch L. (2008). *Modelling and extrapolation of snow and ice melt processes in alpine environments*. Final report of SNOWTRANS project. Austrian Academy of Sciences online publication. ISBN: 978-3-7001-3987-4, (http://epub.oeaw.ac.at/3987-4inhalt).

Koboltschnig G. (2007). *Multivalidation approach of hydrological snow- and icemelt models for high alpine glacierized basins*. Dissertation at the BOKU-University Vienna (in German).

Koboltschnig G., Schöner W., Zappa M., Kroisleitner Ch. and Holzmann H. (2008). Runoff modelling of the glacierized Alpine Upper Salzach basin (Austria): multi-criteria result validation. *Hydrol. Processes*, **22**(19): 3950–3964.

Michlmayr G., Lehning M., Koboltschnig G., Holzmann H., Zappa M., Mott R. and Schöner W. (2008). Application of the *Alpine 3D* model for glacier mass balance and glacier runoff studies at Goldbergkees, Austria. *Hydrol. Processes*, **22**(19): 3941–3949.

Rauch, L. (2007). *Snowmelt modelling with index-based models*. Diploma thesis at the BOKU University Vienna (in German).

Schöner W., Auer I., Böhm R., Hynek B., Holzmann H. and Koboltschnig G. (2004). Extreme glacier melt in Hohe Tauern region (Austrian Alps). In: Herrmann A. (ed.): International Conference on Hydrology of Mountain Environments, 27 Sept.–1 Okt. 2004, Berchtesgaden, Deutschland; *Landschaftsökologie und Umweltforschung*, Extended Abstracts, **47**, 191–195; Selbstverlag Institut für Geoökologie der Technischen Universität Braunschweig, Braunschweig.

MODELLING THE IMPACT OF URBANIZATION ON HYDROLOGICAL EXTREMES

J.P. Nunes[1], J.L.M.P. de Lima[1, 2] and A.J.D. Ferreira[3]

[1] *IMAR: Institute for Marine Research, Portugal*

[2] *Department of Civil Engineering, Faculty of Sciences and Technology, University of Coimbra, Portugal*

[3] *CERNAS, Coimbra Agrarian Technical School, Portugal*

Corresponding author: João Pedro Nunes, e-mail: jpcn@fct.unl.pt

ABSTRACT

Urbanization can have a significant impact on hydrological processes in small catchments, leading in particular to an increase in flash flood frequency. This impact could be enhanced by an increase in the intensity of extreme rainfall events caused by global climate change. This work explores this problem for the Covões catchment in central Portugal which has seen a significant increase in urban density in recent decades. Runoff and peak runoff rates were monitored and used to parameterize a process-based rainfall-runoff model for the study area. The model was later used to simulate the impact of different degrees of urbanization and climate change (in terms of increasing extreme event intensity) on runoff and peak runoff rates in the catchment. Results indicate that an increase in urbanization density could have significant impact on storm runoff and peak runoff rates. Moreover, the impact of climate change on storm rainfall could be amplified by an increase in the number of impervious areas. This can be attributed to the higher connectivity associated with higher urbanization densities and to the low runoff generation ratios currently being observed.

Keywords: Global change, urbanization, climate change, hydrological extremes, hydrological modeling, hydrological connectivity

INTRODUCTION

Urbanization can induce significant changes to the hydrological regimes of small catchments, leading to flash floods which can cause significant damage and put local populations at risk (e.g. Huang *et al.*, 2008). This impact could be enhanced by climate change due to a potential increase in the frequency of extreme rainfall events (Meehl *et al*., 2007). An additional problem is that urbanization could lead to major hydro-meteorological changes over cities due to the urban heat island effect (e.g. Grimm *et al.*, 2008) with unknown impact on rainfall extremes. There have been recent efforts in addressing both problems using modelling approaches (e.g. Chen and Adams, 2007; Kleinen and Petschel-Held, 2007; Cuo *et al*., 2008; Huang *et al*., 2008) but simulation studies coupling both increased urbanization and rainfall are still scarce.

This article presents some preliminary results of an ongoing research project, URBHI – Urban flood risk and pollutant relocation as a result of global change – which is designed to investigate the impact of increased urbanization on hydrological processes on the small catchment scale, and how this could influence catchment response to global climate change. This is being achieved by: (i) installing a detailed monitoring network in a small urban basin near the city of Coimbra (Portugal); and (ii) modelling storm runoff and using it to study the impact of different urbanization and storm patterns on hydrological processes on a catchment scale. This article focuses on the modelling exercises performed within URBHI.

STUDY AREA

The Covões catchment (6.2 km²; Fig. 1) is located in the centre of mainland Portugal. Average annual rainfall is 980 mm with a Mediterranean climate where most of the rainfall occurs during a cold and wet season. In 2000, 21% of the catchment's surface was occupied by discontinuous urban fabric (55% built-up areas interspersed with 45% agricultural and woodland cover); the remainder of the catchment was mostly forested (Fig. 1, right).
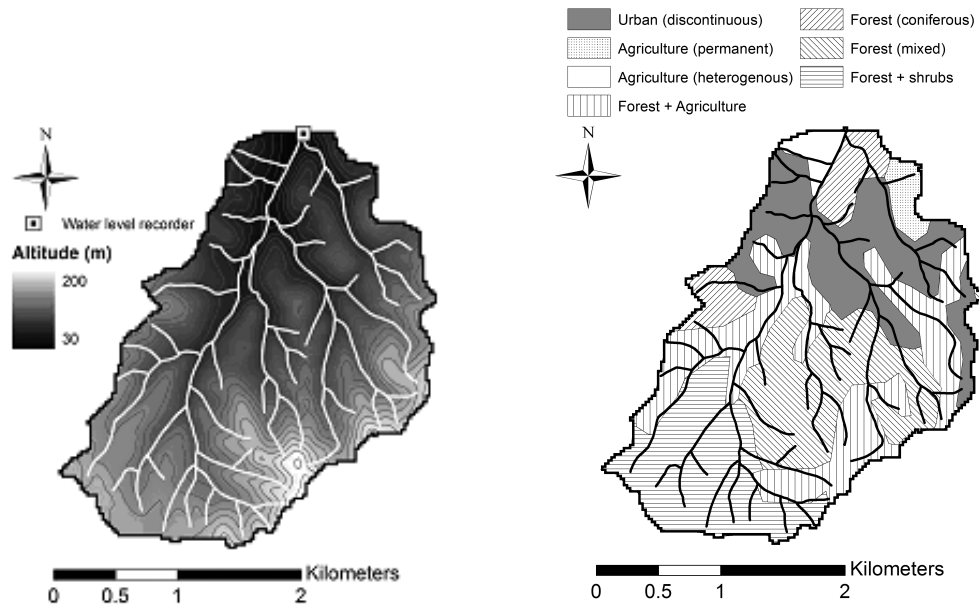
Fig. 1: Map of the Covões catchment showing altimetry and location of the recording stream gauge (left); Land cover according to the CORINE 2000 map (right).

Between 1987 and 2000, the percentage of impervious areas in the catchment increased from approximately 4.5% to 12%, stemming mostly from an increase in urbanization density in the northern part of the catchment. This trend is expected to continue and new urban areas are currently under development further upstream. This process has been identified as having caused a major flood in late 2006, underscoring the need for a modelling approach to study the impact of further urbanization on the catchment's hydrological processes and analyze the effectiveness of different mitigation measures.

RAINFALL AND RUNOFF MONITORING

The Covões catchment was instrumented with a rain gauge, measuring rainfall at 15-minute intervals; and a recording stream gauge, located in a flume at the catchment's outlet (Fig. 1, left) and measuring runoff at 5-minute intervals. Data were recorded between February and October 2005; rainfall during this period was 344 mm, thus being significantly below average totals for these months and reflecting the drought that affected Portugal in the 2004/05 hydrological year. Measured runoff was 13.6 mm, resulting in a runoff generation ratio of 4%. Fig. 2 (left) shows daily rainfall and runoff during the sampling period; baseflow was separated using the method described by Arnold and Allen (1999). Most of the runoff (73%) in this period consisted of surface flow. The low runoff generation and low baseflow could be attributed to drought conditions (leading to low rainfall and potential evapotranspiration ratio) or to the portion of the baseflow exiting the catchment as subsurface flow.
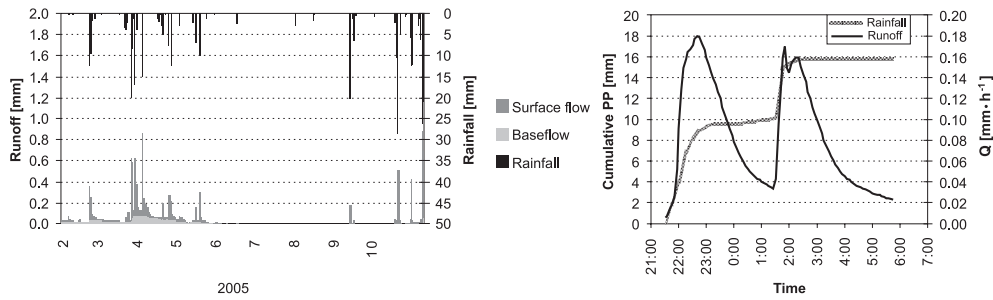
Fig. 2:   Daily rainfall, surface runoff, and baseflow for the sampling period in the Covões catchment (left); Hyetograph and hydrograph for the 25/26-March-2005 storm (right).

The analysis focused on 26 storm hyetographs and hydrographs for this period. Total rainfall was between 1 and 19.2 mm with intensities between 0.3 and 8.8 mm·h^{-1}, and maximum 15-min rainfall between 0.8 and 23.2 mm·h^{-1}; maximum rainfall rates were significantly correlated with total rainfall ($r = 0.71$, $p < 0.01$). Runoff ranged from 0.01 to 0.54 mm per storm; the highest correlation found was that with total rainfall ($r = 0.69$, $p < 0.01$), with a fairly linear relationship independent of storm intensity (Fig. 3, left). The correlation with maximum intensity was noticeably lower ($r = 0.5$, $p < 0.01$).
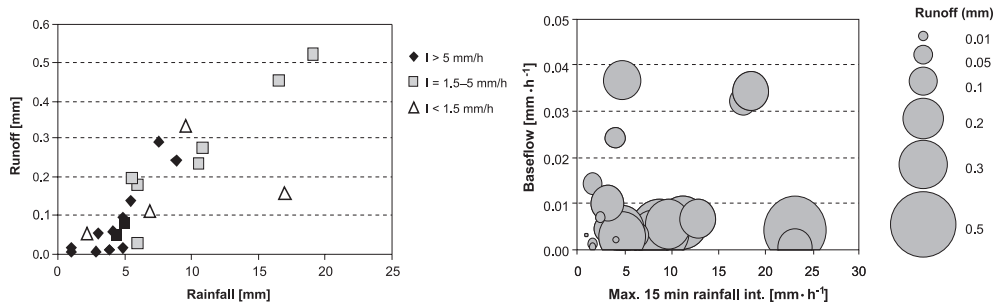
Fig. 3:   Rainfall and runoff for 26 storms in the study period, according to different storm intensity classes (left); Relative runoff for different conditions of maximum rainfall intensity and baseflow with the size of the grey circles indicating the amount of runoff (right).

The relationship between runoff and pre-storm baseflow, an indicator of soil saturation by water (Beven, 2000), was also lower ($r = 0.42$, $p < 0.05$) and appeared to be important only for storms with intensities lower than 5 mm·h^{-1} during 15 min intervals (Fig. 3, right). In comparison, the upper threshold in Mediterranean agricultural catchments can be as high as 60 mm·h^{-1} during 30 min intervals (Castillo *et al.*, 2003). This contrasts with the typically strong relationship between soil water saturation and runoff detected in Mediterranean catchments for medium-intensity storms (e.g. Cammeraat, 2002).

Runoff generation was between 0.2 and 3.7% without significant correlation with any of the above parameters. The runoff generation thresholds shown in Figure 3 (right) appear to be low when compared with typical values reported for Mediterranean catchments of 10 mm·h^{-1} during 30 min intervals (Kirkby *et al.*, 2005); this could indicate an important contribution of runoff from impervious areas.

The catchment responded quickly to most storms with steep rising hydrograph limbs beginning soon after the start of rainfall; an example is shown in Figure 2 (right) for a storm which occurred on the 25th and the 26th of March, 2005. The falling limb of the hydrograph also showed a steep decline. This indicates that most runoff originated close to the river network and possibly close to the catchment's outlet; these areas are preferentially occupied by urban zones (Fig. 1, right). It must be noted that the rainfall-runoff relationships found in this

sampling period could be strongly influenced by prevailing drought conditions. It can be assumed that, in a wetter year, higher intensity storms and wetter soils could lead to different types of dominant runoff generation processes.

MODELLING APPROACH

The MEFIDIS model (Nunes *et al*., 2005) was selected to be applied to the Covões catchment. MEFIDIS is a process-based, spatially-distributed, and dynamic hydrological model for extreme rainfall events. Hydrological simulation is based on the St. Venant equations (Chow *et al*., 1988). Simulated processes include interception, infiltration, surface retention, and runoff generation either through an infiltration deficit or a saturation excess. The spatial distribution of saturated areas is calculated from baseflow using a topographic wetness approach (Beven, 2000). Runoff is routed using a kinematic wave approach (Singh, 1996).

The model was applied to the Covões catchment using existing topographic (25×25 m), landcover, and soil maps; landcover and soil parameters were taken from the scientific literature. The model was calibrated and validated by means of a split-sample approach using the 26 storms described above. The calibration assumed that most of the runoff was generated close to the river network in impervious and saturated areas. Calibration and validation results for total storm runoff and peak runoff rates are shown in Fig. 4. The model performed well for total storm runoff with a Nash-Sutcliffe model efficiency index (Beven, 2000) of 0.82 and with a good correlation ($r^2 = 0.83$) between measured and observed values. The model also performed well when evaluating only peak flow rates for each storm; in this case, both the efficiency index and r^2 were 0.87.
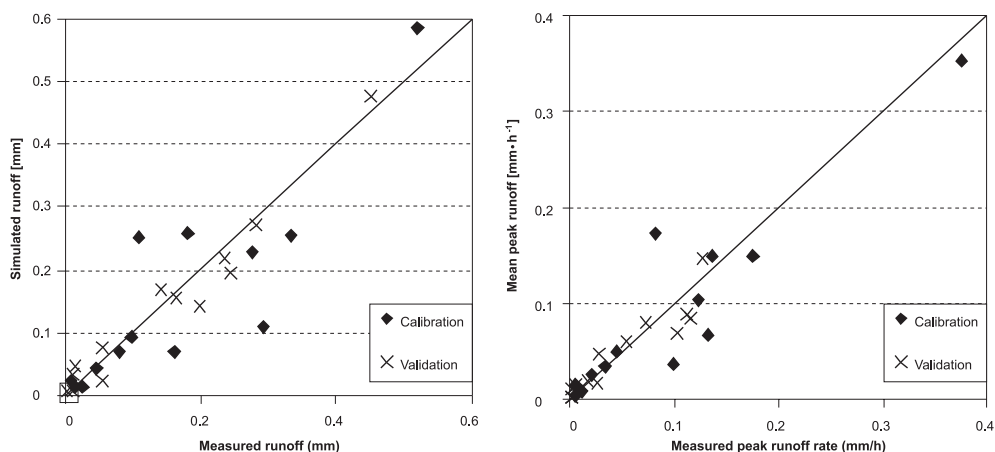
Fig. 4:   Comparison between simulated and observed results for total storm runoff (left) and peak runoff rates (right) for selected storms in 2005.

MEFIDIS was used to assess the impact of different urbanization densities in the study area, occupying only the current urban areas (Figure 1, right); and how these differences could influence the response of the catchment to global climate change. The model was applied with various urbanization and rainfall change scenarios to a subset of 6 storms with rainfall volumes over 10 mm. Urbanization density scenarios included:
- No urbanization;
- 20% urbanization, representing conditions in 1987 (4.5% catchment imperviousness);
- 55% urbanization, representing current conditions (12% catchment imperviousness);
- 80% urbanization as a future scenario (17% catchment imperviousness);
- 90% urbanization as a future scenario (19% catchment imperviousness).

Climate change scenarios considered an increase in storm rainfall up to 25%, in 5% increments, following expected trends caused by global change (Meehl *et al*., 2007). Rainfall changes were applied directly to storm

hyetographs, increasing rainfall intensity by half the amount of total increase (achieved by increasing the duration of the hyetograph, following the method adopted by Nearing *et al.*, 2005). Each rainfall change scenario was applied to each urbanization scenario for a total of 25 scenarios per storm.

RESULTS

Modelling results for runoff and peak runoff rates, for each scenario described above, are shown in Fig. 5. The results indicate that the sensitivity of runoff and peak runoff rates to impervious catchment areas is non-linear; for example, an increase between 4.5% and 12 % imperviousness (not taking into account rainfall changes) leads to a much smaller impact than an increase between 12% and 17%. This can be explained, within the model, by an increase in the connectivity between different impervious areas and the river network, allowing more of the runoff generated in impervious areas to reach the hydrological network. This effect was enhanced by the scenario focus on increasing urban density inside a defined catchment area, forcing
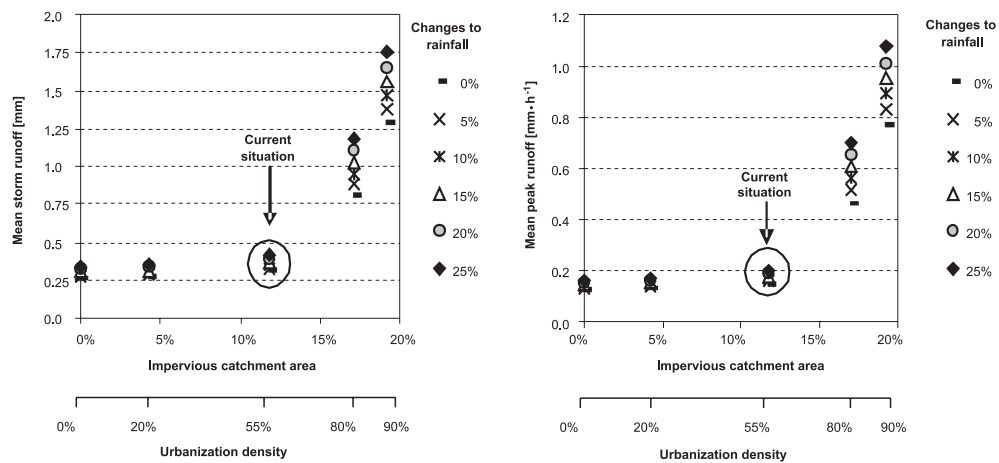
Fig. 5: Average storm runoff (left) and peak runoff rates (right) for the six analyzed storms based on different scenarios of increases in impervious catchment surface area and storm rainfall.

a connectivity increase in these regions. The large increase in connectivity is also reflected in the mean runoff generation ratio, shown in Figure 6; this follows changes to storm runoff and peak runoff rates.

In quantitative terms, the modelling results indicate that the current urbanization density has led to an increase in runoff and peak runoff rates of approximately 20% when compared to "natural" (no urbanization) conditions. The results also indicate a further potential increase in runoff and peak runoff rates by approximately 300% and 400 %, respectively, for an urbanization density increasing from 55% to 90%. However, it should be noted that these large increases still lead to a rather low runoff coefficient (below 10%; Fig. 6), with about half of the rainfall in impervious areas infiltrating or remaining in surface detention.

As for changes in storm rainfall, the results in Fig. 5 indicate that their impact is less important than that of changes in
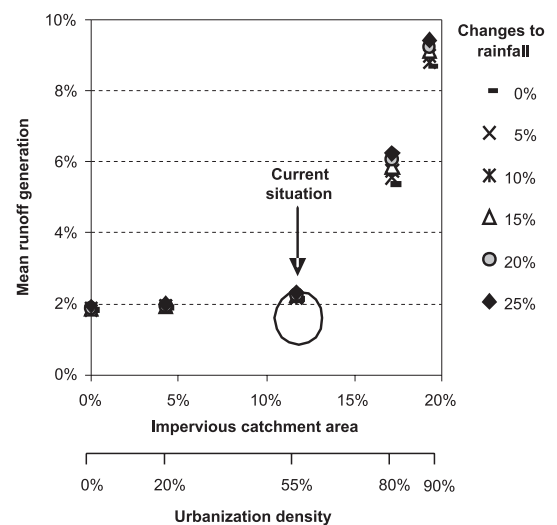
Fig. 6: Increase in the runoff coefficient due to urbanization in the Covões catchment.

45

urban density. For example, for current urbanization rates, the model predicts that a 25% increase in storm rainfall would lead up to a 35% increase in runoff and peak runoff rates, well below the impact of the increased urbanization scenarios. This can be explained by the low runoff coefficients observed in this particular catchment. However, the results also indicate that the impact of changes on storm rainfall may be amplified by an increase in the number of impervious areas (Fig. 5) which can again be attributed to the higher connectivity associated with higher urbanization densities and particularly to the impact on runoff generation ratios.

CONCLUSIONS

This study shows how a modelling approach can help guide urban planning by estimating the hydrological impact of urbanization. The expansion of an urban area can be studied assuming that storm conditions remain unchanged, allowing the impact of urbanization to be separated from that of different storm rainfall patterns. It is also possible to alter storm patterns in line with climate change predictions while keeping urban areas constant and both changes can be simulated simultaneously to study positive feedback from increases in storm intensity and the level of imperviousness of a catchment's surface.

The results indicate that an increase in urbanization density in the Covões catchment could lead to a significant increase in runoff and peak runoff rates for storms of similar magnitude; an increase in storm intensity would have less impact, particularly for current urbanization densities. However, a future increase in urbanization density could enhance the impact of higher storm intensities caused by climate change. The main processes responsible for these changes are an increase in the number of impervious areas generating surface runoff coupled with improved connectivity between impervious areas and the river network.

This work also presents a number of limitations. First, the data available is limited since the Covões catchment has been instrumented only recently. Further work should focus on data with longer observation periods including wetter years (e.g. the hydrological year 2006/07) to assess changes in the dominant runoff generation processes. Second, the work focused on an increase in urban density within a specific area; the analysis can be expanded by comparing these results with simulations for an increase in the area of low-density urbanization, increasing impervious areas without significant changes to connectivity. Finally, further data is required on soil moisture and river runoff rates in other parts of the catchment, particularly upstream of currently urbanized areas, to assess model performance in distinguishing runoff generated in urban and natural areas. Upcoming data from new water level recorders and soil moisture sampling devices in the Covões catchment should allow some of these limitations to be addressed.

REFERENCES

Arnold J.G. and Allen P.M. (1999). Automated methods for estimating baseflow and ground water recharge from streamflow records. *J. Am. Water Resour. As.*, **35**(2): 411–424.

Beven K. (2000). *Rainfall-Runoff Modelling – The Primer*. John Wiley & Sons, Chichester.

Cammeraat L.H. (2002). A review of two strongly contrasting geomorphological systems within the context of scale. *Earth Surf. Proc. Land.*, **27**: 1201–1222.

Castillo V.M., Gómez-Plaza A. and Martínez-Mena M. (2003). The role of antecedent soil water content in the runoff response of semiarid catchments: a simulation approach. *J. Hydrol.* **284**: 114–130.

Chen J. and Adams B.J. (2007). Development of analytical models for estimation of urban stormwater runoff. *J. Hydrol.*, **336**: 458–469.

Chow V.T., Maidment D.R. and Mays L.W. (1988). *Applied Hydrology*. McGraw-Hill, New York.

Cuo L., Lettenmaier D.P., Mattheussen B.V., Pascal Storck P. and Wiley M. (2008). Hydrologic prediction for urban watersheds with the Distributed Hydrology–Soil–Vegetation Model. *Hydrol. Process*es, **22**: 4205–4213.

Grimm N.B., Faeth S.H., Golubiewski N.E., Redman C.L., Wu J., Bai X. and Briggs J.M. (2008). Global Change and the Ecology of Cities. *Science*, **319**(5864): 756–760.

Huang H-j, Cheng S-j, Wen J-c, Lee J-h (2008). Effect of growing watershed imperviousness on hydrograph parameters and peak discharge. *Hydrol. Process*es, **22**: 2075–2085.

Kirkby M.J., Bracken L.J. and Shannon J. (2005). The influence of rainfall distribution and morphological factors on runoff delivery from dryland catchments in SE Spain. *Catena*, **62**: 136–156.

Kleinen T. and Petschel-Held G. (2007). Integrated assessment of changes in flooding probabilities due to climate change. *Climatic Change*, **81**: 283–312.

Meehl G.A., Stocker T.F., Collins W.D., Friedlingstein P., Gaye A.T., Gregory J.M., Kitoh A., Knutti R., Murphy J.M., Noda A., Raper S.C.B., Watterson I.G., Weaver A.J. and Zhao Z-C (2007). Global climate projections. In: Solomon S., Qin D., Manning M., Chen Z., Marquis M., Averyt K.B., Tignor M., Miller H.L. (eds.), Climate Change 2007: The Physical Science Basis. *Contribution of Working Group I to the Fourth Assessment Report of the Intergovernmental Panel on Climate Change*. Cambridge University Press, Cambridge: 747–845.

Nearing M.A., Jetten V., Baffaut C., Cerdan O., Couturier A., Hernandez M., Le Bissonnais Y., Nichols M.H., Nunes J.P., Renschler C.S., Souchère V. and van Oost K. (2005). Modelling response of soil erosion and runoff to changes in precipitation and cover. *Catena*, **61**(2-3): 131–154.

Nunes J.P., Vieira G., Seixas J., Gonçalves P. and Carvalhais N. (2005). Evaluating the MEFIDIS model for runoff and soil erosion prediction during rainfall events. *Catena,* **61**(2-3): 210–228.

Singh V.P. (1996). *Kinematic Wave Modeling in Water Resources: Surface-water Hydrology*. John Wiley & Sons, Chichester.

GIS-BASED SEMI-DISTRIBUTED HYDROLOGICAL MODELLING OF EXTREME EVENTS IN A FORESTED MOUNTAINOUS CATCHMENT

R. Ramsankaran[1, 2], U.C. Kothyari[1], S.K. Ghosh[1] and A. Malcherek[2]

[1] Department of Civil Engineering, Indian Institute of Technology Roorkee, Roorkee 24667, Uttarakhand, India

[2] Institute of Hydro Sciences, German Federal Armed Forces University Munich, Werner-Heisenberg-Weg 39, 85577 Neubiberg, Germany

Corresponding author: Raaj. Ramsankaran – Visiting scholar during 01.10.07-30.9.08 at the Institute of Hydro Sciences, German Federal Armed Forces University Munich, Werner-Heisenberg-Weg 39, 85577 Neubiberg, e-mail: ramsankaran_raaj@yahoo.co.in

ABSTRACT

This paper presents a GIS-based hydrological modelling study and its preliminary results obtained for simulations of several heavy rainfall events that occurred in an ungauged forested Himalayan catchment. In the study, the modelling was done in a semi-distributed manner based on sub-basin discretization designed to capture actual landscape characteristics. The modelling begins by subtracting an empirically-based initial loss caused by the interception of rainfall by vegetation before infiltration is calculated. Next, the Green-Ampt Infiltration hypothesis is adopted for the computation of runoff volumes which are then transformed into direct runoff using the unit hydrograph concept developed by the Soil Conservation Service (SCS). The transformed direct runoff is then routed towards the catchment outlet using the Kinematic Wave Model for channel flows. Based on this hypothesis, several unsteady storm events have been identified during the monsoon season of 2005 and simulated. In the case of simulated events, routed runoff hydrographs exhibit reasonably good agreement with values available from observed runoff hydrographs. Considering the simplicity of the modelling approach, the quality of results obtained in this study vividly demonstrates the applicability of the adopted modelling approach. This type of approach to an ungauged catchment designed to produce a "first look" report is quite useful before going into a detailed analysis of catchment processes.

Key words : Heavy intensity events, hydrological modelling, GIS, ungauged catchment

INTRODUCTION

Generally, in developing countries such as India, there is a lack of proper infrastructure in many catchments, many of which have not been studied hydrologically and are only partially gauged. Reliable rainfall and runoff data are not available for many mountainous Himalayan catchments. Among them, there are many which are meteorologically prone to severe cloud bursts. Many Indian catchments also possess topographic characteristics likely to produce extreme floods.

The destruction caused by extreme floods is unusually devastating in terms of the loss of human life, the collapse of natural systems, and the loss of agricultural products. In order to forge the best possible solutions to tackle such vital problems, scientists should possess firsthand information on existing hydrological conditions in catchments of interest before going on to detailed modelling. As no such information is available for many Indian Himalayan catchments, this research study serves as a pilot study initiated to research an ungauged forested hilly catchment called Pathri Rao in the Shivaliks region of the western Himalaya Mountains (Garhwal Himalayas, India).

The Pathri Rao catchment has never been gauged, therefore, process-based or physical modelling approaches such as the following could not be used: TOPMODEL (Beven and Freer, 2001), SHETRAN (Ewen *et al.,* 2000),

CASC2D (Charles *et al*., 2002), LISFLOOD (Van Der Knijff, 2008). Likewise, purely empirical or conceptual models such as IHACRES (Jakeman *et al*., 1990), L THIA (Harbour, 1998), and other simple models may not be suitable for the purpose of simulating extreme events because of their empirical nature.

Keeping the above in mind, a combination of empirical, conceptual, and simplified physical modelling approaches was adopted. This approach is a hybrid approach which attempts to model extreme flood events in a semi-distributed manner. As no such studies exist for the Indian Himalayan region, this paper presents the preliminary results of an unprecedented attempt to model several extreme events that occurred in 2005 in Pathri Rao, a small lower Himalayan catchment located in the foothills of the Shivalik Range of the Garhwal Himalayas (India).

STUDY WATERSHED DESCRIPTION

The Pathri Rao catchment is situated between the latitudes of 29° 06' N and 30° 02' N and the longitudes of 78° and 78° 06' with an elevation ranging from 290 –730 meters above mean sea level, MSL (Fig.1). The area is densely forested and forms a part of the Rajaji National Park region. The catchment is about 25 km^2 in terms of surface area. It receives an average annual rainfall of 1300 mm with an average of 50 rainy days per year. More than 90% of the rain occurs during the monsoon season between June and September. The mean minimum and mean maximum temperature in the region is 3°C and 42°C, respectively. Mean relative humidity varies from a minimum of 40% in April to a maximum of 85% in the month of July. The overall climate of the area can be classified as humid sub-tropical. The soil is mainly a sandy loam type and the soil depth ranges from 0 to 100 cm. The lower tracts beyond the catchment area have flat slopes and are densely inhabited. An automatic rain gauging station was built in the catchment for the purpose of this research study. It records half-hourly rainfall data necessary for hydrological research studies. Likewise a make shift manual gauging station was established at the watershed outlet for observing discharges during the storm events. The station was used to acquire data during the research period in order to produce a comparative study of observed versus simulated flood hydrographs.
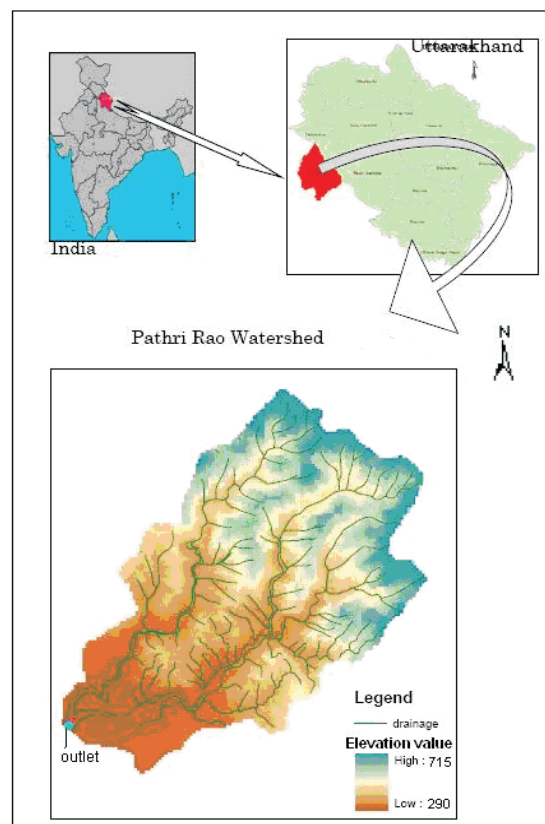
Fig. 1:   Geographic location of the Pathri Rao catchment with a DEM and location of gauging station.

MATERIALS AND METHODS

Data used

- Digital Survey of India toposheet (SOI) at a scale of 1:50,000 with 20 m contour data.
- Hydro-meteorological Pathri Rao catchment data for the year 2005.
- Digital soil map of the Pathri Rao catchment.
- Digital land use map of the Pathri Rao catchment for the year 2005.

Methodology

The hypothesis being put forth in this study is the following: At the beginning of a rainfall event, as rain falls on a vegetated surface, a part of it is held on foliage by surface tension forces. Because it does not reach the soil surface, it has no part in infiltration. The effect of this interception is controlled by two parameters: the interception depth and the fraction of the soil surface covered by intercepting vegetation. The interception depth parameter reflects the average depth of rainfall retained by the particular vegetation type or mixture of vegetation types present on the surface. Accordingly, an interception depth (I) is subtracted from the rainfall before infiltration is calculated. Here, the rainfall rate is reduced until the interception depth (I) has been satisfied. If the total rain falling during the first time increment (At) is greater than I, the rainfall rate is reduced by I/At. If the depth is less than I, the rate is set to zero and the remainder of interception is removed from the rainfall in the following time increments. Next, the Green and Ampt (1911) infiltration approach as described in EM 1110-2-1417 (1994) is used for computing infiltration losses and the obtained excess rainfall is then transformed in each sub-basin outlet using the SCS UH (Soil Conservation Service Unit Hydrograph) transformation approach (NRCS *National Engineering Handbook* 1972). Subsequently, the transformed runoff which enters streams is hydraulically routed towards the catchment outlet using kinematic wave approximations (Singh, 1996) of open surface shallow water equations in order to obtain flood hydrographs. For this purpose, a four point implicit finite difference scheme, as discussed in Fread (1974), is employed.

For this purpose, several geospatial algorithms available in the ArcInfo GIS 9.1 system have been applied to the prepared digital elevation model (DEM) of the catchment to derive sub-basins (Fig. 2) and several corresponding topographic parameters such as slope, longest flow path, and stream length and slope. Based on the digital analysis of soil texture and on land use maps, SCS CNs (Soil Conservation Service – Curve Numbers) are derived and averaged for each of the sub-basins. Likewise, stream parameters have been obtained via a field reconnaissance survey. The details of the derived parameters are reported in Tables 1 and 2. Finally, a few extreme events which occurred in 2005 were simulated using the obtained meteorological data.
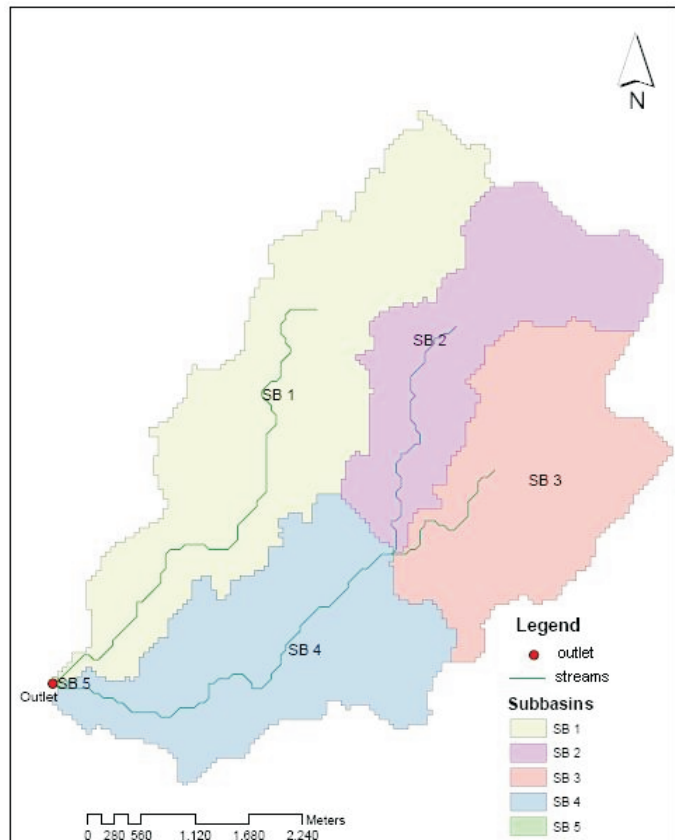
Fig. 2: Discretized sub-basins of the Pathri Rao catchment.

Table 1: Sub-basin topographic parameters.

Element	Area [km²]	Major soil type	Major land use type	Average Curve Number	Fraction of land cover [%]	Interception depth [mm]	Average slope degree	Lag [minutes]
SB 1	8.625	SL	DDF	51.86	50	1.15	27.26	42.0
SB 2	4.89	SL	DDF	54.42	50	1.15	37.40	26.5
SB 3	5.445	SL	DDF	55.34	50	1.15	39.82	21.7
SB 4	5.93	CSL	DC & WL	52.05	35	0.70	12.51	18.4
SB 5	0.505	CSL	DC, WL & DF	82.00	40	0.90	1.28	13.8

SB – Sub-Basin; SL – Sandy Loam; CSL – Coarse Sandy Loam; DDF – Dry Deciduous Forest; DC – Double Crops; WL – Waste Land.

Table 2: Stream routing parameters.

Element	Length [m]	Slope [M/M]	Manning's n	Shape	Bottom width [M]	Side slope [xH: xV]
Stream 1	3752	0.007	0.047	Trapezoid	48	3.0
Stream 2	560	0.003	0.0043	Trapezoid	57	2.8

COMPUTATIONAL PROCESS AND RESULTS

Input data files for all the sub-basins were prepared using GIS analysis. The data file of each sub-basin contains information about average rainfall, slope, lag time, soil type, and land use as well as its associated parameters. Based on the nature of land cover, a rough estimate of initial loss due to interception was prepared. The empirical values of interception depth were taken from Woolhiser *et al.* (1990). Initial water content was quantified using the likely initial soil saturation degree obtained through an analysis of daily rainfall records prior to selected storm events for each of the sub-basins. Next, for each soil type based on the fraction of sand, silt, clay, and organic matter, average initial values of other infiltration parameters such as wetting front depth, porosity, and saturated hydraulic conductivity were derived from work by Rawls and Brakensiek (1989) for each of the sub-basins. For computational purposes, storm events were divided into two groups. The first group of events was "calibration storms" to be used for model calibration. Data from the other group of events referred to here as "verification events" were used for the purpose of model validation. As in Jain *et al.*(2004) and Reddy *et al.* (2007), calibration was performed in order to match peak magnitude, time to peak, and volume of observed and computed runoff by systematically altering the value of parameters dependent on soil type, topography, and land use conditions. Table 3 lists the meteorological information and calibrated infiltration parameters for all the rainfall-runoff events covered in this study. Modelling was performed using the calibrated inputs for the storm events selected for the purpose of validation. The results obtained are shown in Table 4 along with the results obtained for the calibration events. Finally, the model fit is judged by visual matching of observed and computed hydrographs in terms of peak magnitude, time to peak, and hydrograph volume.

In general, the model underestimates runoff volume except for one event that occurred on the 6th of August, 2005. The reason for this may be high antecedent moisture conditions which prevailed before the event in question. The model also underestimates the volume of peak discharge but overestimates the time to peak discharge. The underestimation of peak discharge volume and the delay in computed time to peak discharge in the simulated events may be due to the application of a simplified excess rainfall runoff transformation in each of the sub-basins. Overall, however, the model estimates the shape of hydrographs reasonably well.

Table 3: Meteorological information and calibrated infiltration parameters for all the sub-basins.

Rainfall Event	Rainfall Depth [mm]	Duration [hrs]	~AMC [%]	Volumetric moisture content [ratio]	Wetting front head [mm]	Saturated Hydraulic Conductivity [mm· hr^{-1}]
26.6.05 (c)	36.07	2.5	0.20–0.25	0.335	45	5.6
23.7.05 (v)	40.34	2.5	0.50–0.60	0.182	45	5.6
4.8.05 (v)	39.04	3.0	0.15–0.25	0.355	45	5.6
6.8.05 (c)	24.87	1.5	0.70–0.75	0.151	45	5.6
13.8.05 (v)	11.94	1.0	0.15–0.20	0.382	45	5.6
10.9.05 (c)	17.93	1.0	0.25–0.30	0.325	45	5.6
18.9.05 (v)	73.49	7.0	0.50–0.55	0.213	45	5.6

(c) – Calibrated events; (v) – Validated events.

Table 4: Modelling results for calibrated and validated rainfall–runoff events.

Rainfall events	Total storm runoff [mm]		Peak runoff rate [m^3· sec^{-1}]		Time to peak runoff rate [minutes]	
	Observed	Computed	Observed	Computed	Observed	Computed
26.6.05 (c)	3.84	2.97	14.37	10.63	195	210
23.7.05 (v)	10.73	8.92	23.37	18.07	160	169
4.8.05 (v)	8.34	4.56	31.09	18.11	125	145
6.8.05 (c)	6.41	7.54	37.80	37.39	115	127
13.8.05 (v)	2.56	2.47	13.30	10.33	190	240
10.9.05 (c)	2.75	2.55	12.27	10.91	125	140
18.9.05 (v)	17.34	14.41	42.19	34.66	215	245

(c) – Calibrated events; (v) – Validated events.

SUMMARY AND CONCLUSIONS

An empirical, conceptual, and simplified physical modelling approach, called a hybrid approach, was proposed in this paper. This approach operates in a semi-distributed manner using GIS and has been applied to a number of extreme rainfall events in an ungauged forested hilly catchment. The interception loss component of the developed model is treated empirically rather than physically. The process of infiltration and the subsequent generation of runoff, which is more relevant in determining the quantity of runoff, are treated physically using empirical parameters. The transformation of runoff towards each sub-basin outlet is treated conceptually using the SCS UH Method. Finally, the runoff routing component, which is more relevant in determining the time to peak and the quantity of peak volume, is modelled physically using the well established kinematic wave theory. In general, the preliminary results obtained using the above modelling approach provide satisfactory results. In conclusion, it can be stated that the information obtained via this approach can serve as a first guess about the existing hydrological characteristics of a catchment. This information can be useful for planning catchment management activities. Likewise, the stated requirement of fewer inputs and less complex mathematical formulations makes this modelling approach an efficient way to describe future extreme events using assumed scenarios.

REFERENCES

Beven K.J. and Freer J. (2001). A Dynamic TOPMODEL. *Hydrol. Process.*, **15**(10): 1993–2011.

Charles W.D., Fred L.O., William D.M. and Russell S.H. (2002). Theory, development, and applicability of the surface water hydrologic model (CASC2D). *Hydrol. Process.*, **16** (2): 255–275.

Ewen J., Parkin G. and O'Connell E. (2000). SHETRAN: distributed basin flow and transport modelling system. *J. Hydrol. Eng.*, **5**(3): 250–258.

Fread D. L. (1974). *Numerical properties of implicit four-point finite difference equations of unsteady flow*. NOAA Technical Memorandum NWS HYDRO-18.

Green W.H. and Ampt G. (1911). Studies on soil physics, 1. The flow of air and water through soils. *J. Agr. Sci.*, **4**(1): 1–24.

Harbor J., Grove M., Bhaduri B. and Minner, M. (1998). Long-Term Hydrologic Impact Assessment (L-THIA) GIS. *Public Works*, **129**: 52–54.

Jain M.K., Kothyari U.C. and Raju K.G.R. (2004). A GIS-based distributed rainfall-runoff model. *J. Hydrol.,* **299**: 107–135.

Jakeman A.J., Littlewood I.G. and Whitehead P.G. (1990). Computation of the instantaneous unit hydrograph and identifiable component flows with application to two small upland catchments. *J. Hydrol.*, **117:** 275–300.

National Soil Conservation Service (1972). *National Engineering Handbook*, Section 4: *Hydrology*. USDA, Springfield, VA.

Rawls W.J. and Brakensiek D.L. (1982). Estimating soil water retention from soil properties. *J Irrig. Drain. Div*, ASCE, **108**(IR2): 166–171.

Singh V.P. (1996). *Kinematic wave modelling in water resource resources: surface water hydrology*. New York: Wiley: 1399 pp.

U.S. Army Corps of Engineers. CECW-EH. (1994). *Engineering and Design - Flood-Runoff Analysis*, Chapter 6, Manual. No. EM: 1110–2–1417.

Van Der Knijff J.M., Younis J. and De Roo A.P.J. (2008). LISFLOOD: a GIS-based distributed model for river basin scale water balance and flood simulation. *Int.J. Geogr Inf. Sci.*: 1365–8816.

Venkata Reddy K., Eldho T.I., Rao E.P. and Hengade N. (2007). A kinematic-wave-based distributed watershed model using FEM, GIS and remotely sensed data. *Hydrol. Process.*, **21**(20): 2765–2777.

Woolhiser D.A., Smith R. E., Sharif H.O. and Goodrich D.C. (1990). KINEROS, a kinematic runoff and erosion model: documentation and user manual. *ARS-77,* U.S. Dept. of Agriculture, Agricultural Research Service.

DETERMINISTIC-STOCHASTIC MODELLING
OF HYDROLOGICAL EXTREMES IN SMALL BASINS

O. M. Semenova

Department of Experimental Hydrology and Mathematical Modelling of Hydrological Processes,
State Hydrological Institute, 2-ya liniya V.O. 23, 199053, Saint-Petersburg, Russia,
e-mail: omakarieva@gmail.com

ABSTRACT

This paper presents the results of deterministic-stochastic modelling performed for small basins situated in different landscape and climate zones of Russia. The main features and advantages of an applied universal deterministic-stochastic modelling system (DSMS) developed at the State Hydrological Institute (St. Petersburg, Russia) are discussed.

Keywords: distributed hydrological modelling; principle of universality; the "Hydrograph" deterministic hydrological model; stochastic model of weather; distribution curves

INTRODUCTION

The development of new hydrological approaches for use in research and designed to produce forecasting tools is necessary for the purpose of proper management of water resources under current conditions of high risk of extreme weather events.

Although two fundamental approaches in runoff modelling – deterministic and stochastic – are distinguished, it is the latter approach, based on well-developed mathematical means and reasonable computational complexity, that predominates in engineering calculations, at least in Russia (Code of Rules…, 2004). The main applied task of this approach is the extrapolation of observed flow data in an effort to obtain exceedance probabilities of runoff. However, the use of this method is not fully justified under the changing conditions in the investigated basins. This method must not be used for ungauged basins.

Therefore, a combined deterministic-stochastic approach to the modelling of runoff formation processes is proposed. Here the stochastic models stand as auxiliary features to deterministic models providing them with stochastic input. One example of this is the generation of meteorological forcing fields for use in runoff formation models. Using estimated parameters that represent features of landscape, a deterministic model simulates runoff characteristics. Next, empirical probability distribution functions of annual, monthly, and daily runoff characteristics (including extreme values) are calculated for any past, present or future conditions, taking into consideration climate and landscapes changes.

At this stage, a wide spectrum of approaches and corresponding hydrological models has been developed for the purpose of qualitative description and numerical modelling of hydrological systems. However, it must be noted that many approaches do not necessarily have a universal character and are oriented primarily towards the description and modelling of specific river basins and/or single runoff formation processes. Other models may have a universal applicability but require extensive calibration of parameters. In both cases, the application of such models is limited in ungauged or poorly gauged basins. The fundamental laws of physics require that the process of runoff formation must be the same at any point in space. This implies that the mathematical theory and parameters must be the same for any set of conditions if the model adequately represents natural processes. It follows, then, that models of limited applicability, or with parameters with no physical meaning, present a conflict with the fundamental laws of physics.

The main objective of the research presented herein was the investigation of the possibility of using a single hydrological modelling system and unified informational approach in deterministic-stochastic simulations of extreme hydrological events in small basins situated in different climate and landscape zones. To meet this research objective, ten basins representing different landscape characteristics within the territory of the former USSR were selected (Table 1).

Table 1: Description of basins used in the research study.

No.	River; Outlet	Area [km²]	Geographic location		Landscapes
1	Manga; Manga	243	Karelia, the Onega Lake basin		European boreal forests
2	Nyashenniy; Kotkino	16.1	Nenets district; northern European part of Russia		Tundra
3	Pyasedey-Yaha; 27 km from mouth	113.6	Yamal Peninsula coast		Tundra
4	Tanalyk; Samarskoye	1750	Bashkiria, South Ural Foothills		Steppe
5	Varzob; Dagana	1270	The Kafirnigan and Amudarya river basins; Central Asia		Mountains
6	Timpton; Nagorniy	613	The Stanovoy Range		Mountainus larch taiga
7	Kataryk; Toko	40.2			Mountainous southern taiga, swamps
8	Ebytiem; Ebytiem	1000	The Lena River mouth area	Eastern Siberia	Mountainous tundra headwaters and downstream taiga
9	Suntar; the Saharynya River mouth	7680	The headstreams of the Indigirka River, the Suntar – Hayata Range		Alluvial rocks, mountainous tundra, sparse larch forest
10	Tenke; 2.2 km from Nilkoba River mouth	1820	The headstreams of Kolyma River		Mountainous tundra and taiga

THE DETERMINISTIC-STOCHASTIC MODELLING SYSTEM

The Deterministic-Stochastic Modelling System (DSMS) developed at the State Hydrological Institute (St. Petersburg, Russia) under the guidance of Prof. Yu.B. Vinogradov (Vinogradov and Vinogradova, 2008) was employed in this research work. The DSMS consists of two elements: a deterministic model of runoff formation processes called "Hydrograph" and the Stochastic Model of Weather (SMW). The main feature and advantage of the DSMS is the fact that this system was developed based upon the principle of universality, that is, the possibility of its application to basins of different sizes existing in any physical and geographic conditions without change of model structure. The DSMS uses the simplest meteorological information from weather observation networks such as daily values of air temperature, air moisture deficit, and precipitation.

The "Hydrograph" Deterministic Model

The "Hydrograph" distributed hydrological model is a physically-based runoff formation modelling system. Being constructed on the basis of a general approach to describe runoff formation processes, it covers all types of flow and can be used for simulations of any basin, regardless of its landscape type and size. The model algorithm includes the following computation routines: precipitation interception, snow accumulation and melting, total evaporation, surface flow and infiltration, soil water dynamics and soil flow, heat dynamics and phase change in soil layers, subsurface flow formation, slope and channel flow transformation, and flow discharge.

The parameters and characteristics of the model have a spatial and vertical distribution. Basin schematization is based on an application of a representative point system. This approach, combined with the concept of runoff

elements (Vinogradov, 2003a, 2003b; Vinogradov and Vinogradova, 2008), avoids traditional differential equation schemes that describe water movement such as the kinematic wave for surface and channel flow and the Boussinesq Equation for groundwater. The model calculates all processes and variable states with time intervals of 24-hours or less, depending on the available meteorological inputs.

Model parameters can be divided into five groups:
- Water and physical characteristics of soil layers (density, porosity, specific heat capacity and conductivity, filtration coefficient, maximum water capacity);
- Characteristics of vegetation cover (shadow fraction, albedo, evapotranspiration coefficients, interception rate, phenological dates);
- Nature of slope surface (depression storage, index of snow redistribution over land, hydraulic parameters of surface and subsurface runoff elements);
- Groundwater conditions (distribution indices of incoming water content between modelled groundwater layers and hydraulic coefficients),
- Climate peculiarities.

The model output consists of continuous runoff hydrographs recorded at the basin outlet or in any part of a basin or specified landscape; state variables distributed across the basin reflecting water and heat dynamics in soil layers and snow cover; spatial and temporal distribution of water balance elements including precipitation, transpiration from snow, soil and vegetation cover, as well as surface, subsurface and underground runoff.

The concepts used as a basis for the "Hydrograph" Model – both algorithms and features – are discussed in detail in (Vinogradov, 2003a, 2003b; Vinogradov and Vinogradova, 2008).

The Stochastic Model of Weather (SMW)

The SMW provides simulated meteorological input for the "Hydrograph" Model. Using the Monte-Carlo Method, it generates a series of random numbers that correspond to consecutive daily precipitation sequences, average daily temperatures, and moisture deficits at different points within river basins, taking into account temporal and spatial correlations between meteorological elements and characteristics of their annual variability (Vinogradov and Vinogradova, 2008).

A simulation is performed for a system of representative points (RP) which are distributed according to the nodes of a hexagonal grid covering the basin area. The size of spatial intervals in this grid is determined by basin size and availability of parametric and meteorological inputs.

All SMW parameters are estimated using daily observational data from meteorological stations and are then interpolated into RPs. It is assumed that for the estimation of suitable and stable parameters (especially where it concerns precipitation characteristics), a period of observations of at least 25–30 years is required. The SMW parameters are derived from the climate characteristics of an area. The system of SMW parameters can be divided into three large groups. The first group represents annual parameters, the second group daily parameters and the third group describes the spatial distribution of, and correlations between, parameters. Temporal correlations are preserved because of the explicit consideration of sequentially adjacent members in the time series. Spatial correlations are preserved between nearest neighbors among RPs.

The process of stochastic modelling is as follows: Precipitation is estimated at each RP. At the same time, the presence or absence of precipitation the day before is taken into consideration. If precipitation occurs at an RP, then its daily value is generated. Next, the simulation of daily values of mean air temperature and relative humidity is performed taking into account the current day's precipitation. The meteorological conditions at three neighbouring previously calculated RPs have an effect on the RP currently being analyzed.

Since at most meteorological stations only 20–80 % of precipitation events within the 0–1 mm range are recorded and the annual amount of the precipitation (80–90 %) is determined by the events exceeding 1 mm, the SMW considers the distribution of daily precipitation to be truncated at 1 mm.

The SMW deals with the modelling of relative humidity by factoring its value into the moisture deficit at a given air temperature.

RESULTS

Deterministic-stochastic modelling was performed for small basins situated in different landscapes zones of Russia such as taiga, tundra, steppe, and mountain areas. The model's minimum verification period lasted 3 years for some basins while for others it was more than 20 years (1959-2005).

First, the effectiveness of deterministic modelling was evaluated. The analysis included a simulation of runoff formation processes using daily computation intervals. The evaluation of the model's performance was based on a comparison of observed flow values and (where available) soil and snow state variables. Sample observed *vs* simulated hydrographs are shown in Fig.1. Different types of water regimes allow for the evaluation of the universality of the proposed model which is used with a wide variety of conditions without changing its structure by taking them into account through the use of appropriate parameters. Four of the analyzed basins are situated in the zone of continuous permafrost but actually have completely different factors that govern the specific nature of their runoff processes.
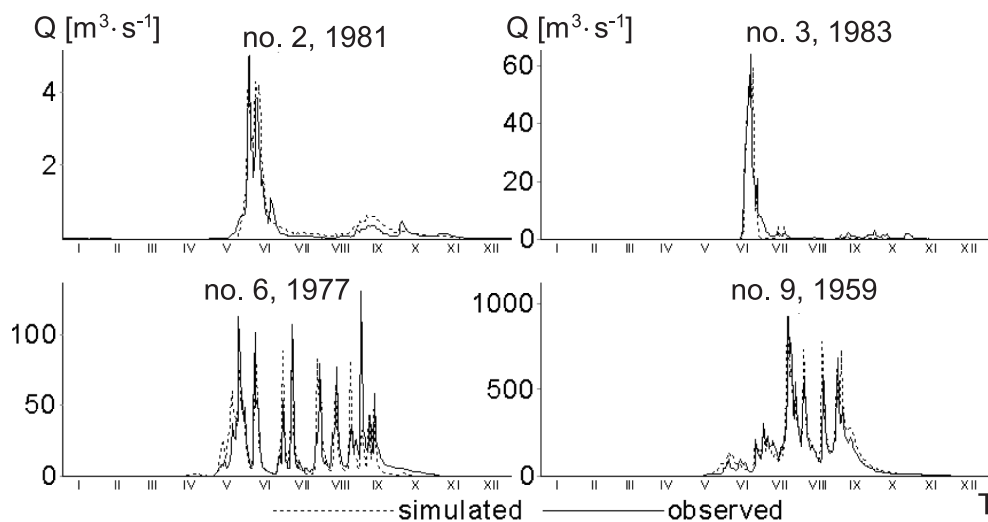
Fig. 1: Observed and simulated hydrographs [$m^3 \cdot s^{-1}$] for four small basins. The above numbers correspond to basin numbers in Table 1.

A thin active thaw layer as well as numerous little lakes, puddles, and surface depressions in conditions of almost flat relief in basins no. 2 and no. 3 result in considerable accumulation of water at the basin surface and slow flow through the drainage network. High runoff values derived from melting snow water are typically observed at the end of spring and are represented primarily by the subsurface flow component.

Basins numbered 6 and 9 are mountainous with an average altitude above sea level of 1000 m for basin no. 6 and 1500 m for basin no. 9. The orographic structure of the basins influences the intensity of runoff processes: altitude, exposure and slope inclination determine the level of incoming solar radiation and the precipitation distribution. The spring flood season is not always clearly defined and is interrupted by rain floods which can have maximum values of peaks and volumes. Numerical experiments and simulation results indicate that there is no surface flow and runoff is mainly formed by rapid ground-type flow. On the other hand, some processes and their reflection in the model structure had to be accounted for in both groups of selected basins. These processes are snow redistribution and thermal processes in the soil matrix.

The Nash-Sutcliffe efficiency for runoff (Nash and Sutcliffe, 1970) exceeds 0.60 for all the studied basins, and in the case of four of them, it exceeds 0.75. It is considered to be a satisfactory result, considering the limitations involved. These were rooted mainly in meteorological forcing data, particular precipitation, which were poor in many cases. A comparison of observed and simulated basin state variables is shown in Fig. 2, indicating a good level of convergence in the case of soil temperature at different depths as well as snow water equivalent values (the example given is for basin no. 4).
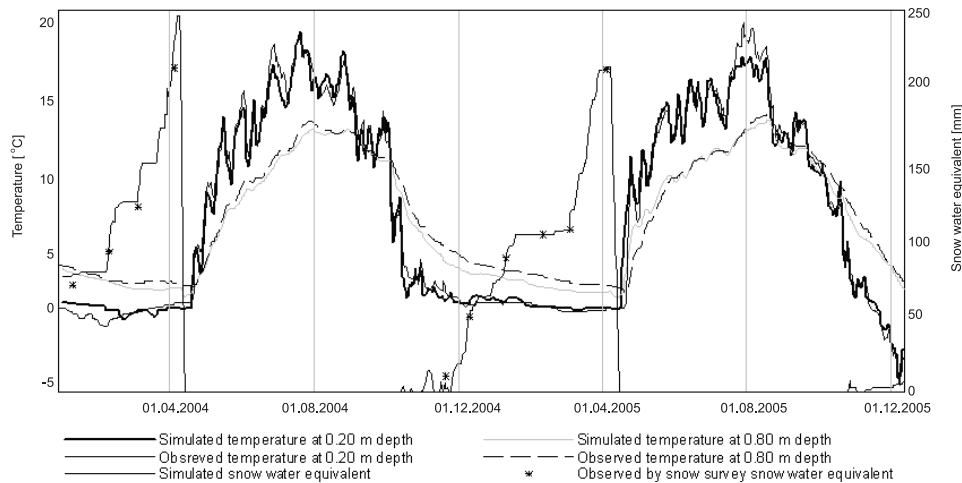
Fig. 2:　　　　Observed and simulated basin state variables (basin no. 4).

SMW parameters were estimated based on daily meteorological data. The weather simulation was carried out for a period of 100 years. In order to assess the performance of the SMW, the model parameters for the simulated series were evaluated and compared with observations.

The precipitation layer still remains the most important and difficult to simulate forcing component. This conclusion is based on the fact that not only do layer values have to be taken into account but also the uneven distribution of solid and liquid phases throughout the year has to be factored in. Figure 3 shows an example of observed and simulated distribution curves of daily precipitation layers for the Toko meteorological station (basin no. 7).
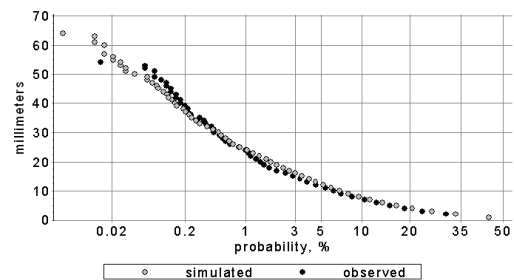
Using simulated runoff hydrographs, distribution curves for daily flow, annual mean, maximum and minimum flow are obtained. Figure 4 presents observed and simulated distribution curves of runoff characteristics for several basins under investigation. It is important to note that the data used were data that were available in all basins. Using weather and streamflow observations, at resolutions higher than one day, most likely would result in different instantaneous peak flows, especially for the smaller basins. For the purpose of this research, peak flows should be understood as "daily peak flows" as opposed to "instantaneous peak flows".

Fig. 3:　Observed and simulated distribution curves of daily precipitation layers for the Toko meteorological station (basin no. 7).

The mean relative error (its absolute value) between observed and simulated distribution curves of daily flow varies from 5 to 27 percent for different basins. The length of the observation period has a substantial influence on error values. For series of observation periods longer than 30 years, the error was less than 10% which can be considered a good result. On the other hand, for the basin with just 7 years of flow observations, it amounted to a sizable value of 27%.
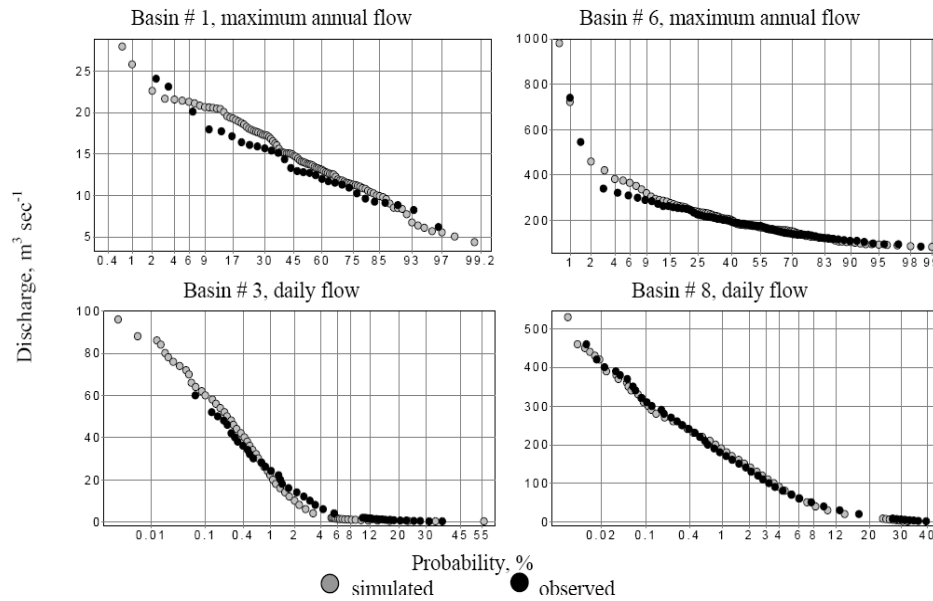
Fig. 4:   Observed versus simulated empirical distribution curves of extreme flow characteristics.

CONCLUSIONS

The results of deterministic-stochastic modelling performed for small basins with different climate and landscape conditions have shown that the output of such a modelling system is highly reliable in comparison to observational data. Some of this success can be attributed to the strong physical basis of this modelling system which includes robust algorithms and a universal structure of the DSMS that can be used in any type of basin without changing the structure of the simulation model.

The method proposed herein can be applied to a wide range of eco-hydrological tasks geared towards the design and safe operation of engineering infrastructure as well as water management in conditions of flood risk. The actual task of factoring in the influence of climate and landscape impact on water resources is quite easy given the adaptable framework of the DSMS. Any number of climate variability scenarios can be taken into account via the introduction of corresponding parameters into the SMW while changes in landscape properties can be reflected via appropriate parameters utilized by the "Hydrograph" deterministic model.

REFERENCES

Code of Rules for Engineering Design and Construction SP 33-101-2003 (2004). *The estimation of main computational hydrological characteristics*. Gosstroy Rossii, Moscow: 73 pp.

Nash J.E. and Sutcliffe J.V. (1970). River flow forecasting through conceptual models: 1 A discussion of principles. *J. Hydrol*., **10**(3): 282–290.

Vinogradov Yu.B. (2003a). River Runoff Modeling in Hydrological Cycle. In: Shiklomanov I.A. (ed.), *Encyclopedia of Life Support Systems (EOLSS)*, Developed under the auspices of the UNESCO, EOLSS Publishers, Oxford, UK, http://www.eolss.net.

Vinogradov Yu.B. (2003b). Runoff Generation and Storage in Watersheds in the Hydrological Cycle. In: Shiklomanov I.A. (ed.), *Encyclopedia of Life Support Systems (EOLSS)*, Developed under the auspices of the UNESCO, EOLSS Publishers, Oxford, UK, http://www.eolss.net.

Vinogradov Yu.B. and Vinogradova T.A. (2008). *Distributed modelling in hydrology*. Academia Publishers, Moscow: 320 pp. (in Russian, in press).

CONCEPTUAL RAINFALL-RUNOFF MODELS VERSUS FIELD OBSERVATIONS DURING FLOOD EVENTS ON THE SMALL GRANITIC STRENGBACH CATCHMENT (VOSGES MASSIF, NORTH-EASTERN FRANCE)

D. Viville[1] and G. Drogue[2]

[1] *EOST-Centre de Géochimie de la Surface (UMR 7517-CNRS/StrasbourgI), 1, rue Blessig, F-67084 Strasbourg Cedex, France, e-mail : dviville@illite.u-strasbg.fr*

[2] *CEGUM,UFR SHA, (U. Paul Verlaine), Ile du Saulcy, F-57045 Metz Cedex, France, e-mail : drogue@univ-metz.fr*

ABSTRACT

In order to test the ability of parsimonious conceptual rainfall-runoff (CRR) models to reproduce flood discharges during low flows conditions on a small (0.8 km²) granitic forested temperate catchment, a hydrological modelling exercise has been undertaken on a set of flood events having affected this catchment. Two CRR models have been run at an hourly time step against the data set available on the 1989–1997 period: the reservoir-based GR4 RR model and the TOPMODEL RR model based on a distributed topographic index used to simulate hydrological processes, especially the dynamics of surface or subsurface contributing areas. Notwithstanding an overall satisfactory ability to reproduce the entire hydrographs, the two tested model structures and assumptions are not able, in certain conditions, to account fully for the complexity of the physical processes involved in flood generation for low flows conditions in the small granitic Strengbach catchment.

Key words: Hydrological models, GR4, TOPMODEL, Strengbach catchment, flood events, field observations

INTRODUCTION

Parameterization and prediction capability of conceptual rainfall-runoff models (CRR) are usually assessed on the basis of their ability to correctly predict lumped hydrograph at catchment outlet. But in some cases, good hydrograph predictions hide actually a poor representation of hydrological patterns and/or internal filling states of catchment flow contributing reservoirs. In other words, a CRR might be efficient for flood prediction but for the wrong reasons. Therefore, the aim of this paper is to give insights regarding two questions : i) Do CRR models offer a satisfying conceptualization of processes and reservoirs involved in flood generation during low flow conditions in a small (0.8 km²) granitic forested temperate catchment? ii) Do hard data (discharge data, groundwater data, etc.) and soft data (isotope tracers, qualitative expertise on hydrological processes, etc.) offer opportunities to improve conceptual RR model structures and parameterizations for better reproducing observed flood hydrographs after a low flow period?

STUDY AREA AND EXPERIMENTAL FLOOD DATA

The granitic Strengbach catchment is a small mountainous experimental catchment of 0.8 km² drainage area located in the Vosges Massif, North-eastern France (Fig. 1). The geological substratum consists of a base-poor leuco-granite, which supports shallow (i.e. <9 m) superficial formations and brown acidic soils.The catchment is mainly covered by Norway spruce. Mean annual precipitation reaches 1400 mm, whereas mean annual runoff is of approximately 850 mm (21.5 dm³·s⁻¹). A connected to the stream variable water saturated area (whose extension can represent up to 3% of the catchment area for a 128 dm³·s⁻¹ discharge), is mainly located on the southern slope, close to the outlet (Fig. 1)''. This location of the water table can be explained by the highest storage capacity of the southern side which is longer, less inclined and covered by thicker superficial formations

than the northern side. The Strengbach main brook is gauged at the outlet (RS) and also upstream at site RAZS which defines a 0.55 km² subcatchment. From 1996 to 1999, groundwater level fluctuations were continuously recorded at piezometers (A, D) located on the southern side at a 30 minutes time step. The equipment of the basin also includes an automatic weather station located on the top of the basin.

A direct method of model control consisting in comparing calibrated parameter values and internal variable states (e.g. reservoir levels) with experimental data to assess how reasonable they are based on field experience, three well-documented floods with hard data (discharge and two groundwater level series) and soft data (contribution of pre-event and event-water throughout the flood, extension of saturated areas) occurring during the low flow period has been preferentially selected (i.e. floods of July 1995, July 1996 and October 1997).

Fig.1: Location and monitoring network of the Strengbach granitic catchment.

DESCRIPTION AND IMPLEMENTATION OF THE CRR MODELS

The GR4 RR model

Structural formulation

The GR4 continuous RR model used in this study corresponds to the hourly version of the daily time step GR4 RR model which is a lumped parsimonious four-parameter RR model (Perrin *et al*., 2003). The hourly version has the same structural formulation as the daily version and differs only through little changes in fixed parameter values for the percolation function, the drainage function of the soil reservoir, and the unit hydrographs.

Through the GR4 RR model, the river catchments are represented by two reservoirs, a soil reservoir and a routing reservoir. After an interception step, the rainfall is divided into a component filling the soil reservoir (drained either by evapotranspiration or by deep percolation), and a component routed to the outlet via a transfer function. This net rainfall is divided into two parts; the first one (90%) is routed by a unit hydrograph UH1 and fills the routing reservoir, the second is routed by a unit hydrograph UH2 and generates the quickflow. The drainage of the non-linear routing reservoir generates a baseflow. A groundwater exchange term that acts on both flow components is also incorporated into the model for simulating catchment water exchange. In order to adapt the model to each particular catchment, four parameters have to be optimized: i) the maximum capacity of the soil reservoir (A) [L], ii) the maximum capacity of the routing reservoir (B) [L], iii) the time to peak of the unit hydrographs (C) [T], iv) the water exchanges term coefficient (D) [L].

Input data

The model calibration was carried out using observed hourly rainfall, PET and discharge data. PET has been determined according to the temperature based on Hamon's formula (Hamon, 1961). The differential split-sample test was performed on the available data set; period 1 (6-y) extended from January 1989 to December 1994 and period 2 (4-y) extended from January 1994 to December 1997. For both periods, the first year was used as a warm-up period to initialize the reservoir levels of the RR model. As the GR4 RR model version we used did not incorporate any snowmelt module, snowfall and snowmelt periods were excluded from the data sets.

Optimization of the RR model parameters

Mathevet (2005) found that local methods of optimization are as efficient as global methods at the hourly time step; the four free parameters of the GR4 RR model were therefore automatically optimized through a step-by-step local method of optimization using a direct start (i.e. the starting point of the optimization is determined through a selection of the best parameter vector among 27 possibilities). As we focused our attention on the ability of the structural formulation as well as internal state variables of the GR4 model to reproduce small flood dynamics during low flow conditions, the objective function used for model calibration was the Nash-Sutcliffe coefficient calculated on the logarithmic transformed flows. Indeed, according to the comparison test performed by Oudin *et al.* (2006), this objective function is ensuring to obtain the most efficient model parameterization for reproducing low flow periods both in calibration and in control mode.

The TOPMODEL RR model

Structural formulation (Donnelly-Makowecki and Moore, 1999)

TOPMODEL represents catchment topography by means of the frequency distribution of a topographic index, $\ln(a/\tan\beta)$, where a is the area drained per unit contour length and β is the local slope angle. In the original version of TOPMODEL, the RR model represents catchments using one linear and one nonlinear storage for each $\ln(a/\tan\beta)$ increment. For each increment, water input first enters the unsaturated zone store (uzs_i) where it then flows vertically to the saturated zone store (szs_i) at a rate $q_{vi} = uzs_i/(td S_i)$ where the parameter td is the unsaturated zone time delay [T], and S_i is the subsurface storage deficit [L], which is equivalent to the quantity of water required to fill the unsaturated store to saturation. The saturated zone acts as a nonlinear reservoir, with the baseflow discharge, Q_b, determined by :

$$Q_b = T_0 \tan\beta \exp(-\overline{S}/m)$$

where T_0 [L^2·T^{-1}] is the lateral transmissivity, $\overline{S}$ the mean catchment moisture deficit [L], and m [L] a parameter that controls the exponential decline of saturated transmissivity with depth. Saturation overland flow, Q_{of}, is generated when the saturation deficit for an increment becomes zero. The frequency distribution of the topographic index is used to compute the fraction of the catchment that generates saturation excess overland flow. For each hourly time step, contributions of Q_b and Q_{of} are summed to give a total discharge for the catchment.

Input data

As we used the original limited Windows version (97.01) of TOPMODEL (i.e. 2500 hourly time steps $\cong$ 3.5 months, 100 x 100 grid cells) provided by the Lancaster University (Beven, 1997a), the model calibration was run with the same data set than for GR4 but twice with two different 3-months periods of low flow conditions (summer 1995 and summer 1996). The model was controlled on the third available low flow period of 1997 (from August to October). The calculation of the topographic index is based on the multiple flow direction algorithm of Quinn *et al.* (1995) and a 14-m grid size DTM.

Optimization of the RR model parameters

With the implemented TOPMODEL version, five parameters have to be calibrated: i) m : the parameter of the exponential transmissivity function or recession curve [L], ii) T_0 : the effective transmissivity of the soil when saturated [L^2·T^{-1}], iii) *S*Rmax : the soil profile storage available for transpiration [L], iv) *S*Rinit : the initial

storage deficit in the root zone [L], v) ChVel: an effective surface routing velocity for scaling the distance/area [L/T]. The optimal values of model parameters have been selected according to a sensitivity analysis applied to each of them with the Nash-Sutcliffe coefficient as objective function.

RESULTS

RR model parameterizations and efficiency

Optimal parameter values obtained for the two CRR models are summarized in Table 1. The numerical values of the model parameters and NSC coefficients were almost the same for GR4 through the differential split sample test with a lower efficiency for the control period (0.59 for period 2; 0.58 for period 1). The optimal value found for the B parameter is representative of catchments having a high storage capacity if we refer to regional investigations made between physiographic catchment characteristics and GR4 RR model parameters (Lang, 2007). As expected, TOPMODEL efficiency appears to be very sensitive to m and Srmax values, which are in the range of previous studies performed with TOPMODEL on similar catchment sizes (see Beven, 1997b for a review).

Table 1: Parameter sets and calibration efficiency for GR4 RR
and the original version of TOPMODEL. (NSC = Nash-Sutcliffe efficiency Coefficient).

GR4			TOPMODEL				
Parameters	Initial values and range	Optimized values	Parameters	Initial values	Run 1 (summer 95)	Run 2 (summer96)	Estimated field values
A [mm]	400 (100–1000)	187	m [mm]	32	23	29	250
B [mm]	100 (10–1000)	384	T_0 [m².h⁻¹]	148	2.5	2.5	10
C [h]	24	4.3	Srmax [mm]	50	65	65	100
D [mm]	-1 (-3–0)	-7.1	Srinit [mm]	400	400	400	
			ChVel [m·s⁻¹]	1	1	1	0.1
NSC		0.68			0.66	0.84	

Looking at selected flood hydrographs, we see that for the small flood of July 1995, maximum peak discharge and storm flow volume are both underestimated, especially for TOPMODEL which produces no saturation excess overland flow (Fig. 2a). The estimations are slightly better for the two other selected floods generated by higher rainfall amounts, especially for the time to peak. Nonetheless, the second observed delayed peak discharge of the flood of July 1996 that had occurred 4 days after the first one, is mismatched both by GR4 RR and TOPMODEL (Fig. 2b).
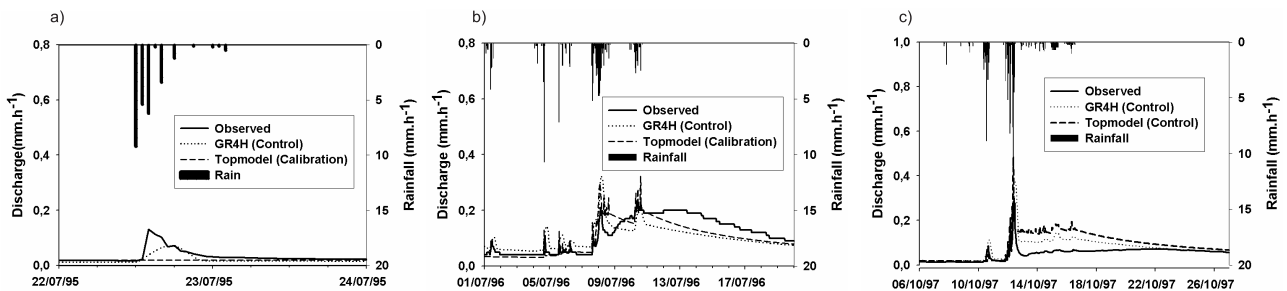
Fig. 2: Observed vs simulated hydrographs for the floods of July 1995 (a), of July 1996 (b) and of October 1997 (c)

Last, a visual comparison of the TOPMODEL simulated hydrograph to the observed one for the control flood of October 1997 reveals that the temporal structure of the observed rising limb seems to be well fitted. Meanwhile, both the main peak discharge and base flow in recession are largely overestimated (Fig. 2c).

DISCUSSION

The two models seem to be able to predict the rapid responses of the stream to the rainfall but they are unable to simulate the delayed responses of the groundwater, which occur several hours or days after the rainfall event.

Structural formulation of the RR models

For moderate wet antecedent conditions and a small rainfall event, (i.e. July 95), the GR4 RR model produces mainly quickflow originating only from the soil reservoir (Fig. 2a). Field observations and flood analysis have shown that, indeed, the hydrological response is generated by the foot-slope/riparian reservoir of small spatial extension (Tab. 2) affected by groundwater ridging, the latter providing the main source of water during

Table 2: Characteristics of the events: amount of precipitation and duration, runoff-precipitation rate (Q/P), Initial Discharge (Q0), Antecedent Precipitation Index for the 20 previous days (API).

	Total Precipitation [mm]	Duration [h]	Q/P [%]	Q0 [mm·h⁻¹]	API 20 [mm]
July 95	30	7	3	0.02	70
July 96	48	20	8	0.04	110
October 97	62	15	4	0.01	4

the flood (i.e. pre-event water). Nevertheless, during this event, measured contribution (determined from tracers) of pre-event water was around 68% vs 32% for event water (Viville *et al*., 2003), whereas the GR4 RR simulated a contribution of the assimilated event water to the flood close to 90%. Concerning TOPMODEL, the choice of the best set of parameters - which is based on the NSE criterion and discharge values does not permit to describe adequately the extension of the saturated area (Tab. 3). This is due to the set of parameters which is spatially uniform, thus not taking into account the local variabilty of the topography as well as the small amount of rainfall which is not sufficient to saturate the soil profile.

Table 3: Extension of saturated areas (% of total catchment area) derived from observations and from TOPMODEL for three flood events.

	Observations	TOPMODEL
July 1995	0.7	0.0
July 1996	1.8	3.2
October 1997	1.7	3.2

For wet antecedent conditions and great rainfall amounts (i.e. July 96), it can be seen on Figure 2b that there is a delayed contribution of the upstream part of the basin (RAZS) still providing water to the catchment outlet (Viville and Gaumel, 2005) several days after the first peak flow (Fig. 3).

The volume of the flood seems to be well predicted (for the first peakflow) but not the temporal distribution by both RR models and the structure of the latter does not permit to fit the delayed rising occuring at a later stage. The high variability of the time response of the contributing areas to the rain is not taken into account and explains the non-capacity of both models to predict the delayed rising.
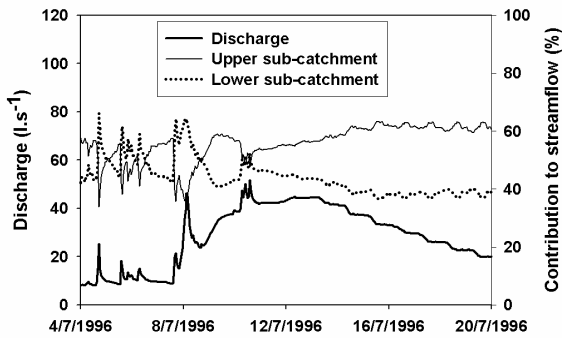
Fig. 3: Contribution of sub-catchments to the total streamflow at the outlet for the flood of July 1996.

TOPMODEL overestimates the spatial extension of the saturated areas and the sharp peak discharge magnitude. Moreover, in the second part of the flood, considering a decreasing value of S (1), the model calculates a decreasing value of Qb and presents a recession, while the field observations indicate a continuous slope sub-surface flow during this period.

For October 97, during the rising limb, the first two peaks are generated by rainfall intensity variations and saturated excess overland flow. Later on, the rainfall intensity variations are no longer replicated and the third peak is generated by saturated excess overland flow and subsurface flow. Even though the shape of the main peak flood is correctly simulated by GR4 RR, the first two peaks generated by rainfall intensity variations during the rising limb are smoothed, contrary to TOPMODEL, which reproduces well the response of saturated areas to rainfall variations but fails to simulate the subsurface flow.

Optimal parameter values and internal state variables vs field observations

The moisture rate of the GR4 RR soil reservoir is a good indicator of the hydric state -except for the flood event of July 1995- of the riparian zone which reacts rapidly to the rain (Fig. 4a). The dynamic of the routing reservoir - which reacts slowly - is well represented by the foot-slope piezometer (A) (Fig. 4b). Comparison of TOPMODEL patterns of hydrological responses to field observations shows a clear deviation from the observed extent of saturated contributing areas (Tab. 3). As a result, small storm flows like the one of July 1995 generated by saturation excess on these areas during low flow periods are systematically underestimated, whereas the biggest floods are overestimated. Hence, saturated contributing area based on topography alone, assuming a homogeneous soil, did not adequately reproduce the observations.
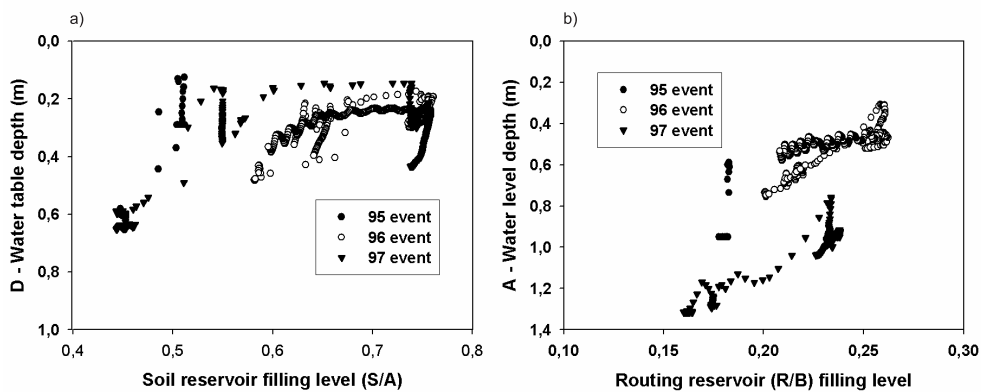
Fig. 4: Scatterplots for three flood events: (a) riparian piezometric levels vs GR4 soil reservoir levels; (b) foot-slope piezometric levels and GR4 routing reservoir levels.

Assessing T_0 in view of field values of lateral transmissivity is much more difficult, because T_0 values depend on the grid resolution of the digital elevation model (DEM) used for derivation of the topographic index. Approximate values derived from groundwater dynamics between piezometer A and D on steep slopes with high effective porosity of $T_0 = 10.0$ m^2·h^{-1} can be regarded as a mean estimation of transmissivity in the study area. The calibrated $T_0 = 2.5$ m^2·h^{-1} is largely below a physically reasonable range. In summary,

the poor correspondence of calibrated TOPMODEL parameters to its field expected values (Tab. 1) revealed that the calibration was influenced by inadequacies of the model structure for the study area, i.e. an overestimation of the dynamics of saturated areas.

CONCLUSIONS AND PERSPECTIVES

Simple conceptual and parsimonious RR models are only a crude approximation to the complex processes in the field. For the GR4 RR model, according to the hard and soft data available, a third reservoir might improve the model predictions. In its original version, although a very attractive conceptualization of catchments having a dominant contribution of variable contributing areas to storm flow as the Strengbach catchment, TOPMODEL is not able to provide a satisfactory representation of the subsurface flow dynamics and patterns of saturated areas during floods in low flow conditions. Underlying subsurface topography would probably be a better «proxy» for simulating saturation excess overland flow instead of topographical patterns of the catchment. Using a parabolic lateral transmissivity function instead of an exponential one might also permit to better simulate the recession part of the flood hydrograph as already demonstrated by Ambroise et al. (1996) for granitic catchments. Improvement of model structures may finally bridge the gap between fiction and representation of reality.

REFERENCES

Ambroise B., Freer J. and Beven K. (1996). Application of a generalized TOPMODEL to the small Ringelbach catchment, Vosges, France. *Water Resour. Res.*, **32**: 2147–2159.

Beven K. (1997a). *TOPMODEL User Notes. Windows Version 97.01*. Centre for Research on Environmental Systems and Statistics, Lancaster University, UK, 14 pp.

Beven K. (1997b). TOPMODEL: a critique. *Hydrol. Process.*, **11**: 1069–1085.

Donnelly-Makowecki L.M. and Moore R.D. (1999). Hierarchical testing of three rainfall–runoff models in small forested catchments. *J.Hydrol.*, **219**: 136–152.

Hamon W.R. (1961). Estimating potential evaporation. In: J.o.H. Division, Editor. *Proceedings of the American Society of Civil Engineers*, **87**: 107–120.

Lang C. (2007). *Etiages et tarissements : vers quelles modélisations ? L'approche conceptuelle et l'analyse statistique en réponse à la diversité spatiale des écoulements en étiage des cours d'eau de l'Est français*. Thèse de 3ᵉ cycle, Université Paul-Verlaine de Metz: 300 pp.

Mathevet T. (2005). *Which rainfall-runoff model at the hourly time-step? Empirical development and intercomparsison of rainfall-runoff models on a large sample of watersheds*. PhD thesis (in French), ENGREF University, Paris: 463 pp.

Oudin L., Andréassian V., Mathevet T., Perrin, C. and Michel C. (2006). Dynamic averaging of rainfall-runoff model simulations from complementary model parameterizations. *Water Resour. Res.,* **42**(7), W07410, doi: 10.1029/2005WR004636.

Perrin C., Michel C. and Andréassian V. (2003). Improvement of a parsimonious model for streamflow simulation. *J. Hydrol.*, **279**: 275–289.

Quinn P. F., Beven K. J. and Lamb, R. (1995). The ln (a/tan beta) index: how to calculate it and how to use it within the TOPMODEL framework. *Hydrol. Process.*, **9**: 161–182.

Viville D., Probst A., Ladouche B., Idir S., Probst J.L. and Bariac T. (2003). Stormflow component determination using hydrological, isotopic and chemical approaches in the small forested Strengbach catchment (granitic Vosges massif, France). [In:] Holko L. and Miklanek P. (eds), Proceedings *of "Interdisciplinary approaches in small catchment hydrology: monitoring and research",* Technical Documents in Hydrology, **67**, UNESCO, Paris 13–18.

THE IMPACT OF SEAWATER INTRUSIONS ON WATER QUALITY IN SMALL COASTAL FRESHWATER BASINS

R. Cieśliński, R. Bogdanowicz and J. Drwal

Department of Hydrology, University of Gdańsk, Dmowskiego 16a, 80-264 Gdańsk, Poland
Corresponding author: Roman Cieśliński, e-mail: georc@univ.gda.pl

ABSTRACT

The main aim of the research was to assess the impact of seawater intrusions on water quality in small basins of river-lake systems and to indicate the most likely factors which produce this phenomenon. For the purpose of the research, five catchments located on the coast of the southern Baltic Sea were selected. Sixteen hydrochemical surveys accompanied by simultaneous determination of the current hydrological situation were conducted from 2002 to 2008. Considering all the surface waters studied, the most pronounced changes in water quality were detected in the mouths of rivers. Significant changes in chemical composition also occurred in a lake with typical freshwater conditions while in lakes with the highest salinity levels (lagoon conditions), saltwater intrusions could not be considered extreme phenomena.

Key words: Baltic Sea, saltwater intrusions, coastal lakes, chloride, small basins

INTRODUCTION

Hydrological extremes are often defined as processes caused by hydrometeorological circumstances which differ markedly from typical weather conditions (Van den Brink *et al*., 2005). Hydrological changes resulting in floods of various origin can be the effects of such a phenomenon in a natural environment (Hall and Anderson, 2002). Such situations are temporal in nature and are related to occasional or episodic changes in geographic conditions (Tarkhov and Treivish, 2007). Typical for coastal areas of the southern Baltic, storm-induced floods occur in rivers mouths when strong winds blowing from the sea obstruct normal river flow. This leads to impoundment and consequently overflow onto riverside plains (Cieśliński and Drwal, 2005).

It is often not recognized that the effect of such a storm is not only freshwater impoundment but also the inflow of saline waters (called intrusions). So far, such incidents have not been considered extreme events. Seawater intrusion is the phenomenon of the penetration of seawater into coastal aquifers and bodies of surface freshwater which have a permanent or periodic connection to the sea. In consequence, a sharp increase in salinity and a number of other chemical and physical parameters is observed. There is not enough information on how the intrusions proceed and what their consequences are in coastal catchments on the Baltic Sea – a semi-enclosed sea with no tides. Another question is whether these inflows can be treated as extreme or rather normal phenomena. The main aim of this research was to assess the impact of seawater intrusions on water quality in selected small basins of river-lake systems and to indicate the most likely factors which produce this phenomenon.

RESEARCH AREA

For the purpose of the research, several hydrographic objects and their catchments were selected (Fig. 1). They are located in the central part of the coast of the southern Baltic with the exception of the Lake Ptasi Raj basin. The surface areas of the five research basins range from 1.4 km^2 (Lake Ptasi Raj) to 107.7 km^2 (Lake Wicko). The surface area of the catchments of Lake Ptasi Raj and Lake Bukowo is dominated by forests (over 40% of basin area) while the catchments of Lake Modła, Lake Kopań, and Lake Wicko are dominated by arable land
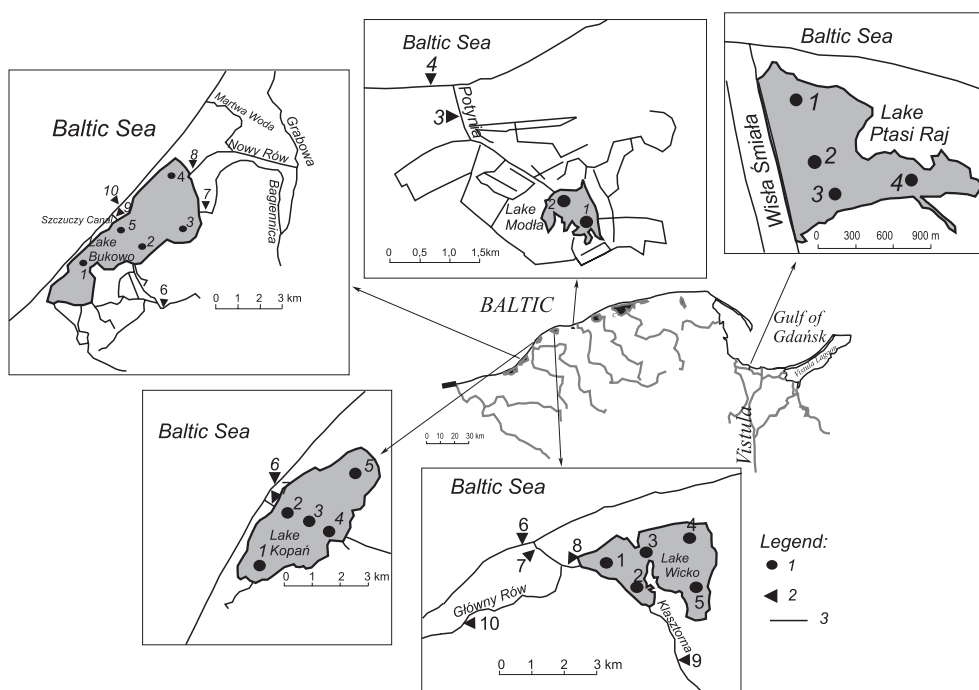
Fig. 1: Research area with the locations of the sampling points.
1 – sampling points on the lake, 2 – sampling points on the sea and on rivers, 3 – rivers and channels.

(over 50% of basin area). In all the basins, the impact of human activity on water conditions can be observed. There are significant changes in the hydrographic network resulting from the development of drainage systems and the formation of polder systems which have in many places replaced natural gravitational water circulation with a forced-flow system (i.e. pumping stations). There are also numerous hydrotechnical structures hampering the free flow of water in particular hydrographic objects including a sluice on the Głownica River which links Lake Wicko with the Baltic Sea. On the other hand, there also exist objects that facilitate the free inflow of saltwater such as culverts in the dike separating Lake Ptasi Raj from estuarine waters.

The research basins were selected in a way where all of them contain lakes as the main hydrographic objects (Tab. 1). The largest of them is the shallow Lake Bukowo with an area of 17.5 km^2 and mean depth of 1.8 m. Like most other lakes on the shore of the southern Baltic, it belongs to a group of coastal lakes formed by the enclosure of a former bay with a sandbar. The only link the lake has with the sea is through the Szczuczy Canal. The largest stream entering the lake is the Bagiennica River. Lake Wicko,

Table 1: `Selected characteristics of the analysed basins.

Lake	Elevation [m a.s.l.]	Lake area [ha]	Maximum depth [m]	Volume [000's · m^3]	Connection with the sea (length/width) [m]	Basin area [km^2]	Freshwater exchange coefficient [year^{-1}]
Bukowo	0.1	1747.4	2.8	32072	Szczuczy Channel (300/18.5)	102.8	0.9
Kopań	0.1	789.7	3.9	14773	Kopański Channel (300/10.0)	38.5	0.8
Wicko	0.2	1058.9	6.1	28495	Głownica River (1900/6.5)	107.7	1.1
Modła	0.4	45.1	2.6	541	Potynia River (2400/5.0)	26.9	1.3
Ptasi Raj	0.0	51.8	2.6	655	Culverts (4/2.0)	1.4	0.0

the second largest of the analysed lakes, has an area of 10.5 km². Its mean and maximum depths, considerably larger than those of the remaining coastal lakes, are 2.7 m and 6.1 m, respectively. The outflow of water from this lake to the Baltic Sea occurs through the natural mouth of the Głownica River. Lake Kopań belongs to a group of smaller sandbar lakes with an area of 7.89 km². Its mean depth is 1.9 m. The only periodic link (40 –50% of the time it is filled with sediment) this lake has with the sea is the Kopański Canal. Lake Modła is the smallest of the lakes with an area of only 0.45 km². Its maximum and mean depths are 2.6 and 0.5 m, respectively.Lake Modła is surrounded by a system of three polders. Only one stream flows out of the lake – the Potynia River – the longest linkage (2.4 km) between a lake and the sea among all the analysed basins. Lake Ptasi Raj (Lake Bird Paradise), located in the Vistula Delta, is a polygenetic lake. The area of this body of water is 0.52 km² and its mean depth is 1.2 m. It has the smallest basin of all the lakes studied and possesses no stream network. There is also no canal linking this lake with the sea. It comes into contact with an estuary via the culverts in the dike separating this lake from the Wisła Śmiała River (the "Brave" Vistula).

METHOD

The employed method involved performing recurring hydrochemical surveys accompanied by simultaneous determination of the current hydrological situation. From 2002 to 2008, about twenty measurement series were completed in each of the analysed lakes (Lake Bukowo, Lake Wicko, Lake Kopań, Lake Modła, and Lake Ptasi Raj) were performed. From 2002 to 2005, surveys were conducted twice a year while since 2006, four times a year. The measurement sites were located on the lakes themselves, on the Baltic Sea, in the lakes' tributaries, and in the canals linking the lakes with the sea. Water samples were taken from surface and intermediate water layers. Water from the latter layers was obtained from the surface of bottom sediment which was collected using a Kajak scoop and a centrifuge. Water samples were analysed in the laboratory of the Hydrology Department of the University of Gdańsk (chlorides, sodium, potassium, magnesium, calcium, sulphates, bicarbonates and specific conductance). The measurements were conducted during normal and extreme weather conditions (stormy weather). Water flow was measured in the canals' outlets to the sea. Additionally, hydro-meteorological data (seawater level, water level in lakes, wind direction, and wind speed) were obtained from the Institute of Meteorology and Water Management (IMGW) in Słupsk and Gdynia. The data were collected for the days of measurement and for two days preceding them. Water level values for the lakes and the sea were standardized using the same reference system.

CHANGES IN WATER QUALITY

An analysis of the average concentration of main ions in the water of the analysed lakes clearly indicated two lakes with water composition similar to sea/lagoon water composition (Lake Bukowo and Lake Ptasi Raj) with appreciable amounts of chlorides and sodium (Bogdanowicz, 2007). The other lakes possessed characteristics more typical for surface freshwater bodies with a larger concentration of calcium and bicarbonates (Fig. 2).

Chloride ions are considered to be the best indicators of the impact of seawater on bodies of freshwater in coastal areas. All further analysis concentrated on their content and variability. Chlorides tend to be "conservative" ions which do not interact with other substances, do not oxidize, and are not reduced. Moreover, they migrate well in aqueous environments. In the scientific literature, certain threshold values have been proposed which could help to assess the scale of seawater influence on the quality of continental freshwater. In surface
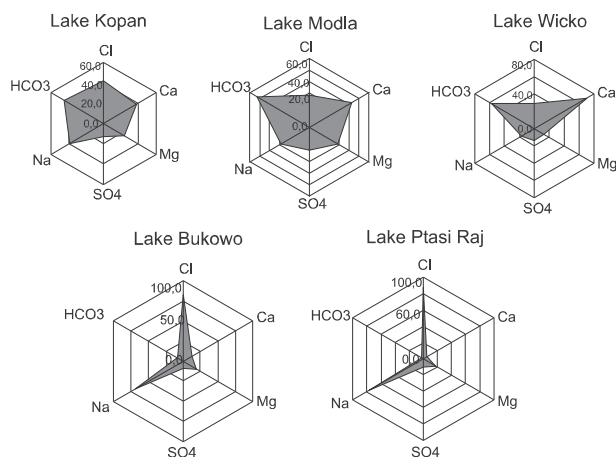

Fig. 2: Chemical composition of water in the selected lakes.

waters, chloride concentration usually stays within the 20–30 mg·dm^{-3} range. An intrusion may be detected when the concentration increases up to around 100 mg·dm^{-3} (Appelo and Willemsen, 1987). In this paper, this threshold value has been adopted for use.

The results of water quality analysis indicated that there was a very high variability in chloride content in the selected basins (Tab. 2). The highest observed values were characteristic for Lake Ptasi Raj where chloride concentration never fell below 2300 mg·dm^{-3}. The high chloride content in this lake, with maximum values over 4000 mg·dm^{-3}, was close to that observed in the Gulf of Gdańsk. Elevated salinity in this small lake may be a result of easy penetration by brackish waters from the Gulf of Gdańsk caused by the frequent opening of sluices in the culverts under the dikes separating the lake from the estuary of the Wisła Śmiała River. Other reasons include inflows of saline groundwater and a disproportionately small catchment area compared to the lake's surface. High chloride concentrations, while not as high as those in Lake Ptasi Raj, have been detected in Lake Bukowo. This lake is located in close proximity to the open sea. The other three lakes have distinctly different characteristics of chloride concentration. The least salty water was typical for Lake Wicko, although even there, water contained more chloride than is typical for inland surface water. The weakest influence of the sea on this body of water can be interpreted as a consequence of the comparatively long distance from the Baltic Sea to the lake through an outlet canal which is additionally obstructed by several hydrotechnical structures. In this lake, seawater intrusions have never been recorded. A similar situation exists in Lake Modła where such a phenomenon has not been observed and maximum chloride concentration rarely reaches 100 mg·dm^{-3}. Occasional seawater intrusions were, however, recorded in Lake Kopań where the result was the highest water salinity in the three lakes of interest.

Table 2: Mean chloride concentrations [mg Cl·dm^{-3}] in the analysed basins.

Lake's Catchment	Surface water in lake (various sampling points)	Intermediate water in lake (various sampling points)	Lake's Tributaries	River or channel outlets
Bukowo	811–985	804–971	19–29	1778
Kopań	94–103	100–115	-	3755
Wicko	41–55	40–55	38	1428
Modła	68–81	67–81	-	224
Ptasi Raj	314–3421	3301–4019	-	-

Chloride concentrations in the intermediate layer were slightly higher than in the surface water in all of the lakes. The sea's influence has not been observed in any of the lakes' tributaries (Tab. 2). Temporal changes in various types of surface waters in the Lake Bukowo basin, where seawater intrusions could be observed, are presented in Fig. 3. The lowest chloride concentrations, typical for surface freshwater, in this area were present in a tributary to the lake (the Bagiennica River) while the highest, and very variable, concentrations were recorded in the Szczuczy Canal linking the lake with the sea. Chloride levels in this lake were also high but in contrast to the canal, they were very stable.

A comparison of extreme chloride concentrations shows clear differences between values observed in seaside lakes and those observed in canals linking these bodies of water with the sea. In all the analysed basins, higher chloride variability has been observed in flowing waters than in lakes, however, significant variability in river water (max/min>5) could be observed only in the catchments of Lake Wicko and Lake Modła (Fig. 4). The highest variability in chloride concentration in lakes (max/min>2) has been observed in Lake Modła – the lake with low average chloride content as well as the longest connecting pathway to the sea.
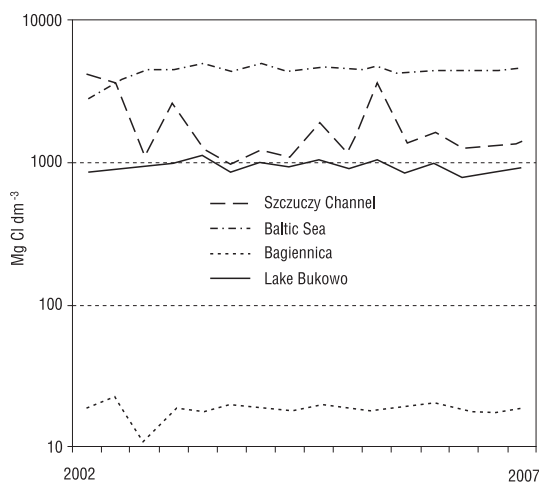
Fig. 3:   Temporal changes in chloride concentration in the Lake Bukowo catchment.
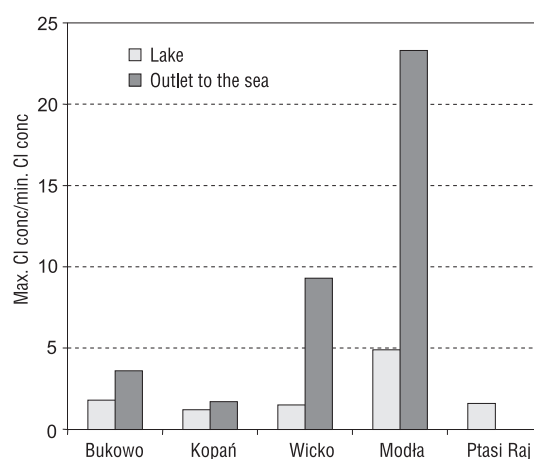

Fig. 4:   Extreme changes in chloride concentration in surface waters of the selected coastal basins.

DISCUSSION

The influence of seawater intrusions on surface waters in coastal areas of the southern Baltic is usually attributed to occasional extreme weather conditions with strong winds blowing landward and elevated sea levels (Cieśliński and Drwal, 2005). An analysis of hydro-meteorological conditions on measurement days and the days preceding them, coupled with a simultaneous analysis of chloride concentrations in the selected small basins, did not fully confirm this thesis. In many cases, the favourable weather conditions did not result in anticipated high levels of chloride. It turned out that some of the basins were more prone to saltwater intrusions and some were much more resilient. Two of the analysed lakes (Lake Bukowo and Lake Ptasi Raj) were strongly impacted by frequent seawater intrusions while in the other lakes, such inflows were occasional or even not recorded. Research has shown that the mechanism of seawater intrusions in small catchments is much more complex than it has been thus far reported in the literature. The most important factors appear to be the characteristics of the pathway connecting the given lake and the sea. Special attention needs to be paid to canal cross sections, flow velocity, waterway continuity, orientation with respect to the coastline, prevailing winds, and currents. In some cases, human impact as reflected in hydrotechnical infrastructure either obstructing (Lake Modła basin) or facilitating seawater inflow (Lake Ptasi Raj basin) was also of significant importance.

The phenomenon of high variability in chloride concentration in various lakes along the southern Baltic coast is well documented (Kavaliauskiene, 1999; Springe et al, 1999; Cieśliński, 2004; Timm et al., 2007). There are bodies of water located very close to the coast where chloride concentrations are below 10 mg·dm⁻³ (e.g. Lake Engure in Latvia) while in other lakes (e.g. Lake Ptasi Raj), these concentrations are frequently well over 1000 mg·dm⁻³. The largest differences were observed between lakes which have a permanent link to the sea and lakes which are permanently separated from the influence of the sea. The lack of a waterway connecting a lake with the sea is not always the factor which eliminates the influence of the sea. There are reported cases where saline intrusions have approached lakes through groundwater aquifers (Macdonald et al., 2006). In lakes, where active river stretches or anthropogenic waterways connect them to the sea, it is important whether this linkage is permanent (as in the case of Lake Bukowo) or perhaps it is often and for long periods of time closed as a result of natural processes (sediment accumulation – Lake Kopań) or human impact (water gates or sluices – Lake Wicko). In the case of the Baltic Sea, the influence of the sea is different than in the case of other seas for two reasons. First, the Baltic is a sea with no tides, therefore, seawater inflows do not occur on a regular basis. Second, it has brackish water with relatively low salt content. For this reason, intrusions of such water cannot elevate chloride concentrations to such high levels as it happens in lakes on the coast of much more salty seas such as the Mediterranean (e.g. Lake Goksu in Turkey) or the Northern Sea (e.g. Lake Grevelingen in the Netherlands). In these lakes, chloride concentrations can even exceed 20,000 mg·dm⁻³ (Gordu et al., 2001; Kamermans at al., 1999).

73

CONCLUSIONS

The results of the research indicate that the influence of seawater intrusions on freshwater quality in small coastal catchments is highly variable. It was discovered that the lakes with the highest salinity were not lakes where such intrusions could be considered extreme phenomena. A permanent and well developed connection to the sea resulted in the creation of unique and quite stable lagoon conditions in such lakes. A very high concentration of chloride ions in these types of basins cannot be, therefore, considered a consequence of exceptional conditions. Of all the surface waters in the analysed catchments, the most pronounced changes in freshwater quality occurred in rivers and waterways that connect lakes to the sea. Significant changes in chemical composition also occurred in the lake with typical freshwater conditions. Therefore, the influence of seawater intrusions can be considered an extreme phenomenon in lakes of this type.

REFERENCES

Appelo C.A.J. and Willemsen A. (1987). Geochemical calculations and observations on salt water intrusions, a combined geochemical/mixing cell model. *J. Hydrol.*, **94**: 313–330.

Bogdanowicz R. (2007). Managing water quality in the Puck Lagoon drainage basin (NATURA 2000 site). In: Nakic Z. (ed.), *Water in protected areas*, CWPCS, Zagreb: 129–133.

Cieśliński R. (2004). Chemical classification of waters of chosen lakes of the central coast of the Polish coastal zone of the Southern Baltic. *Limnol. Rev.*, **4**: 57–66.

Cieśliński R. and Drwal J. (2005). Quasi-estuary processes and consequences for human activity, South Baltic. *Estuar. Coast. Shelf S.*, **62**: 477–485.

Gordu F., Motz L.H. and Yurtal R. (2001). Simulation of seawater intrusion in the Goksu Delta at Silifke, Turkey. In: *Monitoring, Modeling and Management*, Essaouria, Morocco.

Hall J. and Anderson M. (2002). Handling uncertainty in extreme or unrepeatable hydrological processes – the need for an alternative paradigm. *Hydrol. Processes*, **16** (9): 1867–1870.

Kamermans P., Hemmings M.A. and de Jong D.J. (1999). Significance of salinity and silicon levels for growth of a formerly estuarine eelgrass (Zostera marina) population (Lake Grevelingen, the Netherlands). *Mar. Biol.*, **133**: 527–539.

Kavaliauskienė J. (1999). Investigations of biodiversity in freshwater ecosystems of Lithuania. The lakes, In: *Hydrobiological research in the Baltic countries*. UNESCO National Commission of Estonia, Latvia and Lithuania, Vilnius: 104–115.

Macdonald B.C.T., Smith J., Keene A.F., Tunks M., Kinsela A. and White I. (2006). Impacts of runoff from sulfuric soils on sediment chemistry in an estuarine lake. *Sci. Total Environ.*, **329**(1-3): 115–130.

Spriņģe, Briede A., Druvietis I., Parele E., Rodionovs V. and Urtäne L. (1999). Investigations of biodiversity in freshwater ecosystems of Latvia. The lakes, In: *Hydrobiological research in the Baltic countries*, UNESCO National Commission of Estonia, Latvia and Lithuania, Vilnius: 186–230.

Tarkhov S.A. and Treivish A. I. (2007). Geographic location and diffusion of basic innovations, *GeoJournal*, **26**(3): 341–348.

Timm T., Kumari M., Kübar K., Sohar K. and Traunspurger W. (2007). Meiobenthos of some Estonian coastal lakes. *Proc. Estonian Acad. Sci. Biol. Ecol.*, **56(**3): 179–195.

Van den Brink H.W., Können G. P., Opsteegh J. D., Van Oldenborgh G. J. and Burgers G. (2005). Estimating return periods of extreme events from seasonal forecast ensembles. *Int. J. Climatol.*, **25**(10): 1345–1354.

THE INFLUENCE OF WATER CIRCULATION ON STREAM WATER ELECTRICAL CONDUCTIVITY IN CATCHMENTS WITH DIFFERENT LAND USE DURING FLOOD PERIODS (THE CARPATHIAN FOOTHILLS, POLAND)

J.P. Siwek[1], M. Żelazny[2] and W.Chełmicki[2]

[1]*Academy of Physical Education in Cracow, Institute of Tourism and Recreation, Cracow, Poland*
[2]*Jagiellonian University, Institute of Geography and Spatial Management, Cracow, Poland*
Corresponding author: Joanna P. Siwek, e-mail: j.raczak@geo.uj.edu.pl

ABSTRACT

The study aims to identify the influence of water circulation patterns present during flood events on the chemical composition of stream water as represented by the specific electrical conductivity of water (SC). The research catchmens are located within the edge zone of the Carpathian Foothills. The Stara Rzeka catchment is of mixed land use while the two nested sub-catchments, Leśny Potok and Kubaleniec, are wooded and agricultural, respectively. The study takes into consideration stream water SC changes during floods caused by: (i) intensive storm rainfall, (ii) prolonged rainfall, and (iii) snowmelt.

In the woodland catchment area, the water circulation pattern during intensive rainfall-induced floods was different from the pattern in the agricultural catchment. The differences were expressed in the different direction of hysteretic loops of stream discharge vs. SC: clockwise in the woodland catchment and counterclockwise in the agricultural one. In the woodland catchment, the most important supplier of water to the stream was subsurface flow while in the agricultural catchment it was overland flow. The direction of hysteretic loops was the same in all catchments during floods caused by prolonged rainfall and snowmelt, which indicates similar means of water supply to streams independent of the given catchment's land use.

Key words: water circulation, rainfall floods, snowmelt floods, water conductivity, Carpathian Foothills

INTRODUCTION

Alongside geochemical properties, a fundamental role in ion concentration changes in stream water during flood events is played by the water circulation pattern. The given pattern in a catchment area before it reaches a stream channel influences the chemical composition of stream water during and after a flood (Bonell *et al*., 1993). The water circulation pattern determines the arrival time of water from different flow paths at the stream channel and therefore having different chemical composition. The circulation pattern also strictly depends on other factors such as the catchment characteristics, the nature of the given flood event, as well as the water content and the degree of freezing of the regolith and soil cover.

According to Edwards (1973), catchment characteristics such as terrain relief and the nature of lithological formations (solubility and permeability) influence the amount of overland flow and consequently the degree of dilution of river water originating from underground sources ("old water") with flood water ("event water"). Land use within a catchment plays an important role in the shaping of the mechanism that feeds a stream. Streams in woodland catchment areas are fed mainly by subsurface flow which is responsible for the flushing of chemical compounds from soil-regolith deposits and their transport to the channel (Feller and Kimmins 1979). In agricultural and urban catchment areas, overland flow plays a greater role. Based on hysteretic effect analysis of ions during floods in two small catchments in Georgia (USA), Rose (2003) developed a simpler

(two-component) feed model for highly urbanized catchments versus poorly urbanized catchments (three-component feed model). According to Buttle (1994), "old water" plays a much more significant role during flood events in forested and agricultural catchments than in urbanized catchments.

The water circulation pattern during a flood event in a catchment is closely tied to the nature of the given event and to the antecedent conditions of soil cover. While investigating a small agricultural catchment in Great Britain, Foster (1978) determined that decreases in solute concentration are much greater during storms under winter conditions than during storms under autumn conditions. Buttle (1994) explained this phenomenon in terms of a larger proportion of "new water" during snowmelt flood crests compared to rainfall floods. Hooper *et al.* (1990), Evans and Davies (1998) obtained different results: In the course of snowmelt floods, stream ion concentrations did not change as rapidly as during rainfall floods due to a large amount of moisture on soil surfaces and the low precipitation intensity.

The aim of the study is to recognize the influence of water circulation patterns in catchments with different characteristics (land use, relief, soil cover properties) on changes in stream water chemistry during different types of floods, i.e. floods caused by (i) intensive storm rainfall, (ii) prolonged rainfall or (iii) snowmelt. The study is based on specific conductivity (SC) changes in stream water.

RESEARCH AREA

The research was conducted in the northern edge zone of the Carpathian Foothills (Poland) in the Stara Rzeka catchment and two of its sub-catchments: Leśny Potok and Kubaleniec (Fig. 1). The Stara Rzeka catchment area straddles two altitude levels of the Carpathian Foothills: the higher one built of hard "Silesian unit" flysch deposits (S: sequentions sandstones and shales) and the lower of softer "Sub-Silesian unit" flysch deposits. The "sub-Silesian unit" consists of two subunits: Bocheńska Górna (SS-I: sandstones, claystones, shales, clays and conglomerates) and Bocheńska Dolna (SS-II: claystones, marly clays, gypsum, sandstones and a salt series; Olewicz 1973). The entire area of the catchment is lined with a thick layer of dusty loess-like formations,
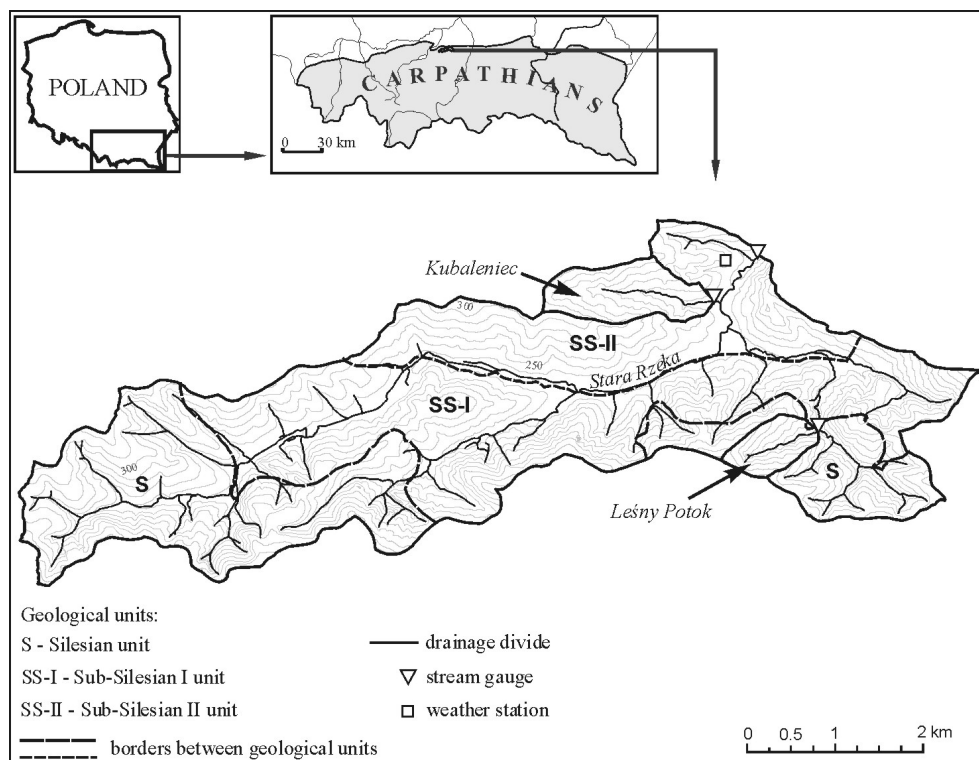

Fig. 1:   Study area.

up to more than ten metres thick with *Haplic Luvisols*, *Stagnic Luvisols*, *Cambic Luvisols* and *Eutric Gleysols* (Skiba *et al.* 1998).

The Stara Rzeka catchment (22.2 km^2) is characterised by a mixed land use structure with woodland accounting for 42%, arable land for 36%, and meadows and pastures for 15% of the area (Święchowicz and Michno 2005). There is a number of villages in the catchment that have substantial influence on the quality of surface and ground waters. Most household and farm wastewater is discharged into roadside ditches and canals and drained into streams.

The Kubaleniec sub-catchment (1.03 km^2) is located within the lower altitude level of the Carpathian Foothills ("Sub-Silesian unit" – Bocheńska Dolna). It is a typical agricultural catchment: arable land accounts for 69% of its area while meadows and pastures account for 20% and forests for just 0.5% (Święchowicz and Michno 2007). It is dominated by small farms with long and narrow plots of land. The high degree of plot fragmentation has produced a dense network of dirt roads (3.6 km·km^{-2}) (Święchowicz 2002). Improper agricultural practices (ploughing along a slope) have led to soil layers *A* and *Eetg* becoming clearly more shallow. The result of this is a layer of poorly permeable argillic (*Bt*) illuvium at a rather small depth. The village of Brzeźnica is located on the boundary of the catchment and constitutes a major source of stream water pollution.

The Leśny Potok sub-catchment (0.48 km^2) lies within the higher altitude level of the Carpathian Foothills ("Silesian unit"). More than 99% of its area is wooded. The forest is mostly composed of beech trees, firs, and complexes closely linked to mixed *Pino-Quercetum* forests. The basin features a wet flat-bedded valley and many side valleys in the form of deep-cutting badlands and v-shaped gullies. So far, the catchment area has not been subject to settlement pressure due to its steep slopes (10–15°). In contrast to the agricultural catchment of Kubaleniec, the illuvial argillic level (*Bt*) occurs here at a larger depth of 40–80 centimetres.

METHODS

SC samplings were performed during the period of 2002 – 2004 at the gauging cross sections of Stara Rzeka, Kubaleniec, and Leśny Potok. The samples were taken manually and then measured in the lab. Altogether, 28 flood events were studied: six caused by intensive rainfalls, seven by long lasting rainfalls and fifteen by melting snow. Water levels were gauged on a continuous basis using a float-type water level recorder until May 2003 and afterwards with pressure-type water level sensors (Aplisens SG-25 and Peltron PLH 27) at ten-minute intervals. Stream discharge was calculated based on rating curves developed experimentally for each cross section. Additionally, during selected floods, ground water, overland flow, and snowpack samples were collected for chemical analysis. This paper presents the results based on SC measurements only.

RESULTS AND DISCUSSION

During intensive summer rainstorm floods, subsurface flow plays the most important role in the process of runoff formation in the woodland catchment. Major role is played by the dense network of badlands and v-shaped valleys incising the slopes and draining the subsurface water. The infiltrating water is drained very quickly. First, at the main channel, water emerges from the side v-shaped valleys incising the ground water table. Generally, overland flow plays a minor role in the supply of water to streams. Water surfaces only after a certain period of time along forest roads and paths and in the wet valley bed. A rapid influx of subsurface flow as well as a small delayed influx of water from overland flow result in higher SC during the rising limb of a flood wave rather than during the falling limb (Fig. 2A). The flushing effect within the soil cover results in a clockwise hysteretic loop direction.

In the agricultural catchment of Kubaleniec, in contrast to the woodland catchment of Leśny Potok, overland flow forms very quickly after rainfall begins. Areas particularly prone to the development of overland flow include highly compacted dirt roads and paths (infiltration excess overland flow). During intensive rains,
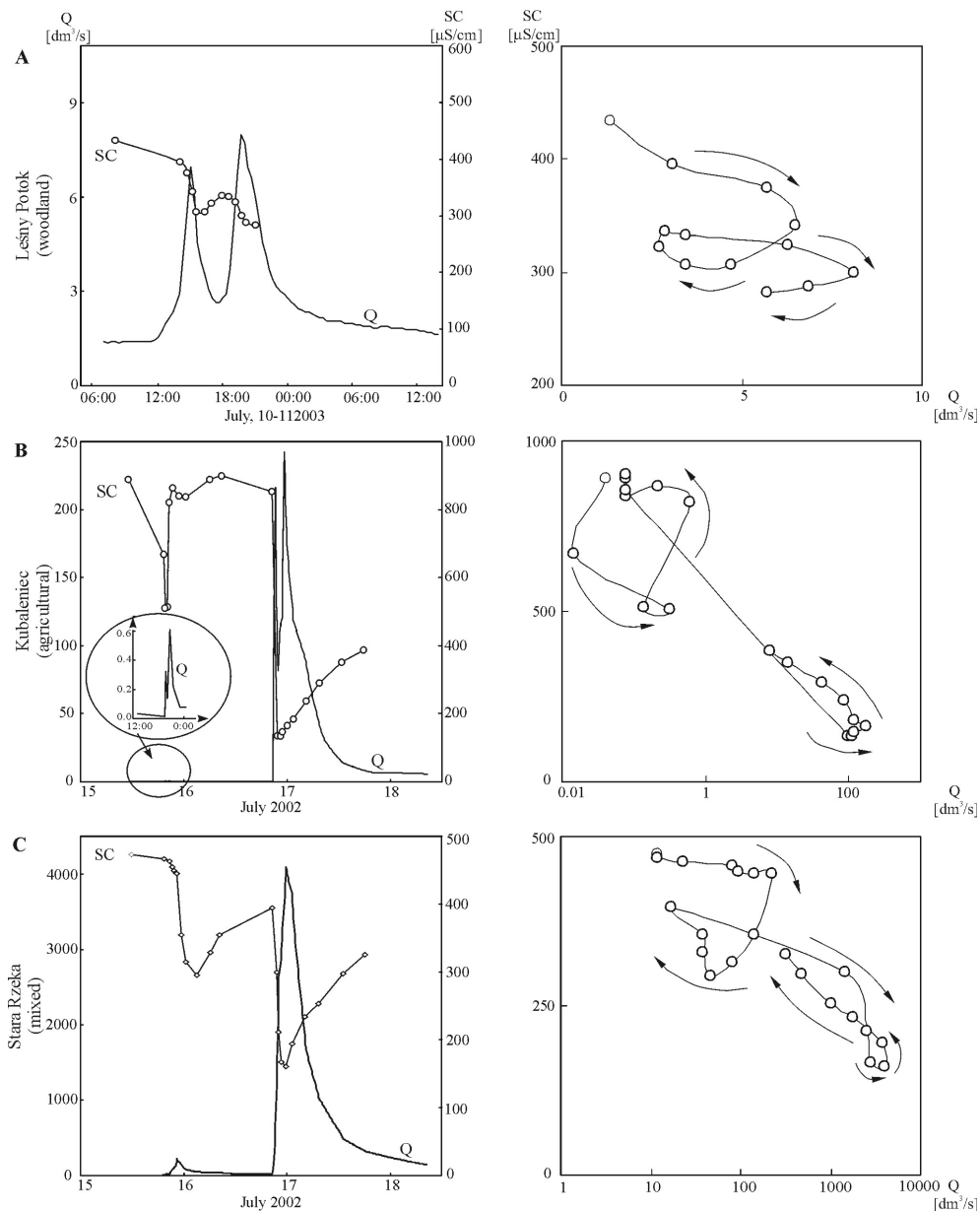
Fig. 2: SC vs. discharge of Leśny Potok, Kubaleniec, and Stara Rzeka during intensive rainstorm floods.

overland flow forms on slope-side fields, albeit with a certain delay compared to runoff on dirt roads and in furrows. A very shallow impermeable *argillic* layer favours the saturation excess overland flow formation. The quick supply of overland flow water causes very low SC to occur prior to peak discharge (Fig. 2B). As the rain stops, overland flow disappears very quickly from the slopes. From that point on, it is subsurface flow that plays a major role in the further development of a flood wave, causing SC to be higher during the recession limb than during its build-up. This results in a counterclockwise hysteretic loop direction.

SC hysteretic loops in the Stara Rzeka that drains the area of a complex land use vary in terms of direction. Sometimes, the loops appear similar to those in Leśny Potok (woodland) and sometimes to those in Kubaleniec (agricultural). Extremely low SC occurs prior to or after peak discharge (Fig. 2C).

The lack of differences in SC behaviour in the three streams during snowmelt floods and prolonged rainfall floods indicates similar water circulation patterns in catchment areas with different land uses (Fig. 3). During snowmelt events, watercourses are supplied primarily by the snowmelt water that is characterised by similar

SC throughout the Stara Rzeka catchment (Fig. 4). The subsurface flow, which determines the chemistry of the rainstorm floods in the agricultural and woodland catchments plays a minor role during snowmelt floods. With a frozen soil cover, i.e. during short floods or in the beginning stages of longer events, subsurface flow represents a negligible proportion in the main watercourse supply because of the restricted infiltration of the snowmelt water. The watercourses take water primarily from the snowmelt water running on top of iced snow, ice or frozen ground.

The thickness of the layer actively supplying water to the stream changes dynamically in this type of situation. According to research by Laudon *et al.* (2004) performed in a small Swedish drainage basin, frozen soil has an impact on the water's access routes to the channel, especially in the initial phase of a flood.

On the other hand, during snowmelt floods, when the soil and regolith cover are not frozen but saturated with water, the subsurface water flow into the watercourse shows very little variation in terms of both quantity and quality of water, which makes the process similar to that resulting from prolonged rainfall floods.
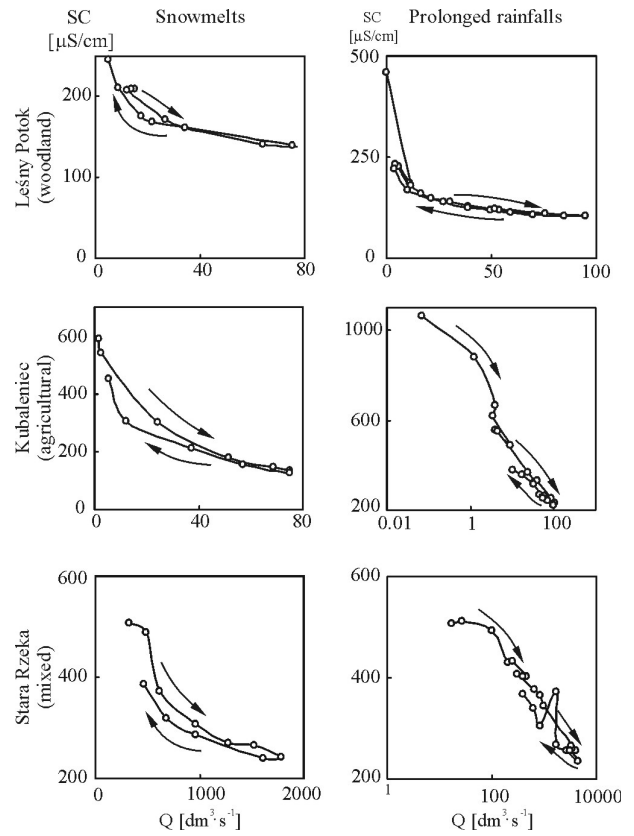
Fig. 3: SC vs. discharge of Leśny Potok, Kubaleniec, and Stara Rzeka during prolonged rainfall and snowmelt floods.
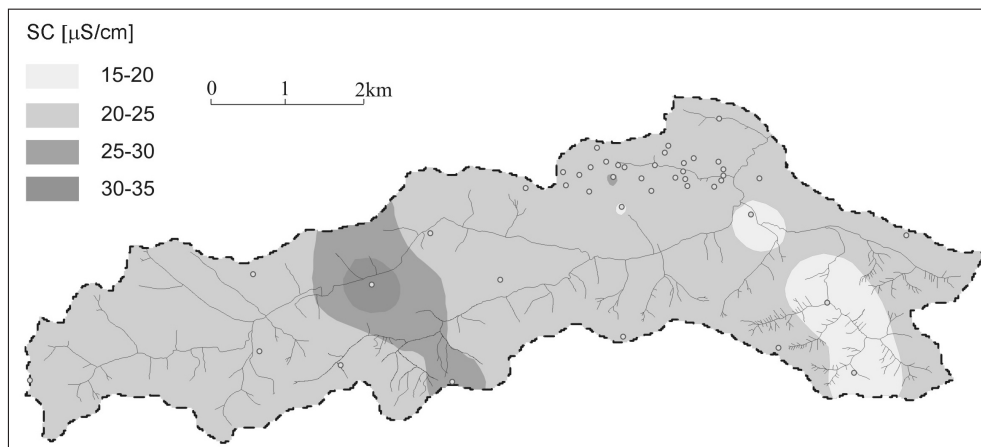
Fig. 4: Snowmelt water SC in the Stara Rzeka catchment on 6-7 January 2004. Small circles depict snow sampling sites. Linear interpolation was applied.

CONCLUSIONS

The water circulation pattern during summer storm floods is clearly different in forested, agricultural, and mixed land use catchment areas. In the forested Leśny Potok catchment, subsurface flow plays the most important role in the process of runoff formation. Water from subsurface very quickly reaches the main channel of the stream thanks to a dense network of badlands and v-shaped valleys. Overland flow plays a marginal role in this type

of catchment. Higher values of conductivity are registered during the rising limb of a flood wave than during the falling limb. The reason for this first-phase spike is a flushing out of compounds accumulated in surface deposits during the precipitation-free period by infiltrating water. As a result, there is a shortage of compounds to be transported during the second phase of the flood event. It is quite a different story in the agricultural catchment Kubaleniec where infiltration excess overland flow plays a very important role by quickly forming along dirt roads and paths. This type of flow is also aided by the saturation excess overland flow developed on shallow and poorly permeable argillic (*Bt*) layer of soil. Once the rainfall ends, overland flow stops very quickly yielding to throughflow. This causes conductivity to be lower during the rising limb of a flood wave when poorly mineralized overland flow water reaches the channel than during the falling limb when well-mineralized throughflow water reaches the channel. The different water circulation patterns in agricultural and forested catchments during storm-induced floods become apparent in the different directions of hysteretic loops: clockwise in woodland catchments and counterclockwise in agricultural catchments. The influence of land use disappears during prolonged rainfall and snowmelt-induced floods when the water circulation pattern in agricultural and forested catchments is similar.

REFERENCES

Bonell M. (1993). Progress in the understanding of runoff generation dynamics in forests. *J. Hydrol.*, **150**: 217–275.

Buttle J.M. (1994). Isotope hydrograph separations and rapid delivery of pre-event water from drainage basins. *Prog. Phys. Geog.*, **18**: 16–41.

Edwards A.M.C. (1973). The variation of dissolved constituents with discharge in some Norfolk Rivers. *J. Hydrol.*, **18**: 219-242.

Evans Ch. and Davies T.D. (1998). Causes of concentration/discharge hysteresis and its potential as a tool for analysis of episode hydrochemistry. *Water Resour. Res*., **34**(1): 129–137.

Feller M.C and Kimmins J.P. (1979). Chemical characteristic of small streams near Haney in Southwestern British Columbia. *Water Resour. Res*., **15**(2): 247–258.

Foster I.D.L. (1978). A multivariate model of storm-period solute bahaviour. *J. Hydrol.*, **39**: 339–353.

Hooper R.P., Christophersen N. and Peters N.E. (1990). Modelling streamwater chemistry as a mixture of soilwater end-members – an application to the Panola Mountain catchment, Georgia, USA. *J. Hydrol*., **116**: 321–343.

Laudon H., Seibert J., Kohler S. and Bishop K. (2004). Hydrological flow paths during snowmelt: congruence between hydrometric measurements and oxygen 18 in meltwater, soil water, and runoff. *Water Resour. Res*., **40**: 1–9.

Olewicz Z R. (1973). Tektonika jednostki bocheńskiej i brzegu jednostki śląskiej między Rabą a Uszwicą. *Acta Geol. Polonica*, **23**(4): 701–761.

Rose S. (2003). Comparative solute-discharge hysteresis analysis for an urbanized and 'control basin' in the Georgia (USA) Piedmont. *J. Hydrol*., **284**: 45–56.

Skiba S., Drewnik M., Klimek M. and Szmuc R. (1998). Soil cover in the marginal zone of The Carpathian Foothills between the Raba and Uszwica Rivers. *Prace Geograficzne*, Instytut Geografii. UJ, **103**: 125–135.

Święchowicz J. (2002). The Influence of Plant Cover and Land Use on Slope-Channel Decoupling in a Foothill Catchment: A Case Study from The Carpathian Foothills, Southern Poland. *Earth Surf. Proc. Land.*, **27**(5): 463–479.

Święchowicz J. and Michno A. (2005). *Obszar badań.* [In]: Żelazny M. (ed.), *Dynamika obiegu związków biogennych w wodach opadowych, powierzchniowych i podziemnych w zlewniach o różnym użytkowaniu na Pogórzu Wiśnickim.* Inst. Geografii i Gospodarki Przestrzennej UJ, Kraków.

HEADWATER CATCHMENT RESPONSE
BASED ON MULTIPARAMETER ANALYSIS OF RUNOFF EVENTS

A. Zabaleta, J.A. Uriarte, I. Cerro and I. Antigüedad

Hydrogeology Group, University of the Basque Country, 48940 Leioa, Bizkaia, Basque Country, Spain
Corresponding author: Ane Zabaleta, e-mail: ane.zabaleta@ehu.es

ABSTRACT

Turbidity (FNU), discharge ($dm^3 \cdot s^{-1}$), and precipitation (mm) are being continuously monitored at the gauging station located at the outlet of the Aixola catchment (Basque Country) since October 2003. Several data sets recorded during flood events were used to estimate continuous suspended sediment concentration (SSC). Electrical conductivity was also measured in samples taken during runoff events. Several event (discharge, precipitation, and suspended sediment concentration) and pre-event (discharge and precipitation) factors have been calculated for all the events analyzed. These factors were used to develop a correlation matrix. A significative level of correlation has been observed between precipitation (P), discharge (Q), and suspended sediment (SS) variables, however, pre-event conditions do not correlate well with event parameters. An analysis of the relation between SSC and discharge during the events indicated that different kinds of hysteretic loops can be observed in the Aixola catchment. Relationships between hysteresis types and event and pre-event factors have also been identified. The evolution of the electrical conductivity of water during flood events indicates that the catchment possesses a considerable regulation capacity.

Key words: discharge, suspended sediment concentration, electrical conductivity, single flood events, hysteretic loops, headwater catchment

INTRODUCTION

Different parameters measured during runoff events in the Aixola catchment (4.8 km^2) have been studied in order to identify the factors that control the hydrological and sedimentological response of the catchment during flood events and also to describe the general behaviour of the catchment during events. For that purpose precipitation (mm), discharge ($dm^3 \cdot s^{-1}$), turbidity (FNU), suspended sediment concentration ($mg \cdot dm^{-3}$), and electrical conductivity ($\mu S \cdot cm^{-1}$) of river water were measured during different length intervals over a period of two years (2003–2005) at the gauging station located at the outlet of the Aixola catchment.

STUDY AREA

The Aixola River is located in the western part of Gipuzkoa County (Basque Country) and drains a headwater catchment of 4.8 km^2 into the Aixola water reservoir (Fig.1). In this catchment, the highest elevation point is 750 m a.s.l., the outlet is 340 m a.s.l., and the mean elevation is 511 m a.s.l. Slopes are generally gentle – inclines under 30%. This catchment is mostly (>80%) woodland with *Pinus radiata* trees dominating the landscape. From a lithological point of view, the catchment is almost entirely homogeneous with the bedrock being Upper Cretaceous Calcareous Flysch with alternating marl and sandy limestone layers. The average annual precipitation for this area is about 1480 mm, distributed quite evenly throughout the year with totals of 1450 and 1375 mm/year during the research periods of 2003–2004 and 2004–2005. Mean annual discharge is about 600 mm with 667 and 810 mm for the research periods, respectively. The discharge water between runoff events has a conductivity of about 370 $\mu S \cdot cm^{-1}$ while being considerably lower (equal to or less than 200 $\mu S \cdot cm^{-1}$) during runoff events. During the 2003–2005 time period, the estimated average suspended sediment yield was 35 $t \cdot km^{-2}$ with mean concentrations of 128 $mg \cdot dm^{-3}$ during events. Since significant sediment loads
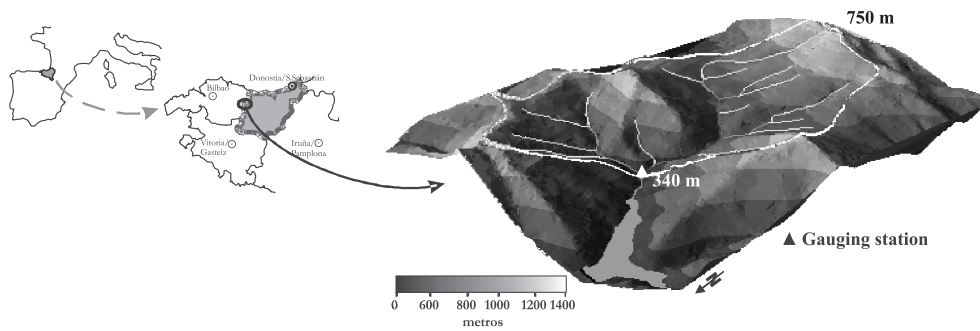
Fig. 1:   Location of the Aixola catchment.

are transported during most events, sediment transport occurs throughout the year, however, it's magnitude is the largest from November to April. A number of relationships between discharge and suspended sediment concentration during runoff events have been identified in the Aixola catchment. Each type of relationship (linear, clockwise hysteretic loop, counter clockwise, figure eight-shaped) is associated with different events and pre-event factors (Zabaleta *et al.*, 2007).

MATERIALS AND METHODS

Turbidity (FNU), discharge ($dm^3 \cdot s^{-1}$), and precipitation (mm) have been measured every 10 minutes at the gauging station located at the outlet of the catchment since October 2003. Turbidity is measured using a Solitax infrared backscattered light turbidimeter (Dr. Lange devices, 0-1000 FNU). Additionally, an automatic water sampler (SIGMA 900) was installed at the station and programmed to take water samples of about 600 ml when discharge rises. Electrical conductivity was measured in these samples before they were taken to the laboratory. Once in the laboratory, turbidity was again measured (WTW 555IR device) and suspended sediment concentration was calculated by means of filtration of the samples through 0.45 µm filters and later weighing the filters. In this manner, the relation between turbidity and suspended sediment concentration (SSC) was calibrated (Zabaleta *et al.*, 2006). Continuous SSC time series have been efficiently derived from *in situ* continuous turbidity series (Lewis, 1996; Zabaleta, 2008).

Taking into account parameters measured every 10 minutes, 76 rainfall-runoff events were characterised using four groups of variables (Zabaleta *et al.*, 2007): event's antecedent conditions, precipitation causing the event, discharge during the event, and suspended sediment delivered during the event. A correlation matrix and factorial analysis that included the variables of interest were performed in order to analyze the factors that control suspended sediment yield during runoff events in the Aixola catchment. The following results were obtained: 38% of events occurred in the autumn, 25% occurred in the winter, another 25% occurred during the spring, and the remaining 12% occurred during the summer.

Electrical conductivity could not be used in these statistical analyses because continuous measurements of this parameter were not available. However, the evolution of electrical conductivity during flood events and its relationship with discharge and suspended sediment were analysed.

RESULTS

Antecedent conditions are described by the amount of precipitation accumulated one hour before an event (aP1h, mm), as well as one day (aP1d, mm), seven days (aP7d, mm) and twenty one days (aP21d, mm) before an event and by the average discharge of the day (24 hours) before the beginning of a given event (aQ1d, $dm^3 \cdot s^{-1}$). Precipitation that caused the given event is characterised by total precipitation (Pt, mm), average intensity

of the precipitation during the rainfall event (IP, mm·h⁻¹), and maximum intensity of the precipitation (IPmax, mm·10min⁻¹). IPmax is the maximum precipitation recorded in a 10-minute interval series. Precipitation data were recorded at the gauging station located in the lowest part of the catchment – no other gauging device is available in the catchment. Discharge during an event is expressed by the total specific water volume of the runoff event (specific runoff) (Qt, mm), average (Qav, dm³·s⁻¹) and maximum discharge (Qmax, dm³·s⁻¹), and the relationship between this maximum discharge and the initial discharge prior to the event of interest (Qmax/Qb). Sediment load was quantified by the average of the suspended sediment concentration – recorded every 10 minutes during each event (SSCav, mg·dm⁻³), the maximum suspended sediment concentration during an event (SSCmax, mg·dm⁻³), and the total suspended sediment yield of the given event (SSt, Kg). In order to analyze the factors that control suspended sediment yield during events in the Aixola catchment, a correlation matrix was produced along with factorial analysis that includes all the variables mentioned above.

Discharge variables are well correlated with total precipitation. Total sediment yield is also strongly related to Pt ($R^2 = 0.58$), while SSCav and SSCmax are much better correlated with the maximum intensity of precipitation ($R^2 = 0.72$, 0.55, respectively). Suspended sediment yield and concentration are also well correlated with Qmax and particularly with the Qmax/Qb parameter. In the same way, suspended sediment average concentration and sediment yield are well correlated. According to Seeger *et al.* (2004), the other important factor that controls the transport of suspended sediment in catchments is antecedent conditions. In the case of Aixola, a very humanly disturbed catchment, antecedent conditions are not significantly correlated with suspended sediment variables.

Table 1: Pearson correlation matrix for parameters calculated for the Aixola catchment (n=76). Correlation is significant at the 0.01 level for bold numbers and 0.05 for italics.

	Pt	Ip	Ipmax	aP1h	aP1d	aP7d	aP21d	aQ1d	Qav	Qt	Qmax	Qmax/Qb	SSCav	SSCmax	SSt
Pt	1.00														
Ip	0.15	1.00													
Ipmax	*0.28*	**0.92**	1.00												
aP1h	0.07	-0.12	-0.10	1.00											
aP1d	-0.01	-0.18	-0.15	**0.49**	1.00										
aP7d	-0.06	*-0.27*	*-0.25*	**0.32**	*0.27*	1.00									
aP21d	-0.15	**-0.33**	**-0.34**	**0.30**	*0.24*	**0.64**	1.00								
aQ1d	-0.04	-0.21	-0.20	**0.31**	**0.34**	**0.71**	**0.61**	1.00							
Qav	**0.50**	-0.10	-0.03	**0.38**	**0.31**	**0.51**	**0.40**	**0.67**	1.00						
Qt	**0.62**	-0.15	-0.06	*0.23*	0.18	**0.33**	*0.23*	**0.45**	**0.88**	1.00					
Qmax	**0.66**	**0.30**	**0.43**	0.20	0.14	*0.26*	0.04	**0.30**	**0.78**	**0.68**	1.00				
Qmax/Qb	**0.54**	**0.54**	**0.70**	-0.12	-0.14	-0.21	**-0.37**	*-0.28*	0.11	0.13	**0.65**	1.00			
SSCav	**0.34**	**0.63**	**0.72**	-0.07	-0.09	-0.15	**-0.35**	-0.17	0.10	0.03	**0.61**	**0.84**	1.00		
SSCmax	**0.33**	**0.40**	**0.55**	-0.06	-0.11	-0.10	*-0.29*	-0.17	0.07	0.03	**0.57**	**0.85**	**0.92**	1.00	
SSt	**0.58**	0.22	**0.37**	0.05	0.00	0.09	-0.11	0.01	**0.49**	**0.51**	**0.83**	**0.76**	**0.72**	**0.80**	1.00

The above data were used to perform principal component analysis with Varimax rotation using the SPSS statistical package. The analysis classified (29% of the variance explained) IP, IPmax, SSCav, SSCmax and Qmax/Qb variables as the first factor and (23% of the variance explained) Pt, Qt, and Qav as the second factor. In this I-II factorial plane, the total sediment yield of an event (SSt) shows a strong relationship with both factors, even if the correlation is better with Factor I, and no meaningful relationship with antecedent conditions can be inferred.

Furthermore, the evolution of discharge and suspended sediment concentration during events was analysed. Hysteretic loops and some event and pre-event characteristics were analyzed using a new factorial approach. In this analysis, precipitation (Pt and IPmax), discharge (Qav), suspended sediment yield (SSt), and antecedent conditions (aP12, precipitation during the 12 hours before an event) were taken into consideration. The two principal factors created explained 71% of the variance calculated: the first factor with total precipitation, average discharge, and suspended sediment yield in the positive part (with 40% of the variance explained), the second factor (31% of the variance) with maximum precipitation intensity in the negative part, and antecedent 12 hour precipitation in the positive part. This distribution indicates a high level of correlation
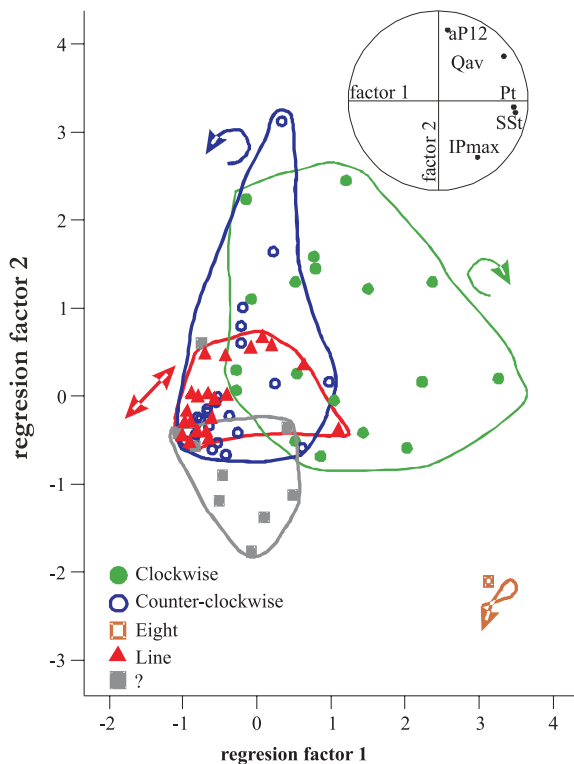
Fig. 2: Distribution of events on a I–II factorial plane based on hysteretic loops.

between precipitation (Pt), discharge (Qav), and suspended sediment yield (SSt). It also indicates a weak correlation of these parameters with precipitation maximum intensity (IPmax) as well as the absence of a meaningful relationship between the mentioned first and antecedent conditions. These results suggest a very rapid response of the catchment to rainfall events, both in the case of discharge and in the case of suspended sediment.

Figure 2 shows the position of different event types in the I–II factorial plane. Events showing a linear relationship between SSC and discharge are events with low levels of precipitation, discharge, and precipitation intensity. Events with clockwise hysteretic loops are located in the positive part of the first factor, therefore, they can be described as events with high precipitation and discharge magnitudes, high suspended sediment yields, and appreciable pre-event precipitation amounts. In these cases, a depletion of the sediment available for transport occurs before water discharge reaches its maximum. This rapid increase in suspended sediment concentration at the beginning of flood event can be explained by the rapid displacement of sediment deposited near the river channel (Regüés *et al.*, 2000). This kind of relationship between sediment and discharge is observed mostly between October and April.

Counterclockwise events differ from others in that they exhibit lower levels of precipitation, discharge, and suspended sediment yield, even though they can be observed under either high or low antecedent precipitation conditions. A figure eight-shaped hysteretic loop was observed for one event only and it was related to very high intensities of precipitation and dry antecedent conditions. This particular event took place at the end of the summer with a maximum precipitation intensity of 6.6 mm in 10 minutes. The rest of the events were not classified. They also took place during dry conditions and with high precipitation intensity, however, sediment discharge relationships are quite difficult to explain.

The evolution of electrical conductivity during runoff events was examined next. The behaviour of conductivity through a series of events was very homogeneous. In all cases studied, a rapid increase in electrical conductivity was recorded following a decrease observed during the rising limb of the hydrograph (Fig. 3). Maximum conductivities measured before and after runoff events were about 370 $\mu S \cdot cm^{-1}$. This value speaks of the chemical properties of the waters that usually are present in the catchment – "the old waters". Minimum conductivities measured during events were always comparatively high, about 200 $\mu S \cdot cm^{-1}$, indicating that a relatively high proportion of old (antecedent) waters (40%–45%) were present in discharge during runoff events (rainwater CE = 60-80 $\mu S \cdot cm^{-1}$). It must be noted that the presence of "old water" does not influence the sedimentological response of the catchment.

The relationship between minimum electrical conductivity (related to the maximum percentage of "new water" present in rivers) and maximum suspended sediment concentration (related to the maximum capacity of runoff to transport sediment) was also studied. However, no clear correlation between the parameters was found zin this catchment. High concentrations of suspended sediment (>2000 mg·dm^{-3}) and low electrical conductivities (<200 $\mu S \cdot cm^{-1}$) were observed only during events with very intense precipitation that occurred under dry summer conditions. Further work is planned on this subject.
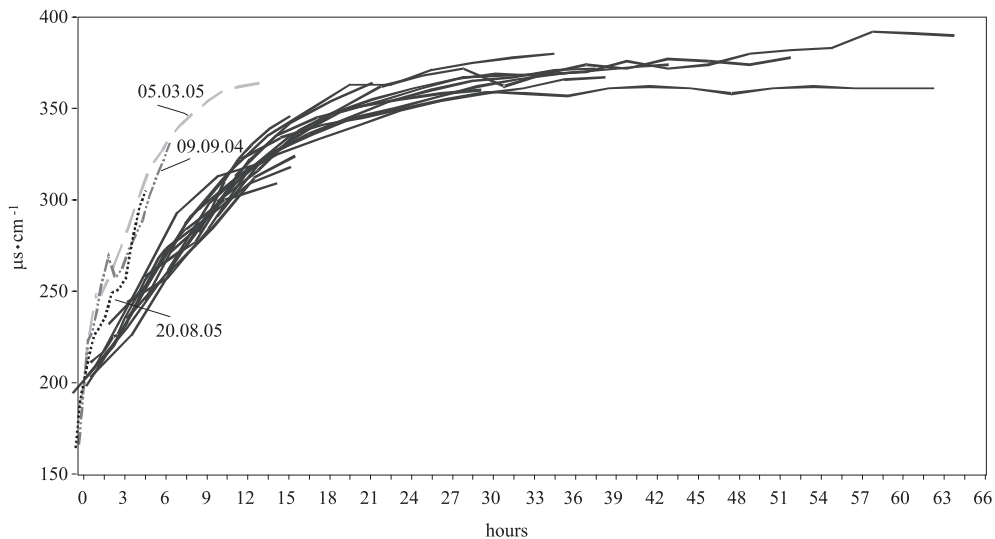
Fig. 3: Evolution of electrical conductivity (µS·cm⁻¹, in hours) in river waters following maximum discharge in the Aixola catchment. t = 0 hours corresponds to electrical conductivity of 200 µS·cm⁻¹, selected as a common point for all the events in order to make comparisons easier.

CONCLUSIONS

The correlation matrices and factorial analysis produced based on the flood events recorded in the Aixola catchment during two years of research show that there is a strong correlation between precipitation, discharge, and suspended sediment variables during flood events but no significant correlation between these variables and antecedent conditions. These results suggest a direct response of the catchment to rainfall events, both in the discharge as well as in the sediment levels. Therefore, the type of runoff events that take place in the Aixola catchment must be classified as a flash flood type.

While event suspended sediment yield is related to total precipitation, suspended sediment concentration is related to precipitation intensity. The relationship between discharge and sediment yield is strong and also positive. However, suspended sediment parameters do not exhibit any dependence on antecedent conditions and sediment response takes place in any type of hydrological situation present throughout the year.

Hysteretic patterns were found to be influenced by event discharge, precipitation characteristics, and pre-event precipitation amounts in the Aixola catchment. In this case, as described by Seeger *et al.* (2004), in small headwater catchments of the Spanish Pyrenees, not only event conditions but also antecedent conditions are important factors controlling sediment transport processes and constitute one significant factor which differentiates types of hysteretic loops. The different patterns of suspended sediment concentration (SSC)-discharge (Q) hysteretic loops observed for Aixola suggest a significant spatial and temporal variability in sediment source areas and the occurrence of different sediment delivery mechanisms depending on event characteristics and humidity conditions of the catchment.

The evolution of electrical conductivity in Aixola catchment waters during events indicates that even if discharge rates and sediment response rates induced by rainfall events are very rapid in all types of hydrological situations, the catchment possesses a considerable regulation capacity (its soils, mainly) as observed in the relatively high electrical conductivity of its river waters. Moreover, there is always a high proportion of pre-event waters in total discharge, including periods of maximum discharge.

REFERENCES

Lewis J. (1996). Turbidity-controlled suspended sediment sampling for runoff-event load estimation. *Water Resour. Res.,* **32**: 2299–2310.

Regües D., Balasch J.C., Castelltort X., Soler M. and Gallart F. (2000). Relación entre las tendencias temporales de producción y transporte de sedimentos y las condiciones climáticas en una pequeña cuenca de montaña mediterránea (Vallcebre, Pirineos Orientales). *Cuadernos de Investigación Geográfica*, **26**: 41–65.

Seeger M., Errea M.-P., Beguería S., Arnáez J., Martí C. and García Ruiz J.M. (2004). Catchment soil moisture and rainfall characteristics as determinant factors for discharge/suspended sediment hysteretic loops in a small headwater catchment in the Spanish Pyrenees. *J. Hydrol.*, **288**: 299–311.

Zabaleta A. (2008). *Análisis de la respuesta hidrosedimentarioa en pequeñas cuencas de Gipuzkoa*. Tesis Doctoral. UPV-EHU. Dpto. Geodinámica: 252 pp., anexos y CD.

Zabaleta A., Martínez M., Uriarte J. and Antigüedad I. (2006). Sediment source variability as origin of uncertainties in sediment yield estimation (Aixola catchment, Basque Country). In: Pfister L., Matgen P., van den Bos R. and Hoffman L. (eds), *Uncertainties in the 'monitoring-conceptualization-modelling' sequence of catchment research*. Abstract book of the ERB conference, Luxemburg: 27–28.

Zabaleta A., Martínez M., Uriarte J. and Antigüedad I. (2007). Factors controlling suspended sediment yield during runoff events in small headwater catchments of the Basque Country. *Catena*, **71**: 179–190.

RUNOFF FROM SMALL BASINS STUDIED FROM A MULTIFRACTAL VIEW POINT

M. I. P. de Lima

Institute of Marine Research – Coimbra Interdisciplinary Centre / Forestry Department,
ESAC/Polytechnic Institute of Coimbra, Bencanta, 3040-316 Coimbra, Portugal
e-mail: iplima@esac.pt

ABSTRACT

This work explores the use of multifractal tools to studying surface flow in watercourses. It explores scale-invariant properties exhibited by this process and the range of scales where such behaviour holds. The discharge data are from different gauging stations in the Douro river drainage basin, in Portugal. The analyses showed that scaling and multifractal behaviour is present in the data, over a considerable range of scales.

Key words: scaling, multifractal analysis, runoff, small basins

INTRODUCTION

The process of watercourse flow is known to be extremely non-linear and variable in time and space, since it depends very much on climatic regimes (particularly rainfall) and complex rainfall-runoff processes occurring over a variety of time scales and across drainage basins. No satisfactory detailed modelling of the complexity of the processes involved and their interactions has yet been achieved, either in mathematical terms or with respect to field data availability at suitable temporal and spatial scales. Moreover, empirical scale truncations are made often (i.e. one scale is studied independently of the others).

One major issue is the characterization of extreme discharges. On the one hand, often there are no discharge records for extreme flood events, and on the other hand, many models fail to adequately describe the violent behaviour of watercourse flows. This matters because the estimation of the probability of exceeding certain large events is highly important to hydrological studies and engineering design, since extreme discharges often lead to flooding that can endanger property and human life. The 'conventional' models frequently used for this type of study, i.e. models developed within non-scaling frameworks, usually involve only weak variability (e.g. exponential probability tails); this is a type of variability characterized by fluctuations of the process singularities that are sufficiently small that divergence of high-order statistical moments does not occur. These models study one scale independent of the other. Moreover, in these frameworks, two or more different distributions are often required to fit different regimes such as the "low-flow", the "regular" and the "extreme" events. These are all factors that limit the full statistical characterization of river and stream discharges.

This work explores an alternative approach to studying this process, developed within a scaling framework, based on the invariance of properties across scales. It uses multifractal theory and models aiming at contributing to the characterization of surface runoff processes in rivers, by exploring scale-invariant properties exhibited by this process and the range of scales where such behaviour holds. The discharge data are from different gauging stations in the Douro river drainage basin, in Portugal.

The approach to the study of river flows based on multifractal theory has been reported in only a few studies, see e.g. Tessier *et al*. (1996), Pandey *et al*. (1998), Hubert *et al*. (2002), Labat *et al*. (2002), Kantelhardt *et al*. (2006), Koscielny-Bunde *et al*. (2006), Sauquet *et al*. (2008). Therefore, the applicability of multifractal theory to runoff processes has still not been fully explored.

MULTIFRACTAL TOOLS

In general terms, in a given process multifractal theory allows us to mathematically investigate the presence of invariance of properties maintained across scales. Scale-invariance leads to a class of scaling rules (power laws) characterized by scaling exponents. This allows the relationship of variability between different scales to be quantified. Statistical properties of scale-invariant systems at different scales (i.e., on large and small scales) are related by a scale-changing operation that involves only scale ratios. Thus scaling theories are developed in non dimensional frameworks.

Multifractal theory (e.g. Schertzer and Lovejoy, 1989, 1991) can play an important role in runoff studies. It has the potential to assess the full range of river flow fluctuations and it offers a single framework to deal with the different flow regimes. Moreover, multifractal methods are innovative for the analysis of extremes, offering practical tools for assessing their probability of occurrence. They can handle heavy tails (i.e., power-law tails) in the flow rate probability distributions. This statistical behaviour may indicate that, in some cases, the probability of exceeding certain high-intensity events is greater than the probability predicted by more 'conventional' models characterized by exponential tails (e.g. Gumbel distribution): power-law tails fall-off slower that exponential tails. This may have important implications in engineering design.

One can use standard spectral methods and analysis to test for scale-invariance. Spectral methods are also known as Fourier transform methods (see e.g. Wu, 1973; Box and Jenkins, 1976; McLeod and Hipel, 1995). For a scaling process, the Fourier energy (power) spectrum is expected to exhibit a power-law behaviour (e.g. Mandelbrot, 1982; Schertzer and Lovejoy, 1987) of the form:

$$E(\omega) \approx \omega^{-\beta} \qquad \text{Eq. 1}$$

where ω is the wave-number, $E(\omega)$ is the energy, and β is the spectral exponent. For temporal processes, the wave-number ω can be approximated by $\omega \sim 1/\tau$, τ being the magnitude of any time interval.

The multifractal temporal structure of the runoff process can be investigated by studying the (multiple) scaling of the statistical moments of the flow rates (Schertzer and Lovejoy, 1987). The scaling behaviour is described by the moments scaling exponent function $K(q)$ that satisfies:

$$\langle Q_\lambda^q \rangle \approx \lambda^{K(q)} \qquad \text{Eq. 2}$$

where λ is the resolution (it is the ratio between the largest scale of interest and the scale of homogeneity of the data or process) and $\langle Q_\lambda^q \rangle$ is the (ensemble) average q^{th} moment of the flow rate on a scale specified by λ. The notion of moment can be generalized to any real value q. The scaling of the moments can be tested with log-log plots of the average q^{th} moment of the flow rate Q_λ, observed on scales of different levels of resolution λ, against the scale ratio λ. The empirical scaling functions K(q), in Eq. (2), are obtained from the regression lines of $\log(\langle Q_\lambda^q \rangle)$ against $\log(\lambda)$ for various moments q of the flow rates.

A Legendre transform (Frisch and Parisi, 1985) establishes a one-to-one relation between orders of singularities γ of the intensities of a process and statistical moments q. This implies, for example, that a single discharge ($Q_\lambda = \lambda^\gamma$) gives a dominant contribution to the qth order moment (q = c' (γ)).

SURFACE FLOW DATA

The river runoff data used in this work are from the river Douro drainage basin, in Portugal. Four measuring stations were selected. Their location is shown in Fig. 1, and a summary of some physiographic characteristics of the water courses and drainage basins are given in Table 1. The area of the drainage basins ranges from about 310 to 1743 km². The time resolution of the data is daily; the time span of the records is more than 40 years. The discharge rates were obtained using rating curves. There are no missing values in the data sets. The 4 daily
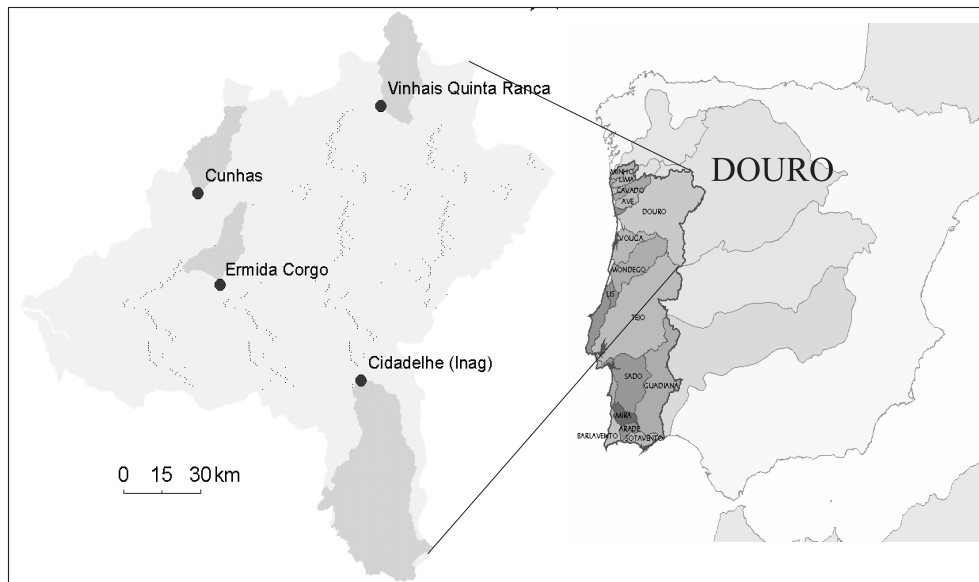
Fig.1: Location of the 4 measuring stations and respective sub-drainage basins, located in the Douro drainage basin (Portugal).

Table 1: Summary of some physiographic characteristics of the water courses and drainage basins, and statistics for 4 locations in the Douro river (Portugal). Symbols are defined in the text.

Station	Ermida Corgo	Cunhas	Vinhais	Cidadelhe
Lat (N); Log (W)	41º14′; 7º45′	41º32′; 7º51′	41º49′; 7º00′	40º55′; 7º06′
Altitude (m)	120.00	198.87	416.16	253.84
Water course	Rio Corgo	Rio Beça	Rio Tuela	Rio Côa
Length (km)	17.522	33.720	39.675	198.316
Mean slope [%]	0.924	1.637	0.809	0.832
Drainage Basin				
Area [km^2]	294.23	337.29	478.55	1743.00
Shape	Asymmetric	Elongated, NE -SW	Elongated, S -N	Elongated, S-N
Altitude (m)	130−1318	196 −1271	544−1347	130−1078
Mean annual precipit. [mm]	700−1600, increasing S-N	800−2000, increasing E-W	800−1600, decreasing E-W	400−1200, decreasing S-N
Land use	Mainly forest and agricultural land	Forest and agricultural land	Forest is dominant; few agric. areas	Mainly forest and agricultural land
Some statistics				
Period	1956−2002	1949−1997	1956−1997	1956−1997
Mean annual discharge [mm]	890	858	747	281
Mean daily discharge [$m^3 \cdot s^{-1}$]	8.4	9.2	11.3	15.5
Max spec. Daily discharge (mm)	84.9	63.8	53.3	36.7
Spectral exponent β	0.51	0.61	0.60	0.70
γ_{max}	0.365	0.357	0.329	0.451
C_1	0.113	0.093	0.107	0.113
α	1.51	1.52	1.93	1.32

flow time series are plot in Fig. 2; statistical test show that they are stationary. The local rainfall regime and its strong seasonality make the surface flow regimes observed in the drainage network highly irregular.
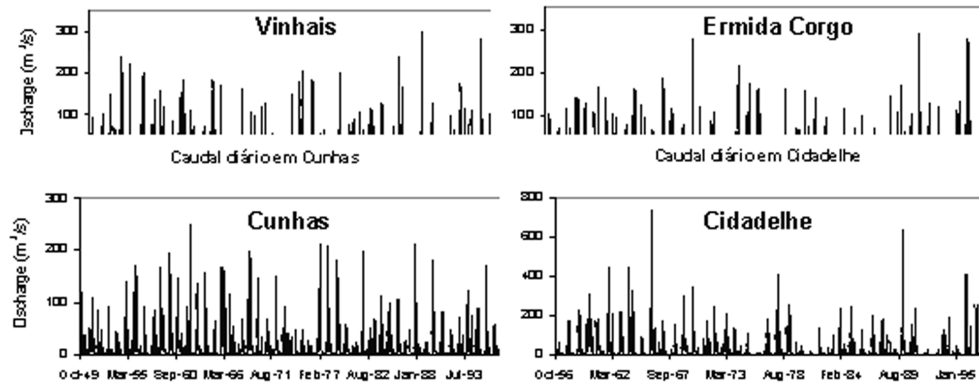
Fig.: 2.　　　River discharge daily time series from 4 locations in the Douro river drainage basin (see Table 1). Note that vertical axes scales are not the same.

RESULTS

Scale-invariance in the surface flow process is first investigated through the energy spectra of the 4 data sets. These spectra are shown in Figure 3, in log-log axis; the strong signal (i.e. spectral peak) observed in the spectra is associated with the annual frequency. The spectra exhibit scaling behaviour over a range of scales ranging form 1 day up to more than 3 months. The spectral exponents β that characterize this behaviour range from 0.51 to 0.70. A smaller exponent indicates larger irregularity in the flow regime. In this case, these lower and upper limits correspond to the smallest and largest drainage basin studied here.
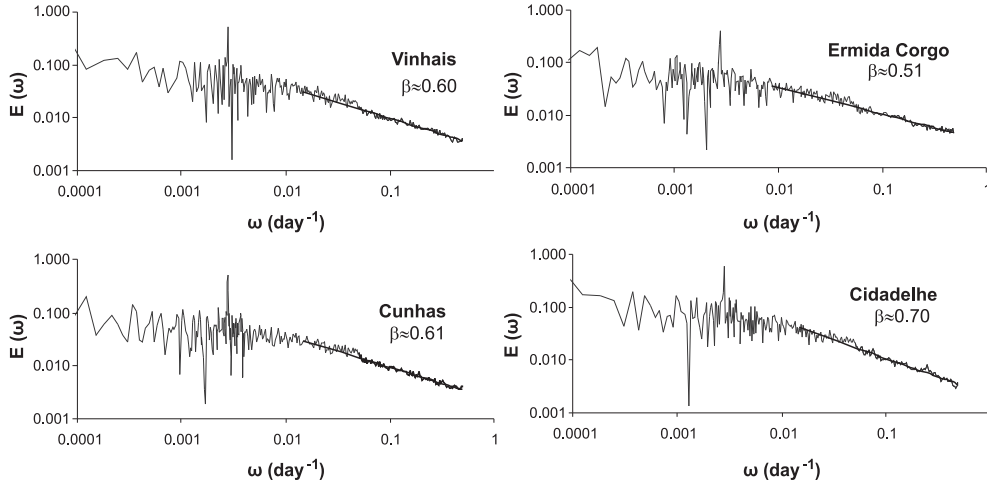
Fig.: 3.　　　Energy spectra for the daily river discharge recorded at 4 locations in the Douro basin, in the north of Mainland Portugal (see Figure 1 and Table 1). The straight lines are fits to the scaling regions, yielding the spectral exponents β.

The daily resolution of the flow data does not allow us to investigate the scaling regime at scales smaller than one day. River flow reflects the interactions between the precipitation input and the local drainage basin characteristics that determine the hydrologic response of the basin. For the data analysed, the spectra of river flow exhibit a spectral slope β larger than the corresponding value found for precipitation in the region (de Lima *et al.*, 2003). The precipitation signal is thus modified by the complexity and variety of processes involved in the precipitation–runoff dynamics.

90

The multifractality of the runoff process is investigated here by testing the scaling behaviour of the statistical moments of the flow rates. Figure 4 shows for the 4 data sets and for the record periods indicated in Table 1 the plots for some moments q>1, for scales from 1 day up to about 5.6 years. The results confirm the presence of scale-invariance across a significant range of scales (from 1 day up to about 128 days).

The scaling exponent functions $K(q)$ that describe the statistics of the flow data over the scaling range are shown in Figure 5. Turning our attention to the large discharge rate part of the statistics, we see that $K(q$ is linear for q exceeding a critical value q_{crit}. Such a discontinuity in the first or second derivative of $K(q$ arises either because
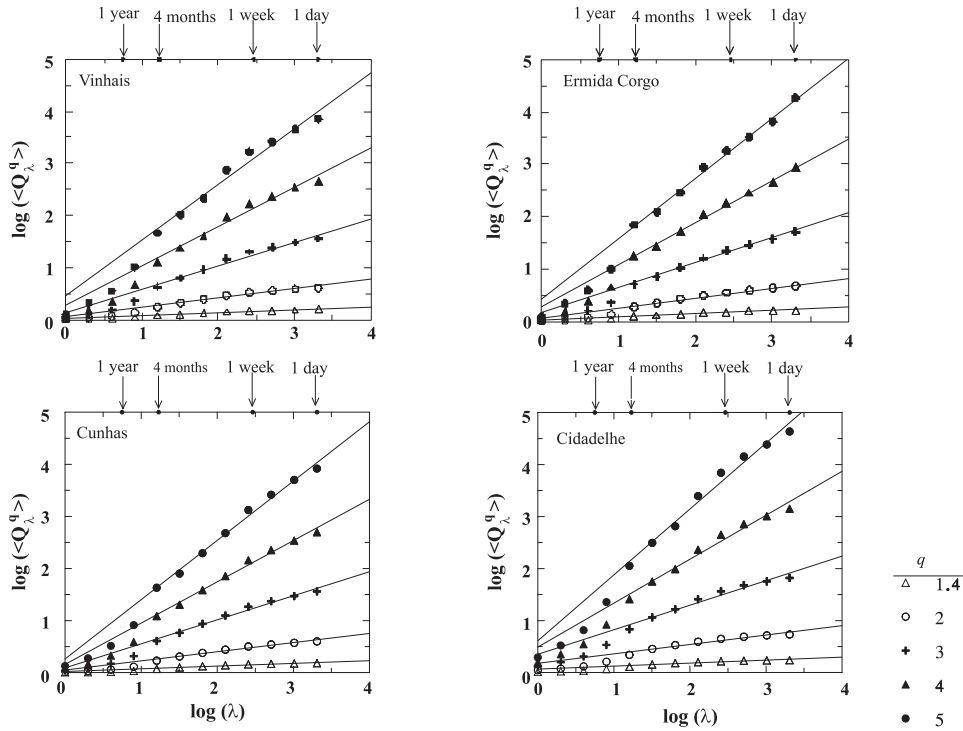
Fig. 4: Log-log plots of the average q^{th} moments of the flow rate against the scale ratio, for the 4 data sets from the Douro river drainage basin. The plot displays scales between 1 day (λ=2048) and 2048 days (λ=1). The straight lines are fits to the scaling regions (assumed to be between 1 and 128 days), aiming at obtaining the scaling exponent functions $K(q)$.
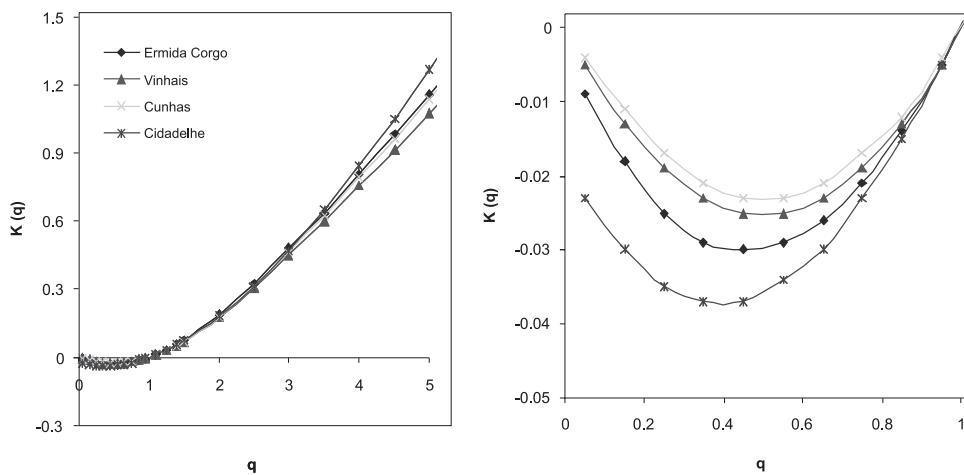
Fig. 5: Scaling functions $K(q)$ of the moments of the discharge rates at the 4 measuring sites in the Douro basin. The plot on the right shows a detail for moments $q<1$. See Table 1, for statistical parameters.

91

of divergence of moments at q_{crit} (called q_D in this first order case) or simply due to the inadequate sample size (at q_s, in the second order case), so that all moments larger than q_s are determined by the largest value present in the sample (see e.g., Schertzer and Lovejoy, 1991). We can determine the corresponding largest singularity present in the sample from $\gamma_{max}=max(K'(q))$, see Table 1. A complete and systematic characterization of the extremes is best done with the help of the complementary scaling function $c(\gamma)$, i.e. by a systematic study of the probability distributions; this is outside our scope here.

Finally, we can characterize the behavior of $K(q)$ for the values near the mean ($q=1$), by using parameter $C_1=K'(1)$ and the radius of curvature R_K at $q=1$ by the parameter α via the relation:

$$R_K (q=1) = \left[\frac{(1 + K'(q))^{3/2}}{K''(q)} \right]_{q=1} = \frac{(1 + C_1)^{3/2}}{C_1 \, \alpha} \qquad \text{Eq. 3}$$

Parameter C_1 is thus the order of singularity of the mean. This characterization of the curvature by α has the advantage that in the case of universal multifractals this single parameter α characterizes the entire $K(q)$ function:

$$K(q) = \frac{C_1}{\alpha - 1} \left(q^a - q \right) \qquad \text{Eq. 4}$$

for q in the non-linear regime (Schertzer and Lovejoy, 1987). Parameter α is called the degree of multifractality. For the data analyzed here we obtained the estimates for these two parameters that are indicated in Table 1: values of α are between 1.32 and 1.93; and C_1 values are low, between 0.093 and 0.113. These estimates are consistent with the results reported in the literature by e.g. Tessier *et al*. (1996) and Pandey *et al*. (1998).

CONCLUDING REMARKS

Results indicate that the scaling framework provides tools that are able to quantify differences in the variability in surface flows, taking into account the behaviour observed across scales. Results also show that the particular signature of a runoff process can be characterized by multifractal parameters which can thus be used complementary to other classical ways of characterization. This signature results from the combined effect of the various non-linear processes involved in the rainfall-runoff transformation. This study will pursue by investigating the relations between the statistical behaviour of river flows and the physical characteristics of the drainage basins as well as the statistics of the rainfall input. These relations were not yet fully explored in the literature. In general terms, the results obtained in this study are consistent with the results reported by e.g. Tessier *et al*. (1996), Pandey *et al*. (1998), Sauquet *et al*. (2008).

REFERENCES

Box G.E.P. and Jenkins G. M. (1976). *Time series analysis: forecasting and control*. Holden-Day, San Francisco, USA.

de Lima M.I.P., de Lima J.L.M.P. and Coelho M.F.E.S. (2003). Spectral analysis of scale invariance in the temporal structure of precipitation in Mainland Portugal. *Rev. Eng. Civil*, Univ. Minho, Portugal, **16**: 73–82.

Frisch U. and Parisi G. (1985). Fully developed turbulence and intermittency. *Turbulence and predicability in geophysical fluid dynamics and climate dynamics*. Proc. of the Intern. School of Physics "Enrico Fermi", Course LXXXVIII, edited by M. Ghil *et al.*, Italian Physical Society, North-Holland, Amsterdam.

Hubert P., Tchiguirinskaia I., Bendjoudi H., Schertzer D. and Lovejoy S. (2002). *Multifractal modeling of the Blavet river discharges at Guerledan*. Proc. of the Third Inter-Celtic Colloquium on Hydrology and Management of Water Resources, National Univ. of Ireland, Galway, 8th-10th July 2002: 131–138.

Kantelhardt J.W., Koscielny-Bunde E., Rybski D., Braun P., Bunde A. and Havlin S. (2006). Long-term persistence and multifractality of precipitation and river runoff records. *J. Geophys. Res.*, **111**, D01106, doi:10.1029/2005JD005881.

Koscielny-Bunde E., Kantelhardt J.W., Braun P., Bunde A. and Havlin S. (2006). Long-term persistence and multifractality of river runoff records: Detrended fluctuation studies. *J.Hydrol.*, **322**: 120–137.

Labat D., Mangin A., and Ababou R. (2002). Rainfall-runoff relations for karstic springs: multifractal analyses. *J. Hydrol.*, **256**(3–4): 176–195.

Mandelbrot B. (1982). *The fractal geometry of nature*. Freeman, San Francisco.

McLeod A.I., and Hipel K.W. (1995). Exploratory spectral analysis of hydrological times series. *Stoch. Hydrol. Hydraul.*, **9**: 171–205.

Pandey G., Lovejoy S. and Schertze D. (1998). Multifractal Analysis Including Extremes of Daily River Flow Series for Basins one to a million square kilometers. *J. Hydrol.*, **208**: 62–81.

Sauquet E., Ramos M.-H., Chapel L. and Bernardara P. (2008). Streamflow scaling properties: investigating characteristic scales from different statistical approaches. *Hydrol. Process.*, **22**: 3462–3475.

Schertzer D. and Lovejoy S. (1987). Physical modeling and analysis of rain and clouds by anisotropic scaling multiplicative processes. *J. Geophys. Res.*, **92**(D8): 9693–9714.

Schertzer D. and Lovejoy S. (1989). Nonlinear variability in Geophysics: multifractal simulations and analysis. In: L. Pietronero (ed.), *Fractals' physical origin and properties*, Plenum Press, New York: 49–79

Schertzer, D., and Lovejoy, S. (1991). Nonlinear geodynamical variability: multiple singularities, universality and observables. In: D. Schertzer and S. Lovejoy (eds.), *Non-linear variability in Geophysics: scaling and fractals*. Kluwer Academic Publishers, The Netherlands: 41–82.

Tessier Y., Lovejoy S., Hubert P., Schertzer D. and Pecknold S. (1996). Multifractal analysis and modeling of rainfall and river flows and scaling, causal transfer functions. *J. Geophys. Res.*, **101**(D21): 26427–26440.

Wu B. (1973). *Mathematical models for the simulation of cyclonic storm sequences and precipitation*. Ph.D. Thesis, Univ. of California, Davis, USA.

SELECTED ASPECTS OF DROUGHT STREAMFLOW DEFICIT VARIABILITY IN SMALL LOWLAND CATCHMENTS

E. Tomaszewski

University of Łódź, Faculty of Geographical Sciences, Department of Hydrology and Water Management
90-131 Łódź, Narutowicza Str. 88, Poland, etomasz@geo.uni.lodz.pl

ABSTRACT

The purpose of this paper is to present an analysis of multi-year and seasonal variability of drought streamflow deficit in small lowland catchments. The identification of low-flow periods and the estimation of streamflow deficit were based on the threshold level method, adopting the seventieth percentile from the flow duration curve as the decision criterion. Basic calculations were performed for daily discharge series at 11 gauging stations located in the basins of the Warta, Pilica, and Bzura rivers for the 1951–2000 time period. The analysis concerns multi-year tendencies and the homogeneity of streamflow deficit determinants as well as the problem of seasonality with respect to streamflow deficit concentration and its time of occurrence. The issue of inertia was also investigated on several different time scales.

Keywords: hydrological drought, low flows, seasonal and multi-year runoff variability

INTRODUCTION

Most elements of river regime demonstrate some level of seasonal and multi-year variability. This also applies to characteristics which are linked to shortage of water resources. Low flows and droughts play important role in river flow regime as they are meaningfully associated with basic water resources. Their extremes indicate limitations in water management. The origin of this phenomenon has not been fully identified because of many indirect factors whose impact is considerably stretched in time. Therefore, multi-year analyses using annual and seasonal intervals may be quite useful both from a scientific and a practical point of view.

The terms "hydrological drought" and "low flow period" are well known in the field of hydrology. However, various methods define these phenomena in different ways. One approach is based on a threshold level. **A** period during which discharge attains values below an established limit is defined as a streamflow deficit period. Its two basic parameters are low flow duration and deficit volume (Fig. 1).

There are two methodological approaches that allow researchers to select a proper threshold: conventional (based on water management) or statistical. The former approach assumes that the threshold can be derived from a flow duration curve such as the percentile Q_{70} or Q_{90} (Hisdal *et al.*, 2004). The latter uses minimum annual daily discharge in the calculation of SNQ (mean minimum runoff), WNQ (the largest of the runoff minima) or ZNQ (median minimum runoff), cf Ozga-Zielińska (1990).
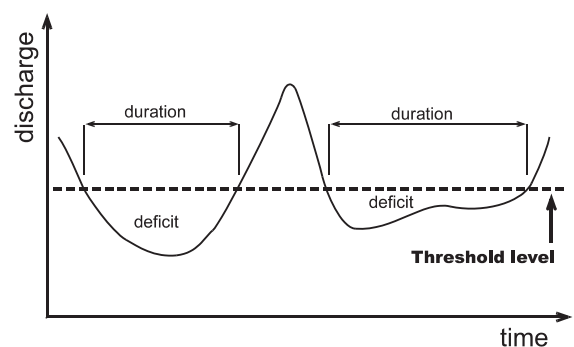
Fig. 1: Basic parameters of a hydrological drought.

RESEARCH LOCATION AND DATA

The research area is located in the central part of Poland. A set of 11 water gauges located in the basins of the Warta, the Pilica, and the Bzura rivers was selected for analysis (Fig. 2). All of the gauges, closing off small and midsize autochthonous catchments, reflected typical conditions vital for low flow formation. Basic calculations were performed on daily discharge series for the 1951–2000 time period. The data had been collected by the Polish Institute of Meteorology and Water Management. In order to estimate streamflow
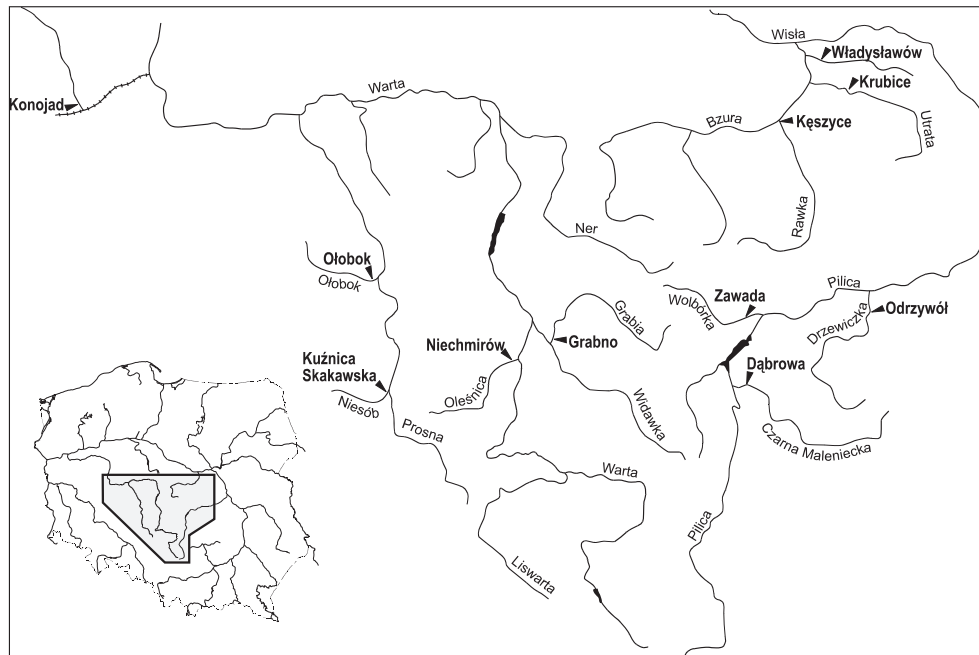
Fig. 2: Locations of the research water gauges.

deficit, the threshold method was applied. The percentile Q_{70} from the flow duration curve was accepted as an appropriate cutoff level on the flow hydrograph. Next, two basic parameters were calculated for each month: the monthly sum of streamflow deficit volume and the number of days with streamflow deficit.

MULTI-YEAR VARIABILITY AND TENDENCY

The multi-year variability of drought streamflow deficit volume was analyzed on the basis of variation coefficient (Fig. 3). Its value was rather high – 0.9 on average. However, differences between catchments did not appear to be large (0.8–1.0) with the exception of one outlier in the case of the Grabia River (1.35).

The multi-year streamflow deficit tendency was statistically significant only in half of the investigated cases (Fig. 4). An upward trend occurred in 2 catchments – Oleśnica and Łasica. A downward trend was demonstrated by 3 rivers (Utrata, Grabia, Niesób). In the other cases, the streamflow deficit tendency was not statistically significant. It is worth noting that no spatial tendencies were observed. This could be taken to imply that determinants and factors which operate on a macroscale and a meso-scale (such as climate) are more or less modified by local conditions.

An analysis of the homogeneity of conditions which determine drought streamflow deficit provided quite interesting results. This was performed using a double mass curve (Fig. 5). It shows the relationship between the cumulated variable of annual streamflow deficit volume and the cumulated variable of annual number of days with streamflow deficit.

96
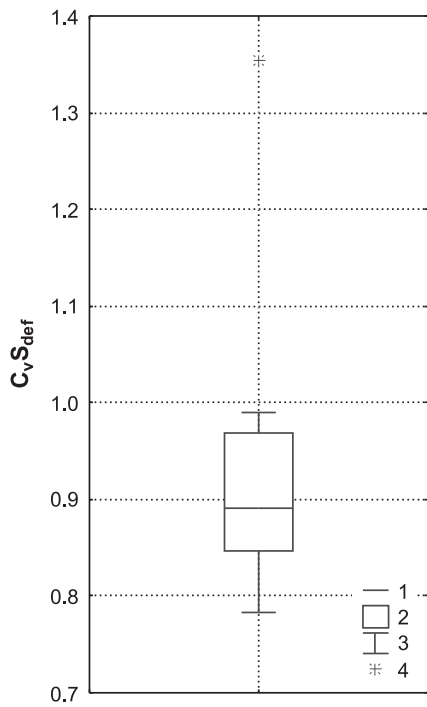
Fig. 3: Distribution of the drought streamflow deficit variation coefficient. 1 – median, 2 – 25–75%, 3 – range less than 1.5 quartile deviations, 4 – outliers.
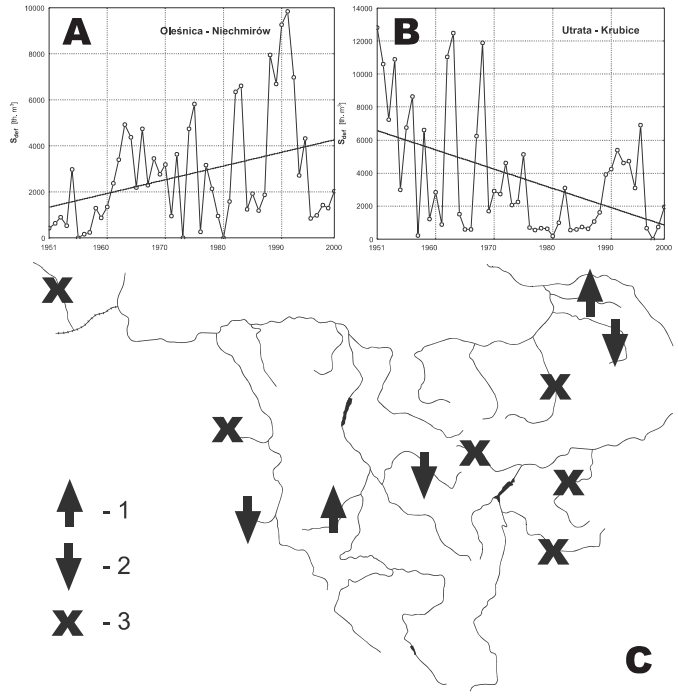
Fig. 4: Examples of statistically significant trends of annual streamflow deficit (A & B) and their spatial variability (C). 1 – statistically significant upward trend, 2 – statistically significant downward trend, 3 – statistically insignificant trend.
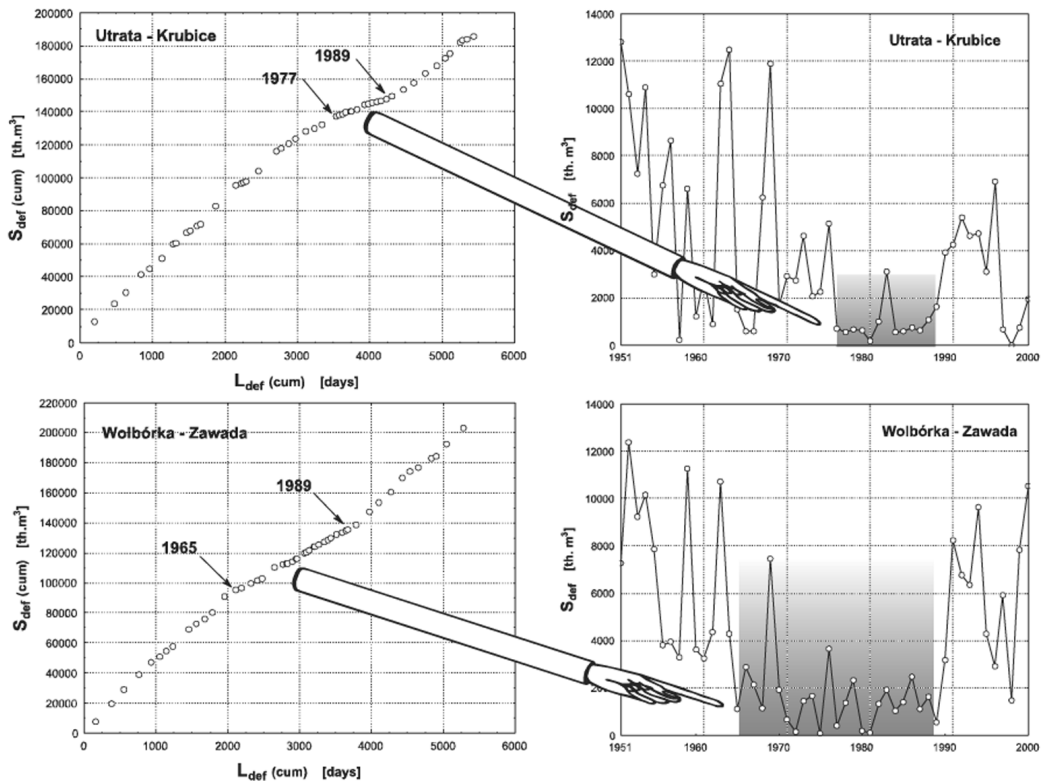
Fig. 5: Double mass curve (1951–2000). L_{def} (cum) – cumulated annual number of days with streamflow deficit, S_{def} (cum) – cumulated annual streamflow deficit volume.

97

Breaks in the curve indicate changes in the relationship between the conditions driving this process. Seven of eleven cases possessed two breaks in their curves. It is interesting to note that the second break occurs near 1989 in each case. This suggests that the beginning of the 1990s was very important for low flow regimes. In the periods between breaks, streamflow deficit volume is in a state of relative decrease while low flow duration is in a state of relative increase. This results in periods with a lower streamflow deficit volume as well as less variability within each period (Fig. 5).

SEASONALITY
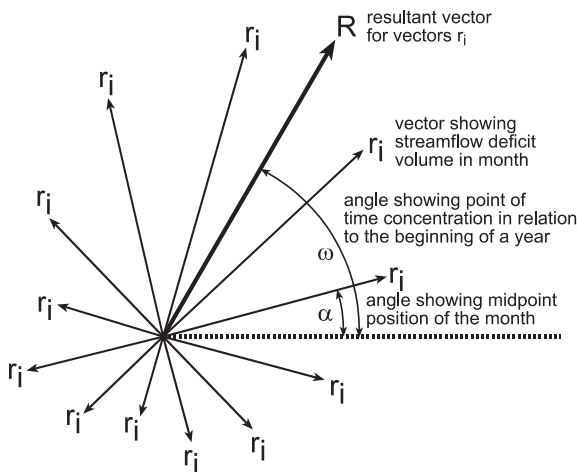
Fig. 6: Idea of Markham Procedure.
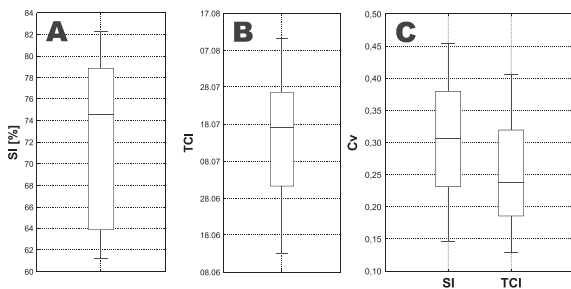
Fig. 7: Distribution of seasonality index (A), time of concentration index (B) and their variation coefficients (C).
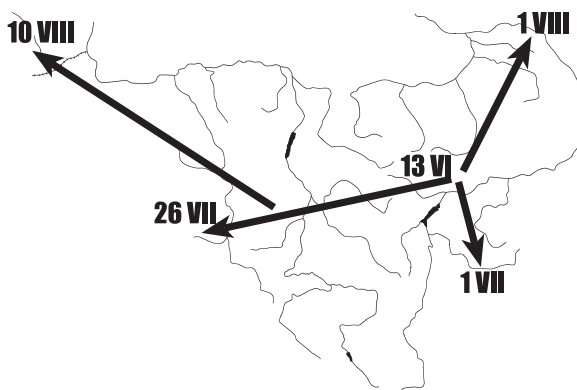
Fig. 8: Spatial course of streamflow deficit concentration time.

The seasonal variability of streamflow deficit was estimated on the basis of Markham (1970) indices. The level of irregularity of annual deficit volume distribution as well as its concentration time were calculated based on angular characteristics. The original version of the procedure was designed for precipitation analysis, however, it has also been adopted for use with total runoff and groundwater runoff (Bartnik and Tomaszewski 2006; Jokiel and Bartnik 2001; Tomaszewski 2001, 2005, 2007). Both characteristics refer to vector analysis (Fig. 6). Each of the 12 months is represented by vector whose length is determined by monthly streamflow deficit volume and its angle depends on midpoint position of the given month in relation to the beginning of the year.

The length of the resultant vector in relation to the sum of the 12 vectors defines the streamflow deficit seasonality index (SI). Its value varies between 0% which means total regularity (the same streamflow deficit volume each month) and 100% which is determined by total concentration where drought streamflow deficit occurs in one month only. The second characteristic – the time of concentration index (TCI) – is represented by the angle of the resultant vector and indicates the day (or the month) of the year of streamflow deficit concentration.

The calculated seasonality index was rather high (74% on average) and oscillated between 60% and 82% which means strong and very strong seasonality (Fig. 7). It is worth noting that the level of irregularity is very high in this case. The same variables attained very different values for groundwater flow (10–20%), precipitation (20–30%), and total runoff (20–40%). The time of concentration index varied between the 13th of June and the 10th of August which clearly indicated a strong role being played by the summer season in the appearance of a streamflow deficit (Fig. 7). In spatial terms, its onset is slightly delayed to the west and to the north (Fig. 8). It appears that climatic influences are significantly modified by hydrogeological conditions, especially by the capacity and the dynamics of groundwater reservoirs which are of a great importance to low flow regime on a time scale. It should also be emphasized that both

seasonality indices remained very stable from year to year. This was confirmed by the low variation coefficients obtained (Fig. 7). Moreover, there was no statistically significant multi-year tendency in any of the investigated cases. This is interesting because precipitation, discharge, and evapotranspiration are very often prone to having some long-term trends. However, seasonality indices are dependent on their own mutual relationships and if their ratios are stable in multi-year periods, then seasonality indices do not vary much either.

INERTIA

The question of the inertia of drought streamflow shortage was examined based on autocorrelation analysis. On a multi-year scale, the first autocorrelation coefficient (shift = 1, 1 year in this case) allowed for the identification of pocket of information about low-flow forming which is transmitted from year to year. In every case, the autocorrelation was quite strong and statistically significant which seems to be determined by the groundwater reservoir regime. Equally interesting was the analysis of autocorrelation based on subsequent shifts. It was possible to group the investigated cases into three categories (Fig. 9). The first category applies to systems with a "long memory" of water shortage episodes where homogenous periods last 9 to 11 years. This category is associated with
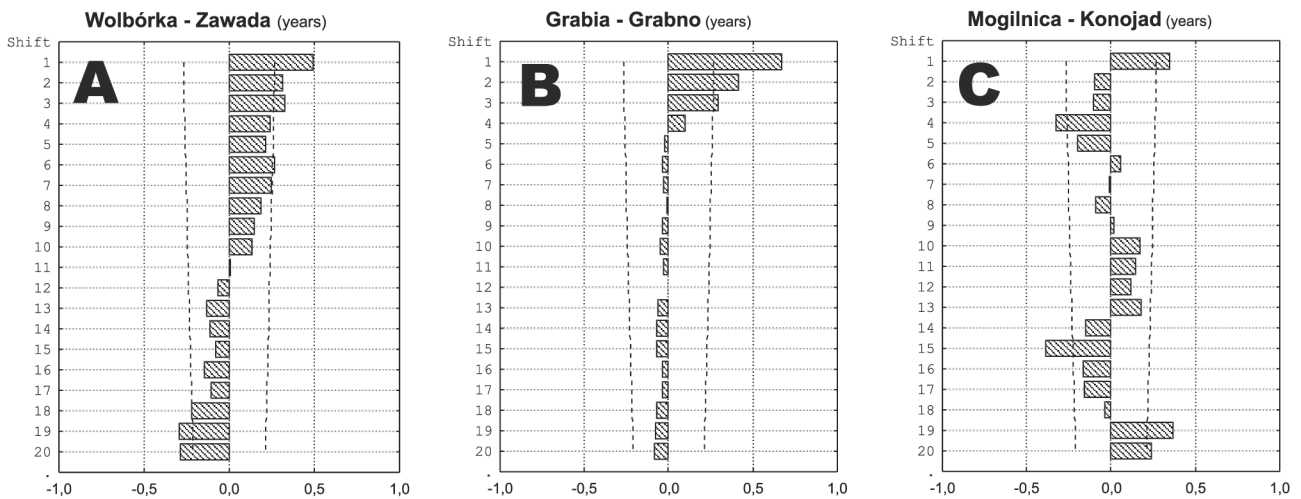
Fig. 9: Autocorrelation of annual streamflow deficit volume in subsequent shifts (1951–2000). The dashed line marks confidence intervals.

basins where the tempo of recession and renewal of groundwater resources is rather low. The second category applies to systems with a very short "memory" of 3 to 4 years. The third category is rather difficult to interpret. It seems to be that the unique nature of some isolated short periods may be the result of the impact of certain specific factors such as lakes which are very important in terms of water retention capacity.

On a monthly scale, all of the rivers demonstrated a clear seasonal rhythm and the only difference was how strong the transition between the seasons was (Fig. 10).
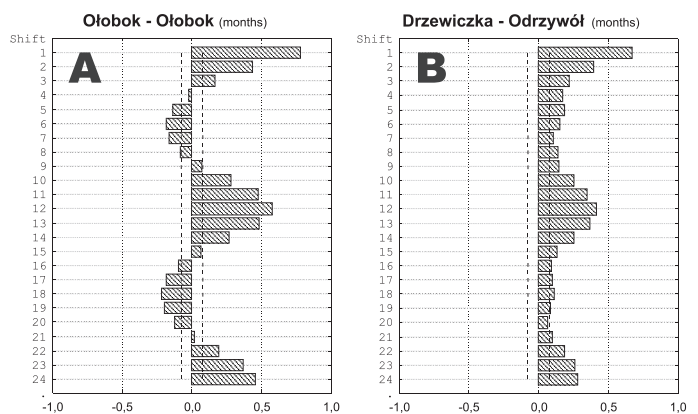
Fig. 10: Autocorrelation of monthly streamflow deficit volume based on subsequent shifts (1951–2000).

99

SUMMARY

It is useful to present diagrams showing drought streamflow deficit volume in relation to years and months (Fig. 11). All analyses have shown that the most common drought periods from 1951 to 2000 were the 1950s and the 1990s. However, hydrological droughts in the 1950s were more severe but those in the 1990s occurred in more catchments. It has also been observed that in rivers where streamflow deficit appeared very often, the time of this event was limited to the summer half-year (Grabia and Łasica examples). In catchments where droughts were weaker, the streamflow deficit occurrence period extended well into the winter half-year (Wolbórka and Rawka examples).

Grabia - Grabno

Łasica - Władysławów

Wolbórka - Zawada

Rawka - Kęszyce

Drought streamflow deficit:

low   middle   high
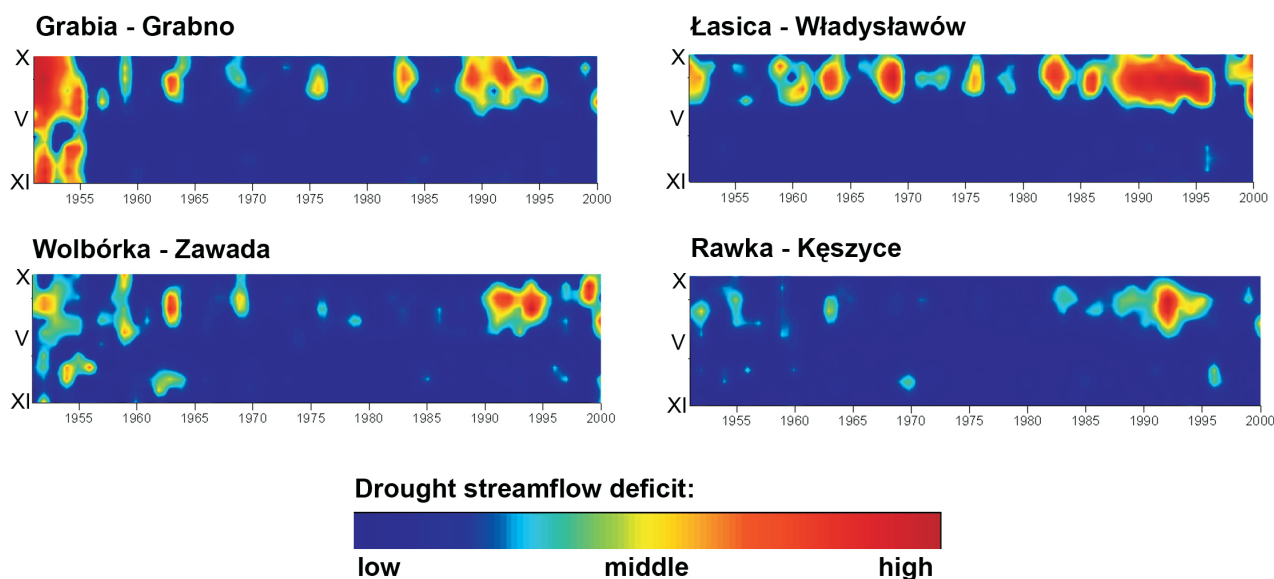
Fig. 11:   The annual course and the long-term course of monthly drought streamflow deficit volume.

The research presented herein produced some interesting results. The conclusions drawn need to be confirmed and expanded by further studies. This is especially true of the spatial aspect of these phenomena as areas with such a high density of catchments have not been analyzed before with respect to such long time series.

REFERENCES

Bartnik A. and Tomaszewski E. (2006). Zastosowanie indeksu pory koncentracji do oceny podatności reżimu rzecznego na formowanie przepływów ekstremalnych w zlewniach nizinnych (Application of the time concentration index to the estimation of river regime receptivity to extreme discharge events in lowland catchments). In: Kostrzewski A., Czerniawska J. (Eds.), *Przemiany środowiska geograficznego Polski północno-zachodniej*, Bogucki Wydawnictwo Naukowe, Poznań.

Hisdal H., Tallaksen L.M., Clausen B., Peters E. and Gustard A. (2004). Hydrological Drought Characteristics. In: Tallaksen L.M. and van Lanen H.A.J. (Eds.), Hydrological Drought. Processes and Estimation Methods for Streamflow and Groundwater. *Development in Water Science*, **48**.

Jokiel P. and Bartnik A. (2001). Zmiany w sezonowym rozkładzie odpływu w Polsce środkowej w wieloleciu 1951–1988 (Changes in the seasonal distribution of outflow in Poland from 1951 to 1998). *Wiadomości IMGW*, **2**.

Markham Ch.G. (1970). Seasonality in the precipitation in the United States. *Ann. Assoc.Am. Geogr*., **3**.

Ozga-Zielińska M. (1990). Niżówki i wezbrania – ich definiowanie i modelowanie (Droughts and Floods – Their Definition and Modelling), *Przegląd Geofizyczny*, **1–2**.

Tomaszewski E. (2001). Sezonowe zmiany odpływu podziemnego w Polsce w latach 1971–1990 (Seasonal changes in groundwater flow in Poland from 1971 to 1990). *Acta Geogr. Lodz.*, **79**.

Tomaszewski E. (2005). Application of the ET algorithm to estimation of groundwater flow dynamics in mountain rivers. *Landschaftsökologie und Umwelforschung*, **48**.

Tomaszewski E. (2007). Pora koncentracji odpływu podziemnego w środkowej Polsce (Time concentration of groundwater runoff in central Poland). In: Michalczyk Z. (Ed.), *Obieg wody w środowisku naturalnym i przekształconym*, Wyd. UMSC, Lublin.

RUNOFF FORMATION IN A SMALL MOUNTAINOUS BASIN DOMINATED BY A FRACTURED ROCK AQUIFER: RESULTS FROM THE TRACER-BASED INTEGRATED CATCHMENT APPROACH (ICA)

A. Herrmann and S. Schumann

Institute of Geoecology, Department of Hydrology and Landscape Ecology, Technical University Braunschweig, Langer Kamp 19c, D-38106 Braunschweig, Germany
Corresponding author: Andreas Herrmann, e-mail: a.herrmann@tu-bs.de

ABSTRACT

Selected results drawn from the application of ICA to the Lange Bramke study basin in the Harz Mountains, Germany are presented. The aim of the experiments was to verify earlier findings and expand the hydraulic knowledge on the runoff generation process based on hydrological and hydrogeological measurements and the use of tracers (environmental isotopes, dyes). The confined fractured rock aquifer was confirmed as the dominant supplier and as the control reservoir of the rain and snowmelt hydrograph generating water fluxes, whereas direct flow from event water and interflow are negligible. Hence groundwater recharge is quantitatively the most relevant and permanent process throughout the year. Piezometric level-discharge relations are often hysteretic, thus permitting various explanations for pathway and travel time of flow of the exfiltrating groundwater during events. Groundwater exfiltration is a combined effect of pressure and mass transfer in the subsurface system which determines the shape of flood hydrographs. These mechanisms can be deduced from developments of pressure heads and tracer mass displacements during single runoff events.

Key words: dye tracers, environmental isotopes, fractured rock aquifer, groundwater dynamics, Lange Bramke, runoff formation

INTRODUCTION

Hydrological processes control storage, turnover and pathways of water and dissolved matter in small headwater basins. Understanding the governing process pattern is absolutely necessary for adequate protection and management of water resources and the environment. Still, big knowledge deficits exist with respect to origin, travel and age of discharge contributing waters particularly on the single event time scale. Runoff formation, as the most complex eco-hydrological key process, should preferably be studied on this scale which is commonly associated with terms like overland flow, inter- or saturated flow, thus surface-near lateral flow processes that are specifically linked to each other. Runoff components of this site-specific category and the system hydrological concepts related to these were widely demonstrated in the anthology by Beven (2006). However, such synthetically-oriented views of precipitation-runoff processes may lead to wrong conceptualisation of reality.

To overcome the methodical restrictions that are set to usual water balance investigations an Integrated Catchment Approach (ICA) was successively developed during the past 25 years in the Lange Bramke basin, Harz Mountains, Germany (Herrmann *et al.*, 2001). It consists in applying natural and artificial tracers to common hydrological investigation methods. Since Lange Bramke will dispose of a 60 years discharge data series in 2009 (Herrmann, 2008), the basin is also a study object for future hydrological trends and simulations in the climate change context. The benefits from tracer hydrological analysis are demonstrated here with respect to flood hydrograph generation and groundwater exfiltration and recharge. Results are also thought to provide the physical background for the changing hydrological behaviour described by Schumann and Herrmann (2008).

EXPERIMENTS

The Lange Bramke basin covers an area of 0.76 km², and its altitude ranges from 540–700 m a.m.s.l.. 90% is forested with 55 years old Norwegian spruce. The unsaturated zone (UZ) is built up of forest soils on silty materials which are of solifluidal origin, rich in skeleton, and that cover the weathered fractured/fissured bedrock. Saturated zones are made up by Lower Devonian sandstones, quartzite and slates (fractured rock aquifer FRA), and by boulders, debris and gravels in the valley filling of the basin's centre (porous aquifer PA). The present instrumentation with special focus upon groundwater experiments and groundwater monitoring under the confined hydrogeological conditions in FRA is shown in Fig. 1. Since 1980 regular and event-based water samples of precipitation, snow cover and snow cover outflows, soil- and groundwater and discharge were analysed for 0–18, H–2 and H–3 contents to allow isotopic hydrograph separations and calculations of mean transit times and other hydraulic parameters of subsurface storages. Special campaigns consisted in the application of artificial tracers (dyes, salts, deuterium) in piezometers as well as on terrain surface to discover and confirm hydraulic connections and to determine travel times.
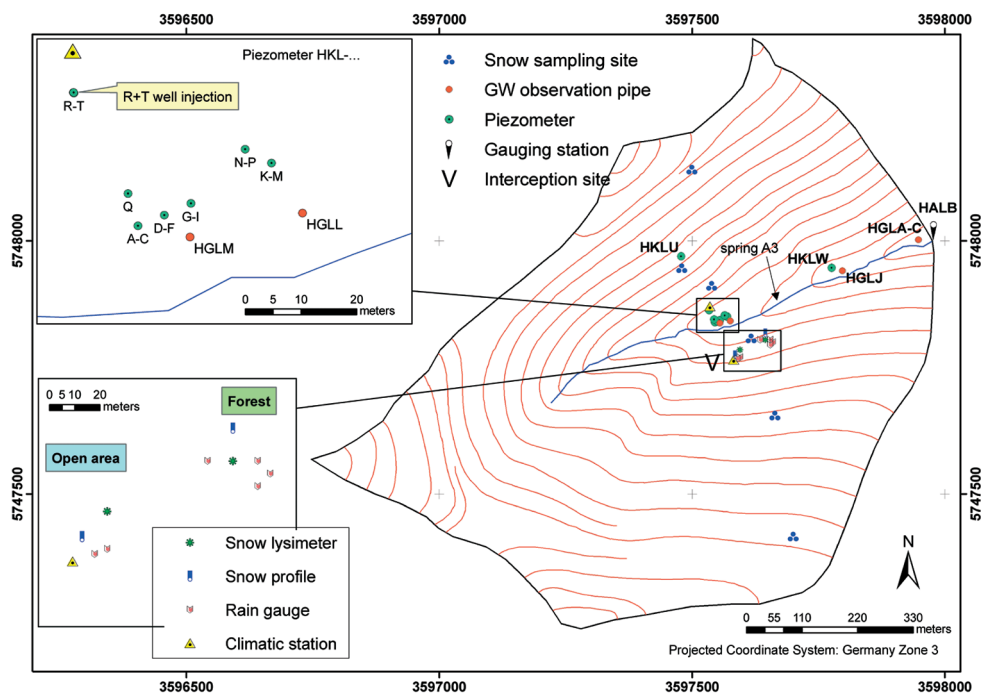
Fig. 1:   Topography and instrumentation of the Lange Bramke basin.

RESULTS

Fig. 2 compiles the conceptual hydrological model of the Lange Bramke basin. Shown are the three main storages (BS=UZ, KS=FRA, PS=PA), the storage characteristics (total volume V, volume of mobile water V_m in 10^6 m³; mean transit time of tracer t_t and of water t_0 in years; total porosity n, effective porosity n_{eff}) and the relevant water fluxes Q (here: mm WC). The following findings are notable:

Interflow (Q_1) is negligible. Direct runoff ($Q–Q_0$) accounts on the average for only 12% of the total discharge as oxygen-18 and tritium results show. UZ and FRA are short-cut by distinct preferential flow paths, which enable fast percolation of infiltration water. These short-cuts were traced with dyes. The mean transit time of groundwater that originates from the reservoir that supplies the mean low discharge is 2.0 years. t_0 was calculated based on tritium values and a dispersive age distribution flow model. The short transit time stands for a quick turnover of groundwater, since 9/10 of total discharge is on average indirect (groundwater) flow
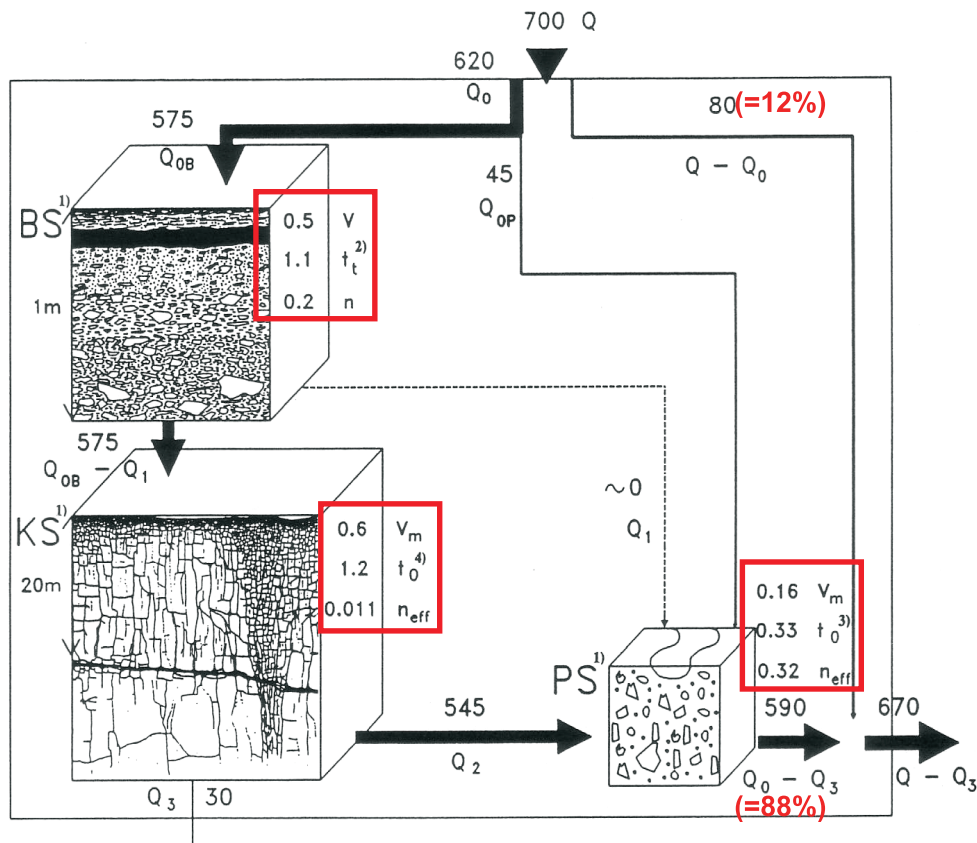
Fig. 2:   Hydrological basin model for the Lange Bramke with mean annual water fluxes [in mm WC] and reservoir characteristics (V: from Herrmann, 2008).

V_t; V_{im} = Total volume; volume of mobile water [in 10^6 m³]
t_t; t_o = Mean transit time of tracer; mean transit time of water [in a]
n; n_{eff} = Total porosity; effective porosity
[1] BS (=UZ) Unsaturated soil zone (residual weathering, allochthonic Pleistocene solifluidals on fissured and faulted rock), PS (=PA) Porous aquifer of valley filling, KS (=FRA) Fissured rock aquifer (folded and fractured Lower Devonian sandstones, quartzite, slates)
[2] From application of Dispersive Model (DM)
[3] From application of Ordinary Dispersive Model (ODM)
[4] $t_o = t_t/R_p$ with R_p=1.45 (from mean area porosities [n_p; n_f])

(Q_0–Q_3). However, residence times of this order are still valid to buffer considerably acid input waters (Herrmann *et al.*, 2001). On the single event time scale, extraordinarily small direct flow portions are confirmed to exist, i.e. total event water corresponds frequently to less than 5% of the actual rain or meltwater inputs. The spontaneous reactions of pressure heads upon basin input, which are observed from the evolution of piezometric levels (cf. Fig. 3 and 4), are an independent indication for the preparedness of the FRA system for increased exfiltration fluxes to stream channels during flood generation. Accordingly, groundwater is by far the dominant runoff component during rain on melting snow and storm floods where the water-bearing major cross faults act as principal subsurface drain channels.

Hence, groundwater recharge that maintains the quantitative balance between basin input and output is a permanent process throughout the year and about three times higher than assessed by conservative methods.

Discharge-groundwater relations may be hysteretic as shown in Fig. 4. The preliminary explanation of this phenomenon by Schöniger and Herrmann (1990) states that flow volumes on the rising limb of the hysteretic loop originate from stream-near and/or little distant but conductive aquifer locations including the major cross-
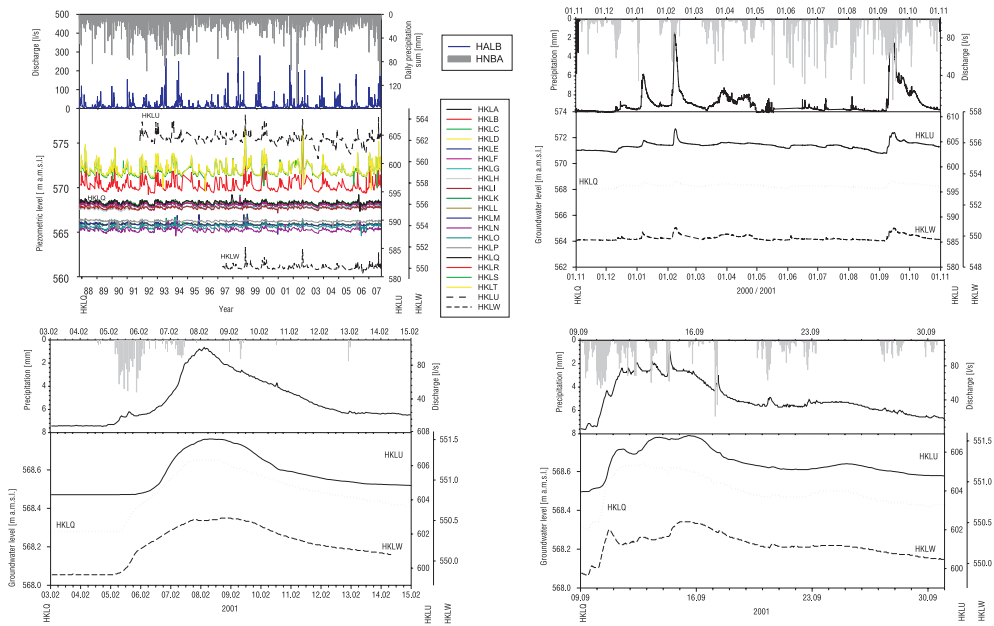
Fig. 3:   Precipitation, discharge and piezometer levels in the Lange Bramke measured manually and automatically (only HKLQ, -U, -W) for 1987–2007 (top left); (b) for 2001 (only HKLQ, -U, -W) (top right); and for single precipitation-runoff events in 2001 with rain on snow (bottom left) and rain (bottom right).
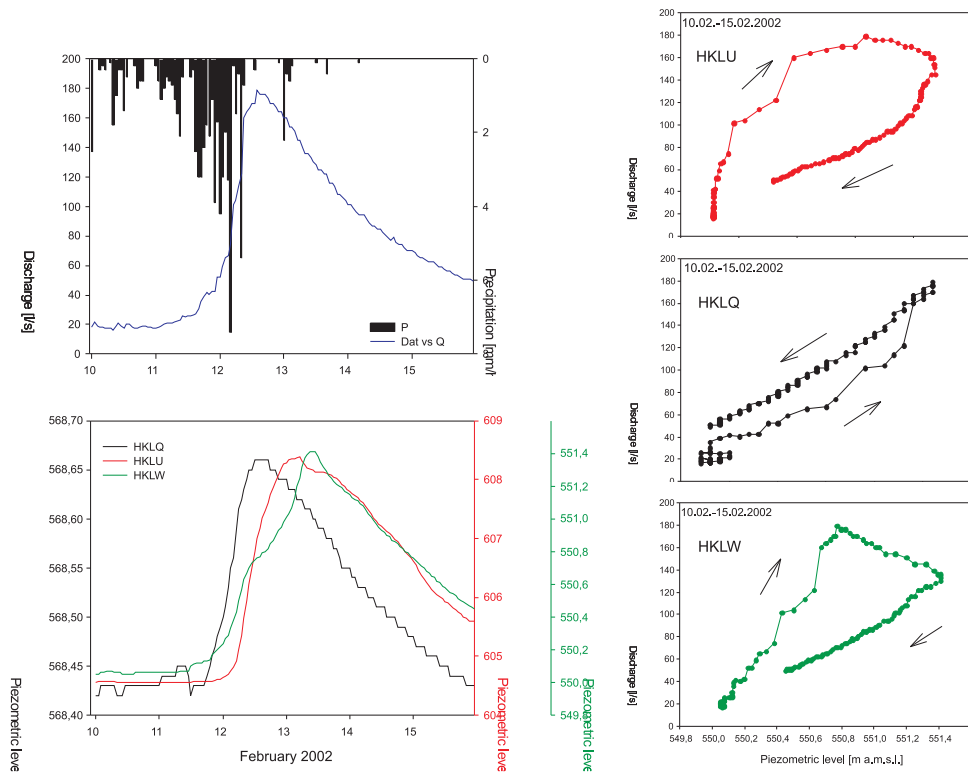
Fig. 4:   Precipitation and flood hydrograph in Lange Bramke from 10–16 February 2002 (top left) with piezometric levels at three different locations (bottom left) and discharge-piezometer level relations (right).

faults, and on the falling limb from more distant and/or less conductive areas thus representing above all matrix flow. This interpretation is still found suitable but not fully convincing by Herrmann and Schumann (2009) mainly because of frequent anticlockwise travel directions on loops like in case of HKLQ in Fig. 4. No hysteresis at all exists in frequent cases where up and down travel paths follow simple exponential lines. For a better physical understanding of the hysteresis phenomenon the whole inventory of 20 years of discharge events with sufficient time resolution will be checked systematically.

The observed synchronous increase of pressure heads and formation of distinct breakthrough curves of stable isotopes and dyes in both FRA and PA aquifers, and the evolution of discharge during an exemplary single event in Fig. 5 indicate a basin-wide pressure transmission in FRA which is followed by the mobilisation of groundwater mass transfer through FRA and PA and ultimately leads to hydrograph formation. Thus, the generation of flood hydrographs primarily consisting of groundwater is bound to the exfiltration mechanism of fractured rock groundwater. The application of artificial tracers to FRA has also shown that the major cross-faults play an important role for the ground water transfer towards channels with flow velocities of more than 10 m/h which correspond to turbulent flow (Maloszewski *et al*., 1999). Other variable flow proportions come from source areas of less hydraulic conductivity according to tectonic fracturing. As compared to FRA
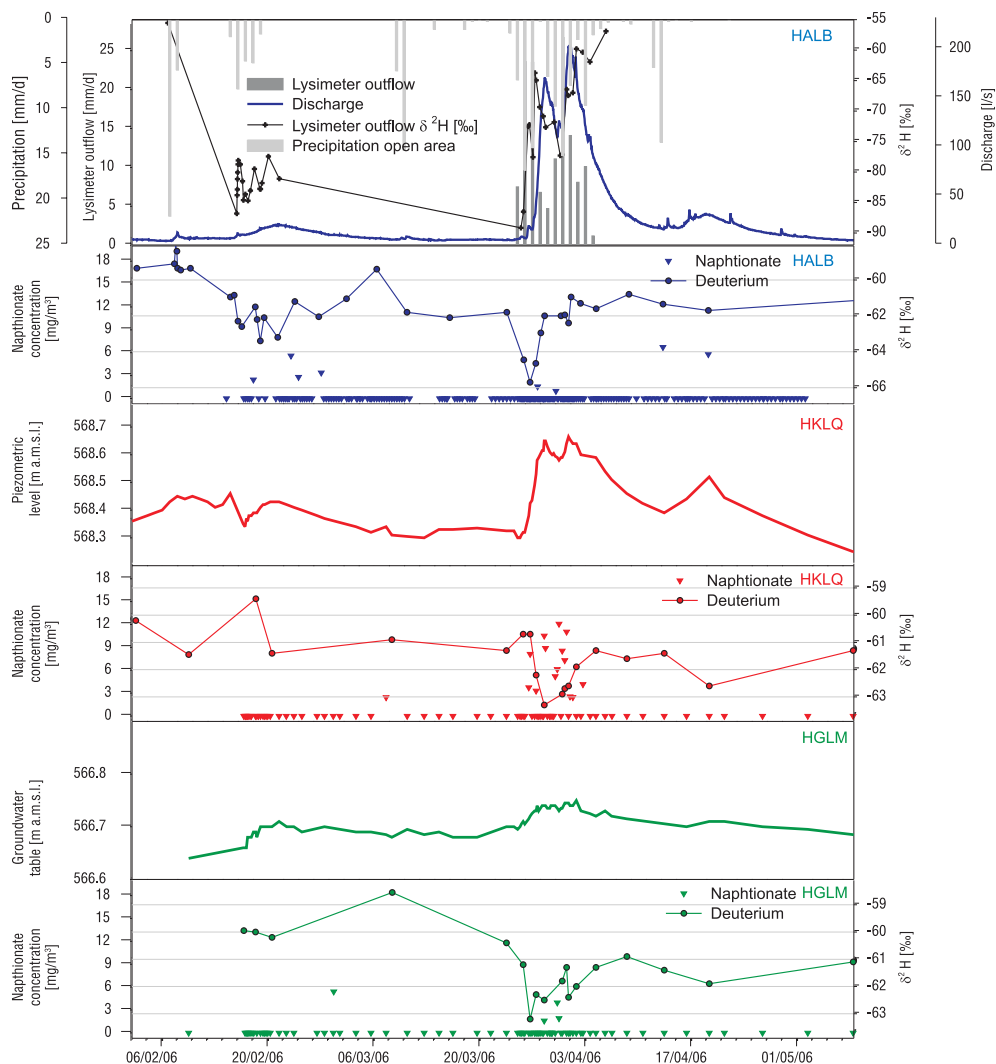
Fig. 5: Hydrological conditions in Lange Bramke basin from February to May 2006 with: Open area precipitation, forest lysimeter outflows with deuterium contents, discharge of Lange Bramke stream at gauge HALB; groundwater tables at piezometer HKLQ and at observation pipe HGLM, deuterium contents (dots and lines) and naphthionate concentrations (triangles) at HALB, HKLQ and HGLM (after Thies 2007).
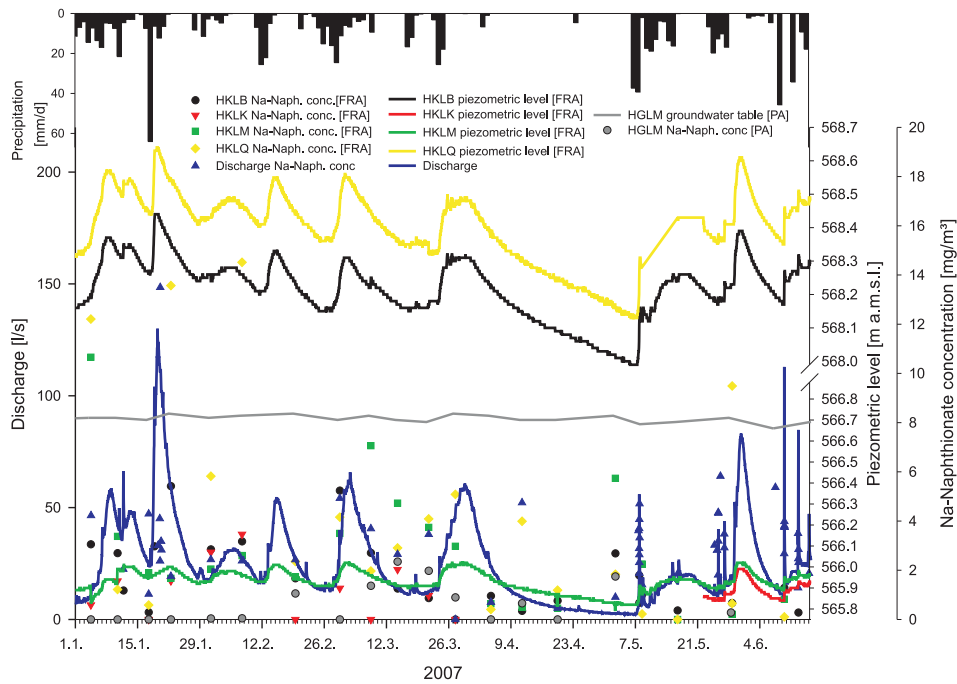
Fig. 6:   Input induced fluctuations of naphthionate concentration with discharge at stream gauge HALB and of groundwater tables at piezometers HKLB (filter section in 8–10 m below ground surface), HKLK (13–15 m), HKLM (3–5 m) and at observation pipe HGLM (whole length).

the porous aquifer of the valley filling PA is considered a steady-state transition storage which can be concluded from the almost constant groundwater table shown in Fig. 5. When we leave the single event time scale that is shown in Fig. 5, for the longer half-year term shown in Fig. 6 the evolution of hydrologic and hydraulic parameters and of dye tracer concentrations confirm these findings in principle. The study basin therefore can be described as a pulsating system depending on the actual basin inputs and filling stages of FRA as the main regulating variables for the system answer, i.e. the runoff. Respective interrelationships will be elaborated in a next step in more detail.

CONCLUSIONS

Runoff formation in the Lange Bramke basin can be understood as a process with three successive stages: (i) Infiltration with saturation of top soils, quick drainage through macropores towards greater depths, and compression of the capillary fringe which may initiate pulse pressure transmission and connected aquifer reactions without mass transfer; (ii) Rise of piezometric table, i.e. increase of subsurface pressure head and subsequent mass displacement, which can be split into vertical seepage in the unsaturated (cf. (i)) and lateral (groundwater) flow in the saturated zone; and (iii) Groundwater exfiltration to stream channels as a combined effect of pressure transmission and mass transfer, with hydrograph generation as a result. To maintain the quantitative input/output balance, short-term groundwater losses are compensated without much delay, i.e. groundwater recharge is a permanent process throughout the year.

Holistic, multidisciplinary ICA concepts seem to be most suitable for a reliable hydrological system analysis on a small basin scale including the runoff formation process complex. The combination of environmental and artificial tracing methods with conventional hydrological and hydrogeological investigations is found to best support traditional water balances, and the calibration and validation of hydraulic basin models. Since

runoff formation largely controls basin storage and transit of water and dissolved matter, it is suggested to intensify the study of the governing hydraulic mechanisms. A primary motivation for realising ICAs is founded in the urgent needs to focus on relevant processes which control hydrological systems behaviours in changing environments. The study shows that in the catchment hydrological context the runoff formation process is the focus of ICA.

REFERENCES

Beven K.J. (ed.) (2006). *Streamflow Generation Processes. IAHS Benchmark Papers in Hydrology*, IAHS Press, Wallingford, UK.

Herrmann A. (2008). 30 Jahre integraler Forschungsansatz zum Abflussbildungsprozess und 60 Jahre Abflussbeobachtungen im Oberharz (30 years of integrated scientific investigations of the runoff formation process and 60 years of runoff observations in the Upper Harz Mountains). *Hydrologie und Wasserbewirtschaftung*, **52**(3): 132–136.

Herrmann A. and Schumann S. (2009). Untersuchung des Abflussbildungsprozesses als Kontrollmechanismus für den Gebietswasserumsatz des Oberharzer Einzugsgebiets Lange Bramke (Investigation of the streamflow generation process as a control mechanism for the basin turnover in the Lange Bramke catchment, Upper Harz Mountains). *Hydrologie und Wasserbewirtschaftung*, **53**(2): 64–79.

Herrmann A., Schöniger M., Schumann S. (2001). Integrated approach of investigating and modelling runoff formation considering information from environmental and artificial tracers. *Freiburger Schriften zur Hydrologie*, **13**: 90–97.

Herrmann A., Schöniger M., Schumann S., Trimborn P., Stichler W. and Groth P. (2001). *Multilateral approach of fissured rock aquifer systems in the Harz Mts., Germany, to assess risk potentials of drinking water reservoirs*. Proceedings XXXI IAH Congress on New Approaches to Characterising Groundwater Flow Munich 10–14 Sept. 2001, Vol. **2**, Balkema: 951–956.

Maloszewski P., Herrmann A. and Zuber A. (1999). Interpretation of tracer tests performed in fractured rock of the Lange Bramke basin, Germany. *Hydrogeol. J.*, **7**: 209–218.

Schöniger M., Herrmann A. (1990). Exfiltration and recharge mechanism in a fissured paleozoic rock aquifer of a small catchment (Lange Bramke, Harz Mountains) from tracer hydrological and hydraulic investigations. *Proceedings XIInd IAH Congress Lausanne 1990,* Mémoires Vol. **22**(1): 582–591.

Schumann, S., Herrmann, A. (2009). Evolution and impact of hydrological extreme years in the Lange Bramke basin, Harz Mountains, Germany. Proceedings 12th Biennial ERB Conference on Hydrological Extremes in Small Basins, Cracow 2008. *Technical Documents in Hydrology*, **84**,Unesco, Paris.

Thies R. (2007). *Determination of runoff generation processes in a fissured rock aquifer (Lange Bramke, Harz Mountains)*. Diploma thesis; Institute of Geoecology, Technical University Braunschweig: 79 pp.

TRENDS IN RUNOFF CHARACTERISTICS AND HYDROLOGICAL REGIME CHANGES IN THE LANGE BRAMKE BASIN, HARZ MOUNTAINS, GERMANY

S. Schumann, A. Herrmann and D. Duncker

Institute of Geoecology, Department of Hydrology and Landscape Ecology, Technical University Braunschweig, Langer Kamp 19c, D-38106 Braunschweig, Germany
Corresponding author: Sybille Shumann, email: s.schumann@tu-bs.de

ABSTRACT

Selected results of a trend analysis carried out on a 59-years discharge and rainfall data series from the Bramke catchment, Harz Mountains, Germany are presented. The results concentrate on the analysis for the summer (May to October) periods 1978 to 2007. The aim of the study was to proof whether the observed rise of temperatures in the region has impacts on the hydrological behaviour of the catchment. The Mann-Kendall trend test coupled with a linear trend analysis has been applied to the data. Furthermore extreme values, i.e. the minimum summer discharges, days below mean low flow (5.8 $dm^3 \cdot s^{-1}$) and the highest daily precipitation sums have been looked at. The years were also grouped according to observed flow regimes of 1: Discharge events throughout the year; 2: Discharge events in winter and autumn and 3: Years when discharge events only occurred in winter (summer-dry years) and looked upon for possible changes. The analyses disclosed that significant negative trends exist for the minimum annual discharges, the runoff and the R:P ratio during hydrological summer period and that the runoff characteristics in Bramke catchment have changed during the past 20 years. Years with long low flow periods (May to October) occur more frequently and tend to last longer, i.e. the regime is developing strongly towards a summer-dry one. Furthermore the data analysis disclosed the high negative impact of extreme years on a reliable trend analysis.

Keywords: climate change, hydrological regime, Lange Bramke, low flow, runoff characteristics, trend analysis

INTRODUCTION

Small basins play a mayor role in hydrological process-, and analytical studies since they feature the advantage that changes in discharge determining factors are far better subsumable than in large basins. In predominantly forested basins the changes in controllable environmental conditions such as land-use variances are even smaller and are further minimized in basins with monoculture plantations. These basins are therefore highly appropriate for the study of governing process pattern and for the study of changes in hydrological conditions, both being indispensable for the proper management of water resources as an essential partial complex of ecosystems.

The Lange Bramke basin, being a small monocultural forest catchment afforested in 1951 with Norwegian spruce, disposed of a 60 years discharge data series in November 2008. It therefore fulfils inter alia the qualification as a study object for hydrological trends and extremes as well as for hydrological forecast.

The presented results zoom in on the changes in hydrological regime in the Lange Bramke basin during the past 30 years, and focus especially on the situation during summer (May to October).

STUDY SITE

The Lange Bramke basin, which is situated in the Harz Mountains (Germany), covers an area of 0.76 km² and an altitude range from 540 to 700 m a.m.s.l. 90% of the area is forested with Norwegian spruce that was reforested in 1951 after the complete clearance of the basin for reparation after the Second World War. The basin is build up of an unsaturated zone made of forest soils on silty materials of solifluidal origin. The soils are rich in skeleton. The unsaturated zone covers weathered and fractured/fissured bedrock that acts as a fractured rock aquifer. Parallel to the Bramke stream a narrow and shallow (<2 m thickness) porous aquifer is developed that consists of boulders, debris and gravels. The hydrological study concept applied in the Lange Bramke catchment as well as the available instrumentation is described by Herrmann & Schumann (2009). The discharge series disposes of a 60 years discharge series by November 2008.

The catchment serves as an inflow to the Oker reservoir that is part of the water supply network of the Harz Wasserwerke (water supply companies). The Oker reservoir also serves as a flood-control reservoir for the Harz foreland.

DATA AND METHODOLOGY

Due to the complete clearing of the Lange Bramke Basin after World War II and the following reforestation in 1951 the hydrological balance in the first years of the catchment monitoring was highly impacted by the growth of the Norwegian Spruce. Unpublished studies taken by the Northwest German Forest Research Station aiming on the real evapotranspiration (ETR) in the Lange Bramke catchment lead to the result that a balanced ETR was reached in the mid seventies. Therefore this study focuses on hydrological data from 1978 onwards, i.e. 30 years time series of daily precipitation and discharge for trend analyses. However, for the detection of regime changes the period 1978 to 2007 is compared to data covering the period 1949 to 1978.

The trend analysis in this paper is based on the Mann-Kendall Trend Test that is widely used to detect trends in hydrologic data (Hamed, 2008). The significance level was subdivided into four categories following Kliwa (2003): 1: $\alpha > 99\%$: highly significant (h.s.); 2: $90\% \leq \alpha \leq 99\%$: probably significant (p.s.); 3: $80\% \leq \alpha \leq 90\%$: weakly significant (w.s.); 4: $\alpha < 80\%$: not significant (n.s.). Trends for the following hydrological characteristics were determined – summer rainfall and runoff, runoff coefficients, maximum daily and 3-day precipitation. The observed regimes at the Bramke river were divided into three groups: G1: Discharge events only in winter (summer-dry); G2: Discharge events in winter and autumn; G3: Discharge events throughout the year. The frequency of occurrence of the three groups over the studied period was evaluated.

RESULTS

The study area is demonstrably affected by global warming effects. Figure 1 demonstrates the increase in mean air temperatures for the winter and summer seasons since 1963 at weather station run by the Deutsche Wetter Dienst (German weather Services, DWD) 5 km air-line distance from the Bramke catchment.

The trend analyses that was carried out for precipitation and runoff data covering the period 1948 to 2007 and the sub-period 1978 to 2007 did not show any trends, neither for the summer half-term nor for the winter half-term. However, in monthly or half-yearly runoff sums or the respective runoff: precipitation ratios (runoff coefficients) trends exist. These results are presented in Table 1 and Fig. 2.

According to Table 1 probably significant downward trends can be detected for the month May to July an a weakly downward trend in August for the monthly runoff sums. This allows for the predication that the monthly discharges are decreasing since 1978 during the summer months May to September. The runoff coefficient does not respond so sensitively since the precipitation sums do not show significant trends. However, still weak to highly significant downward trends exist for the respective summer month except for June and October.

Fig. 2 reveals the probably significant downward trend in the summer period runoff coefficient (linear black line) since 1978. Interesting is the trend displacement if the observed period is shortened to 20 years. The results are displayed as a linear trend in green. This trend is highly influenced by the years 1998, 2003 and 2007 that stand out of the period 1988 to 2007. The significance niveau after Mann-Kendall was not determined in this case though, as the observation period was less than 20 years. However, this result already hints on the impact of extreme years and the length of the studied period on calculated the trends and the difficulties in interpretation that arise from those.

Table 1: Trends in summer months (May-Oct.) for precipitation P, runoff R and runoff coefficient R/P in period 1978 to 2007.

Month	P [mm]	R [mm]	R/P [%]
May	-	↓ 2	↓ 1
June	-	↓ 2	-
July	-	↓ 2	↓ 3
Aug.	-	↓ 3	↓ 3
Sept.	↑ 3	-	↓ 2
Oct.	↑ 3	-	-

Significance levels selected for the Mann-Kendall test: 1: α > 99 %: highly significant (h.s.); 2: 90 % ≤ α ≤ 99 %: probably significant (p.s.); 3: 80 % ≤ α ≤ 90%: weakly significant (w.s.); 4: α < 80 %: not significant (n.s.).
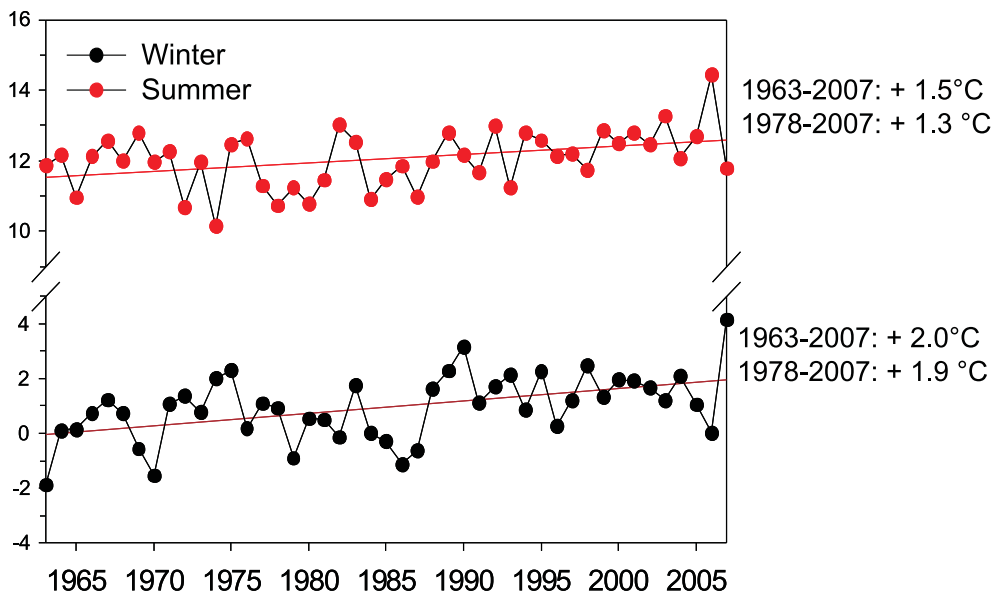
Fig. 1: Development of winter and summer mean air temperatures [°C] since 1963 at DWD station Clausthal-Zellerfeld (data with courtesy from DWD, 2008). Upward trend in both cases: h.s. [1].
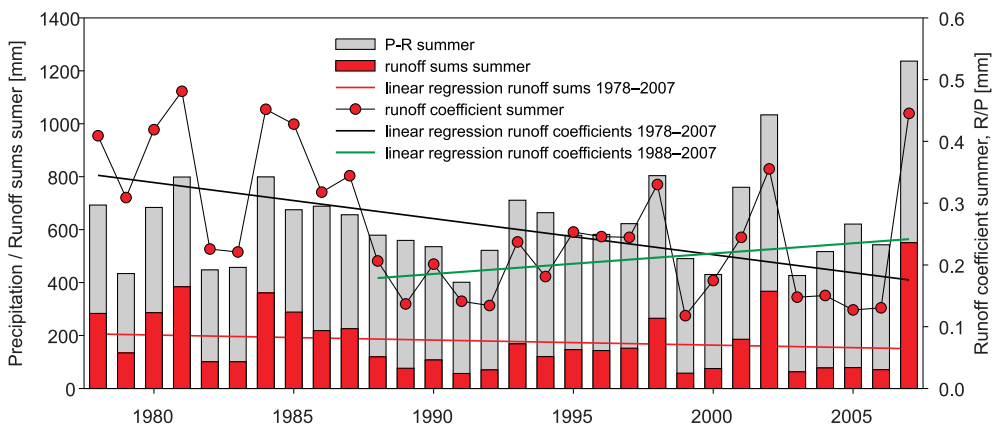
Fig. 2: Runoff sums [mm] and remainder terms of precipitation less runoff [mm] presented in each case for the summer period, as simple bars. Furthermore shown are the runoff coefficients or the summer periods 1978 to 2007 as half-yearly sums (sum May to October) and their linear trend characteristics: runoff-coefficient 1978 to 2007 [p.s: 2], runoff-coefficient 1988 to 2007 [n.s: 4], runoff sums 1978 to 2007 [p.s: 2]).
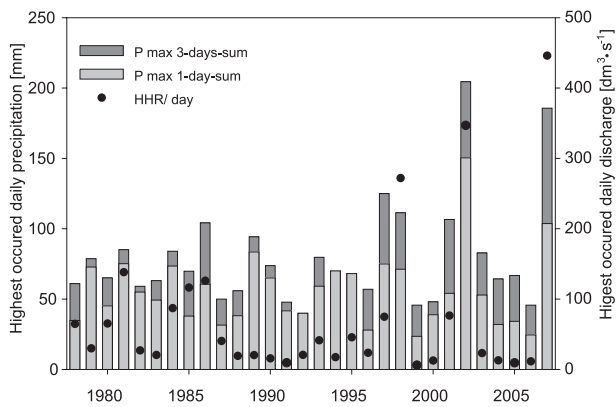
Fig. 3: Highest occurred daily precipitation sums for one day and for three days as accumulated sums [mm] [n.s: 4] measured in the Bramke catchment. Furthermore shown are the highest daily discharges [dm³·s⁻¹] for the summer periods from 1978 to 2007 [n.s: 4].

These extreme years are also noticeable if the maximum occurred 1-day or 3-day precipitation sums are plotted together with the highest occurred daily runoff (HHR). It reveals outstanding daily precipitation sums and HHRs in 1998, 2003 and 2007 (highlighted in the graph) in a 20-years period resulting in an upward linear trend that would be trendless if those three years would not be taken into account.

The analysis for the lowest summer discharges reveals a highly significant downward trend. This is also reflected in the number of days where the discharge stays below the mean low flow discharge (MNQ) of 5.8 dm³·s⁻¹ that show a very significant upward trend for the summer period 1978 to 2007. The results for this analysis are shown in Fig. 4.

The trend towards decreasing minimum annual discharges and the increasing number of days below MNQ during the summer period are also noticeable in a regime change of the Bramke river. Fig. 5 summarizes the observed regimes observed at the Bramke river.

The frequency of occurrence of the three groups has changed in the past thirty years. The distribution of occurrence is shown in Table 2. It is clearly notable that the summer-dry type G1 has occurred more frequently
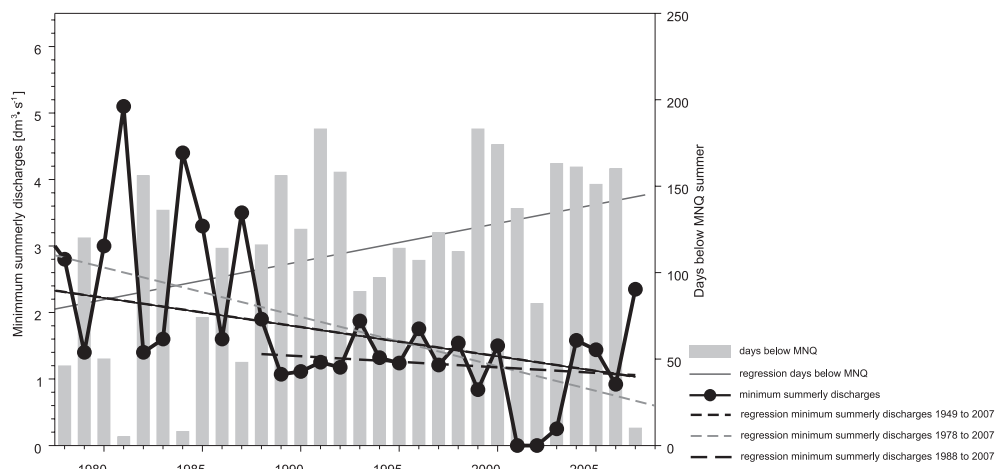
Fig. 4: Minimum annual discharges for the summer periods 1978 to 2007 with their respective linear trend lines for the periods 1949 to 2007, 1978 to 2007 and 1988 to 2007 measured in the Lange Bramke catchment (downward trend: h.s. [1], 1978 to 2007). Furthermore shown are the accumulated number of days with discharges below the MNQ of 5.8 dm³·s⁻¹ (upward trend: h.s. [1]).

Table 2: Occurrence of the regime groups G1: Discharge events only in winter (summer-dry); G2: Discharge events in winter and autumn and G3: Discharge events throughout the year during the past 59 years. The right table represents the 30 years after complete re-growth of the Norwegian spruce.

	G1	G2	G3
1949–1958	1	2	7
1959–1968	1	2	7
1969–1978	1	2	7
Sum	**3**	**6**	**21**

	G1	G2	G3
1978–1987	3	0	7
1988–1997	6	2	2
1998–2007	6	2	2
Sum	**15**	**4**	**11**
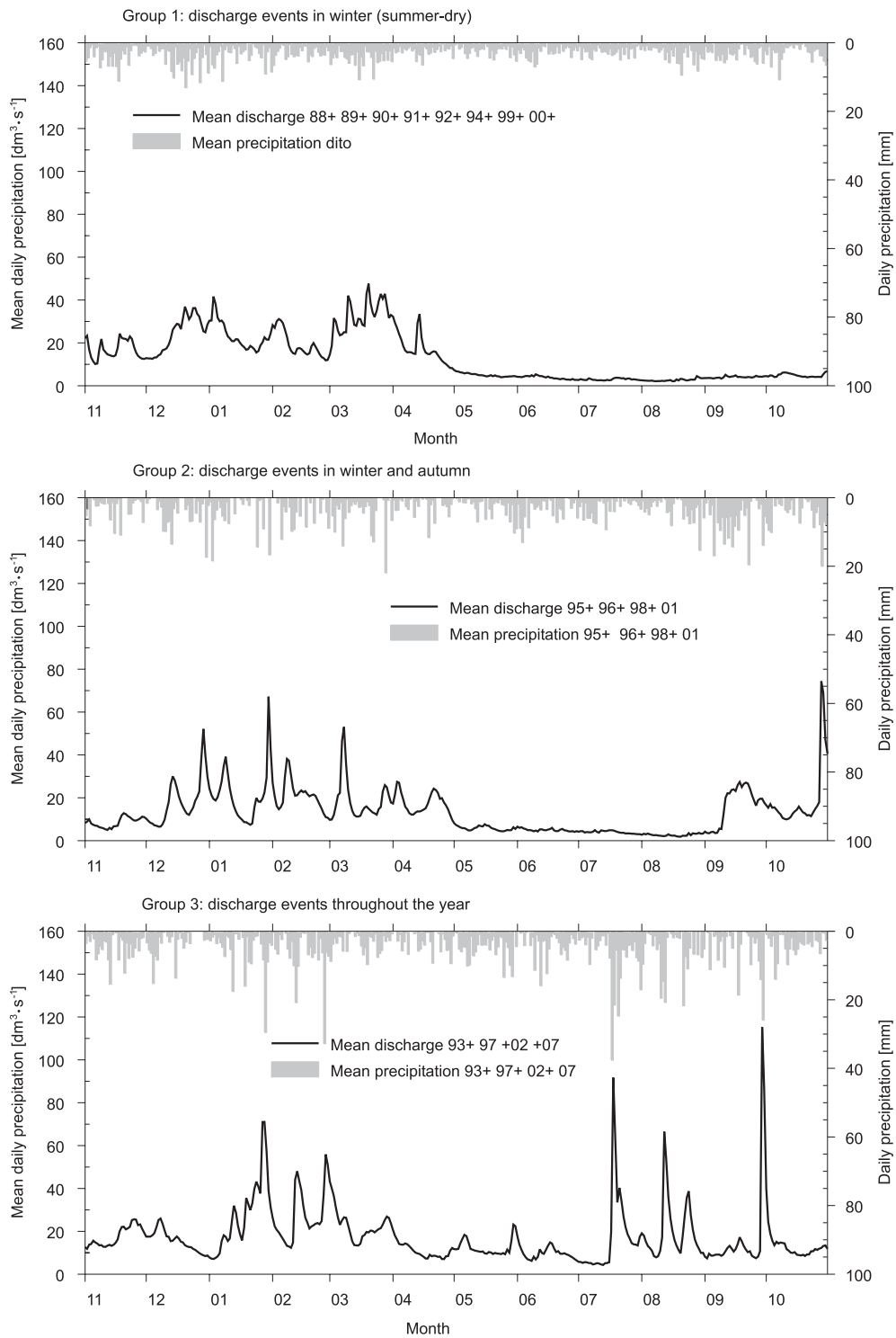
Fig. 5:   Regime groups for the Lange Bramke river. G1: Discharge events only in winter (summer-dry); G2: Discharge events in winter and autumn and G3: Discharge events throughout the year.

during the past years while the type G3, that was the most of all occurring regime from 1949 to 1978 and represents a rather balanced regime with discharge events throughout the year, has lost importance in the catchment especially in the past 20 years.

CONCLUSIONS

It can be concluded that significant downward trends exist for the minimum annual discharges, the runoff and the R:P ratio during hydrological summer period (May to September) in period 1978–2007. If the analysis is shortened to the period after 1988 a trend change exists for the summer R:P ratio towards an upward trend. Both results are, however, dependent on the extreme years 2002 and 2007. Generally it can be stated that the occurrence of extreme years does interfere with the possibility of a reliable trend analysis and hence a predictable forecast.

The regime in the Lange Bramke catchment has changed. Years with long summer low water periods (May to October) occur more frequently during the past 20 years. This may cause problematic situations to the water supply during summer, i.e. reservoirs would need to be filled properly during winter and spring time to account for water needs during the low flow period when reservoirs are not regularly refilled. Though years with considerable discharge events in summer seem to become less frequent, discharges of high volumes still occur but become less predictable and more extreme. If dams are filled to the top to account for the more frequent summerly low flow periods this may cause severe flood risks in the Harz forelands if under these conditions extreme discharges occur as observed in 2002 or 2007.

To verify whether the observed trends are regional trends or may be very distinct for the Lange Bramke catchment, the same analysis should be carried out for other catchments in the Harz Mountains. Furthermore, the characteristics, and more especially the observed low flow periods in summer should be analysed for their correlation with piezometric water levels in order to detect possible changes in groundwater contributions to discharge or changes in available groundwater volumes.

REFERENCES

Hamed K. H. (2008). Trend detection in hydrologic data: The Mann-Kendall trend test under the scaling hypothesis. *J. Hydrol.*, **349**(3-4): 350–363.

Herrmann A. and Schumann S. (2009). Runoff formation in a small mountainous basin dominated by a fractured rock aquifer: Results from the tracer-based Integrated Catchment Approach (ICA). Proceedings 12th Biennial ERB Conference on Hydrological Extremes in Small Basins, Cracow 2008; *Technical Documents in Hydrology*, **84**, Unesco, Paris

IPPC (2007). Climate Change Synthesis Report 2007: 73 pp., *(URL http://www.ipcc.ch/pdf/assessment-report/ ar4/syr/ar4_syr.pdf, verif. 18.08.2008)*

KLIWA (2003). Langzeitverhalten der mittleren Abflüsse in Baden-Württemberg und Bayern. Arbeitskreis KLIWA (*Landesanstalt für Umweltschutz Baden-Württemberg, Bayerisches Landesamt für Wasserwirtschaft, Deutscher Wetterdienst*), **3**, 94 pp. *(URL http://www.kliwa.de/download/KLIWAHeft3. pdf , verif. 18.08.2008)*.

PROGRESS WITH UNIT HYDROGRAPH-BASED RAINFALL–STREAMFLOW MODELS FOR ENGINEERING AND ENVIRONMENTAL HYDROLOGY

I.G. Littlewood

Didcot, UK, e-mail: ianlittlewood505@btinternet.com

ABSTRACT

Two rainfall–streamflow, unit hydrograph (UH) based, modelling methods are compared, one primarily for flood event engineering hydrology and the other mainly for time series environmental hydrology. The latter method is employed to illustrate the often-overlooked sensitivity of calibrated model parameters to data time-step. An empirical method of estimating data time-step-independent parameters is demonstrated for the time series UH-based model, and an important distinction is drawn between the accuracy and precision components of uncertainty in rainfall–streamflow model parameters. It is argued that the parameter values of other rainfall––streamflow models are similarly sensitive to data time-step, causing some of the uncertainty in many model parameter regionalisation schemes. Sensitivities to data time-step are compared for a well-known base flow index (BFI) and an analogous slow flow index (SFI) generated by the time series UH-based method. Suggestions are made for future work.

Keywords: rainfall–streamflow modelling; unit hydrographs; regionalisation; ungauged basins; modelling time-step; base flow index (BFI); slow flow index (SFI).

INTRODUCTION

This short paper compares two rainfall–streamflow modelling approaches used for engineering and environmental hydrology applications respectively. In each case the model comprises a module to estimate effective rainfall followed by a unit hydrograph (UH) module. Statistical relationships between the models' parameters and catchment attributes have assisted with modelling streamflow at ungauged sites. For more than 30 years, since 1975, the first modelling approach has been used extensively in the UK for systematic, flood event, engineering hydrology, e.g. design flood estimation. The prototype of the second approach, which can model continuous hydrographs over several seasons or years (and over single events), was introduced in 1990 and has been applied mainly for environmental hydrology. Variants of the model structure in the second approach have been applied for investigating the impacts of environmental change (e.g. land-use, climate) on streamflow regimes. The second modelling methodology represents substantial progress in the application of UHs for environmental hydrology and could also be useful for engineering hydrology.

The first rainfall–streamflow modelling approach is described in the Flood Estimation Handbook (FEH) (Institute of Hydrology, 1999) and its forerunner the Flood Studies Report (FSR) (NERC, 1975), and will be referred to subsequently as the FSR/FEH rainfall–streamflow method. The second modelling approach is IHACRES (Identification of unit Hydrographs And Component flows from Rainfall, Evaporation and Streamflow data), first introduced by Jakeman *et al*. (1990). For details of the modelling approaches, their applications, and further discussion of many of the points raised in this short paper, the reader is invited to consult Littlewood (2008) and references therein.

An example is presented of IHACRES model parameter sensitivity to the time-step of the data used for model calibration. Similar information is presented for a baseflow index (BFI), comparing it with a slow flow index (SFI) generated by IHACRES. The implications of these results for model parameter regionalisation studies are discussed.

COMPARING THE FSR/FEH AND IHACRES METHODS

The FSR/FEH unit hydrograph (UH) represents a direct flow component of streamflow. The reader is reminded that there is no known method of measuring direct flow. Direct flow for an event is estimated by an intuitively reasonable, though somewhat arbitrary, hydrograph separation. Similarly, effective rainfall for the event in question is estimated by an intuitively reasonable hyetograph separation method. A UH is then identified from the effective rainfall and direct flow. Several events are thus analysed and an average UH computed. To estimate the hydrograph for a different event the relevant hyetograph is first separated to give effective rainfall, which is then convolved with the average UH to generate direct flow for the event, to which is added an appropriate baseflow. The FSR/FEH method is not suitable for modelling hydrographs continuously over seasons or years.

The IHACRES unit hydrograph represents total streamflow, thereby circumventing the problem of having to estimate a rather poorly defined direct flow component prior to UH identification. Hydrograph separation, giving dominant quick- and slow-response components of modelled streamflow, is a by-product of the methodology. IHACRES can model hydrographs continuously over seasons and years (as well as over single events). There are several variants of IHACRES model structure.

Table 1 summarises various features of the FSR/FEH and IHACRES rainfall–streamflow modelling methods. Comparison of the features in Table 1 supports the argument that IHACRES represents an advance in the application of UH theory that has been exploited for environmental hydrology and could, in principle, be exploited additionally for engineering hydrology. Littlewood (2008) compares FSR/FEH and IHACRES unit hydrographs for an event from a 20 km^2 catchment in Scotland. Although the FSR/FEH method has been re-designed and improved recently (Kjeldsen, 2007) it still uses a direct flow UH and remains unsuitable for continuous streamflow simulation over several seasons or years.

Table 1: Summary comparison of FSR/FEH and IHACRES rainfall–streamflow modelling methods.

Feature	FSR/FEH triangular UH (engineering hydrology)	IHACRES UH (environmental hydrology)
What flow is modelled?	Direct flow (Non-measurable)	Streamflow (measurable)
High flows modelled?	Yes ✓	Yes ✓
Low flows modelled?	No ✗	Yes ✓
Event-based modelling?	Yes ✓	Yes ✓
Continuous streamflow simulation?	No ✗	Yes ✓
Prior hyetograph separation required?	Yes ✗	No[1] ✓
Prior hydrograph separation required?	Yes ✗	No ✓
Automated hydrograph separation provided?	No ✗	Yes[2] ✓
Smoothing of UHs identified from hydrometric data required?[3]	Yes ✗	No ✓
UH parameters transferable to ungauged catchments?	Yes ✓	Yes ✓

[1] Automatically by a parameter grid-search method within IHACRES model calibration.

[2] Dominant quick- and slow-flow response components of streamflow.

[3] Using the matrix inversion method stated in the FSR.

REGIONALISATION AND MODEL PARAMETER SENSITIVITY TO DATA TIME-STEP

An IHACRES model structure that has been used for regionalisation has six dynamic response characteristics (DRCs), which for this paper are called model parameters: a catchment drying time constant, τ_w; a temperature modulation factor, f; the depth of a catchment wetness store, c; a quick-flow decay time constant, $\tau^{(q)}$; a slow-flow decay time constant, $\tau^{(s)}$; and the proportional volumetric contribution of slow-flow to streamflow, $v^{(s)}$. The latter DRC is a slow flow index (SFI) that will be referred to again later.

Moderate success has been achieved in relating IHACRES model parameters (and the parameters of other rainfall–streamflow models) to catchment attributes, e.g. Sefton and Howarth (1998), Post and Jakeman (1999), Young (2006), Merz and Blöschl (2004). Merz $et\ al$. (2006) discuss several reasons for the "… relatively low correlations between model parameters and catchment attributes" but not model parameter sensitivity to data time-step. Indeed this source of uncertainty, which is likely to be important in some regionalisation schemes, appears to have been largely overlooked in the rainfall–streamflow modelling literature until quite recently.

Littlewood (2007) and Littlewood and Croke (2008) demonstrate the extent to which IHACRES model parameters can be dependent on the time-step of the data employed for model calibration. Figure 1 shows how each of the IHACRES model parameters for the 10.6 km² Wye at Cefn Brwyn appears to reach or approach a stable value, i.e. insensitive to data time-step, as data time-step decreases to 1 hour. The indicative 95% confidence bands shown in Fig. 1 indicate that precision on the model parameters improves as data time-step decreases from 24 hours to 1 hour. In Fig. 1, the value of a parameter calibrated using 1-hourly data provides a benchmark, and the difference between that benchmark and the same parameter calibrated using n-hourly data can be considered to be a measure of the accuracy associated with that n-hourly parameter. Precision and accuracy thus have quite different meanings. The uncertainty associated with a model parameter is a combination of its precision and accuracy.
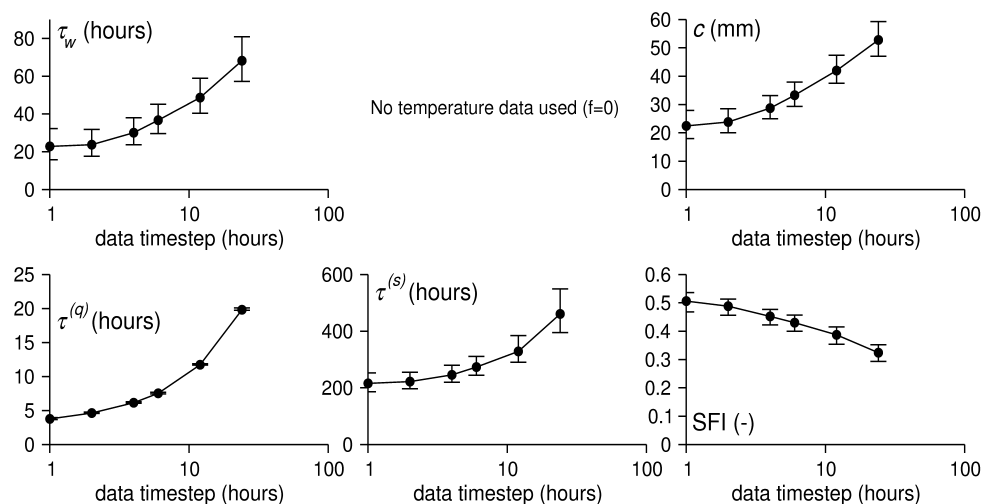
Fig. 1: Wye at Cefn Brwyn DRCs against data time-step: model calibration 6 December 1987–2 July 1988 (Littlewood and Croke, 2008).

It is anticipated that the parameters of other discrete-time rainfall–streamflow models will also exhibit sensitivity to data time-step. When such models are calibrated for many gauged catchments using a common data time-step (e.g. daily), and their parameters are subsequently linked to catchment attributes (regionalisation), a proportion of the uncertainty in the resultant statistical relationships will be due to a common time-step having been used. An alternative modelling approach, which could be useful for regionalisation studies, is the continuous-time data-based mechanistic (DBM) approach introduced by Young and Romanowicz (2004) and Young and Garnier (2006). Continuous-time DBM models yield model parameters that should be insensitive to data time-step.

Such model parameters should exhibit superior statistical relationships with physical catchment descriptors to those from discrete-time models, and therefore lead to a reduction in uncertainty associated with streamflow estimates at ungauged sites.

There is a pressing need to assess the parameter data time-step sensitivity of rainfall–streamflow models that have been, or could be, used to assist with streamflow estimation at ungauged sites. The paper now considers an example. Although the Gustard *et al*. (1992) baseflow index (BFI) is not the output from a rainfall–streamflow model (it is derived solely from streamflow data) it can be considered to have model parameters, and it is interesting to assess its sensitivity to those parameters and data time-step. BFI is a key catchment statistic in floods and low-flow regionalisation studies in the UK and has also been applied for studies in Canada, Fiji, Zimbabwe, New Zealand and Norway (Gustard *et al*., 1992). Period-of-record BFIs derived from daily mean streamflow records are published for more than 1000 UK catchments as "…a measure of the proportion of the river runoff that derives from stored sources" (NERC, 2003).
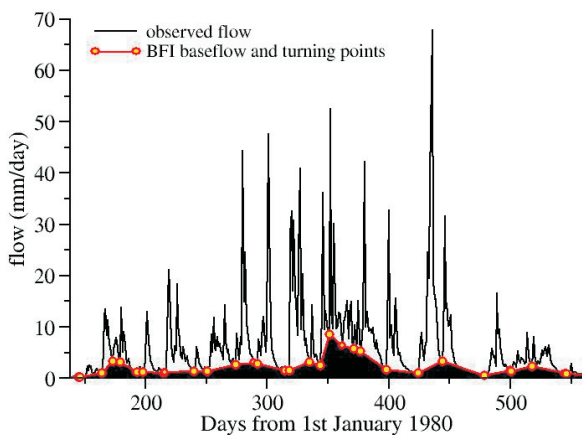
Fig. 2: BFI hydrograph separation for the Wye at Cefn Brwyn (daily data) (Littlewood, 2008).
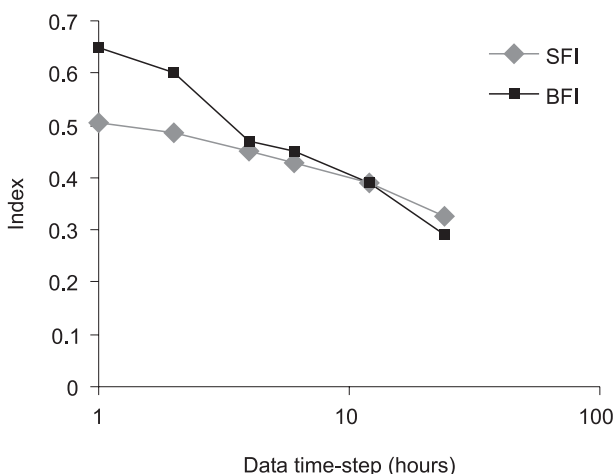
Fig. 3: Wye at Cefn Brwyn
(a) BFIs using different data time-steps,
(b) SFIs and BFIs 6 December 1987 to
2 July 1988 (Littlewood, 2008).

In outline, BFI is usually computed from daily flows, as follows. The minimum flow in each consecutive, non-overlapping, block of five flows (Q_1, Q_2, …, Q_5; Q_6, Q_7, …, Q_{10}; etc.) is identified. The block minima, in overlapping groups of three consecutive values, are then inspected using simple rules to decide if the middle value of each group is a baseflow turning point. An unbroken sequence of daily baseflow values is estimated by interpolating between pairs of consecutive baseflow turning points. Interpolated daily baseflows can occasionally be greater than the corresponding observed streamflows, in which case they are adjusted to the observed streamflows. The area under the adjusted baseflow hydrograph is expressed as a proportion of the area under the observed streamflow hydrograph to give the baseflow index ($0 < BFI < 1$). The BFI algorithm can be considered to include two parameters: the length of non-overlapping flows (L) and a multiplicative factor (F) that is applied to ensure identification of sensible baseflow turning points. Usually, L is 5 (as above) and F is 0.9. Using daily data, values of L and F other than 5 and 0.9 respectively will return different values of BFI for a given catchment. The BFI hydrograph separation (L=5, F=0.9) over a short period of the daily record for the Wye at Cefn Brwyn is shown in Fig. 2, where the shaded area represents the separated adjusted baseflow.

The IHACRES hydrograph separation that gives dominant quick- and slow-response components of modelled streamflow yields a slow flow index (SFI) analogous to BFI. Figure 3 shows how BFI and SFI for the Wye at Cefn Brwyn change as the data time-step varies between 1 hour and 24 hours. While SFI changes by about 18 percentage points, BFI changes by about 36 percentage points, i.e. BFI is twice as sensitive to data time-step as SFI. Furthermore, while SFI shows signs of approaching a stable value at small data time-steps there is no indication of this happening for BFI.

SUMMARY AND CONCLUDING REMARKS

There is seldom information available with which to assess the accuracy of rainfall–streamflow model parameters, though their precision can often be assessed using statistical methods. However, IHACRES model parameters for the Wye at Cefn Brwyn calibrated using hourly data (Fig. 1) provide a reasonable benchmark against which the accuracy of parameters calibrated using other data time-steps can be assessed. The uncertainty associated with a model parameter is a combination of accuracy and precision.

The Wye at Cefn Brwyn case illustrates how model parameters estimated with good precision can be inaccurate, and therefore have large uncertainty. For example, in the lower left panel of Fig. 1 values of $\tau^{(q)}$ estimated using daily and hourly data are about 20 hours and 4 hours respectively, both with good precision. So, although $\tau^{(q)}$ (daily data) is estimated with good precision it is very inaccurate, i.e. about +400% of the benchmark estimated using hourly data, and therefore it has very high uncertainty. The other parameters shown in Fig. 1 are not estimated with precisions as good as that for $\tau^{(q)}$ but they are inaccurate too, though at +190% (τ_w), +132% (c), +110% $(\tau^{(s)})$ and -18 percentage points (SFI) not to the same degree as $\tau^{(q)}$.

From the results presented for IHACRES and BFI it appears likely that the parameters of many, perhaps all, discrete-time rainfall–streamflow models are sensitive to data time-step, unless specific adjustments are made to account for this modelling artefact. Parameters estimated with poor precision may effectively hide the inaccuracy of some model parameters.

Adopting a given data time-step for modelling a set of gauged catchments possessing a range of dynamic responses will account for some of the uncertainty associated with parameter regionalisation equations developed subsequently. The proportion of this uncertainty might be quite high in some cases. Further work is required to investigate and quantify the magnitude of this regionalisation modelling issue.

Much interesting research remains to be undertaken. The PUB[1] Top-Down modelling Working Group (TDWG) provides one forum for researchers interested in rainfall–streamflow modelling and information transfer to ungauged basins. For details of the TDWG and TRUMPER (Towards Reducing Uncertainty in rainfall–streamflow Model Parameter Regionalisation) the reader is invited to visit http://tdwg.catchment.org/.

REFERENCES

Gustard A., Bullock A. and Dixon J. M. (1992). *Low Flow Estimation in the United Kingdom*. Report 108, Institute of Hydrology, Wallingford, UK.

Institute of Hydrology (1999). *Flood Estimation Handbook* (Five Volumes), UK Institute of Hydrology.

Jakeman A.J., Littlewood I.G. and Whitehead P.G. (1990). Computation of the instantaneous unit hydrograph and identifiable component flows with application to two small upland catchments. *J. Hydrol.*, **117**: 275–300.

Kjeldsen, T.R. (2007). *The revitalised FSR/FEH rainfall–runoff method*. Flood Estimation Handbook, Supplementary Report No. 1, UK Centre for Ecology and Hydrology: 68pp.

Littlewood I.G. (2007). Rainfall-streamflow models for ungauged basins: uncertainty due to modelling time-step. In: L. Pfister and L. Hoffmann (eds), Uncertainties in the 'monitoring-conceptualisation-modelling' sequence of catchment research. Proc. Eleventh Biennial Conference of the Euromediterranean Network of Experimental and Representative Basins, *UNESCO Technical Documents in Hydrology* Series, **81**:149–155.

Littlewood I.G. (2008). Characterisation of river flow regimes for environmental and engineering hydrology: unit hydrographs for rainfall-streamflow modelling. *Folia Geogr. ser. Geogr.-Phys.*, **39:** 5–36**.**

---

[1] The Prediction in Ungauged Basins Decade (2003-2012) of the International Association of Hydrological Sciences.

Littlewood I.G. and Croke B.F.W. (2008). Data time-step dependency of conceptual rainfall-streamflow model parameters: an empirical study with implications for regionalisation. *Hydrolog. Sci. J.*, **53**(4): 685–695.

Merz R. and Blöschl G. (2005). Regionalisation of catchment model parameters. *J. Hydrol.*, **287**: 95–123.

Merz R., Blöschl G. and Parajka J. (2006). Regionalization methods in rainfall – runoff modelling using large catchment samples. In: V. Andréassian, A. Hall , N. Chahinian and J. Schaake (eds), Large Sample Basin Experiments for Hydrological Model Parameterization. *IAHS Publication* **307**:117–125.

NERC (1975). *Flood Studies Report* (Five Volumes), UK Natural Environment Research Council.

NERC (2003). *Hydrological data UK*. T.J. Marsh and M.L. Lees (eds), UK Natural Environment Research Council: 208 pp.

Post D.A. and Jakeman J.A. (1999). Predicting the daily streamflow of ungauged catchments in S.E. Australia by regionalising the parameters of a lumped conceptual rainfall-runoff model. *Ecol. Model.*, **123**: 91–104.

Sefton C.E.M. and Howarth S.M. (1998). Relationships between dynamic response characteristics and physical descriptors of catchments in England and Wales. *J. Hydrol.*, **211**:1–16.

Young A.R. (2006). Stream flow simulation within UK ungauged catchments using a daily rainfall-runoff model. *J. Hydrol.*, **320**(1): 155–172.

Young P. C. and Romanowicz R. (2004). PUB and data-based mechanistic modelling: the importance of parsimonious continuous-time models. In: Pahl-Wostl C., Schmidt S., Rizzoli A. E. and Jakeman A.J. (eds.): *Complexity and Integrated Resources Management* (Trans. Second Biennial Meeting of the Int. Environmental Modelling and Software Society, iEMSs, Manno, Switzerland, 2004), **3**: 1141–1146. ISBN 88-900787-1-5. http://www.iemss.org/.

Young P.C. & Garnier H., 2006. Identification and estimation of continuous-time, data-based mechanistic (DBM) models for environmental systems. *Environ. Modell. Softw.*, **21**: 1055–1072.

DEVELOPING SMALL CARPATHIAN CATCHMENTS IN ORDER TO INCREASE THEIR WATER RETENTION CAPACITY

A. Lenar-Matyas, M. Łapuszek, J. Szczęsny and H.Witkowska

Cracow University of Technology, Cracow, Poland
Corresponding author: Anna Lenar-Matyas, e-mail: alenar@iigw.pl

ABSTRACT

In recent years, an appreciable increase in maximum discharge has been observed. The reasons for this include climate changes as well as human activity within river catchments. Thus far, flooding issues have always been addressed at the local level. This often puts downstream areas in danger and has a generally negative impact on the natural environment. Recently, some attention has been directed towards increasing the ability of rivers and catchments to retain water. A number of French research studies in the 1990s explored the idea of a "Dynamic Slow Down". This work presents an application of the DSD method to selected mountain catchments in the Upper Vistula River basin as well as the results of a number of simulations. These suggest that the use of DSD "structures" on a larger scale can result in slower discharge on a global scale.

Key words: Carpathian catchment, flood mitigation, dynamic slow down

INTRODUCTION

In recent years, a significant increase in the intensity of extreme events such as floods and droughts has been observed. The reasons for this include climate changes as well as human activity within river catchments. The same time period has also seen the abandonment of traditional agriculture in the Polish Carpathian Mountains characterized by disappearing field boundaries, the introduction of mechanical logging methods, and an increase in impermeable surfaces such as urban areas, roads, parking areas, *etc*… All of these activities have led to land, gully, and stream channel erosion. The consequences of this have been landslides, increased surface runoff, and higher flood crests. The same is true of streambeds with structures that regulate water flow such as sediment check dams, weirs, sills, and concrete canals designed to protect inhabited areas.

CATCHMENT MANAGEMENT

Historically, flood management techniques have been limited to a single focus on local flood protection and have often caused appreciable disturbances in river and ecosystem dynamics. The concept of a "Dynamic Slow Down" arose in line with growing attention being paid to ecological considerations as well as macro-scale flood protection. The aim of DSD is to solve flood and erosion issues within an entire catchment by increasing its water retention capacity wherever it is possible. So far, DSD has been applied to lowland water basins with few attempts to study its feasibility in mountain regions (*Le Ralentissement...*, 2004). In recent years, forest service crews have attempted to slow down runoff by placing wooden barriers across streams in mountain catchments. However, there are many other "natural" methods that can be used. These include changing agricultural practices, introducing hedgerows, and creating porous parking lots. The "technical" solutions that are currently available are discussed below. These include the construction of small hill slope structures and stream channel structures that slow down water flow. They can be seen here in Figure 1. In order to better retain water, a number of different structures can be constructed. Small temporary ponds called "water traps" can be built within natural hollows in the terrain with low dikes accompanied by transfer trenches designed to redirect overflows to safe thalwegs. Other structures include water infiltration trenches,
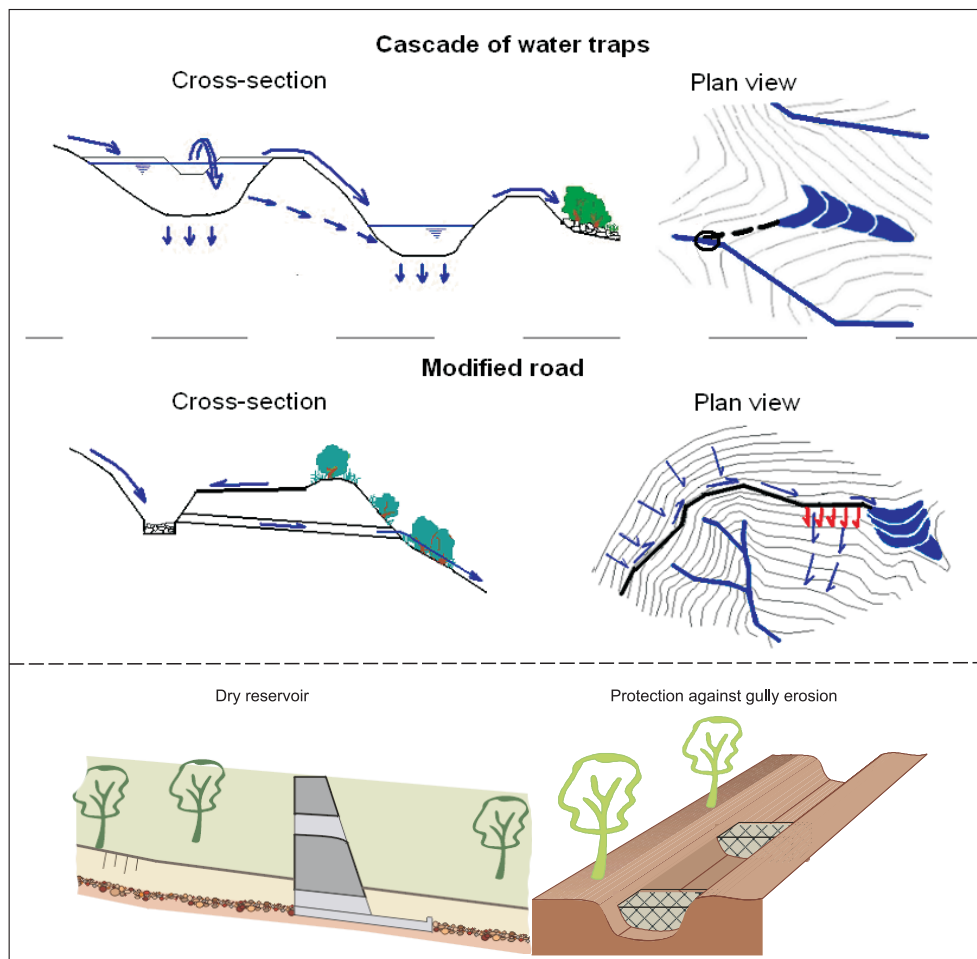
Fig. 1:   DSD cachment structures (Poulard *et al*., 2004).

transversal barriers across gullies, and forest roads built with a transverse slope opposite to that of the hill slope. Discharge can be slowed down in mountain riverbeds using dry reservoirs wherever they do not damage the river channel (Fig. 1).

CASE STUDIES

The authors of this paper conducted a feasibility study for DSD structures in seven Polish Carpathian stream catchments: (1) two catchments in the Beskid Mts. – Trzemeśnianka and Kamieniczanka (Witkowska, 1991); (2) four catchments in the Podhale Region (Poronin County) – Suchy, Bustryczański, Nosków, and Florków (Wątroba, 2004); and finally (3) one catchment in Beskid Żywiecki – Isepnica Stream (Wilczek, 2004; Poulard *et al*., 2004) (Fig. 2).

The authors attempted to assess the effect of different combinations of hill slope structures. With the investigated catchments being ungauged and data being limited, the choice of mathematical models for this study was also limited (Fig. 3).
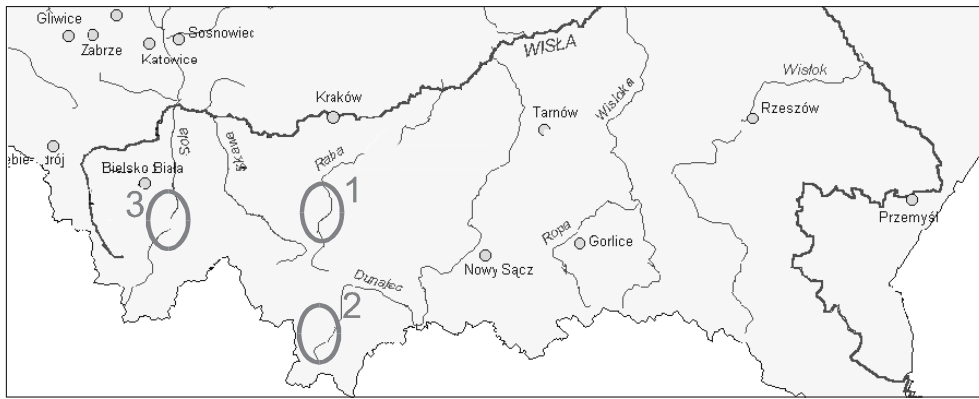
Fig. 2:   Location of the studied catchments.
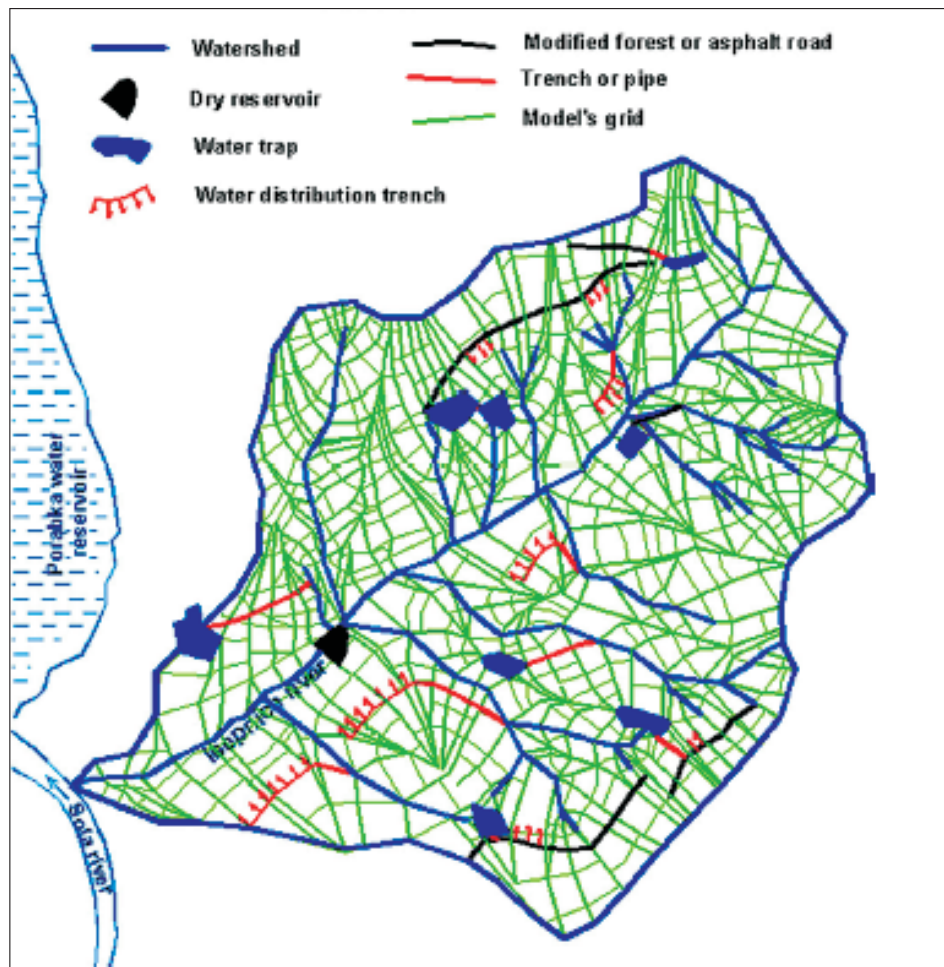
Fig 3:   The Isepnica Stream catchment with a computational net and proposed Slow Down structures (Poulard *et al.*, 2004).

DEVELOPMENT OF THE "ROOF AND PIPE" AND "ONESECOND" MODELS

A review of existing hydrologic precipitation-runoff models indicated that it would be difficult to find a suitable model given our set of assumptions. The existing complex hydrologic models demanded too much data which would be unattainable in an ungauged catchment. Therefore, we developed relatively simple models for our purposes – the Roof and Pipe and the OneSecond models (Poulard *et al.*, 2004). We assumed the most

125

disadvantageous of conditions such as a catchment completely incapable of infiltration (saturated soil and a wet surface) and intense storm-type precipitation. In the models used, the complex topography of the slopes was covered by a very dense irregular computational net (fixed in R&P, based on topography in OneSecond) which allowed one to insert small water retention structures. Both models are distributed parameter models. The difference is that the Roof & Pipe model is very "fast" (ten minutes per run) and the introduction of new management scenarios is very easy. The OneSecond model, on the other hand, more precisely describes the physical nature of runoff but takes a lot more computer time.

For the main stream, the Roof & Pipe model was coupled with a one-dimensional (ID) St-Venent water flow model RubarBE (Łapuszek *et al.*, 2007). This coupling permitted the introduction of water flow control structures in the main stream and the calculation of supercritical and subcritical flows which occur in mountain streams. It also allowed for the introduction of distributed runoff flow into the river section as well as point inputs. The RubarBE model also permitted the calculation of sediment transport rates.

THE RESULTS OF COMPUTATION

In the all the case studies, the Roof & Pipe model was applied to the investigated catchment. The most complete computations with the St-Venant' flood routing system were used only in the case of the Isepnica Stream (3) while in the remaining cases, a simplified routing system was applied. Different scenarios involving catchment structures and reservoirs were studied in cases #1 and #2 in the Podhale catchments (very small and steep) where only a combination of small reservoirs was concluded to be practical. The efficiency of small DSD structures is shown in Figure 4 and Table 1.

Fig. 4:   The results of simulation of dry reservoir impact on the Isepnica Stream.

Table 1: Wave crest reduction via DSD structures.

Stream	Catchment area [km^2]	$Q_{max\,1\%}$ [m$^3 \cdot$s^{-1}]	DSD of Q_{max} reduction structures	
			Dry reservoir Q_{max}	Water traps
Isepnica DR 1	4.3	41	31	
Isepnica DR 2	5.9		25	
Isepnica WT	7.8			29
Florków Potok	1.36	27	11	-
Suchy Potok	6.58	64	23	-
Bustryczański Potok	5.05	51	20	-
Nosków Potok	1.41	30	12	-
Kamieniczanka	5.23	18	6	7
Trzemeśnianka	1.59	21	8	10

RETROFITTING OF SEDIMENT CHECK DAMS

Many sediment check dams have been constructed on Carpathian streams over the years. These dams have not effectively stopped traction load as they quickly became filled (up to 80%) with suspended matter (Ratomski, 1991). Furthermore, they tend to cause quite significant erosion downstream (Wątroba, 2004) and

many have deteriorated since they have been built. Therefore, we have tried to find a solution to this problem by "retrofitting" these dams into dry reservoirs.

A study on the retrofitting process of the sediment check dam on the Isepnica Stream into a dry reservoir has been carried out (Łapuszek *et al.*, 2007). Three sediment check dams are located on the Isepnica Stream. at 412 m, 582 m, and 1510 m (Fig. 4). These sediment check dams were constructed in the 1950s in order to protect the adjacent villages against hillslope erosion. Now their bowls are completely full of sediment and some of them are in very bad technical shape. We recommend that sediment in the bowls be removed, and once they are retrofitted, that they be adopted as dry reservoirs.

Calculations were performed for 31 "natural" cross sections of the stream sections in question. First, we considered the bowls of three sediment check dams (Fig. 4) completely emptied of their accumulated sediment in order to check the efficiency of this strategy. Simulations were conducted for a hydrograph with $Q_{max} = Q = 41$ m^3 s^{-1} without sediment movement (unimpeded water flow). The dimensions of the water outlet were: 1 m high and 2 m wide (Łapuszek *et al.*, 2005).

The computation results showed significant peak-crest diminution (25%) (Fig. 5). This first computation indicated that sediment check dams transformed into dry reservoirs could be a very efficient water flow management solution.
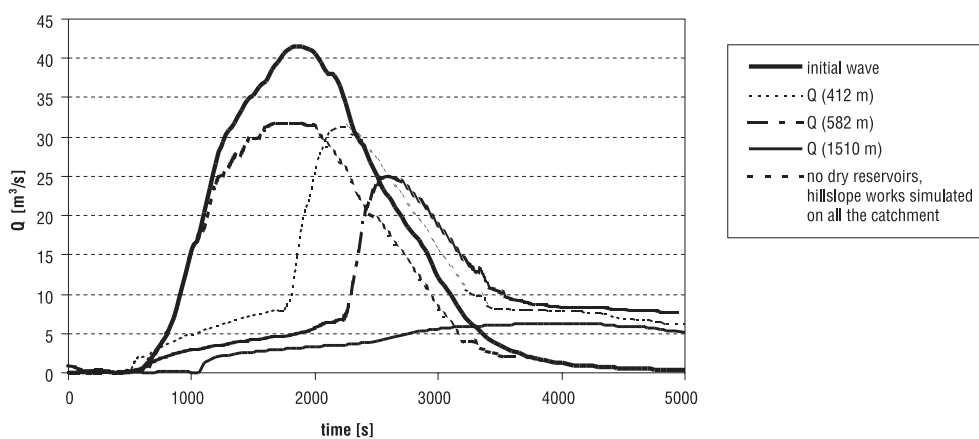
Fig. 5:   Flood wave hydrographs.

CONCLUSIONS

1. A Slow Down structure can effectively reduce the danger of gully erosion and landslides;
2. A special hydrologic model is necessary for quick and efficient computations. A model that is prepared for extreme conditions gives higher discharge values in the main stream than do empirical coefficients for a particular region;
3. The impact of small catchment structures is significant for flood mitigation purposes and for the purpose of reducing wave crests. Such structures could also reduce the need for heavy-duty water control structures in streambeds;
4. When it comes to the protection of urban areas, small Slow Down structures are insufficiently effective. In this case, an integrated system of small structures along with dry reservoirs seems to be the best solution.
5. The retrofitting of ineffective and ecologically harmful sediment check dams into dry reservoirs alters flood wave crest values and allows communities to avoid the construction of concrete channels.

REFERENCES

Le Ralentissement dynamique pour la prevention des inundations – guide (2004). Cemagref.

Poulard Ch., Szczęsny J., Witkowska H. and Radzicki K. (2004). Dynamic SlowDown: a flood mitigation strategy complying with the integrated management concept – implementation in a small mountainous catchment. *Int. J. River Basin Manage.*, **2**(4).

Łapuszek M. and Paquier A. (2007). Practical Application of 1-D Sediment Transport Model. *Archives of Hydro-Engineering and Enviromental Mechanics*, **54**.

Łapuszek M., Witkowska H. (2005). Metoda spowalniania odpływu ze zlewni górskiej (A metod for slowing down runoff in mountain catchments). Infrastruktura i ekologia terenów wiejskich (Rural area infrastructure and ecology), PAN Kraków.

Ratomski J. (1991). Sedymentacja rumowiska w zbiornikach przeciwrumowiskowych na obszarze Karpat fliszowych (Accumulation of traction load in sediment collection traps in the flysch region of the Carpathian Mountains). *Monografia*, **123**, Politechnika Krakowska.

Wilczek A. (2004). *Koncepcja przegród piętrzących na wybranych potokach podhalańskich*. (Different types of barriers on selected streams in the Podhale region). Unpublished master's thesis, Politechnika Krakowska.

Wątroba R. (2004). *Wymiarowanie obiektów spowalniania odpływu z małych zlewniach górskich* (Designing structures that slow down runoff in small mountain catchments). Unpublished master's thesis, Politechnika Krakowska.

Witkowska H. (1991). Erozja poniżej zapór i stopni wodnych (Erosion downstream from dams and weirs) – Materiały XI Ogólnopolskiej Szkoły Hydrauliki (11th Data Set of the Polish School of Water Management), Wola Zręczycka.

RECONSTRUCTION OF SUSPENDED SEDIMENT DATA FROM FLOOD EVENTS USING STOCHASTIC SIMULATION

L. Outeiro, X. Úbeda and F. Asperó

GRAM. Department of Physical Geography. University of Barcelona. Montalegre, 6. 08001. Barcelona, Spain, Corresponding author: Luis Outeiro, e-mail: louteiro@gmail.com

ABSTRACT

The main objective of this paper is to present a methodology for the use of stochastic methods in reconstructing suspended sediment data series acquired during flood events. In this paper, new methodology is compared to other methodologies used in the past by other authors to estimate suspended sediment data. The new methodology involves an innovative approach that has never been used for hydrological purposes but has been used for geostatistical procedures such as mapping techniques of soil variables. Test data for this study comes from a gauging station located within a 2.5 km² woodland catchment. The flood event selected to test the model in question occurred in late winter 2006. Results of the two methodologies used (regression vs. stochastic) portray different behaviors. As has been noted by other researchers, regression techniques tend to underestimate or overestimate suspended sediment estimates. Stochastic techniques, being more complex and more reliant on ancillary variables, yield suspended sediment estimates that are more realistic when compared with field results using suspended sediment from catchments with comparable river beds.

Key words: suspended sediment, discharge, rating curve, stochastic simulation

INTRODUCTION

Extreme rainfall events are increasingly becoming a major concern in terms of the risk of erosion and chemical denudation. This is especially true in Mediterranean environments where, after a dry summer, autumn storms cause significant flash floods (Outeiro *et al.*, 2007). The occurrence of intense storm-induced rainfall in the western Mediterranean results in severe and often catastrophic floods. High resolution temporal data are required in order to assess the effects of such rainfall events and their hydro-ecological response. Unfortunately, pertinent instruments often experience technical problems during such events, and in some cases, are not able to log any data. The extrapolation of suspended sediment concentration has been a traditional topic of discussion given that rating curves relating concentration and discharge always tend to underestimate or overestimate concentrations (Walling, 1977; Walling and Webb, 1988). Several procedures and methods have been developed and applied to correct such bias (Ferguson, 1986; Asselman, 2000; Holtschlag, 2001). Consequently, researchers have been forced to look for cost-effective solutions to such technical problems. Our goal is the reconstruction of "hydro-events" for which there is no available data. The basic strategy is to apply a modeling approach and simulate suspended sediment behavior using methods different from those already described in hydrological estimation literature. Finally, we compare the simulation results with results produced by regression techniques.

STUDY AREA AND MATERIALS

Vernegà Stream is an order 1 stream of the Ter River catchment based on the Strahler classification system. This headwater stream is an intermittent or seasonal type stream due to limited and highly variable rainfall as well as given its geologic structure (granites). The local climate is Mediterranean subhumid with mean annual rainfall in the research area at around 600 mm with the majority of it being collected during the autumn and spring seasons. The hydrologic regime is defined by two Mediterranean features: low discharges and a drought

period between May and October (Sala *et al.*, 2001). The instrumentation used was the following: a water stage recorder (OTT type), an automatic sampler (ISCO 3700). The latter instrument was programmed to take samples every 1 or 2 hours during a flood event from a starting stage of 10 cm.

As stated earlier, the hydrologic regime of this stream makes it necessary to perform suspended sediment simulations only during rainfall events. The event chosen for the simulations occurred in late winter 2006 and the only data available is a time series of 100 hours of discharge ($dm^3 \cdot s^{-1}$) and 24 hours of suspended sediment during the falling limb (Fig. 1). The suspended sediment samples available are not representative of the main event as these were taken during the falling limb and for discharges about four times smaller than peak discharge. Moreover, the variability of the measured concentrations is much higher than the variability of the corresponding discharges, making any kind of modeling of the Q-SSC relationship very difficult.
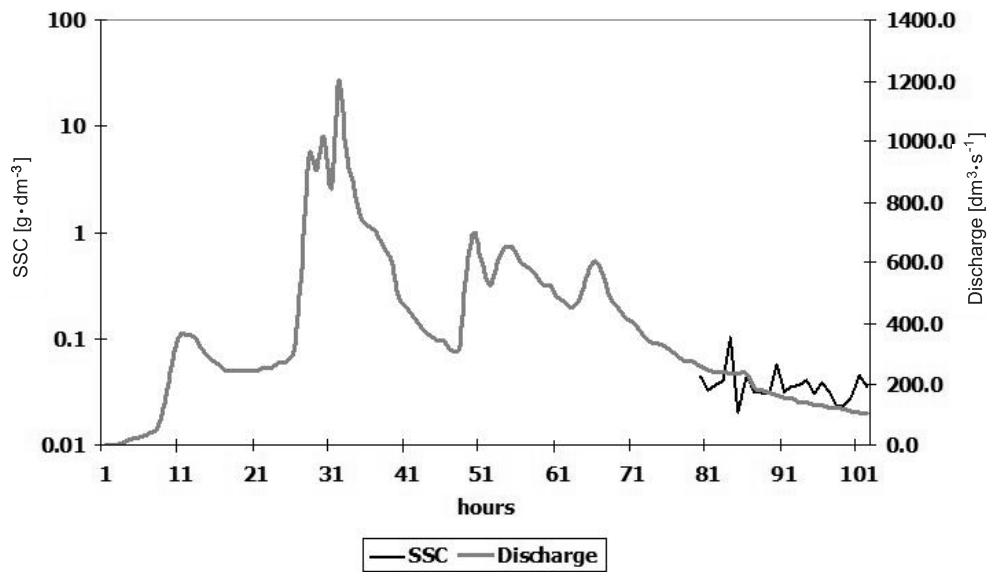
Fig. 1:   Flood event data.

METHODOLOGY

The software used to produce the simulations was GS+ version 7.0 (Gamma Software Inc.) which is based on GSLIB principles (Deutsch and Journel, 1997). The concept of the simulation used in our research is rooted in the sequential conditional simulation (SCS) techniques used by GSLIB. As stated in the book by Deutsch and Journel (1997), the sequential simulation principle allows one to draw the value of a variable $Z(u)$ from its conditional distribution given the value of the most related covariate at the same location u. In this process, the same modeling elements are used for the variable simulated (suspended sediment) as for the most related covariate (discharge). These modeling elements include deterministic algorithms, CDFs, semivariograms, and covariance functions. In their simulation step, the models used include stochastic parameters and algorithms (as randomization seeds), refinement multigrids, the number of simulations for each node, and ratios of searches and numbers of neighbors.

RESULTS AND DISCUSSION

Sequential Conditional Simulation Modeling

SCS measured data were modeled using semivariogram algorithms. A semivariogram fitted to the measured data is presented in Figure 2 with parameter values also being shown. The results of the fitted model in the semivariogram are the following: residual sum of squares (RSS) = 0.0000368, R^2 = 0.448, $C/(C_0+C)$ proportion = 0.998. It is important to note the low number obtained for the RSS parameter which describes how well a model fits a semivariogram. The lower the RSS, the better the fit.

When performing a simulation using this type of simulation model, certain parameters are needed to feed the model for each run. These parameters are: search neighborhood; radius = 6, and number of neighbors = 2. Number of simulations = 1000 for each node (in our case, for each hour). In our simulation runs, a randomization seed was not used in light of the unrealistic output produced when a randomization seed was used. Refinement multigrids were not used in our simulations either. In the following simulation run, the software calculated a standard deviation for each node to give us an idea how much inconsistency the model produces. Our runs obtained a standard deviation of 0.33 g $\cdot$ dm^{-3}
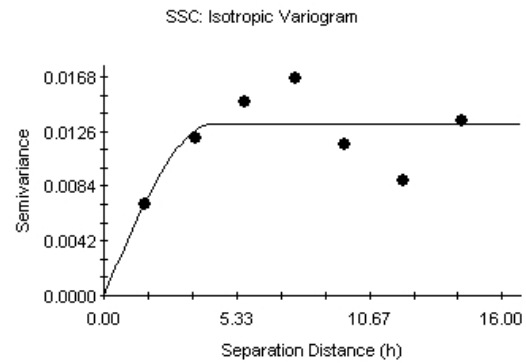
Spherical model (Co = 0.0000300; Co + C = 0.0131600; Ao = 4.39; r2 = 0.448; RSS = 3.687E-05)

Fig. 2: Semivariogram and covariance graph of a model fitted to measured SCS data (g$\cdot$dm^{-3}).

Regression Model

In order to compare the SCS simulation results with other models, we considered two types of fitted regression models: linear and power function. A quite satisfactory R^2 of 0.44 was calculated for the linear regression model of discharge (dm$^3\cdot$ s^{-1}) and SCS (g$\cdot$dm^{-3}). An equally satisfactory R^2 of 0.55 was calculated for the power function model. Asselman (2000) and Walling (1974, 1978) state that the most commonly used sediment rating curve is a power function. Our results from the regression model, therefore, are consistent with what these two autors have stated. In Figure 3, one can see how the power function tends to overestimate SCS values and how the linear model tends to underestimate SCS values. These tendencies were also described by Walling (1977) and Walling and Webb (1988), who stated that rating curves relating concentration and discharge tend to either underestimate or overestimate sediment concentrations.
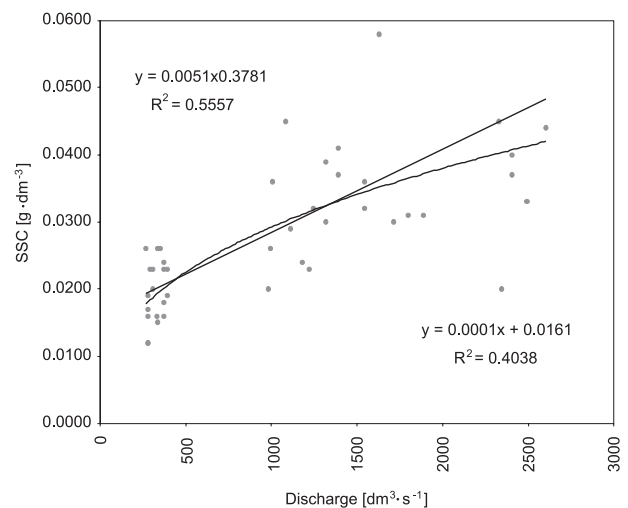
Fig. 3: Regression Model.

presented herein reproduced measured data because of the way the model was used. This method, however, does not guarantee high quality in other types of simulations.

SUMMARY

The simulation model yields a realistic result when calculating SCS for maximum discharge values. During the falling limb, the simulation model yields SCS results of the same order of magnitude as measured values in other catchments with sandy riverbeds as well as measured values for other events occurring in this catchment. Mean values of the series produced by the regression model either underestimate (linear) or overestimate (power function) SCS. The proposed method is an alternative when scarcity of data does not allow for better modeling of SCS relationships. More storm-induced rainfall data are needed to validate both models – especially the regression model. Despite the stochastic nature of hydrologic parameters, these modeling techniques can provide new insight which can also help develop the use of stochastic simulation in hydrologic science. The novel experimental approach presented in this paper can be used in conjunction with other stochastic techniques that involve other hydrologic variables.

Acknowledgement

REFERENCES

Asselman N. (2000). Fitting and interpretation of sediment rating curves. *J. Hydrol*, **234**: 228–248.

Batalla R. (1993): *Contribució del transport de sorres en el balanç de sediment d'una conca granítica mediterrània*. PhD Thesis. Universitat de Barcelona.

Deutsch C. V. and Journel A.G. (1997). *GSLIB: Geostatistical Software Library and User's Guide*. Oxford University Press, New York.

Ferguson R.I. (1986). River loads underestimated by rating curves. *Water Resour. Res.*, **22**: 74–76.

Holtschlag D. (2001). Optimal estimations of suspended-sediment concentrations in streams. *Hydrol. Process.*, **15**: 1133–1155.

Outeiro L., Úbeda X. and Farguell J. (2007). Sequential simulation with external drift of suspended sediment concentration during an extreme rainfall episode in a Mediterranean experimental basin. Proceedings on the European Geoscience Union. Vienna, 2007. *HS30 Experimental river basins*. 15–20 April 2007, Vienna

Sala M., Farguell J. and Llorens P. (2001). Runoff, storm runoff and water quality in two instrumented small catchments in the Catalan Coastal Ranges. *ERB2000 Proceedings* Cd-rom, Gent, 1-19

Walling D.E. (1977). Assessing the accuracy of suspended sediment rating curves for a small basin. *Water Resour. Res.*, **13**: 531–538.

Walling D.E. and Webb B.W. (1988). The reliability of rating curve estimates of suspended sediment yield: some further comments. In: Sediment Budgets. Proceedings of the Porto Alegre Symposium, December 1988. *IAHS Publ.*, **17**: 337–350.

APPLICATION OF ARTIFICIAL NEURAL NETWORKS MODELLING TO THE SÁZAVA AND PLOUČNICE RIVERS

M. Neruda[1], R. Neruda[2] and J. Šrejber[3]

[1] Faculty of the Environment, University of J. E. Purkyně in Ústí nad Labem, The Czech Republic

[2] Institute of Computer Science, Academy of Science, Praha, The Czech Republic,

[3] Czech Hydrometeorological Institute in Ústí nad Labem, The Czech Republic,

Corresponding author: Martin Neruda, e-mail: martin.neruda@ujep.cz

ABSTRACT

The article addresses the modelling of runoff based on precipitation data collected in the Sázava River and Ploučnice River basins. Knowledge acquired in previous research in the Ploučnice River basin was found to be useful in this study. Rainfall and runoff data (both with a 1 hour time step) were obtained from the Czech Hydrometeorological Institute (CHMI). The time period of Aug.1–Sept.11, 2002 was selected, mainly because of the flood event on the 14th of Aug., 2002 in the Sázava River basin. An in-house software system for hybrid computational intelligence modelling, Bang, was used for creating and tuning the model. Calculations were performed with feed-forward neural networks, namely multi-layer perceptron networks trained by back propagation. Network architectures were tested on 1-hour and 2-hour predictions (for the Sázava River) and a 1-hour prediction in the case of the Ploučnice River. The resulting efficiency coefficients measuring the modelling fidelity for the Sázava River tests were: 96.7% (1-hour ahead forecast) and 82.1% (2-hours ahead forecast). This result was in accordance with what was obtained in the previous calculation in the case of the Ploučnice River using daily data (80–93%). It is desired that the experiments in on-line prediction be continued with real-time data from the Smědá River with 6 and 12 hour lead time forecasts.

Key words: artificial neural networks, rainfall-runoff models, Ploučnice River basin, Sázava River basin

INTRODUCTION

Feed-forward artificial neural networks were used in this study as the rainfall-runoff modelling tool for the Sázava and the Ploučnice Rivers. These networks represent a state-of-the-art approach to obtaining an arbitrary input-output function. It was also beneficial to use the knowledge of modelling acquired in the previous research in the Ploučnice River basin. For calculations, two software tools were used – a multi-agent software system called Bang (Neruda, 2005) developed at the Institute of Computer Science, Academy of Science, Praha, and the Weka Library from the University of Waikata in New Zealand. Rainfall and runoff data were obtained from the CHMI, located in Ústí nad Labem and in Prague. Only sub-basins of the Sázava and the Ploučnice Rivers were selected for this study.

RELATED WORK

Kisi (2005) did the river flow forecasting in the form of a numerical and graphical comparison between neural networks and auto-regressive (AR) models. Benchmarking was based on 7-year and 4-year periods of continuous river flow data for 2 rivers in the USA, the Blackwater River and the Gila River, and a 2-year period of streamflow data for the Filyos Stream in Turkey. The choice of appropriate artificial neural network (ANN) architectures for hydrological forecasting, in terms of hidden layers and nodes, was investigated. Three simple artificial neural network (ANN) architectures were then selected for comparison with the AR model forecasts. The sum of squared errors (SSEs) and correlation statistical measures were used to evaluate the models' performance. The benchmark results showed that ANNs were able to produce better results than

AR models when provided the same data inputs. The results obtained with ANNs for 1-day ahead forecasts are better than those reached using the AR models and confirm the ability of this approach to provide a useful tool in solving a specific problem in hydrology, that of streamflow forecasting. The results suggest that the ANN approach might provide a superior alternative to the AR models for developing input - output simulations and forecasting models.

Sohail *et al.* (2008) found that to achieve a desired level of accuracy during the training process of a Back Propagation Artificial Neural Network (BPANN) model, the appropriate stopping criteria were very important. The extended iterations beyond requirement in the training of a BPANN model might result in over-fitting of the model, behaving extraordinarily well on the training data but poorly on the testing data. A cross–validation approach became the standard technique for the generalization of BPANN models and was used in Sohail study. In cross-validation, it was customary to divide data into three sets labeled training, validation, and test sets. The model counted the number of epochs. The monitoring of validation error after every 100 epochs was used due to large amounts of data. After a certain level of training, although the training set error would be decreasing, the error in the validation set would start increasing or become stable. At that moment, the training was stopped and the network was said to be generalized.

Aquil *et al.* (2007) used 2 types of ANN architectures: feed forward and recurrent ANN and 3 types of training algorithms. Levenberg-Marquardt, Bayesian regulation, and Gradient descent with momentum and adaptive learning rate back propagation algorithms were used. Six types of ANN architectures were developed for 1 to 5 hours ahead prediction in the Cilalawi River in Indonesia. The best results were obtained by a recurrent and a feed forward network trained using the Levenberg-Marquardt algorithm.

The ASCE Task Committee in Application of Artificial Neural Networks in Hydrology (2000) produced two parts of description of ANN usage in rainfall-runoff modelling. It was stated that an attractive factor of ANNs was their ability to extract the relation between inputs and outputs of a process without knowing the physics of it. The physics was locked up in the set of optimal weights and threshold values. Optimal training data were very important. Less training data made the network work poorly and more training data should bring better performance to the model.

Jayawardena and Fernando (1995, 1996) and Fernando and Jayawardena (1998) also used RBF (Radial Basis Function) networks for flood forecasting. Hourly rainfall and runoff data from a 3.12 km^2 basin were collected and used in developing an ANN. The autocorrelation of runoff and the cross-correlation between rainfall and runoff indicated that runoff, at a certain time, was influenced by antecedent rainfall from up to three previous hours. The input layer contained three antecedent discharges and two precipitation values: Q (t-1), Q (t-2), Q (t-3), R (t-2), and R (t-3). The output was runoff at the current hour, Q (t). Both a multiple layer perceptron (MLP) neural network and an RBF network were developed and compared with the statistical ARMAX model. Even though both the RBF and MLP networks worked well, it was found that RBF networks could be trained faster than MLP networks using back propagation. Also, both networks performed better than the ARMAX model.

Thirumalaiah and Deo (1998) selected a three-layer ANN for predicting flood situations for the city of Jagdalpur. The ANN was trained with back propagation, a conjugate gradient, and a cascade correlation algorithm. It was found that all three training algorithms performed really well. Back propagation needed the most training epochs and the cascade correlation algorithm needed the fewest. The ANNs predicted lower water levels well but generally underestimated high water levels. That was because not enough training data were available for training of high water level periods.

In the Czech Republic, the Czech Hydrometeorological Institute uses AquaLog software for rainfall-runoff modelling and for real-time flood forecasting. The present setting of AquaLog has been operated since 2001; however, the system and its components are developed continuously according to operational needs and changes (data availability and formats, new subroutines etc.). AquaLog was used for several research projects and studies in the last few years. The modelling system AquaLog was developed based on the strategy and certain procedures used by NOAA NWSRFS (National Weather Service River Forecasting System), and were operated by the US National Weather Service for more than 30 years. The software system is used in the MS Windows environment with a user friendly GUI. AquaLog uses a special database called AquaBase, which is

a tool for data quality checking, correction, and editing. AquaBase prepares in advance data on time series of precipitation, temperature, and discharge for AquaLog. Unfortunately, there is no common format of operational meteorological and hydrological data, such as a SHEF format used in the NWSRFS. As there are different sources of operational data (precipitation data, data from river authorities, different types of data-acquisition water gauges etc.), the first step of hydrological modelling must be data unification and quality control. That is done in this special AquaBase software. AquaBase imports data from different sources (databases, data files), performs the first automatic control of missing data and produces automatic interpolation or extrapolation of time series according to set criteria. AquaBase also unifies the time step of time and serves as a GUI for data correction by a hydrologist. AquaLog incorporates a snow accumulation and ablation model called SNOW17 and a rainfall-runoff model called SAC-SMA. In order to provide a 48 hour forecast for all forecasting profiles (some of the forecasting profiles represent an area of less than 50 km^2; the typical size of a basin is about 200–300 km^2) the meteorological measurements and forecast (NWP ALADIN) must provide an input for hydrological modeling purposes. The model is computed regularly once a day in the morning with additional runs during the day in case of a flood. AquaLog is an interactive system demanding a forecaster's involvement in the process which means changing settings and parameters during the computation based on the forecaster's knowledge of the model, his or her skills and experience, and the given basin being modelled. The real-time flood-forecasting version of AquaLog operates in a 1-hour time step and produces a standard 48 hour lead time forecast for more than 130 profiles in the Labe River basin. The AquaLog modelling system was set to a 6-hour time step, therefore a new calibration of model parameters had to be done using daily precipitation, minimal, and maximum temperature time series for the 1961 to 2003 time period.

METHODOLOGY

An important property of the neural network is its ability to learn the function from examples of input and desired output data, analogically to its biological counterpart. A multi-layer perceptron network architecture was used in this research. Neurons in the feed-forward network are arranged in layers which are connected by synapses. These networks are typically trained by a standard back propagation algorithm or back propagation with a momentum term. Hourly data were used for the time period of Aug. 1,2002–Sept.11, 2002 forthe Sázava River, mainly because of the inclusion of the flood on the 14th of Aug., 2002 (critical flood flow 7:00–9:00 AM with runoff 169 m$^3 \cdot$s^{-1}). According to the CHMI, it was more than Q_5 (5 –years runoff). Rain gauging stations were located in the following towns: Habry, Horní Krupá, Humpolec, Světlá nad Sázavou. (Fig. 1) For the calculation of weight rainfall averages, the Thiessen polygon method was used in ArcGIS version 9. In the Sázava River study, the data from the time period of Aug.1–Aug. 31, 2002 were designated to be training data while for testing (verification) data, the time period of Sept.1–Sept.11, 2002 was selected. Two variants of perceptron neural network architecture, 2-7-1 and 3–7–1 with a back propagation algorithm were used. The first variant was associated with a 1 hour ahead forecast, with rainfall and runoff data at the time of calculation. The second variant was associated with a two hour ahead forecast, with rainfall and runoff data at the time of calculation, and rainfall data from a two hour ahead prediction.

Fig 1:   Sázava River Basin – the selected part (Source: CHMI).

Data from two rain gauging stations (in the town of Jablonné v Podještědí and the town of Stráž pod Ralskem) and runoff data from the Mimoň water-stage recorder were used for the Ploučnice River calculations (Fig. 2). The data were normalized to the program in the interval <0; 1>. After calculations, the data were changed back to runoff in [m$^3 \cdot$s^{-1}] and then the efficiency coefficients were calculated (Nash-Sutcliffe). The dataset contained 17 521 hourly data (2 years 2006–2007). It was divided into two parts where 90% became training

Fig. 2: Ploučnice River Basin
         – the upper part (CHMI).

data and 10% became testing data. Back propagation with a momentum term was used to train the multi-layer perceptron networks for 500 epochs (presentations of the training set). The reported results were obtained based on the training data and the testing data. Networks with 1-hour, 2-hour, and 3-hour histories were tested. In each category, there were several architectures differing in the number of hidden layers (1 or 2) and the number of neurons in them (5–10 in the first, and 2–4 in the second hidden layer). The number of neurons within hidden layers was based on experience and previous calculations.

Training data are used to set the network parameters during the training process while testing data are used to verify a network's ability to model previously unseen data. In order to quantitatively measure the performance of all models, a so-called efficiency coefficient (EC) is used, as expressed in equation 1. The EC value can be mostly in the interval between 0≤EC≤1, and the closer the value to 1, the better performance.

$$EC = \left[1 - \frac{\sum (Q_m - Q_p)^2}{\sum (Q_m - \overline{Q})^2} \right] \cdot 100 \ (\%)$$

Eq. 1

Where: Q_m – hourly measured flows at the ČHMU profile (mm)
       Q_p - hourly flows computed by a neural network (mm)
       $\overline{Q}$ – average measured flow value (mm)

RESULTS

Sázava River: The efficiency coefficients for the first variant (1 hour ahead forecast) were: for training 99.6%, for testing 96.7%; for the second variant (2 hours ahead forecast) were for training 99.4%, for testing 82.1%. On graphs, the term „řada 1" means measured values and „řada 2" means predicted values. In future experiments, forecasts will reach further in time, i.e. larger lead time forecasts (6, 12 hours).
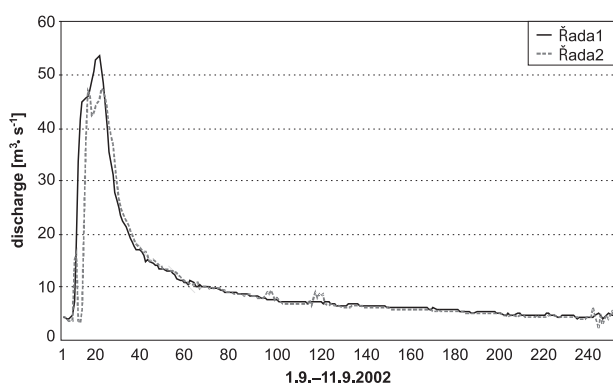
Fig. 3: Prediction with 2 hours lead time, network 3-7-1, testing in the Sázava River.

Ploučnice River: In general, networks with more hours of history perform slightly better than those with 1-hour historical data. It seems that 3-hour history networks will require more time for proper learning, since they contain more parameters to be set by the learning process. Nevertheless, all the networks were quite successful in learning assigned tasks. Results have been compiled in Table 1 where training and testing data are compared. The testing was performed on a previously unseen 10% of the data. It can be seen from the second column that the bigger the network, the bigger the testing error, resulting in poorer generalization of bigger networks. Comparing the training errors in column one, it can be seen that two-hour history networks achieved the best performance.

138

Table 1: Results for the Ploučnice River experiments.

Network architecture	Absolute training error	Absolute testing error
1 hour history		
3;5;1	0.0394	0.009
3;10;1	0.0428	0.011
3;5;2;1	0.0394	0.013
2 hour history		
6;5;1	0.0246	0.010
6;10;1	0.0253	0.015
6;5;2;1	0.0263	0.019
6;10;4;1	0.0267	0.022
3 hour history		
9;5;1	0.0629	0.034
9;10;1	0.0581	0.033
9;5;2;1	0.0644	0.037
9;10;4;1	0.0682	0.042

CONCLUSION

It is desired that the experiments in on-line prediction with real-time data from the Smědá River basin be continued. The aim is to compare two modelling software approaches, AquaLog on the one hand, and Bang/Weka on the other. Until now, no comparisons of results with other statistical methods or deterministic models have been performed. These experiments, so far, indicate a successful application of neural networks to rainfall-runoff modelling. Most of the previous experiments (from the year 2000) were done using daily data with very good results (EC = 57-93% for testing). Experimenting with hourly data began in order to achieve a better fit of the model to flood events (peaks). With hourly data, calculations were performed first for the Sázava River (year 2002 – 50 days) and the Ploučnice River (2006-2007) basins. The main goal of all this work is to improve flood management strategies – mainly flood warning systems – by employing these models in real world on-line scenarios.

REFERENCES

Aquil M., Kita I., Yano A. and Nishiyama S. (2007). Neural networks for real time catchment flow modeling and prediction. *Water Resour. Manag.*, **21**: 1781–1796.

ASCE Task Committee in Application of Artificial Neural Networks in Hydrology (2000). Artificial Neural Networks in Hydrology II: Hydrologic Applications. *ASCE J. Hydrol. Eng.*, **5**(2): 124–137

Eberhart R .C. and Dobbins R.W. (1990). *Neural network PC tools: A practical guide*. Academic Press, San Diego, 414 pp.

Fernando D.A.K and Jayawardena A.W. (1998). Runoff forecasting using RBF networks with OLS algorithm. *J. Hydrol. Eng.,* **3**(3): 203–209.

Jayawardena A.W. and Fernando D.A.K. (1995). ANN in hydrometeorological modeling. [In:] Topping B.H.V. and Khan A.I. (eds.): *NN and Evolutionary Computing for Civ. and Struct. Enineering*, Proc. 4th Conf. in the Application of Artificial Intelligence to Civ. And Struct. Engrg., Devel, Civil-Comp Ltd., Edinburgh, UK: 115–120.

Jayawardena A.W. and Fernando D.A.K. (1996). *Comparison of multi-layer perceptron and radial basis function network as tools for flood forecasting*. Proc. North Am. Water and Envir. Conf., ASCE, New York: 457–458.

Kisi Ö. (2005). Daily river flow forecasting using Artificial neural networks and Auto-regressive models. *Turkish J. Eng. Env. Sci*, Tübitak, **29**: 9–20.

Neruda M., Neruda R. and Kudová P. (2005). Forecasting runoff with Artificial Neural Networks, UNESCO, International Hydrological Programme, *Progress in surface and subsurface water studies at plot and small basin scale*, 10th Conference of the Euromediterranean Network of Experimental and Representative Basins (ERB), Turin, Italy, 13-17.10.2004, IHP-VI, No. **77**, Paris, France: 65–69.

Neruda R. (2006). Computational Intelligence Agent-Oriented Modelling. *WSEAS Transactions on Systems,* 5(2): 430–433.

Sohail. A., Watanabe K. and Takeuchi S. (2008). Runoff analysis for a small watershed of Tono area, Japan by Back Propagation Artificial Neural Network with seasonal data. *Water Resour. Manag*, **22**:1–22.

Šíma J. and Neruda R. (1997). *Theoretical issues of neural networks*. Matfyz Press, Charles University, Prague (in Czech).

Thirumalaiah K. and Deo M.C. (1998). River stage forecasting using ANN. *ASCE J. Hydrol. Eng.*, **3**(1): 26–32.

Witte I. H. and Eibe F. (2005). *Data Mining: Practical Machine Learning Tools and Techniques*, Second Edition, Morgan Kaufmann Series in Data Management Systems.

A NEW TREND IN STREAMWATER BALANCE AND SEDIMENT DELIVERY INDUCED BY INCREASING VEGETATION COVER IN A SMALL BASIN

C. Pelissero, F. Maraga, F. Di Nunzio, F. Godone, R. Massobrio and G. Rivelli

National Research Council (CNR), Department of Earth and Environment,
Research Institute for Geo-Hydrological Protection (IRPI), Turin Branch
E-mail: chiarapelissero@libero.it, franca.maraga@irpi.cnr.it

ABSTRACT

The results of 25 years of field observations of sediment transport (1982–2006) in a gravel stream can be seen in a small instrumented basin in the northwestern Italian Alps called Valle della Gallina, (1.08 km^2). The basin is equipped for long-term water and bed load measurement in order to determine the variability of sediment supply from year to year. This particular small basin is representative of a reduction in erosion magnitude in a mountain region with a continental Mediterranean climate. The precipitation in the area mainly consists of rainfall. Annual sediment yield data collected at the mouth of the basin, namely the product of erosion, indicates that there has been a decrease in sediment load delivery and also in the runoff coefficient since the end of the 1990s. This decrease in sediment transport at the basin mouth can be explained by the development of vegetation cover on the upper slopes and towards the drainage divide. In the 1970s, these slopes were denuded by logging and became more sensitive to rain erosion and channel bank erosion which, in turn, led to higher sediment supply in the stream channel system.

Key words: hydrologic change, mountain basin, Alps, Italy

INTRODUCTION

This paper presents data on bed load delivery from a small mountain basin representative of the Piedmont area of the Alpine region of northwestern Italy under geomorphological conditions of erosion processes shaping steep drainage basins and regoliths with regosols (Biancotti, 1981). Hydrological records on this small basin have been kept since 1982 in order to provide a long-term estimate of sediment transport in relation to runoff and precipitation (Fig. 1). The sediment transport data refer to the volumes and grain size of sediments delivered from the main stream and trapped at the basin outlet (Anselmo and Maraga, 1985; Caroni *et al*., 2000; Maraga, 2007).

Since data analysis of the 25-year period of interest revealed a significant reduction in sediment transport during the last decade, research efforts became focused on the identification of the changing slope features. Soil erosion was recognised as the dominant process that feeds sediment into the hydrographic network.

STUDY AREA

The small basin's drainage divide belongs to the Alpine hydrographic system in the Piedmont area – or buffer zone – between the Alps and the upper Po River plain (NW Italy). Some characteristics of the study area are reported in Table 1.

The local pluviometric regime reflects the characteristics of a continental Mediterranean type with two rainfall maxima with a first peak in the spring and a second peak in the autumn as well as storms during the summer
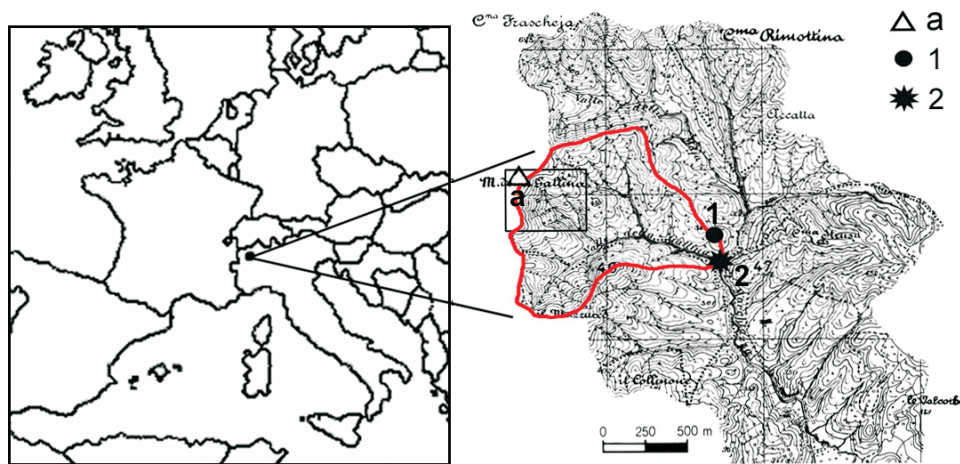
Fig. 1:   *Left*: Location of the small basin *Valle della Gallina* (Italy), 1.08 km². *Right*: Topographic map of the drainage basin with contour lines showing erosional landforms representative of the Alpine Piedmont region: a – head of the small Piedmont basin *Valle della Gallina* (522 m a.s.l.); 1 – meteorological station (375 m a.s.l. ; 2 – hydrometric and sediment collection station (330 m a.s.l.) as well as the mouth of the small basin (45°38'28''N, 8°18'48''E). The area delineated with a rectangle at the head of the small basin (a) contains the headwater slope detail presented in Figure 4.

Table 1: Small basin Valle della Gallina characteristics.

Area	1.08 km²	Temperature (mean 1982–2006)	10°C
Lithology	rhyolites	Precipitation (mean 1982–2006)	1283 mm·year⁻¹
Altitude (mean)	417 m a.s.l.	Runoff (mean 1982–2006)	735 mm·year⁻¹
Inclination (mean)	43%	Runoff coefficient (mean 1982–2006)	0.57
Main channel length	1.50 km	Discharge (mean 1982–2006)	0.02 m³·s⁻¹
Soil cover (regolith)	0–2 m	Peak flow max (19 Sept. 1995)	6.44 m³·s⁻¹

season (Caroni, 1979). The meteorological characteristics of this small Piedmont basin are comparable to regional climatic conditions. Regolith soil cover (0.7 m thick, on average) and rhyolite bedrock outcrops characterize the lithological conditions in the basin. The morphometry of the geomorphological features describes a stream erosional landscape characterized by a main stream with a 6% slope and a dendritic drainage network with a density of 52 km·km⁻². There is no permanent human activity in the basin.

SEDIMENT TRANSPORT

The mechanism of sediment transport was observed in the main stream along its terminal reach. It was found to be primarily related to bed load type based on the grain size distribution of the sediment transported and collected at the sediment collection station at the mouth of the small basin and via field experiments using tracers and seismic detectors (Giussani *et al.*, 1991; Govi *et al*., 1993; Maraga 2007).

Accumulated sediment volumes at the sediment collection station vary between about 1 m³ (1985) and 73 m³ (2002) from year to year, depending on the availability of sediment in the main stream in its terminal reach moving from the basin stream network towards the stream mouth and the sediment trap. In fact, the sediment

142

Fig. 1:   *Left*: Location of the small basin *Valle della Gallina* (Italy), 1.08 km². *Right*: Topographic map of the drainage basin with contour lines showing erosional landforms representative of the Alpine Piedmont region: a – head of the small Piedmont basin *Valle della Gallina* (522 m a.s.l.); 1 – meteorological station (375 m a.s.l. ; 2 – hydrometric and sediment collection station (330 m a.s.l.) as well as the mouth of the small basin (45°38'28''N, 8°18'48''E). The area delineated with a rectangle at the head of the small basin (a) contains the headwater slope detail presented in Figure 4.

Table 1: Small basin Valle della Gallina characteristics.

Area	1.08 km^2	Temperature (mean 1982–2006)	10°C
Lithology	rhyolites	Precipitation (mean 1982–2006)	1283 mm·year^{-1}
Altitude (mean)	417 m a.s.l.	Runoff (mean 1982–2006)	735 mm·year^{-1}
Inclination (mean)	43%	Runoff coefficient (mean 1982–2006)	0.57
Main channel length	1.50 km	Discharge (mean 1982–2006)	0.02 m^3·s^{-1}
Soil cover (regolith)	0–2 m	Peak flow max (19 Sept. 1995)	6.44 m^3·s^{-1}

season (Caroni, 1979). The meteorological characteristics of this small Piedmont basin are comparable to regional climatic conditions. Regolith soil cover (0.7 m thick, on average) and rhyolite bedrock outcrops characterize the lithological conditions in the basin. The morphometry of the geomorphological features describes a stream erosional landscape characterized by a main stream with a 6% slope and a dendritic drainage network with a density of 52 km·km^{-2}. There is no permanent human activity in the basin.

SEDIMENT TRANSPORT

The mechanism of sediment transport was observed in the main stream along its terminal reach. It was found to be primarily related to bed load type based on the grain size distribution of the sediment transported and collected at the sediment collection station at the mouth of the small basin and via field experiments using tracers and seismic detectors (Giussani *et al.*, 1991; Govi *et al*., 1993; Maraga 2007).

Accumulated sediment volumes at the sediment collection station vary between about 1 m³ (1985) and 73 m³ (2002) from year to year, depending on the availability of sediment in the main stream in its terminal reach moving from the basin stream network towards the stream mouth and the sediment trap. In fact, the sediment

142

yield in the main stream is clearly augmented by its dense drainage network, which has developed as far as the hillcrests with numerous first-order streams in various states of regressive erosion. One source of sediment in this basin is weathered bedrock which yields regolith soil on the basin slopes. Another source of sediment is fractured bedrock, eroded in the basin's stream channels.

A detailed analysis was performed on erosive rainfall events for the 1991–2000 time period in order to assess their impact on sediment transport. The analysis revealed 280 erosive rainfall events at the standard threshold of 12.6 mm/event in the considered period, and they had recurrence of 20 to 37 events per year. The study revealed that the correlation between accumulated sediment volumes – year to year – and the corresponding number of annual erosive rainfall events is almost equivalent to the correlation between the sediment volumes and the total annual rainfall, with correlation coefficients of about 0.8 (Maggi *et al.*, 2003). In the 1970s, the main sources of sediment were areas of bare soil and sparse vegetation as well as emerging bedrock outcrops that characterized the headwater slopes of the small basin. At the time, woodlands only covered about 75% of the basin area, mostly distributed from the streams to just over halfway up the slopes (Bellino and Maraga, 1995).

Average bed load transport has been measured to be 35 $m^3 \cdot year^{-1} \cdot km^{-2}$ (1982–2006) with a maximum sediment load of 73 m^3 accumulated during the extreme hydrological year of 2002 characterized by frequent high peak flows. The trapped sediment normally consists of sand and gravel, ranging from 0.06 to 128 mm in size, with rare cases reaching 200 mm in grain size.

Suspended sediment transport at the mouth of the main stream is insignificant compared to bed load. The average suspended sediment value was 0.17 $g \cdot dm^{-3}$ during a recorded peak flow of 1.6 $m^3 \cdot s^{-1}$ after a precipitation event with 202 mm of rainfall in 62 hours in 1981 (Anselmo *et al.*, 1982). Sediment yield collected in the trap during a "recent" period (1999–2006) was characterized by grain size larger than previously with some cases of cobbles in the 128–256 mm size class. Such occurrences can be attributed to an increase in stream bank erosion and a decrease in soil erosion in the basin.

In fact, vegetation cover has spread from the slopes to the hillcrests on the basin's drainage divide and now covers the entire surface area of the basin. The previously observed soil erosion has essentially disappeared. The Atlas of Forestry of the Italian Piedmont presents vegetation typologies and their distribution in the small basin. These include: chestnut (49%), false acacia (16%), and oak (15%). The *Valle della Gallina* small basin is equipped for meteorological, hydrometric, and sediment detection.

DATA COLLECTION AND PROCESSING

The meteorological station is situated on the drainage divide of the small basin towards the mouth of the basin area (see no. 1 in Fig. 1). The hydrometric station is situated in the channel bed in the terminal reach of the main stream at the outlet of the small basin. The data collected therein is representative of the amount of water and sediment coming from the basin's stream system (see no. 2 in Fig. 1). The sediment collection station was set up in the channel bed near the hydrometric station (see no. 2 in Fig. 1) by reshaping a natural pool in the bedrock. It has a collection capacity of 40 m^3 capable of trapping bed load sediment being transported downstream (Fig. 2).

The sediment in the main stream channel is captured directly within the pool in the channel bed and the accumulation inside the trap is measured periodically (at least once a month) using a detailed topographic survey. A small mechanical digger is used to empty the trap and transfer the sediment into the channel downstream of the weir, so that sediment delivery outside the small basin remains unaltered.

Pluviographic, hydrographic, water balance, and discharge data are recorded every five minutes and stored in a database. An azonal soil survey (depth and grain size) was carried out in 1992 by means of 57 manual cores distributed throughout an area featuring the soil cover of interest. They were located in basin soils with or without vegetation cover. The barren surface areas riddled with bedrock outcrops were then observed (Bellino and Maraga, 1995).
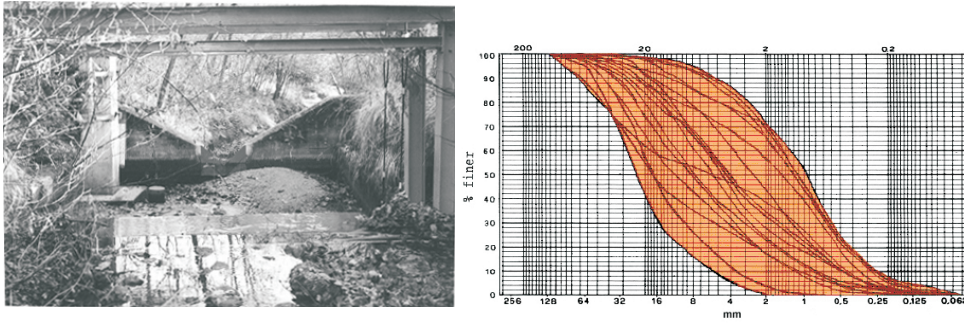
Fig. 2: *Left*: A hydrometric and sediment collection station at the basin outlet (about 20 m³ of sediment can be seen amassed in the trap); *Right*: Grain size frequency curves for sediment trapped on 19 different occasions.

The soil cover was measured to be 0.7 m deep, on average, with a maximum depth of 2 m. 313 soil samples were selected for grain size analysis from the 57 cores used. Stratigraphic measurements of soil grain sizes revealed a significant level of heterogeneity in soil texture and dominant grain sizes (68%) within medium and coarse sands, ranging from 0.125 to 2 mm.

The locations of the measurement stations possess climatic characteristics as well as erosion and drainage conditions which are comparable to those of the Piedmont region under examination. The instruments in the basin have been operating since 1982.

RESULTS AND FINAL CONSIDERATIONS

During the last decade of the 25 years of stream sediment observation (1982-2006), sediment delivery measurements at the small basin's mouth revealed a decrease in the spread of erosion in the headwater region of the basin. Landscape changes were observed by comparing current photographs with those dating back to the 1970s. The archival 1970s photographs had been taken by the Research Institute for Geo-Hydrological Protection – Turin Branch. It was also observed that the grain sizes of sediment accumulated at the stream channel measurement station are similar to those present in the soils of the basin. The only exceptions were the larger sizes (>64 mm), produced by the action of channel bank erosion on fractured bedrock.

Annual rainfall data indicate a decrease in the amount of rain received during the last decade (Fig 3). Therefore, the increase in natural vegetation and the decrease in rain amounts have led to a reduction in soil erosion on
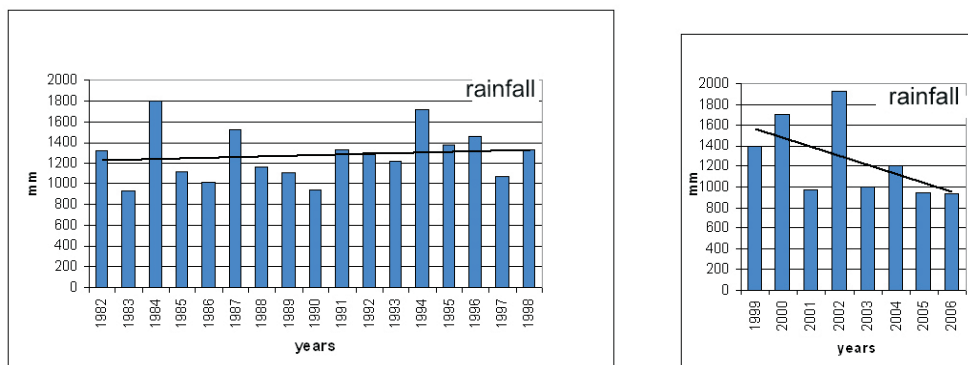

Fig. 3: Rainfall amounts from 1982 to 1998 (left). The trend line on the right shows an appreciable decrease in rain amount values for the last decade of the research study.

144

the basin's slopes and to a subsequent reduction in sediment delivery to the numerous streams that constitute the drainage network feeding the main stream that reaches the basin mouth.

The evolution of the basin's landscape, characterized by the encroachment of woodland onto the upper slopes and headwater areas, is illustrated in Fig. 4. The 1975 photograph (*left*) shows the basin's headwater areas partially denuded and with extensive gully and rill erosion. A comparison of this photograph with a 2008 photograph (*right*) illustrates the growth of new vegetation as far as the basin's drainage divide. The lower annual accumulation of sediment trapped during the last decade is related to the smaller quantity of sediment being delivered to the sediment trap due to fewer floods with the exception being the year 2002. That particular year was a year of extreme flood frequency. In 2002, the largest volume of annual sediment accumulation for the 1982–2006 time period was recorded to be 73 m³ (Fig. 5).
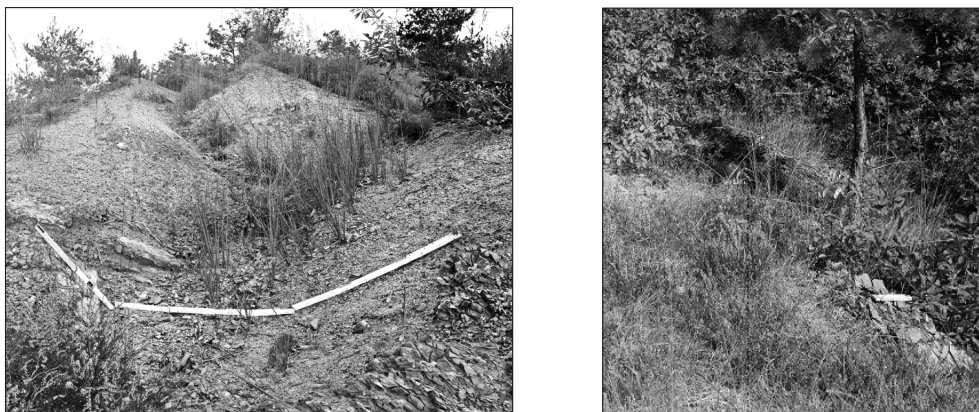

Fig. 4: View of the slopes at the headwaters of the *Valle della Gallina* small basin. Photograph taken from the head of the main stream (northern view). *Left*: 1975 photograph. Bare area of regolith soil and fractured bedrock (3 m tape measure). *Right*: 2008 photograph. Vegetation cover and remnants of bedrock outcrops (20 cm tape measure).
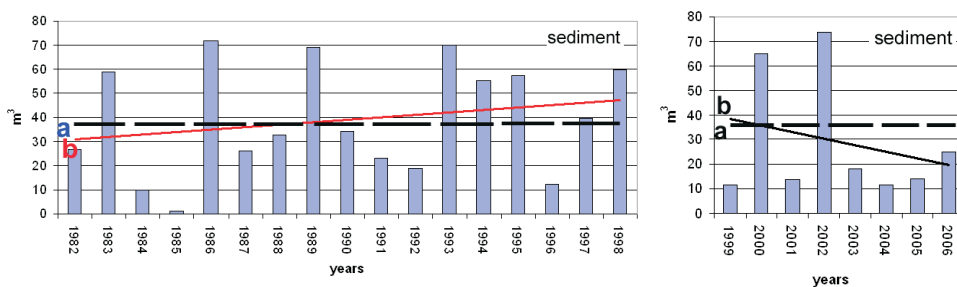

Fig. 5: Sediment transport response to woodland encroachment in the small basin over the last decade of the research study in relation to sediment yield at the basin outlet. *Left*: 1982-1998 and *Right:* 1999–2006 volumes in the sediment trap; a – average value for the observation period (1882–2006) and b – 1982–1998 and 1999–2006 trends that illustrate decreased sediment delivery during the last decade of the research study.

The expansion of woodlands helps the soil to retain rainwater which would otherwise cause soil erosion and facilitate the transport of sediment through the stream channel system. Indeed, the water balance is sensitive to the processes of infiltration and evapotranspiration as well as to water retention potential (Tesar *et al*., 2000; Anselmo *et al*., 2004). Vegetation cover in the basin has been shown to prevent direct runoff from the surface, resulting in a reduction in runoff of more than 10%. Runoff coefficients indicate a similar reduction due to the observed increase in vegetation cover.

Annual sediment trapped at the basin outlet at the end of the 1990s showed a degrease in relation to the reduction in sediment supply. Average sediment transport values were about 25% lower while average runoff and rainfall values were about 10% lower.

The annual water balance in the basin of interest was characterized by a growing frequency of minimal runoff coefficients during the last decade of the research study. In fact the minima values of the runoff coefficients reached 0.4 in 1985, 1997, 1998, 2000, 2001, and 2005. The maximum value of the runoff coefficient reached 0.8 in 1988.

An investigation is in progress to evaluate heavy rainfall, peak flow, and sediment supply trends in the basin. Relationships between hydrological trends and sediment delivery should be more clear once a detailed correlation analysis of event data is carried out. The trend described in this paper reflects the increase in woodland area in the basin and the corresponding reduction in runoff coefficients as well as the reduction in sediment supply within the stream system. These reductions are the result of decreased surface runoff in the basin.

CONCLUSION

This sediment transport study has identified a reduction (since 1999) in sediment yield due to the constant expansion of natural vegetation cover towards the basin headwater areas. This expansion, in turn, has caused a reduction in soil erosion on the slopes that feed sediment transport routes leading to stream channels. Both the very presence of new vegetation and its growing density are responsible for the reduction in erosion.

An increase in vegetation cover has also occurred in some regions of the adjoining French Alps and is commonly held responsible for reductions in sediment delivery to watercourses (Liébault and Piégay, 2001). The *Valle della Gallina* small basin is representative of a natural reduction in the erosion of basin landscape. This reduction has been shown to decrease sediment delivery volumes to the hydrographic stream network which illustrates a broader trend that can be observed on a regional scale.

REFERENCES

Anselmo V., Godone F. and Tropeano D. (1982). *Eventi idrologici in piccoli bacini montani: osservazioni sulla relazione afflussi-deflussi.* Atti Convegno Associazione Italiana Genio Rurale, Padova (Italy). 19 Nov. 1982: 309–324.

Anselmo V., Guiot E. and Tesar M. (2004). *SCS-curve number derivation from rainfall-runoff data collected in forested experimental catchments of the ERB network*. Proc. of "Progress in surface and subsurface water studies at the plot and small basin scale" conference, Turin (Italy) 13–17 Oct., CNR publ.: 131–134.

Anselmo V., Maraga F. (1985). *Cobble Movement and Sediment Transport in a Streambed*. In: CNR-PAN Meeting on "Progress in Mass Movement and Sediment Transport Studies", Turin (Italy), 5–7 Dec. 1985: 245–264.

Biancotti A. (1981). Morfologia, suoli ed erosione in Valle Marchiazza. *Geogr. Fis. Dinam. Quat.*, **4**: 30–38.

Bellino L. and Maraga F. (1995). *Tempi di saturazione in bacino idrografico montano*. Atti II Incontro Internazionale dei Giovani Ricercatori in Geologia Applicata, Peveragno (Italy), 11–13 ott. 1995, Politecnico di Torino, Dipartimento di Georisorse e Territorio: 254–259.

Caroni E. (1979). Pluviometria del Biellese Orientale. *Bollettino dell'Associazione Mineraria Subalpina*, **16**(4): 889–909.

Caroni E., Arattano M. and Maraga F. (2000). Results from bed load measurements in a small catchment (Rio della Gallina, Italy). *Quaderni di Idronomia Montana*, Editoriale Bios, **20**: 99–110.

Giussani F., Maraga F., Pirastru E. and Zuppi G.M. (1992). *Use of activated sediment in field measurements of bed load transfer in a mountain stream*. Proc. "Isotope techniques in water resources development 1991, Vienna (Austria) 11–15 March 1991, IAEA Proceedings Series: 755–757.

Govi M., Maraga., Moia F. (1993). Caratterizzazione granulometrica dei terreni superficiali del bacino sperimentale della Valle della Gallina (VC). CNR-IRPI, Internal Report I.I. 93/9.

Liébault F. and Piegay H. (2001). Assessment of channel changes due to long-term bed load supply decrease, Roubion River, France. *Geomorphology*, **36**: 167–186.

Maggi I., Maraga F. and Ottone C. (2003). Relationship of heavy rainfall to in-channel sediment delivery in a small Alpine basin (North-Western Italy). Proc. of ERB2002 9th Int. Conf. "Interdisciplinary approaches in small catchment hydrology: monitoring and research", Demanovska dolina (Slovakia), 25–28 Sept. 2002, IHP-VI UNESCO, *Technical Documents in Hydrology, UNESCO, Paris*, **67**: 91–98.

Maraga F. (2007). *Charge de Fond dans un petit cours d'eau équipé des Alpes piémontaises (Italie)*. Colloque d'hydrotecnique "Transport solides et gestion des sediments en milieu naturel et urbain, Publications S.H.F: 165–168.

Tesar M., Buchtele J., Sir M. , Di Nunzio F. (2000). Simulation and verification of evapotranspiration and rainfall-runoff processes in the Liz (Czech Republic) and Gallina (Italy) experimental basins. Proc. of ERB1998 8th Int. Conf. "Catchment hydrological and biochemical processes in a changing environment", Liblice (Czech Republic), Sept. 22–24, 1998, IHP- VI UNESCO, *Technical Documents in Hydrology, UNESCO, Paris*, **37**: 131–138.

WATER MANAGEMENT MEASURES ANALYSED FOR DUTCH BASINS TO REDUCE FLOODING

E. Querner

Alterra, P.O. Box 47, 6700 AA Wageningen, The Netherlands, e-mail: erik.querner@wur.nl

ABSTRACT

Flooding in the northern part of The Netherlands has caused serious economic threats to densely populated areas. Therefore a project has been carried out in a pilot area to assess the retention of water in two river basins as a way to reduce flooding. The physically-based groundwater and surface water model SIMGRO was used to model the hydrology of the basins. The model was calibrated using discharges and groundwater levels. Scenarios of measures to assess the possibility of retaining water in the basin were then defined and tested. The first measure was the retention of higher discharges using culverts or gates in the upstream part of the basin. The second measure was to make the streams shallower and thereby, increase flood plain storage. The last measure was flood water storage in a designated area in the downstream part of one basin. The analysis indicates that holding water in the upstream parts of the basins proved to be feasible and can result in significant reductions of peak flows.

Keywords: Drainage basin, rainfall, evapotranspiration, groundwater, surface water, modelling, river basin, scenario

INTRODUCTION

Worldwide there has been an increase in the number of floods and droughts that effect large number of people and cause enormous economic losses. In the period 1990 to 1998 the number of recorded flood disasters in Europe was higher than in the previous three and a half decades. Because of this situation it is clear that measures have to be taken to reduce the impact of these extreme hydrological events. During recent extreme rainfall events in the northern part of The Netherlands the rapid flow from the upper parts of the basin caused flooding of some polders and resulted in a serious threat of flooding of densely populated areas. After a Dutch national study "Water Management in the 21st Century" a policy was adopted to retain more water in the upper part of river basins in order to avoid flooding in the downstream parts. In this study the SIMGRO model was used. This model simulates the flow of water in the saturated zone, the unsaturated zone and the surface water. The model is physically-based and therefore suitable for use in situations with changing hydrological conditions.

In order to give solutions for an integrated river basin management plan for the northern part of the Netherlands, one of the problems to solve is how to reduce the peak discharge. The question is how to retain more water in a river basin. To analyse such situations and possible mitigation measures, tools were used to evaluate them in terms of eco-hydrological impact and the effect on agriculture. In this paper a report is made on a project carried out to assess the possible retention of water in the upper and lower part of two adjacent river basins. First a very brief description of the SIMGRO model is given, followed by the schematisation of the study area, a comparison of measured and calculated discharges, the scenarios and the results.

THE COMBINED SURFACE AND GROUNDWATER FLOW MODEL SIMGRO

SIMGRO (SIMulation of GROundwater and surface water levels) is a distributed physically-based model that simulates regional transient saturated groundwater flow, unsaturated flow, actual evapotranspiration, sprinkler irrigation, stream flow, groundwater and surface water levels as a response to rainfall, reference

evapotranspiration, and groundwater abstraction. To model regional groundwater flow, as in SIMGRO, the system has to be schematised geographically, both horizontally and vertically. The horizontal schematisation allows input of different land uses and soils per subregion, in order to model spatial differences in evapotranspiration and moisture content in the unsaturated zone. For the saturated zone various subsurface layers are considered (Fig. 1). For a comprehensive description of SIMGRO, including all the model parameters readers are referred to Querner (1997) or Walsum *et al.* (2004).
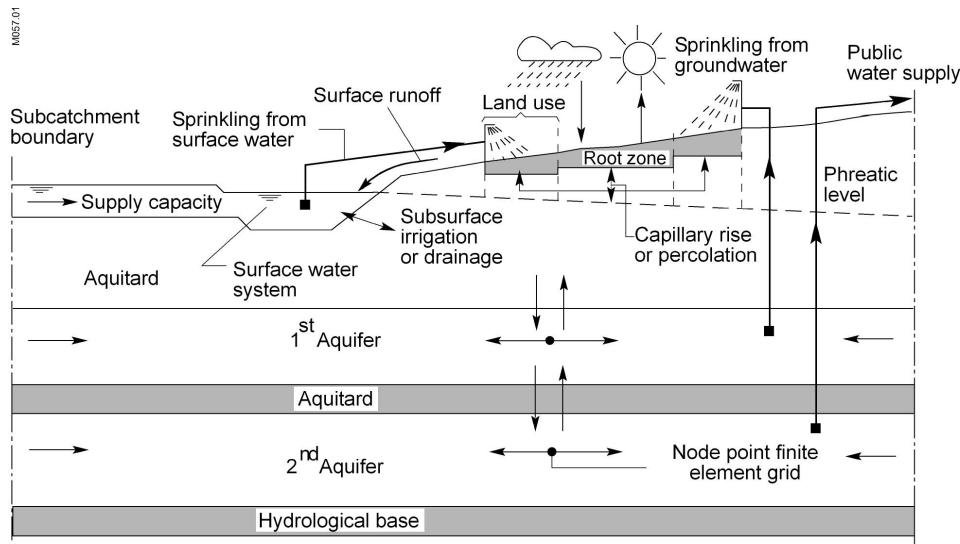

Fig. 1:   Schematisation of water flows in the SIMGRO model. The main feature is the integration of the saturated zone, unsaturated zone and surface water systems (Querner, 1997).

In SIMGRO the finite element procedure is applied to approach the flow equation which describes transient groundwater flow in the saturated zone. The unsaturated zone is represented by means of two reservoirs, one for the root zone and one for the underlying soil (Fig. 1). The calculation procedure is based on a pseudo-steady state approach, using generally time steps of up to one day. Evapotranspiration is a function of the crop and moisture content in the root zone.

In the model, four different categories of ditches (related to its size) are used to simulate the drainage. This interaction between surface water and groundwater is calculated for each category using a drainage resistance and the difference in level between groundwater and surface water (Ernst, 1978). The surface water system is modelled as a network of reservoirs. The outflow from one reservoir is the flow entering the next reservoir, and surface water levels depend on the amount of storage and discharge from a reservoir.

The SIMGRO model is used within the GIS environment ArcView. It gives the possibility of using digital data, such as a soil map, land use, watercourses, etc., to serve as input data for the model and to show results. It is also a tool for analysis and discussion, because interactively data and results can be presented.

STUDY AREA AND MODEL SCHEMATISATION

The modelling area covers 1200 km^2 and is located in the northern part of the Netherlands (see Fig. 1). The area of main interest is approximately 750 km^2 and covers the basins of the river Drentsche Aa and Peizerdiep. The ground surface slopes from about 24 m+MSL in the south to about −1 m in the north. The area consists of sandy soils in the upper parts with clay and peat in the stream valleys and the lower part. Land use is predominantly agricultural and forest. About 42% is in pasture, 24% is arable land, 18% is

woodland, 11% residential and 5% is other. For the meteorological input data five stations spread over the area were used (Querner *et al.*, 2005).

For the SIMGRO model the groundwater system needs to be schematized by means of a finite element network. The network, comprising 49 050 nodes, is spaced at about 200 m in the interest area, but in the stream valleys it is spaced at 75 m. For the modelling of the surface water the two river basins were subdivided in 5625 sub-basins. The difference in height of about 25 m means that 570 weirs were constructed in the past to control the water level and flow. Most of the weirs are adjustable, so that the target water level in summer can be raised. In the lower part, the polders with a water level near or below sea level, there are 58 pumping stations and 41 inverted siphons.

The geology of the area is quite complex, due to influences from the Pleistocene period, permafrost, tectonic movements, and influences from wind and water. A major influence on the groundwater flow patterns is the resistant impermeable layers formed by boulder clay that cause large areas with perched water tables. The groundwater system in the model is build up of four aquifers that are interlaid with three less permeable layers. The second layer consists of the boulder clay. The interaction between groundwater and surface water is characterized by a drainage resistance. This resistance is derived from hydrological parameters and the spacing of the water courses.

The initial SIMGRO model was not able to simulate the perched water tables caused by the boulder clay (model layer 2). In large areas this resulted in phreatic groundwater levels that were 1-3 m too low. Therefore the model was improved that, on the basis of the hydraulic head below and above the boulder clay, the vertical resistance is adjusted to simulate the flux through this clay layer correctly. Also the storage coefficient above and below the clay layer was changed during the calculations depending on the presence of the perched water table. After the model was improved, calculated phreatic levels were close to the measured ones (see next section).

RESULTS OF SIMGRO MODELLING

Present situation

Simulations were carried out for a period of 10 years (1989-1999). The results were compared with measured river discharges (nine locations) and groundwater levels (about 800 piezometers). For three main gauging stations, as shown in Fig. 2, Table 1 gives the measured and calculated discharges. The discharges are given for a recurrence interval of once in five years to a recurrence interval of 15 times per year (denoted as 15x/year). The last column in Table 1 gives Q95, the flow occurring less than 5% of the time. For the Drentsche Aa the calculated discharge is a bit higher than measured (about 8–20%). For the other two streams the differences

Table 1: Measured and calculated discharges for three gauging stations ($m^3 \cdot s^{-1}$) as shown in Fig. 2 (for recurrence intervals see text).

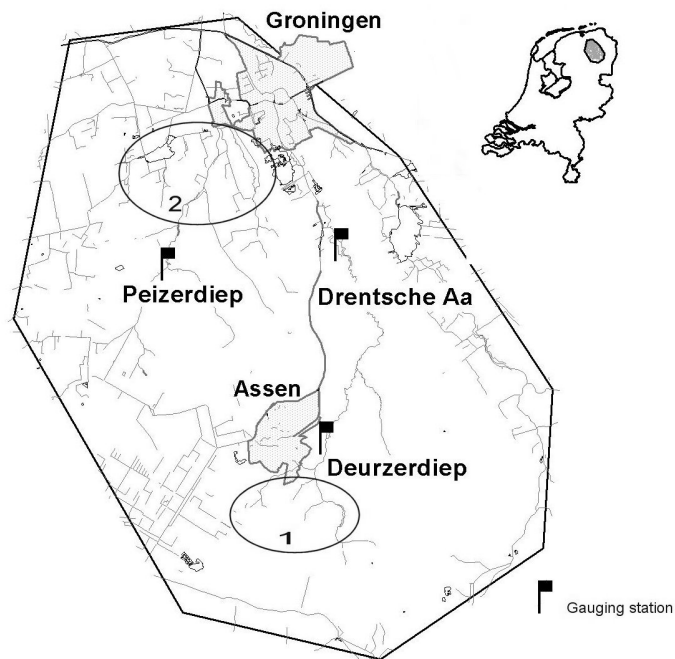| Gauging station		Discharge for the given recurrence interval:				
		5 year	1 year	5x/year	15x/year	Q95
Drentsche Aa	Measured	11.02	8.91	6.97	5.48	0.57
	Calculated	13.63	11.57	7.58	6.24	0.36
Deurzerdiep	Measured	14.45	11.52	6.34	4.00	0.27
	Calculat ed	14.05	11.59	6.24	4.31	0.14
Peizerdiep	Measured	13.64	10.45	6.57	5.01	0.08
	Calculated	13.44	10.47	5.97	4.37	0.12

Fig. 2:   Location of the modelling area and the main water courses in the northern part of The Netherlands (Rakhorst, 2005). In region 1 measures are taken in the upper part of the basin and in region 2 in the lower part.

are smaller, in the order of 2–14%. When comparing hydraulic heads, for more than half the total number of piezometers, the difference in measured and calculated head is less than 0.25 m. Comparing only the phreatic levels: for the 332 phreatic piezometers there are 239 with a difference less than 0.5 m and 145 with a difference less than 0.25 m. These differences between measured and calculated results were regarded as small, so it was concluded that the final model can be used to analyse possible measures to hold water in the upstream part of the basin.

Mitigation measures and the impact

Mitigation measures were defined that would reduce the peak discharges to acceptable volumes. In this research the following measures were analysed:

- Restrict peak discharges:
  Peak flows can be restricted by installing sluice gates or culverts of such a dimension that only the higher peaks are reduced. In the simulations, the opening of these constructions was such that the flow will be restricted when the flow is higher than occurring once a year.
- . Make the brooks shallower:
  Reducing the depth of the water course will result in water overtopping the side banks and it will be stored on the flood plain. The storage of the water on the over banks will reduce the flow propagation and thus reducing the peak flow.
- Flood storage:
  In a designated area in the lower part of the Peizerdiep under high water conditions flood water is stored.

In Figure 3 the measures in the upstream part of the Drentse Aa are shown. At eight locations the flow was restricted and over a length of 29 km the streams were made shallower. In Table 2 the results are given for the

152

two sub basins; it gives the discharge for the reference situation, the two measures and the change in flow. The impact of the first measure (restrict peaks) is more than the second (shallower streams). Limiting the flow by introducing gates or culverts, means a decrease in peak flow in the order of 25–50%. The large variation depends on local conditions and the number of structures in a stream. Limiting the flow has very little influence on groundwater levels, because the water flow is obstructed only for a number of days or weeks. Local flooding may occur and thus groundwater levels rise. This small and short rise, often in winter time, has no apparent effect on agriculture or nature.

In the second scenario, when the stream is made shallower, the reduction of peak discharges is in the order of 5–20% (Table 2). The consequence of this measure is higher water levels in both wet and dry periods. The flow reduction is mainly caused by the water overflowing the river banks and flooding the valley. As a consequence, the groundwater levels adjacent to the stream will be higher. In general the higher levels may have a positive influence on the presence of rare and protected marsh species.
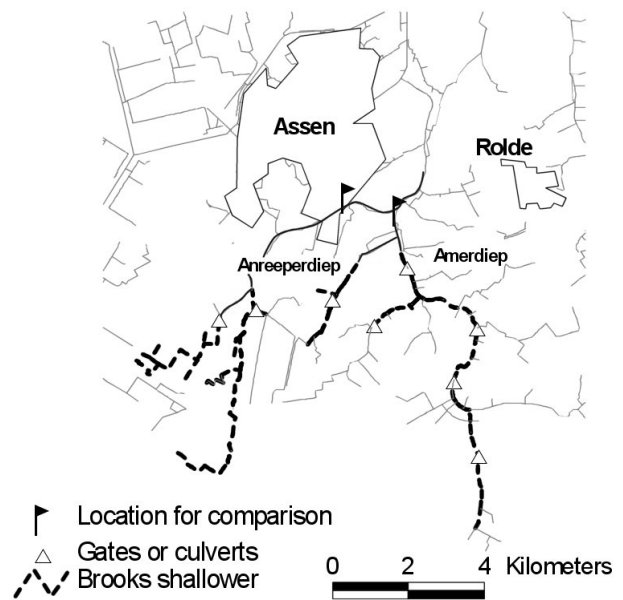

Fig. 3: Location of the mitigation measures carried out in the water courses of the upstream part in the Drentsche Aa. See Fig. 2 for the location in the pilot area.

Table 2: Change in discharges [$m^3 \cdot s^{-1}$] for 2 sub basins and the two scenarios as shown in Figure 2.

Location	Scenario	Discharge for a given recurrence interval				
		10 year	5 year	1 year	5x/year	15x/year
Amerdiep	Reference	13.18	9.62	5.42	3.08	2.23
	Gates	5.32	4.98	4.60	3.14	2.25
	Reduction [%]	60	49	15	-2	-1
	Shallower streams	10.08	9.06	4.99	3.07	2.25
	Reduction [%]	24	7	8	0	-1
Anreeperdiep	Reference	9.12	5.81	3.38	1.94	1.47
	Gates	6.97	3.74	3.02	1.97	1.48
	Reduction [%]	24	36	8	-2	0
	Shallower streams	8.47	5.53	3.44	1.93	1.43
	Reduction [%]	7	4	2	1	1

Flood water storage is considered in the downstream part of the Peizerdiep basin (Fig. 4), where an area is designated for flood water storage (Royal Haskoning, 2006). This area used to be agricultural, but over the last fifty years it was partly changed to a nature area, because of the too wet conditions encountered. The region consists of peat land and subsidence of the soil surface has resulted in a situation that excess water from the area had to be pumped into the river, thus it became a polder. The anticipated flood storage area is around 22.1 km^2.

In scenario 3 (flood storage) it has been considered that the water flow in the brooks Peizerdiep and Eelderdiep is flowing thru the flood storage area (Fig. 4). The dikes along both sides of the rivers, separating it from the polders, will be removed. During flooding of this area, water retention will take place and results in lower

Fig. 4:   Location of the flood storage area in the lower part of the Peizerdiep basin. See Fig. 2 for the location in the pilot area.
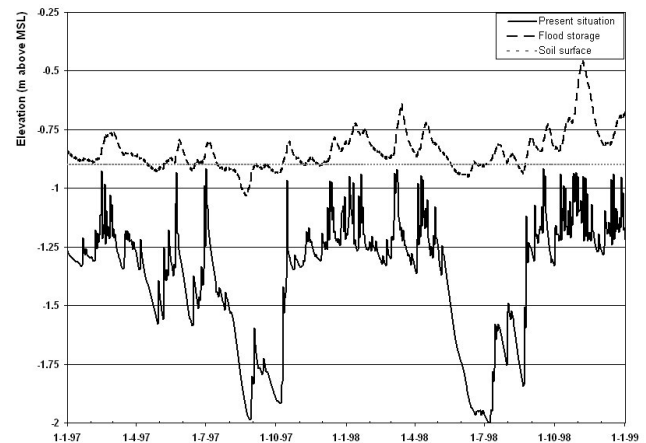
Fig. 5:   Groundwater table for the present situation and the flood storage scenario (Fig. 4 shows the location of the node).

surface water levels. Before and after the flooding there will be in the polder a strong interaction of the surface water with the groundwater. Such complicated situation made it clear that a model was needed to simulate the effects of measures which integrates groundwater and surface water.

In Figure 5 the groundwater table is shown for a location in the anticipated flood storage area. In the present situation the target water level for the polder is -1.30 m above MSL, but the groundwater table is in summer (dry period) even lower. In winter time the groundwater table is close to ground level, being -0.9 m+MSL. In the flood storage scenario the groundwater table remains very close to the ground level, and during wet periods the area is inundated and surface water level and groundwater table are above ground level. Under these situations water is stored in the area, as occurs frequently (Fig. 5). Especially during the months Oct-Nov. 1998 the inundation is around 0.45 m deep.

DISCUSSION ON MEASURES FOR EXTREME RAINFALL EVENTS

In the present situation extreme rainfall extreme events would cause flooding in the low laying areas, which are often densely populated. This situation occurred as well in the autumn of 1998, when in the upper part of the brooks intense rainfall occurred for a number of days. This caused high stream flows and in the lower parts, in the city of Groningen (see Fig. 2), very serious threats of flooding occurred. In this analysis it has been demonstrated that it is feasible to restrict peak flows when they are higher than the discharge occurring once a year. Another approach could be as well to reduce the peak flows which occur once in 10 or 50 years. Take these measures in the upper parts of the basin, thus storing water in extreme events in areas which are not so densely populated. In that way the choice is explicitly accepting local flooding in the upper parts of a catchment where mostly agricultural land is situated, instead of flooding densely populated areas more downstream.

CONCLUSIONS

The physically-based Simgro model was able to simulate stream flow in basins with different land use and climate conditions. The model calibration was limited, but the simulation results show that the model gives satisfactory estimates of the discharges and groundwater levels. The model is therefore an adequate tool to simulate stream flow, and has the potential to assess the impact of measures to reduce flooding.

This study has shown that ecosystems of lowland catchments where the groundwater levels have been lowered by extensive land drainage can be restored by restricting the flow from the upper parts. Holding water in the upstream parts of the basins is feasible. The delay of the peak flow is significant. Also the storage of water in designated areas is effective, but is an expensive measure.

For extreme situations, such as occurred in October 1998, it is also possible to use measures to reduce peak flows that have a recurrence of once in 10 or 50 years. In that way the choice is explicitly to accept local flooding in the upper parts of a catchment where mostly agricultural land is situated, instead of flooding high densely populated areas more downstream.

REFERENCES

EEA (2001). Sustainable water use in Europe. Part 3: Extreme hydrological events: floods and droughts. *Environmental issue report,* **21**, European Environment Agency. Copenhagen.

Ernst L.F. (1978). Drainage of undulating sandy soils with high groundwater tables. *J. Hydrol.*, **39**: 1–50.

Querner E.P. (1997). Description and application of the combined surface and groundwater model MOGROW. *J. Hydrol.*, **192**: 158–188.

Rakhorst M. 2005. Reduction in peak discharges for the Brooks in Northwest Drenthe; estimated with the SIMGRO model (in Dutch). MSc thesis. Wageningen University.

Querner E.P. (2002). Analysis of basin response resulting from climate change and mitigation measures. In: van Lanen H. and Demuth S. (Eds.), FRIEND 2002, Bridging the gaps between research and practice. 4th Int. Conf. on Friend, Cape Town, South Africa, March 2002. *IAHS Publ.* **274**: 77–84.

Querner E.P., Rakhorst M., Hermans A.G.M. and Hoegen S. (2005). Exploring the possibilities to retain water on the Drents Plateau; Pilot in Northwest Drenthe (in Dutch). Wageningen, Alterra, *Alterra- Report,* **1240**.

Royal Haskoning (2006). *Environmental assessment study on flood storage* (in Dutch). Groningen. Report 9R3320, July 2006.

Van Walsum P. E. V., Veldhuizen A. A., Van Bakel P. J. T., Van Der Bolt F. J. E., Dik P. E., Groenendijk P., Querner E. P.and Smit M. F. R. (2004). SIMGRO 5.0.1, Theory and model implementation. *Alterra- Report,* **913.1**. Alterra, Wageningen, The Netherlands.

CHANGES OF THE SOIL MOISTURE REGIME IN LOWLAND CATCHMENT IN CURRENT AND FUTURE CLIMATE CONDITIONS

U. Somorowska

The University of Warsaw, Faculty of Geography and Regional Studies, Department of Hydrology, Krakowskie Przedmiescie 30, 00-927 Warsaw, Poland, e-mail: usomorow@uw.edu.pl

ABSTRACT

Considerable increase in the severity of hydrological events has been registered in Europe in the recent decades and this concerns also the territory of Poland. Signals of climate change are subject to many investigations as future evolution of the climate may have further impact on modification of the hydrological cycle. The objective of this study was to investigate changes of soil moisture in a lowland catchment located in central Poland. The focus was on the soil water storage evolution that has occurred in the past decades as well as on possible shifts in the soil water regime induced by a change of climatic conditions. The study was facilitated by data sets from ensemble simulations from all over Europe with the Regional Climate Model CLM, available from Max Planck Institute for Meteorology, Hamburg, Germany. The soil water content data were extracted from simulations for the last four decades of the 20th century as well as for the 21st century with respect to two IPCC climate scenarios (A1B and B1). Acquired data comprised six subsurface levels with boundaries at depths: 0.01, 0.04, 0.10, 0.22, 0.46, 0.94 m. Using soil water content at given soil depths, area-averaged estimates of water storage have been calculated for the 0–30 cm and 0–50 cm soil layers. Long term variability of soil water storage in the 20th century shows slight downward tendency, statistically significant in last two decades. Monthly mean values for the years 1960–2000 were compared with values projected for the years 2060–2100. The potential evolution of the seasonal cycle of soil water storage was explored. It was shown that considerably drier conditions may appear in summer months. The amount of soil water storage may decrease in the future, as evaluated by the difference between control values and those projected for the 21st century.

Key words: soil water storage, soil moisture projections, differential response

INTRODUCTION

Among different hydrological variables, soil moisture is of special importance as it controls exchange processes between soil, vegetation and atmosphere. Increase of temperature and change in precipitation can have significant impact on terrestrial ecosystems through changes in soil moisture. Decreased soil moisture under higher temperature may limit productivity of terrestrial ecosystems and it may drive vegetation evolution. Changes in the soil moisture regime can also significantly influence the generation of stream flow. For these reasons, the investigations of possible effects of climatic change on soil moisture are currently subject to many research studies (e.g. Yang *et al.,* 2003, Jasper *et al.*, 2006).

The Fourth Assessment Report of the Intergovernmental Panel on Climate Change states that "…continued greenhouse gas emissions at or above current rates would cause further warming and induce many changes in the global climate system during the 21st century…" (IPCC Climate Change, 2007). By the end of the 21st century, the global average surface temperature is expected to increase by about 1.8–4.0°C, if emissions are within the range of the SRES scenarios. Along with the increase of temperature, most General Circulation Models predict a precipitation change. Annual precipitation over Poland may decrease even up to -100 mm, as evaluated by the difference in mean precipitation between a control period of the 20th century and future projection for the 21st century (Kundzewicz *et al.*, 2006). The question arises, how big of a change in the soil moisture regime may be expected, as a consequence of the modified recharge by precipitation and modified losses of evapotranspiration.

Accurate estimates of soil moisture are difficult to obtain even for present conditions. This is due to a high variability of soil moisture in time and space and difficulty of measurement. Although *in situ* data from reference sites are the most accurate estimates, they are rarely available for longer periods and give only an information at a point. Alternative source is microwave remote sensing of soil moisture but these products at fine scale are still urgently needed to be improved. This concerns both the accuracy of data and their assimilation into hydrological applications (Wagner *et al*., 2007). Other estimates of soil moisture can be acquired from the Global Land Data Assimilation System (Rodell *et al*., 2004) or as outputs from regional and local land surface models.

The overall aim of this study was to investigate possible changes of the soil moisture regime in lowland catchment (Fig. 1) by comparing current and future soil moisture values. Selected data sets were from ensemble simulations from all over Europe with the Regional Climate Model CLM which has been forced with output of the ECHAM5/MPIOM global climate model (Hollweg *et al*., 2008). These experimental simulations of regional climate have been computed by the group "Model and Data" of Max Planck Institute of Meteorology (MPI–M) in Hamburg, in close cooperation with Brandenburg University of Technology in Cottbus, the GKSS Research Centre in Geesthacht and the Potsdam Institute for Climate Impact Research (PIK). The climate version of the local model (CLM) of the German Weather Service (DWD) was used to simulate the regional climate of the 20th century (1960–2000) and the 21st century (2001–2100) in Europe. The climate of the 21st century was modeled with respect to two IPCC climate scenarios (A1B and B1).
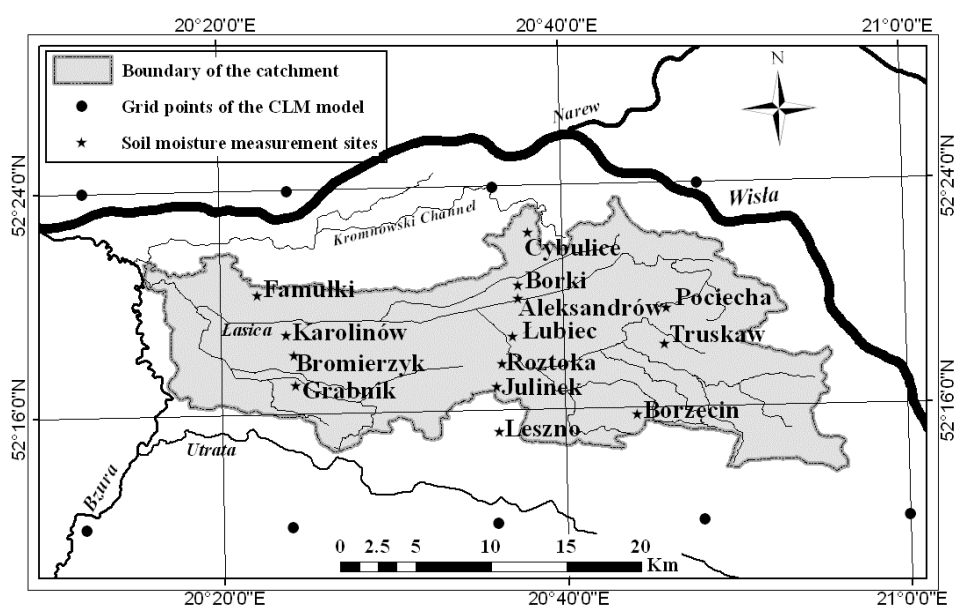

Fig. 1: Location of the soil moisture measurement sites and grid points of the CLM model in the vicinity of Lasica catchment, central Poland.

To give a general picture of how the soil moisture regime may look like in the future at scale of the analyzed catchment, results of model runs were acquired in selected grid cells embracing the catchment area. Soil water storage was characterized by the soil water depth and as the effective relative soil moisture (dimensionless parameter). Long-term monthly mean values have been evaluated for selected periods of the 20th and the 21st century by comparing the time periods of 1960–2000 and 2060–2100.

DATA

The extracted data from the CLM runs comprise sets corresponding to 9 grid cells covering the latitudes from 52°12'N to 52°24' N, and longitudes from 20°12'E to 21°00'E. They have been retrieved by the Net-CDF

format and processed using the Net-CDF Toolbox for Matlab. For each grid cell data were extracted for unevenly spaced layers with the following depth boundaries: 0.00 to 0.01 m, 0.01 to 0.04 m, 0.04 to 0.10 m, 0.10 to 0.22 m, 0.22 to 0.46 m, 0.46 to 0.94 m. The name of the variable extracted from database is "thickness of moisture content of soil layer", which is the soil water storage expressed in mm. Additionally, data from the *in situ* soil moisture measurements in the Lasica catchment (Somorowska, 2007) were applied to check how the CLM model reproduces the soil moisture variability.

METHODS OF ANALYSIS

The soil profiles have been schematized in a number of soil layers, taking into account the extent of unevenly spaced soil layers of different depth in the CLM model. Soil water storage in the soil layer of the depth of 30 cm and 50 cm was calculated according to the following expressions:

$$WS_{30cm} = WS_{0.00-0.01} + WS_{0.01-0.04} + WS_{0.04-0.10} + WS_{0.10-0.22} + (1/3) \cdot WS_{0.246} \qquad \text{Eq. 1}$$

$$WS_{50cm} = WS_{0.00-0.01} + WS_{0.01-0.04} + WS_{0.04-0.10} + WS_{0.10-0.22} + WS_{0.22-0.46} + (6/50) \cdot WS_{0.46-0.94} \qquad \text{Eq. 2}$$

where: $WS0_{30cm}$ and WS_{50cm} represent soil water storage in the surface layers of 30 cm and 50 cm respectively, $WS_{0.00-0.01}$, $WS_{0.01-0.04}$, $WS_{0.04-0.10}$, $WS_{0.10-0.22}$, $WS_{0.22-0.46}$ and $WS_{0.46-0.94}$ – soil water storage in the soil layers at depth range indicated in m in lower index. To express soil water storage in a dimensionless way, the parameter of effective relative soil moisture was applied. Effective relative soil moisture was defined as $X = (WS - WS_{min})/(WS_{max} - WS_{min})$, where WS_{min} – minimum soil water storage, corresponding to the wilting point and WS_{max} – maximum soil water storage, corresponding to the field capacity.

Series of annual mean values of the soil water storage and evapotranspiration/precipitation ratio (ET/P) were analyzed in selected periods to detect long term tendencies in the 20th century. Time series were checked for normality by the Shapiro-Wilk test, using the *KyPlot* Program in version 5.0. Temporal independence of data was checked by the Wald-Wolfowitz runs test, using the *Hydrospect* software in version 2.0 (Radziejewski, Kundzewicz, 2004). Using *Hydrospect* software, parametric linear regression method was used to test whether trend in time series was statistically significant.

Monthly mean values for the years 1960–2000 were compared with values projected for the years 2060–2100. Soil water storage in the 20th century (WS_{CTL}) was assumed to be a control value for the water storage estimated for the 21st century (WS_{SCEN}). The value of a differential response expressed in percentage of a change, related to the control period, was obtained from the expression: $\Delta WS = (WS_{CTL} - WS_{SCEN})/WS_{CTL}$.

RESULTS AND DISCUSSION

Future soil moisture changes should be predicted by models that can produce reliable simulations of soil moisture for past climate conditions. An evaluation of the performance of the IPPC models for the second half of the twentieth century was done e.g. by Li *et al*. (2007). Generally, these models have limited capacity to reproduce observed seasonal cycle of the soil moisture, although some of them, including ECHAM5, were identified as effectively representing circulation patterns in Europe (Seneviratne *et al.*, 2006). The ability to calculate accurate soil water storage depends on several factors. Extremely important are accurate precipitation and radiation forcing and accurate land surface model. In quality control of the CLM model with reference to precipitation, simulations were compared to different reference data sets (Hollweg *et al.*, 2008). It was found that the uncertainty of the reference data for the monthly averages was slightly smaller than the error of the simulated data. The values from the model were merely higher than precipitation averaged over all reference data, but reference data were not corrected with regard to the collective losses. Before considering possible changes of the soil moisture regime in the 21st century in the analyzed catchment, the CLM model simulations of the soil water storage were compared to the *in situ* data.

Comparison between the soil water storage calculated from the *in situ* and simulated data

The soil water storage calculated from the CLM simulations was compared with the values estimated from the *in situ* soil moisture measurements collected from September 1999 to December 2000 (Fig. 2). Mean bias, root mean squared error (RMSE) and the determination coefficient (R^2) were used to evaluate the CLM model performance with reference to the mean *in situ* soil water storage (Table 1). The values were compared at intervals of 1 month (Fig. 2a) and 2 weeks (Fig. 2b). The edge curves for the *in situ* data (very wet profiles - type I, wet profiles – type II and dry profiles – type III) represents the range of uncertainty which concerns various reference profiles. In general the model simulations reproduced temporal patterns of the soil water storage, however differences are observed (Fig. 2c). Variation in the soil water storage was less adequately reflected during summer months. Bias of *X* for June reached 0.28 (mean value). It gave values closer to those estimated for wet sites (bias=0.13) and greater discrepancy (overestimation) for drier sites (bias=0.34). Although discrepancies are observed, the CLM simulation reproduces temporal rhythm which has slightly better performance for time interval of 1 month. Thus considering projections for the 21st century, the temporal interval of one month was applied.
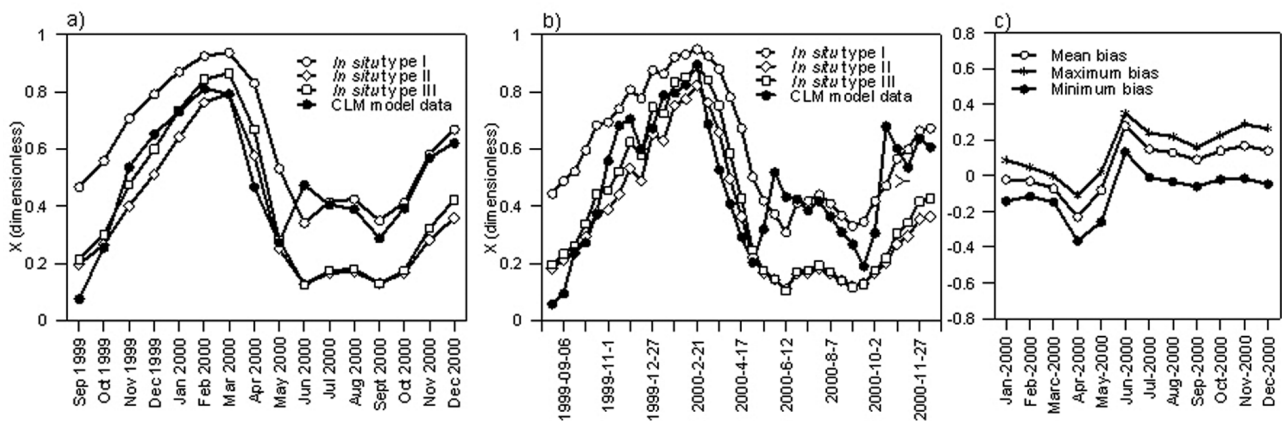

Fig. 2:   Comparison of the modeled and measured soil water storage in the 0–50 cm soil layer: a) temporal interval: 1 month, b) temporal interval: 2 weeks, c) monthly bias range of the soil water storage.

Table 1: The evaluation of the CLM soil water storage simulations with regards to the *in situ* data.

Soil layer	Accuracy measure	In situ (mean) / CLM interval: 2 weeks	In situ (mean) / CLM interval: 1 month
0–50 cm	Mean bias	0.02	0.02
	RMSE	0.15	0.14
	R^2	0.56	0.62

Long term changes of the soil water storage in the 20th century

Standardized cumulative annual deviation (SCAD) was applied to detect trends in the annual time series of the soil water storage from the CLM data (Fig. 3a). Two wet periods and two dry periods has been distinguished. A positive slope, indicating a wet period in which the soil water storage was above the mean, was detected in years 1960–1966 and 1981–1986, assuming six consecutive years as a minimal length of the period. A negative slope, indicating a dry period in which the soil water storage was below the mean, was observed in years 1967–1980 and 1987–2000, with some oscillations. Thus in years 1960–1980 one wet period and one
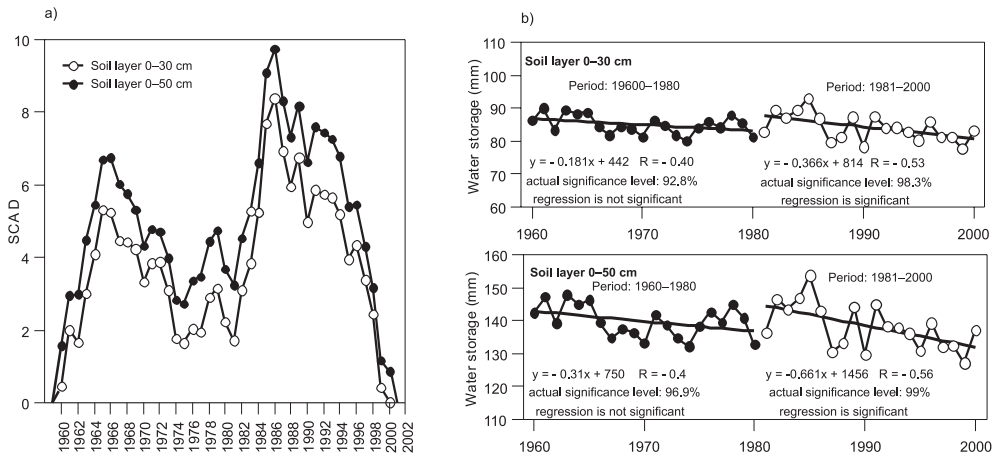
Fig. 3:   Detection of trends in the series of the mean annual soil water storage in years 1960–2000 based on the CLM data: a) standardized cumulative annual deviation (SCAD) of the soil water storage, b) variability of the annual soil water storage.

dry period have appeared, and a similar sequence has been observed in years 1981–2000. Series of the soil water storage show no significant changes in the years 1960–1980, whereas in the years 1981–2000 decreasing trends are statistically significant (Fig. 3b). In last two decades of the 20th century mean annual soil water storage decreased twice as rapidly as in the years 1960–1980. In these years, rate of change in the 0–30 cm soil layer was 3.7 mm/10 years and 6.6 mm/10 years in the 0–50 cm soil layer. The observed patterns of the soil moisture at interannual scale can be explained by the variability of the ET/P ratio. Decrease in the SCAD of the soil moisture corresponds to an increase in the SCAD of the ET/P ratio (Fig. 4a). Slight upward tendency of the ET/P ratio was observed in years 1960–2000 (Fig. 4b), although not statistically significant. In general, it was found that there was strong negative corelation between the ET/P ratio and the soil water storage (Fig. 5).
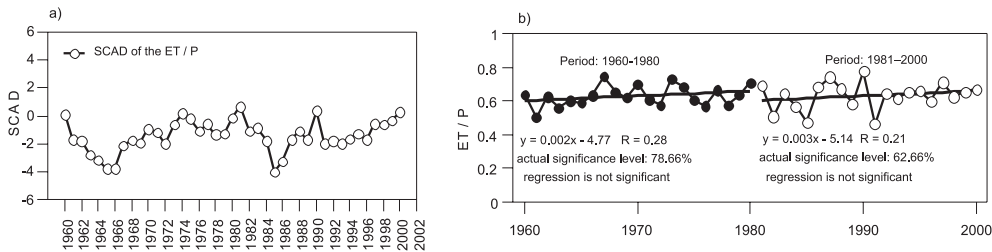

Fig. 4:   Standardized cumulative annual deviation (SCAD) of the evapotranspiration/precipitation ratio (ET/P) in years 1960–2000 (a) and long term variability of the annual ET/P ratio (b).
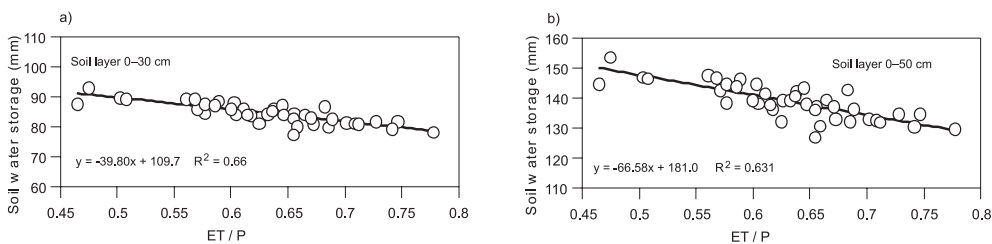

Fig. 5:   Relation between the evapotranspiration/precipitation ratio and the soil water storage in the 0-30 cm soil layer (a) and in the 0–50 cm soil layer (b).

161

Changes in temporal patterns of the soil water storage

The two scenarios affected the monthly mean of the soil water storage to different degrees (Fig. 6). Long term mean annual values of forcing variables are presented in Table 2. Most pronounced changes were indicated by the A1B projection. Expressed as an average over the entire catchment, changes in April-October months amounted to –8% and –13% in the case of the 0–30 cm and the 0–50 cm soil layers respectively. A decrease also appears in the winter months (January–March), whereas an increase is expected in the months April–June and November–December. Predicted variability range of the monthly values for the future conditions as compared to the control period is much narrow for January-March and September (Fig. 6c). This suggests possibility of appearance of much drier conditions in winter and late summer in future.
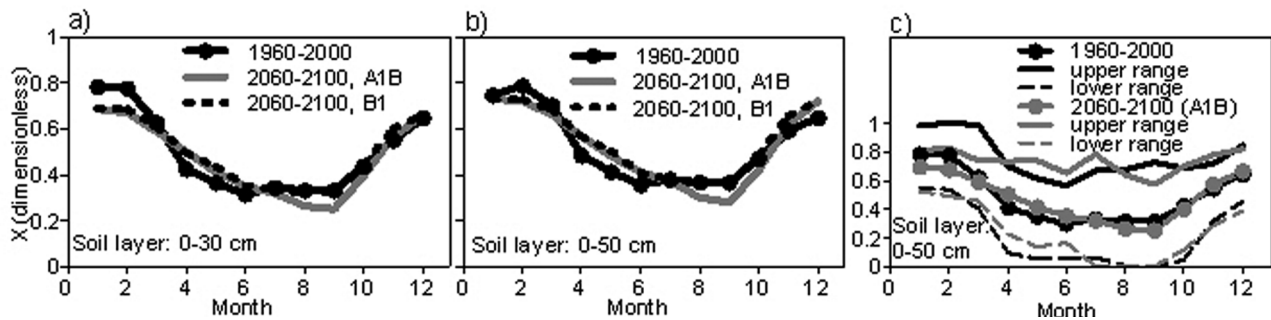

Fig. 6: Seasonal variability of the effective relative soil moisture (dimensionless) according to the CLM simulations for the 20th and the 21st century: a) the soil layer 0–30 cm, b) the soil layer 0–50 cm, c) the soil layer 0–50 cm; solid and dashed lines marks range of simulated variability.

Table 2: Mean annual values of precipitation, evapotranspiration, ET/P ratio and air temperature.

Variable	1960–1980	1981–2000	1960–2000	2060–2100 (A1B)	2060–2100 (B1)
Precipitation	776 mm	705 mm	743 mm	724 mm	795 mm
Evapotranspiration	455 mm	442 mm	449 mm	493 mm	491 mm
ET/P	0.60	0.64	0.62	0.68	0.62
Air temperature at 2 m	7.43ºC	7.65 ºC	7.54 ºC	10.51 ºC	9.65 ºC

CONCLUSIONS

This contribution provides an insight into intensification of the local hydrological cycle resulting from climate change projections based upon results from the CLM climate experiment. Results shown here suggest that during the 21st century a decrease in the soil water storage in late summer months is predicted to appear. This already have occurred in the latter decades of the 20th century. Thus the soil water resources may become more limited in the future which consequently may facilitate formation of more intense soil and hydrological droughts. Considerable changes concern components of the hydrological cycle (precipitation and evapotranspiration) upon which the soil moisture regime develops.

REFERENCES

Hollweg H-D., Böhm U., Fast I., Hennemuth B., Keuler K., Keup-Thiel E., Lautenschlager M., Legutke S., Radtke K., Rockel B., Schubert M., Will A., Michael Woldt M. and Wunram C. (2008). *Ensemble Simulations over Europe with the Regional Climate Model CLM forced with IPCC AR4 Global Scenarios.* Tech. Rep. No. **3**, http://www.mad.zmaw.de/fileadmin/extern/documents/reports/.

IPCC Climate Change (2007). *The Physical Science Basis, 2007*. Working Group I Contribution to the Fourth Assessment Report of the IPCC Intergovernmental Panel on Climate Change. Cambridge University Press, Cambridge, UK & New York, NY, USA.

Jasper K., Calanca P. and Fuhrer J. (2006). Changes in summertime soil water patterns in complex terrain due to climatic change. *J. Hydrol.*, **327**: 550–563.

Kundzewicz Z. W., Radziejewski M. and Pinskwar I. (2006). Precipitation extremes in the changing climate of Europe. *Climate Res.*, **31**: 51–58.

Li H., Robock A. and Wild M. (2007). Evaluation of Intergovernmental Panel on Climate Change fourth Assessment soil moisture simulations for the second half of the twentieth century. *J. Geophys. Res.*, **112**.

Radziejewski M. and Kundzewicz Z. W. (2004). Detectability of changes in hydrological records. *Hydrolog. Sci. J.,* **49**(1): 39–52.

Rodell M., Houser P. R., Jambor U., Gottschalck J., Mitchell K., Meng C.-J., Arsenault K., Cosgrove B., Radakovich J., Bosilovich M.,. Entin J. K, Walker J. P., Lohmann D., and Toll D. (2004). The Global Land Data Assimilation System. *B. Am. Meteorol. Soc.*, **85**(3): 381–394.

Seneviratne S.I., Luethi D., Litschi M. and Schär C. (2006). Land-atmosphere coupling and climate change in Europe. *Nature*, **443**: 205–209.

Somorowska U., 2007. Quantifying the uncertainties in the terrestrial water storage-runoff relation using in-situ soil moisture data. [In:] Pfister L., Hoffmann L. (Eds.), Uncertainties in the 'monitoring-conceptualisation-modelling' sequence of catchment research. *Technical Documents in Hydrology*, **81**: 35–41. UNESCO, Paris.

Wagner W., Blöschl G., Pampaloni P., Calvet J.-C., Bizzarri B., Wigneron J.-P. and Kerr J. (2007). Operational readiness of microwave remote sensing of soil moisture for hydrologic applications. *Nord. Hydrol.*, **38**(1): 1–20.

Yang Y., Watanabe M., Wang Z., Sakura Y. and Tang C. (2003). Prediction of Changes in Soil Moisture Associated with Climatic Changes and Their Implications for Vegetation Changes: Waves Model Simulation on Taihang Mountain, China. *Climatic Change*, **57**(1): 163–183.

IMPACT OF LAND COVER CHANGE ON FLOOD RUNOFF CHARACTERISTICS OF THE HEADWATER SUB-CATCHMENTS IN THE NYANDO RIVER BASIN, KENYA

L.O. Olang [1,2], P. Kundu[1], T. Bauer[3] and J. Fürst [2]

[1] *Egerton University, Faculty of Engineering and Technology, Department of Agricultural Engineering, P. O. Box 536, Njoro, Kenya*

[2] *Institute of Water Management, Hydrology and Hydraulic Engineering (IWHW), University of Natural Resources and Applied Life Sciences, Vienna. Muthgasse 18, A-1190, Vienna, Austria*

[3] *Institute of Surveying, Remote Sensing and Land Information (IVFL), University of Natural Resources and Applied Life Sciences, Vienna. Peter Jordan-Strasse 82, 1190, Vienna, Austria*

Corresponding author: Luke Omondi Olang, e-mail: olanglk@yahoo.com

ABSTRACT

The effects of land cover change on runoff characteristics of four sub-catchments located in the headwaters of the Nyando River Basin (3500 km^2) of Kenya were simulated in this study. Land cover change data were obtained by classifying Landsat satellite images based on six major land cover classes prevalent in the basin. The accuracy of the classifications was assessed with the help of reference datasets acquired from the FAO-Africover land cover dataset and digitized topographic maps (1:50 000) of the basin. The mapped land cover data, together with a DEM and a digital soil map, were used to estimate the parameters for parsimonious conceptual rainfall-runoff models, namely the Natural Resource Conservation Service-Curve Number (NRCS-CN) and Clarks Unit Hydrograph (C-UH) used to generate and transform runoff from a typical rainfall storm characteristic of the basin. Land cover classification results obtained revealed that, over the study period, forest cover declined by 20% while agricultural fields expanded by 16%. The headwater sub-catchment with the highest reduction in forest coverage exhibited the highest simulated change in runoff, leading to increased runoff volumes and peak discharges by up to 22%. Generally, simulated runoff peak discharges were noted to have increased in the study sub-catchments by factors of 1.1 to 1.22 over the study period.

Key words: Landsat satellite images, land cover change, rainfall-runoff models

INTRODUCTION

Over the last fifty years, the Nyando River basin (NRB) of Kenya has witnessed significant land cover changes epitomized by the rampant deforestation in its headwaters. This degradation has largely been caused by an upsurge in its human population in pursuit of socio-economic sustenance from the existing natural resources. Today, these land cover changes are believed to be amplifying flood flows through increased runoff rates during rainfall seasons. Few studies carried out in this basin have attempted to relate this land degradation to the flood runoff characteristics of the basin (www.worldagroforestrycentre.org/~/TransVic) This is because the basin lacks adequate stream gauge representation within the affected upstream sub-catchments. Moreover, the available stream flow data from the few existing stations in the basin cannot be fully relied on due to the uncertainties related to large data gaps and poor recording practices. Understanding the influence of land cover changes on hydrological regimes also requires high resolution spatio-temporal land cover data with the ability to identify change statistics and directions (Coppin *et al*., 2004). Quality land cover change monitoring requires precise land information such as orthophotographs. However, the costs associated with the acquisition of such datasets are still a major challenge to many rural basins in developing countries such as Kenya.

The availability of cost-effective multi-temporal satellite imagery in recent times, therefore, has to some extent alleviated the data difficulties experienced by such rural basins. Satellite imagery has the ability to provide

historical, repetitive, and statistically representative land cover data that can be used to quantify multi-temporal alterations of land cover components (Miline, 1998). Such land cover statistics, in combination with other spatial datasets, can be used to simulate the impact of land cover changes using rainfall-runoff models whose parameters can be established physically. In this study, multi-temporal land cover changes in the NRB were investigated and their impact on flood runoff characteristics simulated using a range of flood-generating rainfall events. In this paper, only one typical storm event characteristic of the uplands of the basin is used to illustrate the impact of the changes on runoff peak discharges and volumes in four selected sub-basins (Fig. 1).
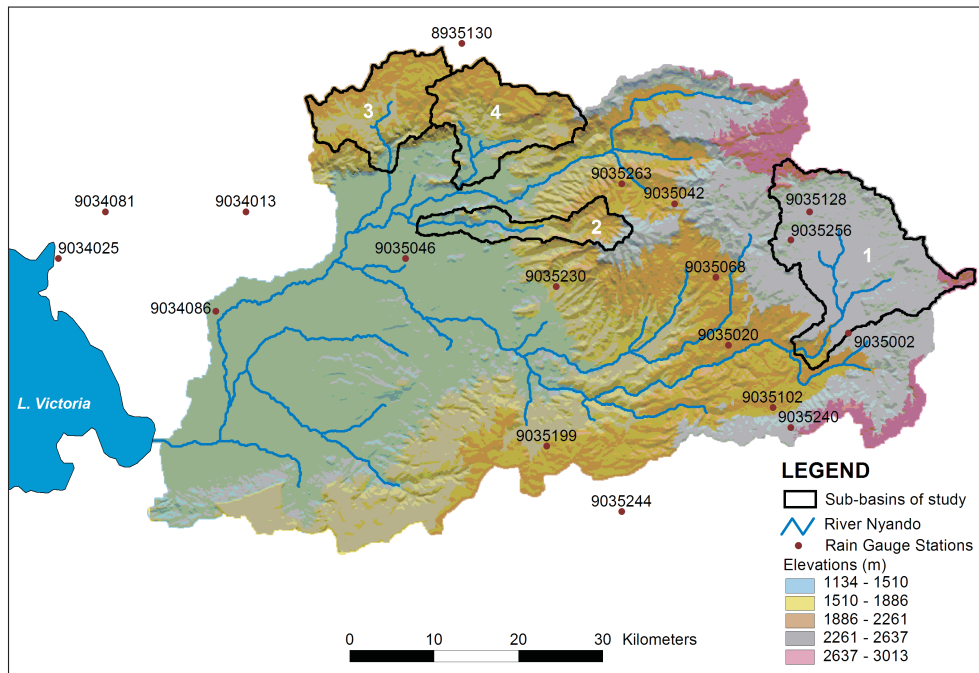

Fig. 1:   Rain gauges, location, and elevation of the selected study sub-basins.

STUDY AREA

NRB covers an area of about 3550 km² in western Kenya. The basin spans the equator between latitudes 0˚25'S & 0˚10'N and longitudes 34˚50' & 35˚50' E. It is located in the scarps of the Kavirondo Gulf formed as a result of a rift fault. The basin is drained by the Nyando River with a total length of about 170 km, originating in the upland hills of Nandi and Londiani and draining into the transboundary Lake Victoria at an altitude of about 1100 m a.s.l. The climate of the basin is largely influenced by the Equatorial Convergence Zone (ITCZ), modified by local orographic effects. Land cover in the basin generally varies from forests in the uplands to mixed-type agriculture in the mid to lowland parts of the basin.

DATASETS AND METHODS

Hydro-meteorological data

Daily rainfall data for the basin were obtained from seventeen pluviometric stations located within the basin (Figure 1). Interpolated depths for the basin were calculated using ordinary Kriging procedure based on a spherical variogram model (Cressie, 1993). A rainfall event which occurred in April, 1972 during the long rainy season was selected for use in this simulation. Based on rainfall data analysis, this event has a return

166

period of two years within the basin. The areal daily rainfall depths for the study sub-basins were derived by lumping the interpolated values with the help of GIS. Table 1 provides the physical characteristics and areal rainfall depths for the study basins.

The modeling procedure adopted for this study required hourly rainfall data as input for the models. Since only daily data were available for the sub-basin, it was important to disaggregate the data into hourly time intervals based on assumed spatio-temporal patterns of the rainfall. Generally, the whole NRB exhibits significant rainfall variability. In the lowlands, intensive short-duration (1–3hours) storms are predominant. In the uplands, long-duration but less intense storms are prevalent. Therefore, rainfall disaggregation was done by assuming that the storms had durations of 5 hours which also corresponds approximately to the times of concentration.

A comparison of the daily time series plots of rainfall and runoff for the sub-basins revealed a lot of inconsistencies in the stream flow gauge data that were acquired. Either no rainfall was noted (or occurred) on the corresponding days when flood events were noted to have occurred in the immediate downstream river gauge. The converse was also noted to be true. Due to these data uncertainties, added to the other fact that the runoff values were also daily data, the discharge data were not used for systematic calibration and validation of the selected models but rather for plausibility checks. Nonetheless, the locations of the river gauges were used to define the sub-basins and their geometric characteristics.

Land cover

Land cover data were a principal part of this study. The data were obtained from classifications of Landsat satellite images acquired for the years, 1973 and 2000 from the global Landsat database (http://www.landsat.org). Images for the year 1973 were produced using Landsat-1 which used a Multi Spectral Scanner (MSS) satellite sensor. Images for the 2000 were produced by Landsat-7 which uses an Enhanced Thematic Mapper plus (ETM+) satellite sensor. Characteristically, Landsat MSS had a spatial resolution of about 80 m and four spectral bands that can be used to discriminate land cover changes. Landsat ETM+ has a spatial resolution of about 30 m for the first seven bands (bands 1-7) and a resolution of 15 m for band 8 (panchromatic band). For each year of study, two image scenes encompassing the study area were obtained. Seven land cover classes, namely *agriculture*, *forest*, *grassland*, *shrubland*, *wetland*, *tea/coffee*, and *water* were selected for classification purposes. Land cover reference dataset for validating classifications for the year 2000 was obtained from the FAO Africover land cover Program (http://www.africover.org). This data was processed and reclassified to conform to the selected seven land cover classes. Land cover reference data for 1973 image classifications was obtained by processing 12 topographic maps (1:50,000) covering the entire study basin. The maps were digitized, geo-referenced and reclassified into the selected land cover classes with the help of ground truthing and field interviews.

In order to identify the spectral bands to be used in the classification process, the transformed divergence technique was applied. Transformed divergence is a statistical method for identifying the minimum yet optimal image bands for use in a classification procedure (Jensen, 2005). Consequently, image bands 4–3–2 were selected for classifying Landsat ETM+ (2000) images. As for the Landsat MSS (1973) classification, all the image bands were found sufficient for use. Because of the different spatial resolutions for the 1973 and 2000 satellite images, the selected optimal bands were merged and later resampled using the nearest neighbor technique (NN) to a common resolution of 80 m. The NN interpolation scheme does not alter pixel brightness values important for discriminating land cover classes. Classification of the images was done on per pixel basis using a hybrid of supervised and unsupervised classification approach known as guided clustering (Yuan *et al.*, 2005). This was achieved by delineating selected land cover polygons on the images with the help of the reference datasets and an initial unsupervised clustering done to enhance careful identification of clusters with similar statistics within the delineations. Supervised classification was then performed using the maximum-likelihood parametric decision rule with a priori probabilities which were estimated from the classified Africover reference data. To remove small isolated image pixels arising during the classification process, a 3x3 majority filter was finally applied on the classified land cover classes.

The procedure adopted in this study was such that the image scenes for each year of study were processed and classified independently to minimize radiometric anomalies. The classified image scenes were then mosaicked and later clipped to the study area for subsequent analysis. Assessment of classification accuracy was done by comparing the classified images and the reference datasets via an error (correlation) matrix. Two procedures, namely the overall classification accuracy and the *Kappa* statistics index were used. *Kappa* statistics is a multivariate measure of the agreement between classified images and reference datasets. The index considers the combined effects of properly classified land cover classes, as indicted by the major diagonal of the error matrix, and the agreement by chance, as indicated by the marginals of the error matrix (Congalton, 1991). A total of 170 and 181 auxiliary points were used to generate error matrices for the assessing image classifications for Landsat ETM+ (2000) and Landsat MSS (1973) respectively.

Digital Elevation Model (DEM)

Derivation of the morphometric and topological characteristics of the basin was performed using a grid-based DEM with a resolution of 90 m. The data was acquired from the USGS-Shuttle Radar Topographic Mission (SRTM) web portal at http://srtm.usgs.gov and hydrologically corrected in a GIS to fill the sinks. Based on the eight direction pour point procedure (D8), the DEM was used to derive stream and basin characteristics. In the D8 method, a moving 3x3 cell assigns flow by comparing the elevation gradient of eight surrounding cells. This was done via the automated procedures provided in a GIS for the determination of flow direction, flow accumulation, stream definition and delineation of the sub-catchments at selected sites (Burrough and McDonell, 1998). In this study, the sub-catchments were delineated based on the geographic locations of existing river gauging points. The derived river network, especially in the flat floodplains of the basin, was later realigned to its actual position with the help of the panchromatic band of Landsat ETM+ (Callow *et al*., 2006). In total, 14 sub-catchments were derived for the whole NRB together with their morphometric properties. Four upstream sub-catchments (Table 1) were then selected for this study based on the areas known to have undergone significant land cover changes over the years.

Table 1: Physical characteristics and areal rainfall depth of the sub-basins.

Id	Sub-basin	River gauge	Area of sub basin [km^2]	Average slope [%]	Areal rainfall depth [mm]
1	Masaita	1GC05	285.6	8	30
2	Mbogo	1GB06	77.3	19	20
3	Kapchure1	1GB07	130.7	13	27
4	Ainapsiwa	1GB11	147.7	17	24

Soils Data

Soils data were obtained from the Global Environment Facility Soil Organic Carbon (GEFSOC) project available at the World Soil Information web portal at URL: http://www.isric.org. This dataset is currently available at a scale of 1:1M for Kenya (Batjes and Gicheru, 2004). This data was pre-processed in a GIS and reclassified into the required classes with the help of the FAO/UNESCO revised manual for soil maps of the world. Based on their infiltration characteristics, hydrological soil groups (HSG) were derived and later used in combination with the classified land cover data to derive the parameters for the selected models.

SELECTED MODELS

The Natural Resource Conservation Service-Curve Number (NRCS-CN) model was used in runoff generation. This model assumes that the effective rainfall in the basin is the portion of the total rainfall occurring in the basin less the initial abstractions. No runoff, therefore, is produced in the catchment until the rainfall equals the initial abstractions. The other assumption of the model is that infiltration is less than or equal to the value of potential maximum retention. The depth of runoff, therefore, is entirely the result of total rainfall minus infiltration or water retained in the basin (Maidment, 1993). Under these conditions, the model generates runoff based on the premise that the ratio of infiltration and potential maximum retention equals the ratio of actual runoff and effective rainfall. The model estimates that the potential maximum retention ability of the basin is a function of a dimensionless parameter called the curve number (CN). This parameter accounts for land cover, soil types, and antecedent moisture conditions (AMC). By assuming a mean AMC value, the CN value can be estimated as a function of the land cover and soils datasets. In this study, the initial abstraction was assumed to be 20% of the potential retention ability since the selected rainfall event for the study occurred under wet catchment conditions (that is, during the long rainy season). Since the same hydrological soils were used in the model for the respective years of study, it was also assumed that the changes in the derived CN values were largely consequent of the land cover changes in the basin.

Runoff transformation, on the other hand, was achieved by using the Clark Unit Hydrograph (C-UH) model. The model is based on UH assumptions where direct runoff is modeled from a unit of excess precipitation assumed to occur instantaneously over the basin (Chow *et al*., 1988). Clarks UH ideally derives the UH of sub-catchments by accounting for its translation and attenuation. Translation defines the movement of rainfall excess from its production points throughout the drainage area to the outlet. Translation hydrographs are generated from time-area relationships and routed based on the linear reservoir model concept (USACE, 1994). Attenuation, on the other hand, defines a reduction in the discharge magnitude as excess rainfall is stored in the basin. Unlike other conceptual UH procedures, the Clark UH model provides an opportunity to relate its processes to catchment characteristics. Generally, the application of this model requires the determination of travel time and storage coefficients of the basin. With the help of other empirical equations, these two main parameters can be established from catchment characteristics. In this study, time of concentration was obtained from the United States Department of Agriculture – Soil Conservation Service (USDA-SCS, 1985) method, which relates this parameter to CN, the hydraulic length and slope of the sub-basins. The storage coefficient, an indicator of the temporary storage capacity of a basin, was obtained from the procedure defined by Sabol (Sabol, 1988).

RESULTS AND DISCUSSION

Land cover classification results obtained revealed significant spatio-temporal land cover changes over the study period. Overall classification accuracies obtained for the 2000 and 1973 classifications were 84% and 76%, respectively. *Kappa* statistics values for the respective years stood at 80% and 67%. These accuracies are considered good image classification estimates (Jensen, 2005). Generally, forests declined by 20% while agriculture increased by 16%. The area covered by shrubland also increased by about 4% depicting a gradual transition from forests to other types of land cover. While it could be true that some land cover changes such as a shift from pasture to agriculture and vice versa can be attributed to seasonal or normal cover conversions experienced by any region, the majority of the land cover changes, especially those from forest to agriculture and vice versa, revealed by the classification procedures can be more accurately described as land cover modifications which involved long term or complete replacement of one type of cover by another. These modifications were more prevalent in the upstream sub-basins where the results revealed significant forest decline and consequent agricultural expansion. Table 2 provides the results obtained when effects of land cover changes were simulated using the selected models in the four sub-basins.

Table 2: Simulated runoff characteristics.

Id	Sub-Basin	Mean CN		Runoff coefficient		Peak runoff (Q_p)		Changes in Q_p
		1973 [%]	2000 [%]	1973 [%]	2000 [%]	1973 [$m^3 \cdot s^{-1}$]	2000 [$m^3 \cdot s^{-1}$]	[%]
1	Masaita	66.1	71.9	60.4	67.2	180	206	14
2	Mbogo	68.0	74.3	61.1	71.0	30	37	22
3	Kapchure1	67.7	72.1	75.4	83.0	93	104	12
4	Ainapsiwa	68.0	74.3	75.8	85.0	111	127	15

Based on the model and study assumptions, it was noted that the value of CN changed significantly in the sub-basins. Higher values of CN in river basins are usually construed to mean more runoff production with the converse also being true. It should be noted that the empirical formula of the NRCS-CN procedure used in this study provides average values of the CN parameter. In reality, however, this parameter is a continuous variable in time and space due to the high variability and nonlinearity of the AMC of the soils. In fact, the determination of its actual value for large scale modeling studies is still a challenge for sub-basins with limited data. Chow *et al.* (1988) provided adjustment factors for the CN parameter for use in wet and dry catchment conditions. Mean values of CN provided in Table 2 were obtained after applying the adjustment factors for wet conditions. Generally, sub-basin no. 2 (Mbogo), which was relatively the smallest in size but with the largest slope, provided the highest percentage change (22%) in the peak runoff value. A retrospective check of the land cover changes in this sub-basin indicates that the basin suffered more deforestation than other areas.
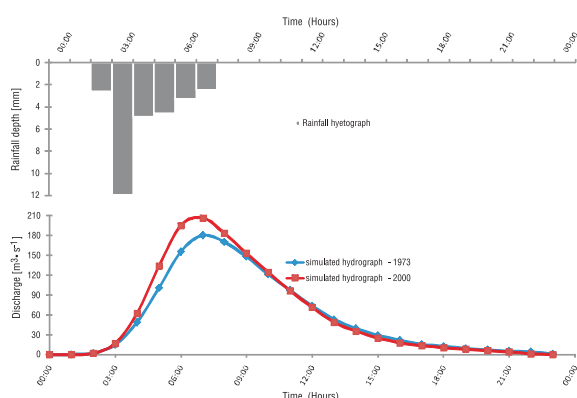

Fig. 2: Simulated runoff hydrographs for 1973 and 2000 land cover in the Masaita sub-basin.

The runoff coefficient is a ratio or a proportion of rainfall that becomes runoff. Changes in runoff volume, therefore, can be deduced from changes in this coefficient. While it may be interesting to relate CN to the runoff coefficient in as far as runoff production is concerned, the obvious deduction that becomes apparent from our results is that the runoff coefficient values obtained were higher than the CN values as indicated in a similar study elsewhere (Merz *et al.*, 2006). The highest jump in the value of the runoff coefficient was noted sub-basin no. 2 (Mbogo) where the runoff coefficient increased by about 10%. That notwithstanding, sub-basins no. 3 (Kapchure1) and no. 4 (Ainapsiwa) were noted to be more likely to produce higher flood runoff volumes than the rest as shown by their high values of the runoff coefficient. Such catchments can, therefore, be targeted with appropriate land use management systems aimed at reducing the magnitude of local flows. A typical simulated runoff hydrograph for sub-basin no. 1 (Masaita), which was the largest in size, is shown in Fig. 2.

Generally, it was noted that for the study periods and at least in the selected study sub-catchments, simulated land cover changes increased peak discharge by factors of 1.10 to 1.22 from its initial value. These factors were considered relatively high considering the depth of the rainfall used for the study and the relative sizes of the sub-catchments studied.

CONCLUSION AND RECOMMENDATION

The study demonstrated the potential of using multispectral Landsat satellite data as an alternative source of land cover data for hydrological modeling. Model results showed that land cover changes have, in fact, impacted on the hydrological response of the basins of interest leading to increased peak discharges and consequently higher runoff volumes. This increase was more apparent in sub-basins where deforestation was more prevalent, with a likely dwindling of soil moisture retention capability and lower rates of infiltration. However, further research is recommended for the whole basin, especially during large flood events, so that the effects of land cover changes in the whole basin can be further quantified for proper and enhanced land and water management.

REFFERENCES

Batjes N.H. and Gicheru P. (2004). Soils data derived from SOTER for studies of carbon stocks and change in Kenya (GEF-SOC Project, Version 1.0). In: Technical Report **2004/01**, ISRIC – World Soil Information, Wageningen.

Burrough P.A. and McDonnel R.A. (1998). *Principles of Geographical Information Systems*. Oxford.

Callow J.N., Van Niel K.P. and Boggs, G.S. (2006). How does modifying a DEM to reflect known hydrology affect subsequent terrain analysis? *J. Hydrol.*, **332**: 30–39.

Chow V.T., Maidment D.R. and Mays L.W. (1988). *Applied Hydrology*. McGraw-Hill.

Congalton, R.G. (1991). A review of assessing the accuracy of classifications of remotely sensed data. *Remote Sens. Environ.*, **37**: 35–46.

Coppin P., Jonckheere I., Nackaerts K., Muys B. (2004). Digital change detection methods in ecosystem monitoring: a review. *Int. J. Remote Sens.*, **25**: 1565–1596.

Cressie, N.A.C. (1993). *Statistics for Spatial Data*. Wiley, New York: 928 pp.

Finished Shuttle Radar Topographic Mission (SRTM) Data. United States Geological Survey (USGS). Acquired on the 31st August, 2007, from http://srtm.usgs.gov

Food and Agriculture Organisation (FAO) of the United Nations – Africover. Multipurpose Africover Databases on Environmental Resources (MADE). Retrieved on the 12th, June, 2007, from http://www.africover.org

Global Orthorectified Landsat Land Cover Data. Retrieved on 3rd, May, 2007 from http://www.landsat.org

Jensen J.R. (2005). *Introductory Digital Image Processing: A Remote Sensing Perspective*. 3rd ed. Prentice Hall series in Geographic Information Science.

Maidment D. R. (1993). *Handbook of Hydrology*. McGraw Hill.

Merz R., Blöschl G. and Parajka J. (2006). Spatio-temporal variability of event runoff coefficients. *J. Hydrol.*, **331**: 591–604.

Miline A. K. (1998). *Change direction analysis using Landsat Imagery: a review of methodologies*. In: Proceedings of the IGARSS'88 Symposium in Edinburgh, Scotland, ESA SP-284 (Noordwijk, Netherlands: ESA): 541–544.

Sabol G.V. (1988). Clark unit hydrograph and r-parameter estimation. *J. Hydraul. Eng.,* **114**(1): 103–111.

TransVic project . International Center for Research in Agro-Forestry. Retrieved on the 21st, April 2007 from http://www.worldagroforestrycentre.org/sites/TransVic

USACE (1994). *Flood-Runoff Analysis. Engineering Manual* No. 110-2-1417, Washington.

USDA-SCS (1985). *SCS National Engineering Handbook*, *Section 4: Hydrology*. USDA, Washington D.C.

World Soil Information (ISRIC). SOTER database for Kenya (version 2.0). Retrieved on 12th January, 2008 from http://www.isric.org

Yuan F., Sawaya K.E., Loeffelholz B.C. and Bauer M.E. (2005). Land cover classification and changes analysis of the Twin Cities (Minnesota) Metropolitan Area by multitemporal Landsat remote sensing. *Remote Sens. Environ.*, **98**: 317–328.